Mathematical Modelling and Analysis of Vehicle Frontal Crash using Lumped Parameters Models

Bernard B. Munyazikwiye

UiA University of Agder

Doctoral Dissertations at the University of Agder 261

Bernard B. Munyazikwiye

Mathematical Modelling and Analysis of Vehicle Frontal Crash using Lumped Parameters Models

A dissertation submitted to the University of Agder for the degree of Doctor of Philosophy, Specialisation in Mechatronics

University of Agder
Faculty of Engineering and Science
2020

Doctoral Dissertations at the University of Agder 261
ISBN: 978-82-7117-961-8
ISSN: 1504-9272

Printed by Media 07
Kristiansand

Acknowledgments

Upon presenting this thesis, I would like to acknowledge the valued support of several people or institutions. I am highly indebted to the University of Agder (UiA) for funding this project. I would like to thank Professor Frank Reichert and Associate Professor Ghislain Maurice Norbert Isabwe for initiating the cooperation between UiA and the University of Rwanda (UR). It was through this cooperation that I had the opportunity to pursue my PhD studies.

I would like to thank my supervisors Professor Kjell G. Robbersmyr, Professor Hamid Reza Karimi, and Associate Professor Dmitry Vysochinskiy, for their guidance and constant supervision as well as providing necessary information regarding the project. I certainly could not have done this work without them. Also I would like to thank Professor Van Khang Huynh, who has provided detailed insights and suggestions on the structure of this document. His contribution is extremely valuable in producing the final document.

I would also like to thank my colleagues and the Dynamic research group at UiA for their constructive discussion and comments. I would like to express my sincere gratitude towards Mrs. Emma Elizabeth Horneman, PhD coordinator, for her care and kindness and encouragement during my stay at UiA.

Last but not least, thanks to my wife, Mrs. Immaculée Uwineza, for her support and endurance to bear my absence in the family during the whole period of study. This thesis is dedicated to my wife Immaculée Uwineza and my children Blessing Sam Irumva, Joy Gwiza, Joël Ganza, and Joshua Manzi.

Thesis details

Thesis Title: Mathematical Modelling and Analysis of Vehicle Frontal Crash using Lumped Parameters Models

PhD Research Fellow: Bernard B. Munyazikwiye

Supervisors:
Main supervisor, Dr. Kjell G. Robbersmyr, Professor at the University of Agder, Norway; Co-supervisors: Dr. Hamid Reza Karimi, Professor at Politecnico di Milano, Italy, up to the end of 2016 and Dr. Dmitry Vysochinskiy, Associate Professor at the University of Agder, Norway, from Spring 2017.

The following listed articles have been published in peer reviewed journals and conference proceedings. The version presented in this thesis differs only in formatting and minor errata.

Paper A: Bernard B. Munyazikwiye, Hamid Reza Karimi, and Kjell G. Robbersmyr, "Mathematical Modelling and Parameters Estimation of Car Crash Using Eigensystem Realization Algorithm and Curve-Fitting Approaches," *Hindawi: Mathematical Problems in Engineering, Vol. 2013, 2013, pp. 1-13.*

Paper B: Bernard B. Munyazikwiye, Kjell G. Robbersmyr, and Hamid Reza Karimi "A state-space approach to mathematical modelling and parameters identification of vehicle frontal crash," *Tylor & Francis: Systems Science & Control Engineering: An Open Access Journal*, Vol. 2, 2014, pp. 351–361.

Paper C: Bernard B. Munyazikwiye, Hamid Reza Karimi, and Kjell G. Robbersmyr, "A Mathematical Model for Vehicle-Occupant Frontal Crash using Genetic Algorithm," *UKSim-AMSS 18th International Conference on Computer Modelling and Simulation (IEEE)*, Cambridge, UK, 6-8 April 2016.

Paper D: Bernard B. Munyazikwiye, Hamid Reza Karimi, and Kjell G. Robbersmyr, "Optimization of Vehicle-to-Vehicle Frontal Crash Model Based on Measured Data Using Genetic Algorithm," *IEEE Access. Special Section on Recent Advances on Modelling, Optimization and Signal Processing Methods in Vehicle Dynamics and Crash-Worthiness, Vol.5, 2017, pp. 3131–3138*.

Paper E: Bernard B. Munyazikwiye, Hamid Reza Karimi, and Kjell G. Robbersmyr, "Application of Genetic Algorithm on Parameter Optimization of Three Vehicle Crash Scenarios," in *International Federation of Automatic Control (IFAC)*, Toulouse, France, 9-14 July 2017.

Paper F: Bernard B. Munyazikwiye, Dmitry Vysochinskiy, Mikhail Khadyko and Kjell G. Robbersmyr "Prediction of Vehicle Crashworthiness Parameters using Piecewise Lumped Parameters and Finite Element Models", *Designs, Special Issue Road Vehicle Safety: Design and Assessment, 2018 Vol.2(4) pp. 1-16.*

In addition to the main articles included in the dissertation, the following papers have also been published:

1. Bernard B. Munyazikwiye, Hamid Reza Karimi, and Kjell G. Robbersmyr, "Mathematical Modeling of Vehicle Frontal Crash by a Double Spring-Mass-Damper Model," *International Conference on Information, Communication and Automation Technologies (ICAT)*, Sarajevo, Bosnia and Herzegovina, 30 October – 01 November, 2013.

2. Bernard B. Munyazikwiye, Hamid Reza Karimi, and Kjell G. Robbersmyr, "Fuzzy logic approach to predict vehicle crash severity from acceleration data," *International Conference on Fuzzy Theory and Its Applications (iFUZZY)*, Yilan, Taiwan, 18-20 November, 2015.

Contents

List of Abbreviations

AEMS	Absorbable Energy Monitoring Scheme
ARMA	Autoregressive Moving Average
ARMAX	Autoregressive Moving Average with exogeneous input
ASI	Acceleration Severity Index
CCT	Component Crash Test
CF	Curve Fitting
CFC	Chanel Frequency Class
EoM	Equations of Motion
ERA	Eigensystem Realization Algorithm
FEM	Finite Element Model
FMVSS	Federal Motor Vehicle Safety Standard
FSCT	Full-Scale Crash Test
GA	Genetic Algorithm
IIHS	Insurance Institute for Highway Safety
IPA	Interior Point Algorithm
LB	Lower Bound
LC-CDE	Linear Constant-Coefficient Difference Equation
LPM	Lumped Parameter Model
LSCF	Least Squares Curve Fitting
MAE	Mean Absolute Error
MSD	Mass Spring Damper
NCAP	New Car Assessment Program

NHTSA	National Highway Traffic Safety and Administration
PWLPM	Piecewise Lumped Parameter Model
RD	Residual Deformation
RMSE	Root Mean Square Error
SAE	Society of Automotive Engineers
SIA	System Identification Algorithms
SS	State Space
UB	Upper Bound
V-Occ	Vehicle-Occupant
VTB	Vehicle To Barrier
VTV	Vehicle To Vehicle

List of Symbols

$\hat{y}_i$	Simulated variables
$\ddot{q}_1$	Acceleration of chassis
$\ddot{q}_2$	Acceleration of passenger compartment
$\ddot{x}_o$	Acceleration of occupant
$\ddot{x}_v$	Acceleration of vehicle
δ	Restraint slack
$\dot{q}_1$	Velocity of chassis
$\dot{q}_2$	Velocity of passenger compartment
$\dot{x}_o$	Velocity of occupant
$\dot{x}_v$	Velocity of vehicle
$a(t)$	Acceleration time-history
$a_{k=0\ldots2}$	Linear constant coefficients for the numerator of the difference equation
$b_{k=1\ldots2}$	Linear constant coefficients for the denominator of the difference equation
c_1	Damper coefficient of the vehicle's frontal structure

c_2	Damper coefficient of the vehicle's rear structure
c_e	Equivalent Damping coefficient
C_{mo}	Maximum occupant travel
C_m	Dynamic crush
c_{nl}	Nonlinear damper
CG_x	Longitudinal location
CG_y	Lateral location
CG_z	Vertical location
$d(t)$	Displacement time-history
$Den(s)$	Denominator of a transfer function
E_{est}	Estimated acceleration
E_{exp}	Experimental acceleration
E_r	Error between the estimated and the measured accelerations
E_{st}	Estimated variables
E_{xp}	Experimental variables
k_1	Spring stiffness of the vehicle's frontal structure
k_2	Spring stiffness of the vehicle's rear structure
k_e	Equivalent Spring stiffness
k_{nl}	Nonlinear springs
M_1	Mass of bullet vehicle
M_2	Mass of target vehicle
M_e	Effective mass
M_o	Mass of occupant
M_v	Mass of vehicle
N	The number of samples in the measured data
$Num(s)$	Numerator of a transfer function
p	Unknown parameter
q_1	Position of chassis

q_2	Position of passenger compartment
R_i	Residuals or squared deviations
r_1	Mass 1 reduction factor
r_2	Mass 2 reduction factor
$T_e(s)$	Transfer function from experimental data
$T_{model}(s)$	Transfer function of the model
t_m	Time at dynamic crush
$v(t)$	Velocity time-history
V_0	Initial velocity
V_r	Rebound velocity
$X(z)$	Input sampled signal
x_o	Displacement of occupant
x_v	Displacement of vehicle
$Y(z)$	Output sampled signal
y_i	Experimental variable

Abstract

A full-scale crash test is conventionally used for vehicle crashworthiness analysis. However, this approach is expensive and time-consuming. Vehicle crash reconstructions using different numerical modelling approaches can predict vehicle behavior and reduce the need for multiple full-scale crash tests, thus research on the crash reconstruction has received a great attention in the last few decades. Among modelling approaches, lumped parameters models (LPM) and finite element models (FEM) are commonly used in the vehicle crash reconstruction. This thesis focuses on developing and improving the LPM for vehicle frontal crash analysis. The study aims at reconstructing crash scenarios for vehicle-to-barrier (VTB), vehicle-occupant (V-Occ), and vehicle-to-vehicle (VTV), respectively.

In this study, a single mass-spring-damper (MSD) is used to simulate a vehicle to-barrier or a wall. A double MSD is used to model the response of the chassis and passenger compartment in a frontal crash, a vehicle-occupant, and a vehicle-to-vehicle, respectively. A curve fitting, state-space, and genetic algorithm are used to estimate parameters of the model for reconstructing the vehicle crash kinematics. Further, the piecewise LPM is developed to mimic the crash characteristics for VTB, VO, and VTV crash scenarios, and its predictive capability is compared with the explicit FEM. Within the framework, the advantages of the proposed methods are explained in detail, and suggested solutions are presented to address the limitations in the study.

PART I

Introductory chapters

Chapter 1

Introduction

1.1 Background

Car accidents contribute significantly to the rate of mortality in the modern world. To reduce this rate, vehicle manufacturers usually perform crash tests on a sample of vehicles to analyse the impact of the crashes, and make sure that the final products meet the requirements of safety standards. For this reason, vehicle crashworthiness analysis is a significant problem to be addressed.

Traditionally, vehicle crash analysis relies on physical crash tests, which are subdivided into (1) component crash test (CCT) and (2) full-scale crash test (FSCT). The former is usually carried out on an isolated component subjected to dynamic or static loading, while the latter is a collision of a guided vehicle, being accelerated into a barrier or another vehicle at a predetermined initial velocity. To assess the vehicle crashworthiness, there exist crash test programs responsible for setting up the standard test procedures to be followed. Among others, there are the New Car Assessment Program (NCAP), a department of the National Highway Traffic Safety and Administration (NHTSA) [1], and the Insurance Institute for Highway Safety (IIHS) [2]. According to the NHTSA, the main objective of the crash test is to assess how a vehicle would protect the occupant during a crash event [3]. Car producers incorporate safety devices into the design of their vehicles for assessing the crashworthiness performance.

Although FSCT is a useful technique to assess crashworthiness, it is costly because it requires expensive infrastructure and highly qualified personnel to conduct such a test. Analytical or numerical approaches are utilized to assess the vehicle crashworthiness before FSCT. The earliest method used for crashworthiness assessment is the lumped parameter model (LPM) but nowadays, because of rapid devel-

opment in computer-aided software, the LPM is out-performed by the explicit finite element model (FEM).

The frontal structure of the vehicle plays an important role in vehicle crashworthiness because it is the most affected part during a frontal crash event. The frontal structures of modern vehicles are generally designed with deformable zones, which can absorb the kinetic energy during a crash. The structural cage surrounding the occupant should be robust enough so that it does not crumple around the occupant. During a collision, the occupant is subjected to inertia forces that can result in a severe injury. When a vehicle crashes against a rigid barrier or another vehicle, reaction forces causing the vehicle to stop suddenly are generated. A crashworthy vehicle structure should be able to absorb the kinetic energy from a sudden crash event. The frontal structure of a lightweight vehicle is mainly composed of: bumper, crash boxes, longitudinal beams, sub-frames, and upper rails. These parts should be deformed plastically during a crash scenario and withstand the impact forces as indicated by arrows on the three load paths in Figure 1.1. In most frontal crashes, the crash boxes absorb more than 50 % of the total energy [4]. The passenger compartment, framed by A-pillar and B-pillar, roof, firewall, sill beams, and floor panel, should be rigidly assembled. When designing a vehicle for crashworthiness, the firewall should be strong enough so that it can prevent any intrusion into the passenger compartment. Hence, the firewall ensures enough survival space for the occupant. Nowadays, the physical structures of vehicles are manufactured mainly of steel panels of different tensile strengths, being connected using various fastening techniques [5]. For example, A and B-pillars are made from high to ultra-high-strength steel alloys with a yield strength from 800 to 1000 MPa [6–8] while the crash boxes are made from low to medium strength materials that can easily absorb the kinetic energy [9]. Based on the capabilities of the crash box to absorb the kinetic energy, a vehicle can be modeled as a mass-spring-damper system, because spring and damper are energy absorbing elements.

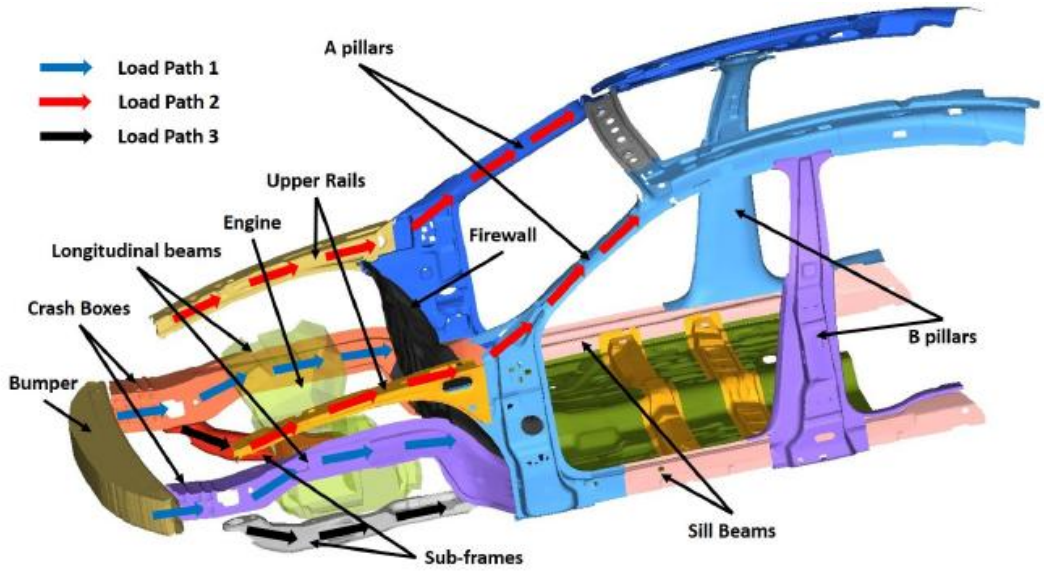

Figure 1.1: Modern vehicle structure with load paths [4].

1.2 Research Motivation

With the advancement in computer simulation software, all car manufacturers today incorporate the explicit finite element model (FEM) into the car design process. The FEM became the most common technique for crash simulation and crashworthiness analysis.

However, the finite element models (FEM) are a double-edged sword. On one hand, these models can provide detailed information about vehicle behavior during the crash event. On the other hand, the price of this detailed information is the overall complexity of the model. This complexity leads to long computational time and, more importantly, a high amount of man-hours put into assembling and debugging a model for vehicle crash simulation. The former is easily handled by the availability of powerful computers, while the latter severely limits the possibility of using the finite element models for vehicle crash reconstruction and crashworthiness research. The amount of man-hours required to assemble a finite element model of a vehicle is often beyond a single researcher's capacity. This is reserved for large research and development centers. Simple mathematical models for vehicle crash reconstruction are less informative than FEM, but they still might be able to provide relevant information about the vehicle crashworthiness. Therefore, it is important to investigate various techniques used for vehicle crash reconstruction to gain deeper knowledge of the applicability of each technique. The motivations of this thesis are

summarized in the following research questions:

- Can a double mass-spring-damper system mimic the responses of the chassis and passenger compartment in a vehicle frontal crash? If yes, is it possible to estimate the responses of the chassis and passenger compartment from only one acceleration measurement? The capabilities of curve-fitting (CF), eigen-system realization (ERA), and the state space (SS) approaches for estimating the parameters of the proposed model are investigated to address the above questions.

- When it comes to vehicle-occupant crash analysis, full-scale crash would be quite expensive because of the extra cost of dummies. Therefore, to reduce the overall cost, FEM or LPM may be used to simulate the vehicle–occupant frontal crash and validate the model results with the actual crash test. Does an LPM have the capabilities to simulate a vehicle-occupant during a frontal crash scenario? This challenge can be investigated with the help of a double-mass-spring-damper system.

- When a full-scale crash test is conducted for a vehicle-to-vehicle crash configuration, the cost will be doubled because of two vehicles being involved in the crash event. Which efficient and accurate approach could cut down the cost and mimic a vehicle-to-vehicle crash without performing a FSCT? An LPM is investigated for addressing this research question.

- It is well known that FEM has the predictive capability to analyse vehicle crash but it has its significant draw backs. Can LPM predict the crashworthiness parameters in a similar manner as the well established FEM? This can be confirmed by comparing the two approaches.

- Which optimization algorithm could estimate the physical structure characteristics of a vehicle during a frontal crash? This could help car designer to use simple models in the earlier design phase without relying only on the complicated and expensive approaches.

1.3 State of the Art

In vehicle crash analysis, as it is for other dynamical systems, parameters estimation is the most challenging step. In many cases, laws of physics are used to obtain a model of the system. However, in some situations, including crash events, laws

of physics cannot provide sufficient insight into the specific behavior of a physical system. Hence, the model has to be tuned using information from experimental data. This leads to a research area referred to as system identification [10]. Figure 1.2 shows a typical flowchart of a system identification procedure.

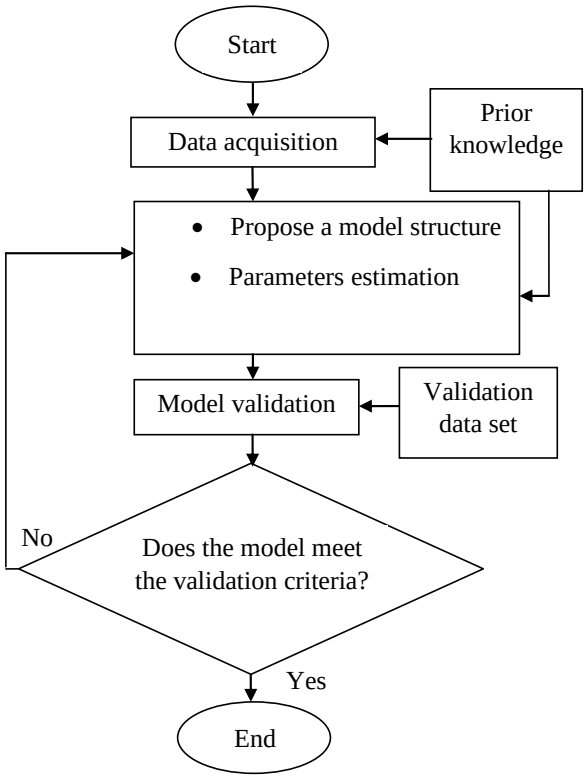

Figure 1.2: System identification flowchart. [11]

In general, the system identification can be subdivided into the theoretical and experimental modelling.

Theoretical modelling: The physical knowledge about the system, is employed to obtain a model consisting of differential or algebraic equations among physical parameters. When a model is identified based purely on physical knowledge of the system, the approach is termed as white box identification [11]. FEM and LPM belong to this type of system identification.

Experimental modelling: Measurements of several variables of a dynamical system are taken and a model is constructed by identifying a model that matches the measured variables. The situation that a model is identified from experimental data, and without taking particular account of the physical parameters of the system, is referred to as black box system identification [11]. Data-based models, Artificial Neural Networks and Fuzzy logic are typical examples of this category of system

identification.

System identification algorithms (SIA) have been developed for different applications. Examples of SIA include: State-space identification, eigensystem realization algorithm (ERA) and data-based regressive model approaches. Typical examples of using SIA can be found in literature [12–15].

Gandhi and Hu in [16], made a significant contribution to the data-based approach in modelling vehicle crash. In their work, the authors reconstructed the vehicle crash by developing analytical model directly from crash test measurement using system identification approach. The analytical model was in two parts: (1) a differential equation consisting of a mass, a spring and a damper, and (2) the transfer function consisting of the autoregressive moving average (ARMA) structure. In [17–21], much work was conducted for reconstructing the vehicle crash using the data-based modelling techniques with linear parameters, varying autoregressive moving average with exogeneous input (ARMAX), and ARMA structures.

1.3.1 Vehicle crash modelling by a double LPM using curve-fitting and state space approaches

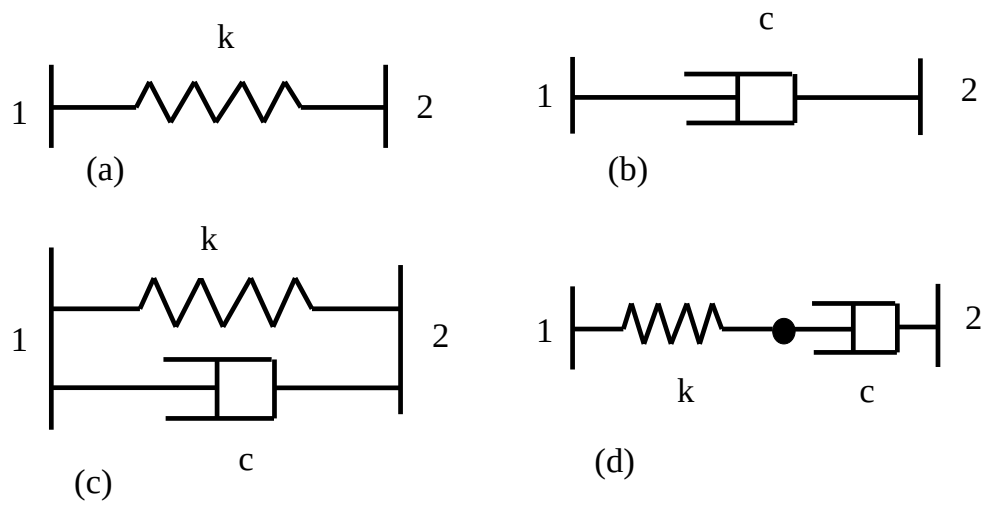

Figure 1.3: Schematic representation of energy absorbing elements (a) Spring, (b) Damper, (c) Kelvin, and (d) Maxwell elements [22].

Constructing mathematical models of dynamical systems based on measured input-output data is very challenging in an accident reconstruction. In case of a vehicle crash, a system identification algorithm using lumped parameter models

(LPM) or mass-spring-damper systems, consists of retrieving the unknown parameters such as the spring stiffness and damping coefficient. A possible approach is to identify these parameters directly from experimental dynamical data.

LPM have been utilized in crashworthiness analysis since the early 1970s. These models are extensively used in the field of vehicle crashworthiness due to the advantage of reducing computational burdens of FEM. Figure 1.3 shows the symbolic representations for the energy absorbing elements commonly used to represent an LPM [22].

Pawlus et al. [23–25] developed several mathematical models based on the mass-spring-damper system. In [23], the authors developed a mathematical model of a vehicle crash based on elastoplastic unloading scenarios of spring-mass models. In [24], the authors used a double mass-spring-damper system to simulate a vehicle into a barrier, while in [25], the authors proposed a model being suitable for localized collisions simulation.

Another method most used for extracting model parameters is the eigensystem realization algorithm (ERA). It is a system identification approach used mostly in civil engineering, particularly in structural health monitoring (Junfeng et al. [26], Li et al. [27], Angelis et al. [28] to name a few). This technique consists of generating a system realization using the time domain response (multi input-output data). The theory of ERA can be found in Juang et al. [29–31]. Juang and Pappa [31] developed an ERA to extract the natural frequencies and damping ratios of a dynamical system. Yang and Yeh [32] determined the model parameters of vibrating structures from experimental data. The authors used the ERA to identify the system matrices of the structure from displacement and excitation forces. Guida et al [33] used a state space system identification approach to identify the parameters of a two degrees of freedom mechanical system. The identification process was based on the ERA to extract the model's parameters where the algorithm was tested on a light-damped mechanical linear apparatus. Brownjohn in [34] used an ERA to study the performance of a building under wind and seismic loads. The application of ERA for vehicle crashworthiness analysis is missing from the current state of the art. In this framework, it is thus useful to apply this concept to vehicle crash analysis.

Another time-domain based method used for system identification is the state space (SS) approach, which has been used in different fields. Minh Quach et al. in [35] used the SS approach in modelling a biological network. Ali Emadi in [36] used a SS approach for modelling and analyzing multi-converter DC power electronic systems. Marzbanrad and Pahlavani in [37, 38] used a system identification

algorithm to identify the parameters of a vehicle lumped parameter model in frontal crash analysis.The authors developed the state space model from the dynamic equation of a five degrees of freedom system for a vehicle frontal crash.

The computational burden in the eigensystem realization and curve-fitting (CF) techniques for vehicle crash is challenging, requiring a better approach. Since it was found that the SS approach was effective in many fields, it can be utilized to reduce the burden of the ERA and CF in vehicle crash reconstruction.

1.3.2 Mathematical model for vehicle-occupant frontal crash

In modern society, traffic road accidents are one of the leading causes of mortality or disability. To address this issue, vehicle manufacturers have tried to incorporate a wide range of safety devices and features into their vehicles. The common safety devices include airbags, energy-absorbing steering columns, side door beams, etc. To evaluate the effectiveness of these protective devices would require investigating the dynamic response of the human body in a traffic accident scenario, which is hard to analyse.

Finite element model (FEM) is the most used approach to model the effect of vehicle-occupant during a crash scenario because of the advancements in computer-aided software. Dummies are used in FEM of vehicle-occupant in a crash event to mimic the occupant behavior [39]. Yehia A, and Abdel-Nasser [40] used a FEM developed with ABAQUS model to simulate a vehicle frontal crash against lighting columns. FEM required detailed dimensions and proper material parameters as a general description of the model design, starting from meshing up to model validation.

Different methods have been attempted to simulate a vehicle-occupant in crash events without using the finite element analysis. Tso et al. [41] analysed the dynamic response of vehicle-occupant in frontal crash using a multi-body dynamics method. The authors assessed the injuries sustained to the occupant's head, chest and pelvic regions, respectively. Sousa et al. [42] and Carvalho [43], proposed optimization procedures to assist multi-body vehicle model development. The authors devised the topological structure of the multi-body system representing the structure of a vehicle and described the most relevant mechanisms of deformation. Alnaqi et al. [44], proposed an approach for controlling the seat belt restraint system force during a frontal crash to reduce thoracic injury. Application of lumped parameters models to simulate vehicle-occupant frontal crashes is limited and hard to find in literature.

1.3.3 Optimization of vehicle frontal crash model based on measured data

In the last few decades, much effort has been made in the area of vehicle crash reconstruction. Jonsén et al. [45] identified an LPM based on results from crash tests of a Volvo S40. In [46], the authors developed a simple LPM for reconstructing the kinematics behaviour in vehicle-to-vehicle crash. Elmarakbi in [47] used a mass-spring-damper system to investigate and to enhance crashworthiness of vehicle-to-vehicle full and offset frontal collisions.

Some drawbacks of LPMs have been reported in literature. In [48], it was concluded that LPMs were only valid for data used for their creation. Hesham in [49] highlighted that LPMs require prior knowledge of the spring characteristics of the system. It is observed from the current state-of-the-art that many published papers could reconstruct the kinematics of the car crash, but the nonlinear behavior of the deformed vehicles involved in vehicle-to-vehicle crash scenarios was not well taken into consideration. The problem of reconstruction of a piecewise linear model for a vehicle-to-vehicle frontal crash scenario based on the genetic algorithm, has not yet been completely considered in literature.

The pioneer in developing the LPM for vehicle crash analysis is Kamal, who first simulated a frontal car crash at velocities ranging from 0 to 48 km/h [50]. After the Kamal's initiative, many others intensively contributed to the development of LPMs for vehicle crash reconstructions. Huang [22] developed a good number of vehicle crash models based on the LPM, which became an inspired source to many researchers. Pawlus et al. in [24, 48] used the theory from Huang to develop several models based on one mass-spring-damper system. Klausen et al. in [51, 52] introduced a nature-inspired approach (a firefly optimization technique) to optimize the parameters of a single LPM for reconstructing a vehicle crash test. Ofochebe et al.in [53] expanded the Kamal's model to a five degrees of freedom system to study the performance of a frontal vehicle's structure subjected to a full-frontal crash. Ofochebe et al. [54], presented the absorbable energy monitoring scheme (AEMS) by suggesting a new design protocol that attempted to overcome problems associated with the high-order numerical computational models such as the dynamic finite element model. The authors used a two degrees of freedom lumped-mass-spring (LMS) model for evaluating the vehicle structure crashworthiness.

The common challenge for LPM in a vehicle crash reconstruction is to find an accurate method to extract the unknown model parameters from acceleration mea-

surements. Vehicle crash is a complex phenomenon, which is difficult to describe using traditional mathematical models. A SISAME (Structural Impact Simulation And Model Extraction) software developed by NHTSA is dedicated mainly to extract optimal lumped-parameter structural impact models from actual or simulated vehicle crash event data. Typical examples, where SISAME was applied, include the work of Lim [55] and Mentzer et al. [56, 57]. However, difficulties of using SISAME software have limited its application as reported in [58]. FEM is informative, being known as the most used technique for vehicle crash reconstruction. Many researchers have developed the FEM for simulating the crash event and came up with outstanding results. Top records in the development of explicit finite element codes are credited to John Hallquist's work at Lawrence Livermore laboratories when he released the DYNA code in 1976 as reported by Belytschko in [59] and also in the LS-DYNA Keyword user manual [60]. LS-DYNA succeeded in simulating vehicle large deformation for the first time in 1986 and the commercial version was distributed in 1989 for vehicle crashworthiness. Other explicit nonlinear finite element softwares such as RADIOS, HYPER-CRASH, ABAQUS, PAM-CRASH [61], are also reported to perform crash simulation and reconstruct the crash event effectively. An overview of the theoretical background for explicit finite element formulation and an associated code for crash analysis can be found in the manual of particular simulation programs such as LS-DYNA in [62]. The FEM procedures can be found in many textbooks such as *Finite Element Procedure*, by K.J. Bath [63] and *An Introduction to the Finite Element Method*, by J.N.Reddy [64], to name a few. Explicit FEM has been frequently used to calibrate the LPM for simulating vehicle crash effectively. Deb and Srinivas in [65], Ofochebe et al. in [66], Tanlak et al. in [67] applied FEM to simulate crash events. Although FEM outperformed the LPM in many applications, it has significant drawbacks. An explicit finite element model of a vehicle may be complex and hence needs lots of crash simulation cycles, increasing the computation time and cost. The cost and time of finite element model are increased by the extensive representation of the major mechanisms in the crash event. This approach requires powerful computational tools for producing accurate results. Additionally, selecting proper material properties of the colliding vehicle and its surrounding is the biggest challenge of this approach [18, 68]. Evidence from literature showed that the two methods used for vehicle crash reconstruction have their merits and limitations. Although outstanding results for reconstructing the crash using LPMs can be found in literature [24, 45, 48, 51–53, 69], their predictive capabilities have not yet fully exploited. A comparison between the predictive

capability of LPM against the well established FEM would give a better evaluation on the mentioned approaches in the field vehicle crashworthiness.

1.4 Contributions

This thesis presents simplified and accurate lumped parameters models which reconstruct vehicle crash scenarios. The vehicle crash configurations investigated are: vehicle to barrier, vehicle-occupant and vehicle-to-vehicle crashes. The parameters of the model are optimized using the genetic algorithm. Further, the predictive capability of the lumped parameters model (LPM) to reconstruct crash kinematics for a vehicle-to-rigid wall, is compared with that of the FEM. For all configurations, the computation time taken to reconstruct the crash with the LPM was short as compared to that of a FEM. Much efforts have been made to verify if simple LPMs could reconstruct the crash event. It was proved that with the application of appropriate algorithm, it was possible to predict the spring and damper characteristic of the model from the acceleration measurement. Different approaches for vehicle crash reconstruction were investigated. The main contributions of this thesis can be summarized as follows:

- A double spring-mass-damper system was developed to model the real vehicle frontal crash scenario. It was found that a nonlinear least-square curve fitting approach could quickly determine the structural parameters, namely natural frequencies, damping factors, spring stiffness, and damping coefficients of a vehicle from only one acceleration measurement.

- An eigensystem realization algorithm (ERA) was proposed to formulate the state space (SS) matrices of the double mass-spring-damper model from only one acceleration measurement. From the formulated SS, the natural frequencies and damping ratios of the system were extracted.

- A state space (SS) system identification procedure based on the time-domain analysis of input and output signals was presented to model a vehicle frontal crash. It was found that the ratio of the two-mass system influenced the responses (displacement-time histories) of the chassis and passenger compartment, respectively. Further, the estimated dynamic crush was closer to the real crash when the mass of the front mass is 2/3 of the total mass of the vehicle. The SS approach could give a better estimation of the dynamic crush

than the curve-fitting approach. The poles of the system have a significant influence on the response of the chassis and passenger compartment.

- A lumped parameter model for reconstructing the kinematic time-histories of both vehicle and occupant was developed in this work. The developed double-mass-spring-damper system could reconstruct the response of both the vehicle and the occupant with high accuracy. Within the framework, linear and nonlinear springs and dampers were combined to develop the studied model, and a genetic algorithm was proposed to accurately estimate the model parameters, namely spring and damping coefficients.

- A mathematical model was proposed to predict the behavior of the vehicle frontal structures during a vehicle-to-vehicle crash, and a piecewise linear LPM was found to be able to estimate both vehicles' frontal structures. The genetic algorithm is proved to be an accurate optimization approach for extracting the model parameters. The proposed algorithm could assist car designers or vehicle manufacturers in reducing the cost of multiple full-scale crash tests.

- This work presents a simple piecewise LPM for vehicle crashworthiness analysis. It was found that the piecewise LPM could greatly assist the modelling of a vehicle crash with a less computational burden as compared to the well established FEM. The parameters of the presented piecewise LPM were accurately estimated by genetic algorithm, allowing predicting the crashworthiness parameters (dynamic crush and acceleration severity index) effectively at different impact velocities. Hence, this approach was proposed for avoiding multiple crash tests. It was found that a good agreement between the developed model and FEM in terms of vehicle crash reconstruction confirms that the LPM was valid even outside the calibration point.

1.5 Thesis outline

This thesis is composed of two parts. Part I comprises four chapters organised as follows: Chapter 1 is a general introduction comprising the motivations of the research, state-of-the-art, and scientific contributions. Next, Chapter 2 provides the methodology and a step-by-step procedure followed to address the research questions mentioned in Chapter 1. Chapter 3 outlines important results from this research and detailed discussions of the findings. Finally, the concluding remarks and further work are provided in Chapter 4. Part II is a collection of publications.

Chapter 2

Research Methodology

This thesis comprises four phases as shown in Figure 2.1. The preliminary work (Phase 0) consists of data acquisition and pre-processing of the measured signals. The data of interest are acceleration signals measured from the center of gravity of the vehicle. Any noise observed from the acceleration measurements is filtered before further analysis. After the filtering process, the acceleration signals are integrated twice for extracting the velocity and displacement responses, respectively. The main parameter for monitoring the impact severity level is the dynamic crush, being determined from the maximum displacement on the displacement-time history curve. After determining the maximum dynamic crush, mathematical models of reconstructing the kinematics time-history are developed and presented in Phase I and II.

Phase I uses crash test data from the University of Agder vehicle crash test database. The response of the front and real parts of the vehicle crashing into barrier are estimated using least-squares curve fitting (LSCF) and state space approaches. The state space model is formulated using the system identification toolbox and the eigensystem realization algorithm (ERA). Initially, the model parameters (spring stiffness and damper coefficients) are assumed as constants during the crash event.

In Phase II, mathematical models for three vehicle crash configurations (vehicle-to-barrier, vehicle-occupant and vehicle-to-vehicle crashes) are developed. The frontal structure of the vehicle is modeled by piecewise linear lumped parameters, which are expressed as functions of displacement and velocity, respectively. Then a genetic algorithm (GA) is applied to estimate and optimize the model's parameters.

Phase III presents a verification of the LPM against a finite element model (FEM) and a full-scale crash test (FSCT) at various impact velocities. This verification is only performed for a vehicle-to-rigid wall.

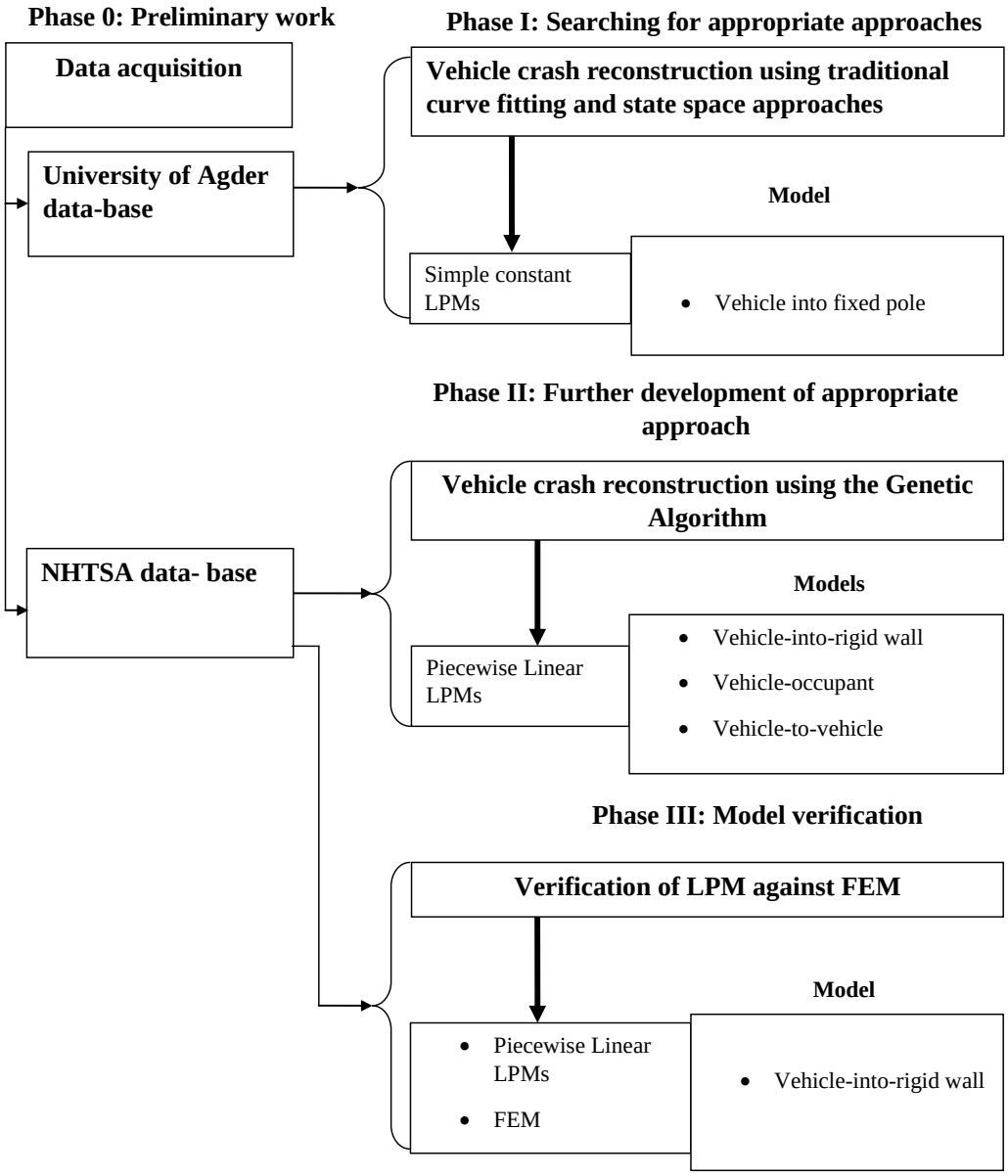

Figure 2.1: Flowchart summarizing the thesis structure.

2.1 Crash tests data acquisition and pre-processing

Two sources of data, one from the University of Agder [70] and the other from the National Highway Traffic and Administration (NHTSA) open database [71], were used to verify the mathematical models proposed in this thesis.

2.1.1 University of Agder crash test data-base

Two sets of data, raw and filtered acceleration signals, for vehicle frontal crash into a fixed pole, were obtained from the research center at the University of Agder, under the initiative of professor Kjell G. Robbersmyr [70]. The raw data were filtered according to the International Standard, ISO 6487 [72]. The following instruments were used to collect the data: 1) A 3-D accelerometer, 2) a gyroscope, 3) and an inductive vehicle speed monitor. The accelerometer was a piezoresistive tri-axial sensor with an accelerometer range of ± 1500 g. This accelerometer was mounted on a steel bracket at the center of gravity (COG) of the vehicle. Screws fastened the bracket to the vehicle's chassis. The acceleration measurements in longitudinal (X), lateral (Y), and vertical (Z) directions were taken from the COG of the vehicle. The yaw rate was measured using a gyroscope at a rate of $1°/ms$. The location of the COG was determined by weighing the vehicle in different positions using four load cells. The dimensions of the tested vehicle are listed in Table 2.1, being illustrated in Figure 2.2 with all dimensions in meters [m].

Table 2.1: **Relevant Vehicle's Dimensions [m]**

Width	Height	Frontal overhang	Wheel track: front axle
1.58	1.39	0.66	1.38
Length	Wheel base	Rear overhang	Wheel track: rear axle
3.64	2.28	0.70	1.34

The locations of the vehicle's COG in longitudinal, lateral, and vertical directions are calculated as follows [73]:
Longitudinal location: the horizontal distance between COG and centerline of the front axle:

$$CG_x = \left(\frac{m_3 + m_4}{m_v} \right) \cdot l \tag{2.1}$$

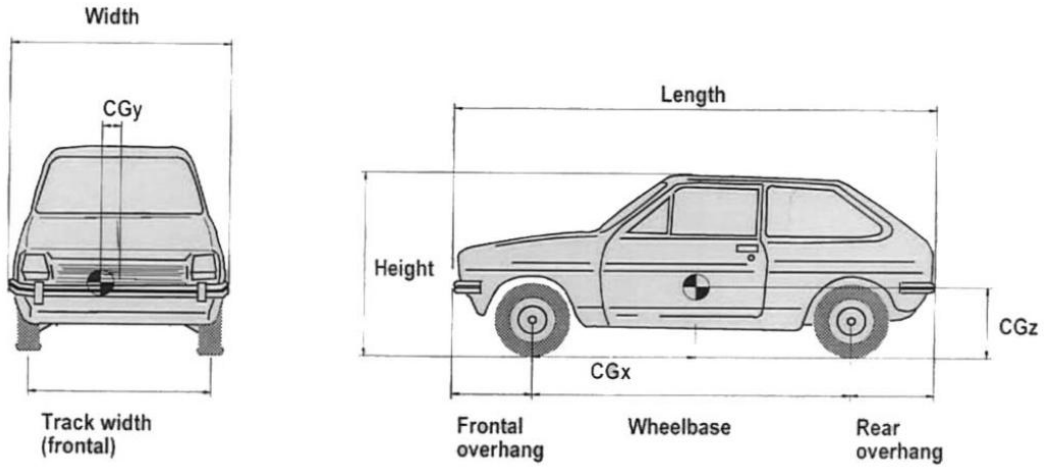

Figure 2.2: Characteristic dimensions of the tested vehicle [73].

Lateral location: the horizontal distance between the COG and the longitudinal median plane of the vehicle:

$$CG_y = \left(\frac{m_1 + m_3 - (m_2 + m_4)}{m_v} \right) \cdot \frac{d}{2} \tag{2.2}$$

Vertical location: location of COG above a plane through the wheel centers

$$CG_z = \left(\frac{m_1 + m_2 - m_f}{m_v \tan\theta} \right) \cdot l \tag{2.3}$$

where

- m_1 = 257 kg: mass of the front left wheel,
- m_2 = 237 kg: mass of the front right wheel,
- m_3 = 154 kg: mass of the rear left wheel,
- m_4 = 150 kg : mass of the rear right wheel,
- m_v = 798 kg: total mass of the vehicle,
- m_f = 444 kg: front mass in the tilted position,
- m_b = 354 kg: rear mass in the tilted position,
- θ = 28.4°: tilted angle,
- l = 2.28 m: wheelbase,

- d = 1.73 m: distance across the median plane between the vertical slings from the lift brackets at the wheel centers and the load cells.

Substituting the above values in Equations 2.1 to 2.3 results in $CG_x = 1.0971\ m$, $CG_y = 0.0260\ m$, $CG_z = 0.3337\ m$.

Data from the accelerometer were fed to an eight-channel data logger having a sampling rate of 10 kHz [73]. The initial velocity of the vehicle was 35 km/h, and its mass (including instrumentation) was 873 kg. The sequence of a vehicle undergoing the deformation is shown in Figure 2.3 and the kinematic time-histories for both the raw and filtered acceleration signals are shown in Figure 2.4.

The challenge was that the data from the University of Agder did not contain all specific information required for the completion of this work. For example, no data for the vehicle-to-vehicle crash was available from the University of Agder database. Hence, another set of data was useful for model calibration and verification.

(a) (b)

Figure 2.3: A full-scale frontal crash test of a standard Ford Fiesta 1.1 L 1987 model at 35 km/h, (a) Test vehicle during impact (b) Test vehicle after impact [70].

The filtered acceleration was first imported and processed into MATLAB, then the dynamic crush was obtained by double integrating the acceleration signal. The maximum dynamic crush is the pick on the displacement-time history, where the relative velocity approaches zero. When the acceleration tends to zero, the vehicle rebounds and gets separated from the barrier. From Figure 2.4b, the maximum dynamic crush, the time of dynamic crush, and the rebound velocity are 50.63 cm, 0.0748 s, and 2.7 km/h, respectively.

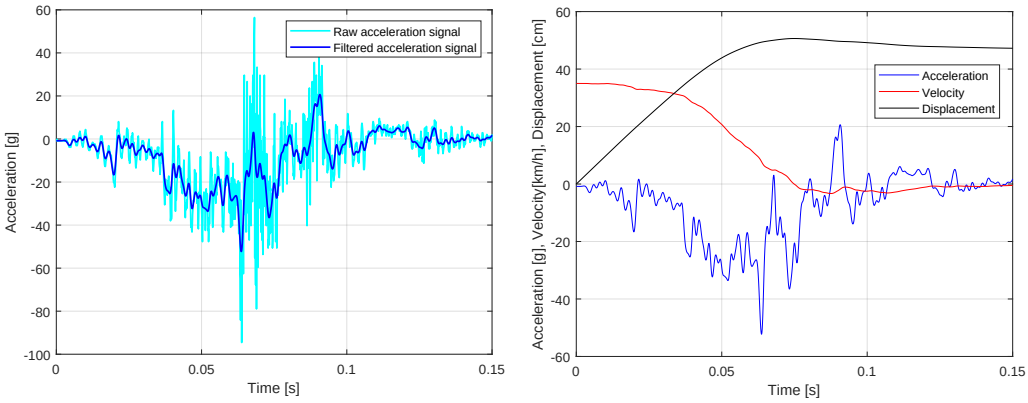

(a) (b)

Figure 2.4: Data post-processing for vehicle into barrier (a) Noizy and filtered acceleration. (b) Kinematics time-histories after filtering.

2.1.2 NHTSA crash test data-base

The new data set was obtained from the National Highway Traffic and Safety Administration (NHTSA) database. A set of crash test data (acceleration signals) for the vehicle into a barrier, vehicle-occupant, and vehicle-to-vehicle, was collected. It was challenging to interpret the data since they contained noises of high-frequency components. The noise signals cause imperfect representation in the data. Therefore, the data had to be filtered before a further analysis. Filtering is the most important step in the processing of crash signal. The American Society of Automotive Engineers' standard, SAE J211-1:1995 [74] and the International Standard, ISO 6487 designate four chanel frequency classes (CFC) of filters for crash data processing, which are abbreviated as CFC 60, 180, 600, and 1000.

CFC filters are derived from analog Butterworth filters that have the cut off frequency of $\frac{CFC}{0.6}$ [75]. The CFC 60 and 180 are mainly used to filter vehicle structural accelerations integrated for velocity or displacement. CFC 600 is used for a component analysis, while CFC 1000 is used for head accelerations.

In this work, a CFC 180, 4^{th} order Butterworth low pass filter with a sampling rate of 10 kHz was used to filter the acceleration signals following the mentioned standard. The noise signal was eliminated from the useful acceleration signal. This was achieved by filtering the acceleration signal twice using the difference equation. Let $X[t]$ be the input sampled at intervals of T seconds in the sequence of the unfiltered digital signal, and $Y[t]$ the corresponding sample in the filtered output signal. A general transfer function of an N^{th} order digital Butterworth filter, in z domain, between the output and input signal is expressed as

$$H(z) = \frac{Y(z)}{X(z)} = \frac{\sum_{k=0}^{M} a_k z^{-k}}{1 - \sum_{k=1}^{N} b_k z^{-k}}, \quad N \geq M. \tag{2.4}$$

For the 2^{nd} order Butterworth filter, the transfer function becomes

$$\frac{Y(z)}{X(z)} = \frac{a_0 + a_1 z^{-1} + a_2 z^{-2}}{1 - (b_1 z^{-1} + b_2 z^{-2})}, \tag{2.5}$$

Equation 2.5 can be converted into a linear constant-coefficient difference equation (LCCDE) via the z-transform as follows

$$Y[z] = a_0 X[z] + a_1 X[z^{-1}] + a_2 X[z^{-2}] + b_1 Y[z^{-1}] + b_2 Y[z^{-2}]. \tag{2.6}$$

The block diagram of a Butterworth low pass filter is illustrated in Figure 2.5. Converting Equation (2.6) to the discrete form by replacing (z) with (t) yields an

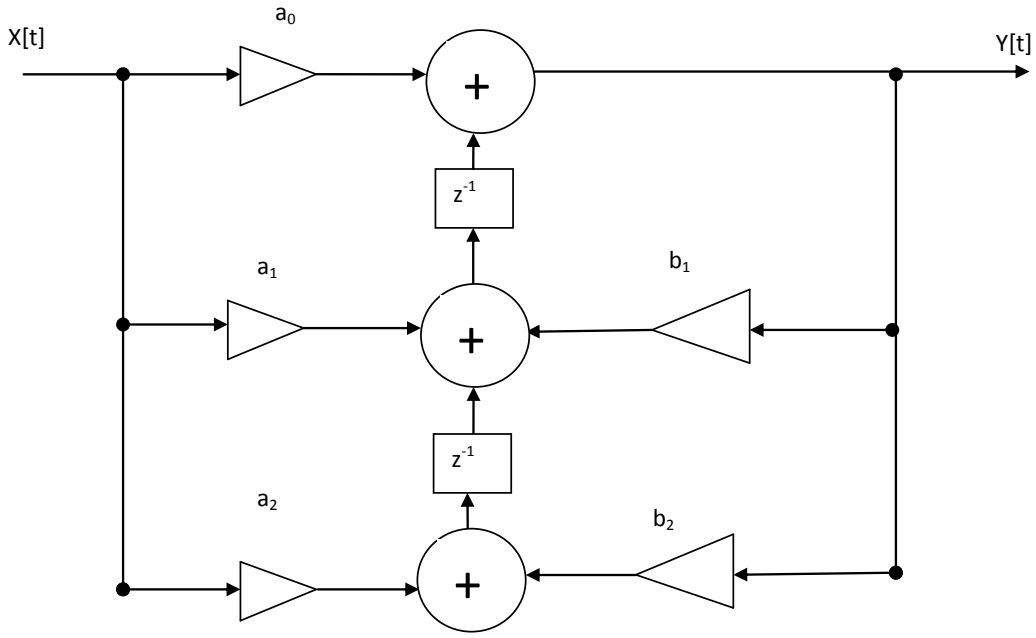

Figure 2.5: Second order Butterworth low pass filter block diagram.

output equation:

$$Y[t] = a_0 X[t] + a_1 X[t-1] + a_2 X[t-2] + b_1 Y[t-1] + b_2 Y[t-2], \tag{2.7}$$

where:

- $X[t] = X[z]$ is the current filter input,
- $X[t-1] = X[z^{-1}]$ is the previous one sample old the filter input,
- $X[t-2] = X[z^{-2}]$ is the previous two samples old filter input,
- $Y[t] = Y[z]$ is the current filter output,
- $Y[t-1] = Y[z^{-1}]$ is the previous one sample old filter output,
- $Y[t-2] = Y[z^{-2}]$ is the previous two samples old filter output,
- t is the sampling instant in time,
- a_0, a_1, a_2, b_1, b_2 are the coefficients of the 2^{nd} order Butterworth low-pass filter and are dependent on a particular CFC.

The goal of a filter design is to find the coefficients a_k and b_k such that the filter meets specific characteristics. The digital filter algorithm in Equation 2.7 is the 2^{nd} order Butterworth filter, which may introduce a phase shift in the output signal. To avoid phase shifts in the filtered signal, the 4^{th} order filter is designed such that the signal passes through the 2^{nd} order filter twice (i.e.once forward and once backward). According to the society of automotive engineers (SAE J211-1) standard, the constants in Equation 2.7 are defined as follows [74]:

$$a_0 = \frac{\omega_a^2}{1+\sqrt{2}\omega_a+\omega_a^2}, \qquad a_1 = 2a_0, \qquad a_2 = a_0$$
$$b_1 = \frac{-2(\omega_a^2-1)}{1-\sqrt{2}\omega_a+\omega_a^2}, \qquad b_2 = \frac{-1+\sqrt{2}\omega_a-\omega_a^2}{1+\sqrt{2}\omega_a+\omega_a^2}$$

where

$$\omega_a = \tan\left(\frac{\omega_d T}{2}\right), \qquad \omega_d = 2\pi\left(\frac{CFC}{0.6}\right)1.25$$

and T is the sample period in seconds and $\frac{CFC}{0.6}$ is the cut-off frequency of the Butterworth filter. A CFC180 was chosen for filtering the noisy signal and a zero-phase filtering was implemented using the following MATLAB routine

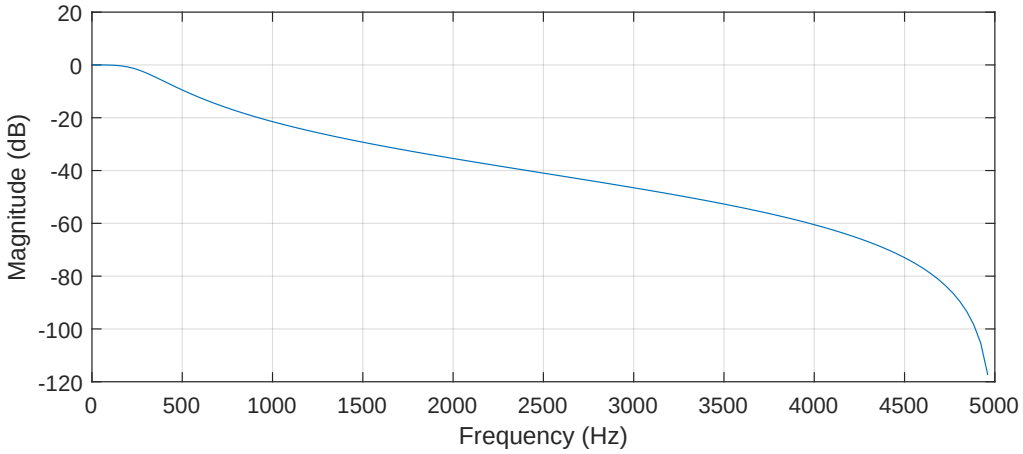

Figure 2.6: Frequency response for CFC180 Butterwoth low pass filter.

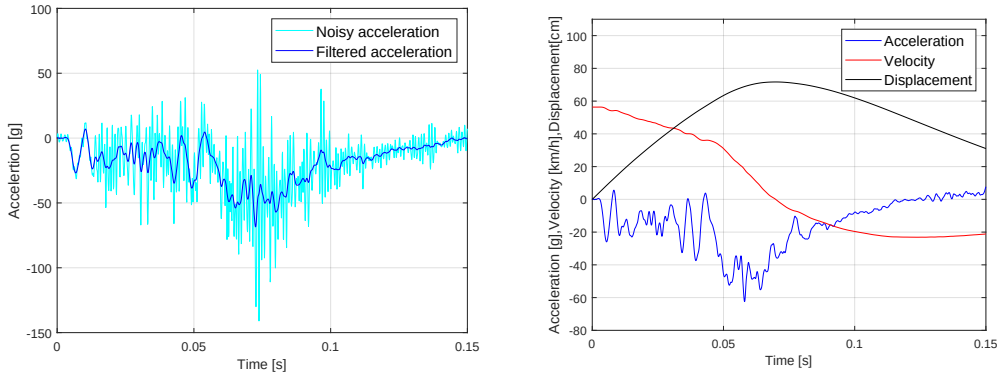

(a) (b)

Figure 2.7: Data pre-processing for vehicle into barrier (data from the NHTSA) (a) Noizy and filtered acceleration. (b) Kinematics time-histories after filtering.

$$Y = filtfilt(b, a, X) \tag{2.8}$$

where $a = [a_0, a_1, a_2]$ and $b = [1, -b_1, -b_2]$. Equation 2.8 performs a zero-phase digital filtering by processing the input data, X, in both the forward and reverse directions. After filtering the data in the forward direction, $filtfilt$ reverses the filtered sequence and runs it back through the filter. The characteristics of the designed filter is shown in Figure 2.6.

In crash dynamics, one is often concerned with the magnitude and duration of the acceleration signal at a low frequency that will be input into the passenger through the structure to the seat. Consequently, the high-frequency component is now of little interest [76].

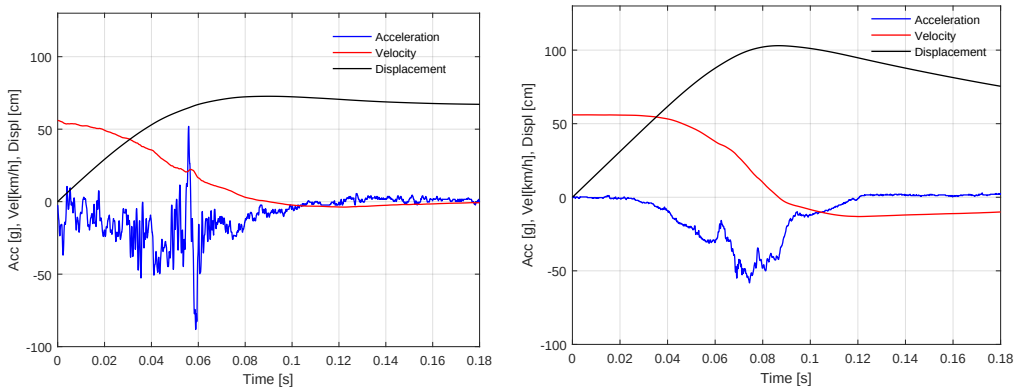

(a) (b)

Figure 2.8: Filtered kinematics time-histories for vehicle-occupant crash (a) Vehicle, (b) Occupant

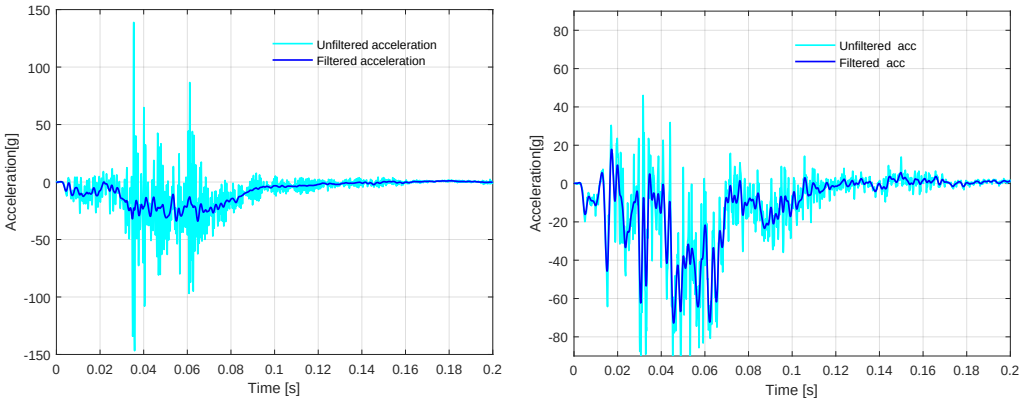

(a) (b)

Figure 2.9: Data pre-processing for vehicle-to-vehicle (data from the NHTSA) (a) Bullet vehicle. (b) Target vehicle.

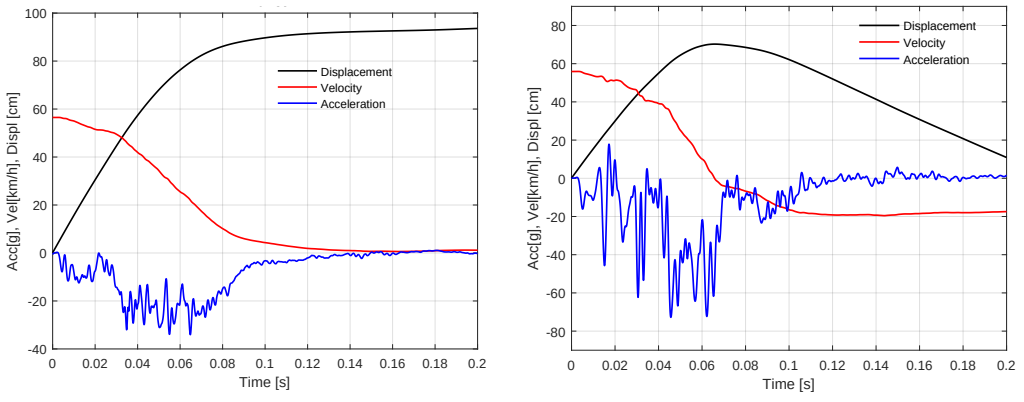

(a) (b)

Figure 2.10: Filtered kinematics time-histories for vehicle-to-vehicle crash (a) Bullet vehicle. (b) Target vehicle.

The unfiltered and filtered acceleration signals, for vehicle-to-barrier, vehicle-occupant, and vehicle-to-vehicle (Bullet and Target vehicles) are shown in Figures 2.7 to 2.10. The filtered data were then used for verification of the mathematical models developed in this thesis as reflected in the published papers.

2.2 Approaches to reconstruct the crash pulse

A crash pulse signal of interest is the acceleration measurement from the center of gravity of the vehicle. The model described in Papers A and B is a lumped parameter model (LPM) composed of the double mass-spring-damper system, as shown in Figure 2.11. This model was used to estimate the response of the chassis and that of the passenger compartment. The nonlinear least-squares curve fitting (LSCF) algorithm, the eigensystem realization algorithm (ERA) and the state space (SS) approach were applied to estimate the parameters of a vehicle frontal crash model.

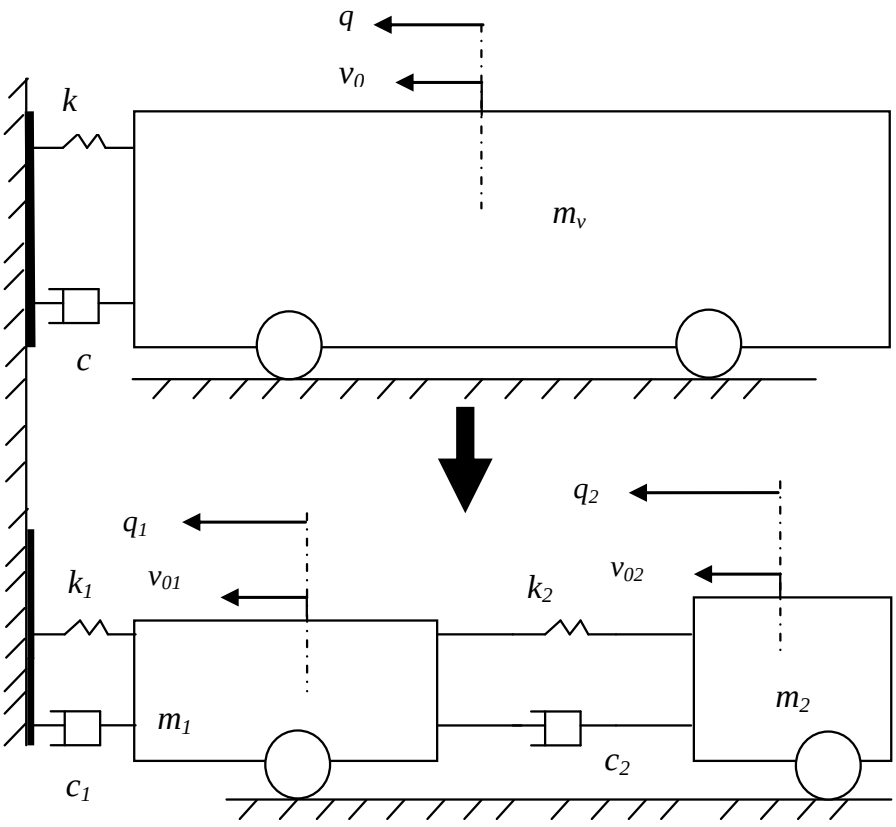

Figure 2.11: A double mass-spring-damper model of a vehicle frontal crash.

2.2.1 Nonlinear least squares curve fitting approach

A nonlinear least squares curve fitting (LSCF) problem is a minimization of an error between the model and experimental observation. Having a set of n experimental data points (t_i, y_i) $(i = 1, 2, \ldots, n)$, and a function $f(t; \mathbf{p})$, $\mathbf{p} = (p_1, p_2, \ldots, p_m)$, with $m \leq n$, the LSCF consists of finding the vector $\mathbf{p}$, such that $f(t; \mathbf{p})$ fits the experimental data.

To optimize the parameters ($\mathbf{p}$) of the model, the fitting error defined as the sum of squared deviations (residuals, R_i) should be minimized. The residuals R_i are defined in the following equation

$$R_i = f(t; \mathbf{p}) - y(t_i), \tag{2.9}$$

and the fitting error (E_r) between the data and $f(t_i, \mathbf{p})$ is

$$E_r = \sum_{i=1}^{n} R_i^2 = \sum_{i=1}^{n} \Big(f(t; \mathbf{p}) - y(t_i) \Big)^2. \tag{2.10}$$

The minimum sum of squares is obtained by setting the gradient or the first derivative of the error to zero. Because the model contains m parameters, there are m gradient equations, i.e

$$\frac{\partial E_r}{\partial p_j} = 0 \implies 2 \sum_{i=1}^{n} \Big(f(t; \mathbf{p}) - y(t_i) \Big) \frac{\partial f(t; \mathbf{p})}{\partial p_j} = 0, (j = 1, 2, \ldots, m) \tag{2.11}$$

where m is the number of parameters to be estimated. Solving Equation 2.11 results in the values of vector $\mathbf{p}$.

The objective of curve fitting is to describe the experimental data by a model function and find the parameters of the model so that it fits the experimental data as accurately as possible. The best-fitting depends on the estimated parameters.

To develop a mathematical model of the crash test data, the data points were first plotted, and subsequently, a model was developed for describing the general trend in the displacement-time history as shown in Figure 2.4b.

The developed model is the second-order system represented by a double mass-spring-damper system in Figure 2.11. The mass of the vehicle is split into two masses, m_1 and m_2. The mass m_1 represents the mass of frame rail (chassis) and the mass m_2 represents the passenger compartment such that the average deceleration of

the two masses is equivalent to that of COG of the vehicle. The decelerations of the two masses in the double mass-spring-damper model are defined in the following equations:

$$\ddot{q}_1 = \frac{1}{m_1}\Big[-(c_1+c_2)\dot{q}_1 - (k_1+k_2)q_1 + c_2\dot{q}_2 + k_2 q_2\Big], \tag{2.12}$$

$$\ddot{q}_2 = \frac{1}{m_2}\Big[c_2\dot{q}_1 - c_2\dot{q}_2 - k_2 q_2 + k_2 q_1\Big], \tag{2.13}$$

where the springs k_1 and k_2, dampers c_1 and c_2 are parameters to be estimated, $\dot{q}_1$ and $\dot{q}_2$, q_1 and q_2 are the velocities and positions of masses m_1 and m_2, respectively. The challenge was to estimate the parameters (k_1, k_2, c_1 and c_2).

2.2.2 Eigensystem realization algorithm

Eigensystem realization algorithm (ERA) is a method developed for identification of model parameters from test data. This algorithm consists of determining the state space representation of a system, (i.e system state matrix **A**, input matrix **B**, and output matrix **C**) by making the Hankel matrix using singular value decomposition [77]. The following are the main steps to implement the ERA as referred to Jer-Nan Juang [78]:

- Assemble the experimental data into a Hankel Matrix,
- Factorization of the Hankel Matrix using singular value decomposition,
- Extract the controllability and observability matrix and calculate the system realization matrix,
- Solve the eigenvalue problem for the system realization matrix,
- Calculate the natural frequencies and the damping factors from the obtained eigenvalues.

In this thesis, the ERA was used to formulate the state space realization model from vehicle crash test data (acceleration signal), then the natural frequencies and the damping factors were extracted. A detailed description of the application of ERA for vehicle crash analysis is presented in Paper A.

2.2.3 State space modelling approach

A state space model of a system is a structured form of a set of the first-order differential equations. The state space formulation of a double mass-spring-damper system for a vehicle to a rigid pole was obtained by reducing the second-order differential equations (2.12) and (2.13) into a system of four first-order differential equations. The state variables (positions and velocities) of the two masses (m_1 and m_2) in Figure 2.11 were defined as follows: $x_1 = q_1, x_2 = \dot{q}_1, x_3 = q_2, x_4 = \dot{q}_2$ and the output variables as positions of m_1 and m_2 are : $y_1 = x_1 = q_1, y_2 = x_3 = q_2$.

$$
\begin{aligned}
\dot{x}_1 &= \dot{q}_1 = x_2, \\
\dot{x}_2 &= \ddot{q}_1 = \frac{1}{m_1}(-(c_1 + c_2)x_2 - (k_1 + k_2)x_1 + c_2 x_4 + k_2 x_3) + \frac{1}{m_1}u, \\
\dot{x}_3 &= \dot{q}_2 = x_4, \\
\dot{x}_4 &= \ddot{q}_2 = \frac{1}{m_2}(c_2 x_2 - c_2 x_4 - k_2 x_3 + k_2 x_1) + \frac{1}{m_2}u.
\end{aligned} \tag{2.14}
$$

The system of the first order equations 2.14 is written in state space form as

$$
\underbrace{\begin{bmatrix} \dot{x_1} \\ \dot{x_2} \\ \dot{x_3} \\ \dot{x_4} \end{bmatrix}}_{\dot{\mathbf{X}}} = \underbrace{\begin{bmatrix} 0 & 1 & 0 & 0 \\ -\frac{k_1+k_2}{m_1} & -\frac{c_1+c_2}{m_1} & \frac{k_2}{m_1} & \frac{c_2}{m_1} \\ 0 & 0 & 0 & 1 \\ \frac{k_2}{m_2} & \frac{c_2}{m_2} & -\frac{k_2}{m_2} & -\frac{c_2}{m_2} \end{bmatrix}}_{\mathbf{A}} \underbrace{\begin{bmatrix} x_1 \\ x_2 \\ x_3 \\ x_4 \end{bmatrix}}_{\mathbf{X}} + \underbrace{\begin{bmatrix} 0 & 0 \\ \frac{1}{m_1} & 0 \\ 0 & 0 \\ 0 & \frac{1}{m_2} \end{bmatrix}}_{\mathbf{B}} u, \tag{2.15}
$$

$$
\underbrace{\begin{bmatrix} y_1 \\ y_2 \end{bmatrix}}_{\mathbf{y}} = \underbrace{\begin{bmatrix} 1 & 0 & 0 & 0 \\ 0 & 0 & 1 & 0 \end{bmatrix}}_{\mathbf{C}} \underbrace{\begin{bmatrix} x_1 \\ x_2 \\ x_3 \\ x_4 \end{bmatrix}}_{\mathbf{X}} + \underbrace{\begin{bmatrix} 0 & 0 \\ 0 & 0 \end{bmatrix}}_{\mathbf{D}} u. \tag{2.16}
$$

where equations (2.15) and (2.16) are the state and output equations, respectively. In a frontal crash, a deformation force equivalent to the inertia of the car is applied to the system. This inertia force is defined as

$$
u = -m \times a_x, \tag{2.17}
$$

where m is the total mass of the vehicle and a_x is the longitudinal acceleration.

The input and output (inertia force(*u*) and acceleration) signals from the crash test were imported into the MATLAB system identification toolbox for being suitable for identification of the model. A state space and transfer function models from the crash test were thereafter estimated using the system identification toolbox. The physical parameters (spring stiffness and damping coefficients) are embedded in the input state matrix **A**.

A transfer function of the LPM, which is derived from the state matrix, is

$$T_{model}(s) = \frac{Num(s)}{Den(s)} \tag{2.18}$$

where

$$\begin{aligned} Num(s) &= c_2 s + k_2 \\ Den(s) &= m_1 m_2 s^4 - (m_1 c_2 + m_2(c_1 + c_2))s^3 + (m_1 k_2 + m_2(k_1 + k_2) + c_1 c_2)s^2 \\ &\quad + (c_1 k_2 + c_2 k_1)s + k_1 k_2, \end{aligned}$$

and the estimated four-pole transfer function from the experimental data is

$$T_e(s) = \frac{-0.0139s + 0.5942}{s^4 + 97s^3 + 3810s^2 + 87170s + 35718}. \tag{2.19}$$

Then by inspection, the unknown parameters are obtained by comparing the denominators of Equations (2.18) and (2.19). A nonlinear system of equations with unknown stiffness and damper coefficients is formed and solved. The estimated parameters (k_1, k_2, c_1, c_2) are finally substituted in the following two dynamical equations of the model

$$\begin{aligned} \ddot{q}_1(i) = \frac{1}{m_1}\big[&- (c_1 + c_2)\dot{q}_1(i)(q_1(i))^{0.5} - (k_1 + k_2)q_1(i) + c_2 \dot{x} q_2(i)(q_2(i))^{0.5} \\ &+ k_2 q_2(i)\big], \end{aligned} \tag{2.20}$$

$$\ddot{q}_2(i) = \frac{1}{m_2}\big[c_2 \dot{q}_1(i)(q_1(i))^{0.5} - c_2 \dot{q}_2(i) q_2(i))^{0.5} - k_2 q_2(i) + k_2 q_1(i)\big], \tag{2.21}$$

where $i = 1 : (length(t) - 1)$, where t is a time vector, whose length equals to that of the acceleration signal in real crash. A detailed discussion of the results from a double mass-spring-damper model using the state space approach is presented in Paper B.

2.3 Further improvement of the developed models

The frontal structure of the car was modeled as piecewise linear spring ($k(x_i)$) and damper ($c(x_i)$) and optimized by a genetic algorithm (GA). An initial population, a guess of parameters, was chosen randomly and substituted in the piecewise spring and damper defined as functions of displacement and velocity, respectively as shown in Figure 2.12, and defined as follows:

$$k(x_i) = \begin{cases} k_{i1} + s_1 x_i & x_i \leq x_{i1}, \\ k_{i2} + s_2(x_i - x_{i1}) & x_{i1} \leq x_i \leq x_{i2}, \\ k_{i3} + s_3(x_i - x_{i2}) & x_{i2} \leq x_i \leq C_i, \end{cases} \tag{2.22}$$

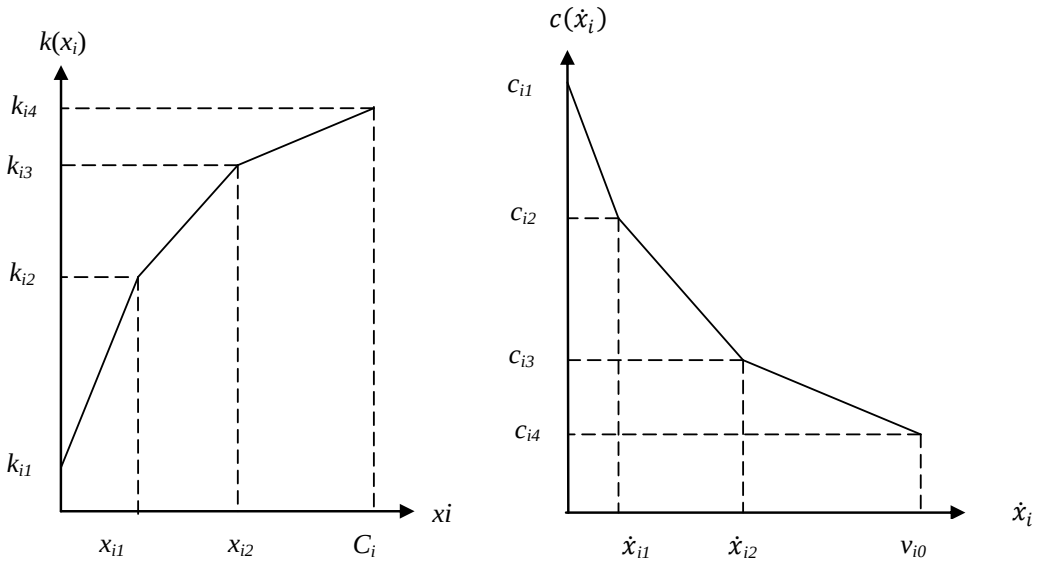

a. Stiffness constant characteristics b. Damper constant characteristics

Figure 2.12: Proposed piecewise lumped parameters characteristics

$$c(\dot{x}_i) = \begin{cases} c_{i1} - d_1 \dot{x}_i & \dot{x}_i \leq \dot{x}_{i1}, \\ c_{i2} - d_2(\dot{x}_i - \dot{x}_{i1}) & \dot{x}_{i1} \leq \dot{x}_i \leq \dot{x}_{i2}, \\ c_{i3} - d_3(\dot{x}_i - \dot{x}_{i2}) & \dot{x}_{i2} \leq \dot{x}_i \leq v_0, \end{cases} \tag{2.23}$$

where the subscript $i = 1, 2$ stand for the 1^{st} and 2^{nd} mass, respectively. C_i is the dynamic crush of the vehicle or occupant maximum displacement, and v_0 is the initial impact velocity. The slopes for spring stiffness and damping coefficients functions are s_i and d_i, respectively. The same piecewise functions, without the subscript i, are used to model the vehicle-to-barrier (Figure 2.13). The equations of motion (EoM) for vehicle-to-barrier, vehicle-occupant, and vehicle-to-vehicle crash models shown in Figures 2.13 to 2.15 were solved using the Newton's second law of motion.

A genetic algorithm was tuning the piecewise lumped parameters until when an optimum solution was obtained. Then the optimum values of stiffness and damping coefficients were substituted into the dynamic equations of the models defined in Subsection 2.3.1 to 2.3.3. The kinematic time-histories from the model results were finally compared with the kinematic time-histories from the crash test.

2.3.1 Vehicle-to-barrier model

The dynamic equation of the model- with linear spring and damper- for a vehicle-to-barrier shown in Figure 2.13 is defined as follows:

$$\ddot{x} = \frac{1}{M}(-c\dot{x} - kx), \tag{2.24}$$

where M, x, and $\dot{x}$ are the mass, displacement, and velocity of the vehicle, respectively. k and c are spring stiffness and damping coefficient of the vehicle's front structure, respectively.

When the nonlinearity of the spring and damper is considered, Equation 2.24 can be rewritten as

$$\ddot{x} = \frac{1}{M}(-c\dot{x} - c_{nl}\dot{x}^3 - kx - k_{nl}x^3), \tag{2.25}$$

where k_{nl} and c_{nl} are the cubic nonlinear components for the spring and damper, respectively.

A classical approach to estimate the linear spring and damper in the model presented in Figure 2.13 is to extract the circular natural frequency and damping factor from the crash test as referred in [22].

Initially, a vehicle crash test was conducted on a typical mid-speed vehicle to pole collision. Based on the response from the test, a piecewise linear lumped parameters model (LPM) was developed and a nature-inspired algorithm was used to

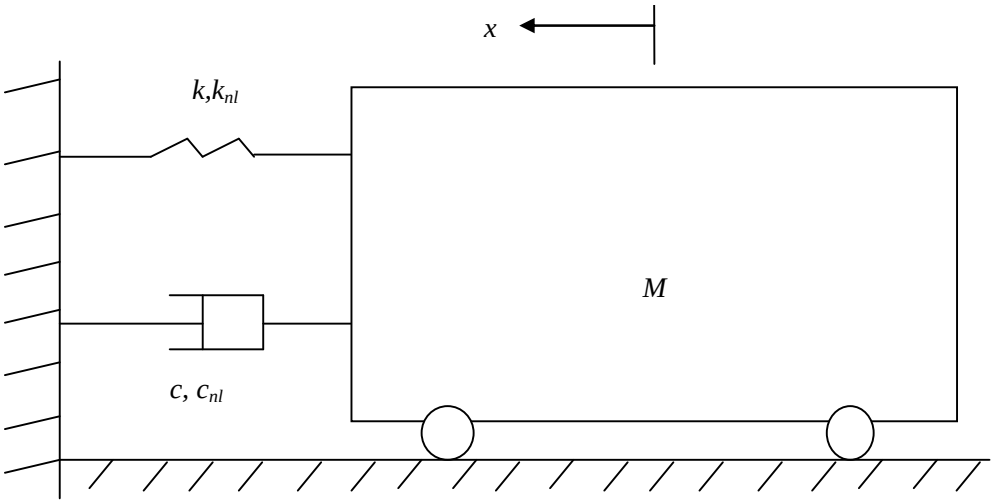

Figure 2.13: Vehicle into barrier model.

optimize the parameters. This algorithm is described later in the text (see Section 2.3.4). Under an assumption that the deforming spring and damping forces - developed at the time of the crash- are piecewise functions in x and $\dot{x}$, respectively. A comparison between the model response and the experimental test results for a vehicle into a fixed pole is shown in Paper E. It was observed that the model results agree with the crash test. The maximum dynamic crushes (maximum displacements), the times at dynamic crush, the rebound velocities for both the model and the crash test are similar. This is a proof of the accuracy of the piecewise linear lumped parameters modelling approach for vehicle frontal crash.

2.3.2 Vehicle-occupant model

The accelerations of the vehicle-occupant model, presented in Figure 2.14, are defined in the following:

$$\ddot{x}_v = \frac{1}{M_v}\Big[- k_o(x_v - x_o - \delta) - c_o(\dot{x_v} - \dot{x_o}) - (k_v x_v + c_v \dot{x}_v)\Big], \tag{2.26}$$

$$\ddot{x}_o = \frac{1}{M_o}\Big[k_o(x_v - x_o - \delta) + c_o(\dot{x_v} - \dot{x_o})\Big], \tag{2.27}$$

for $x_v - x_o \geq \delta$,

where

• $\ddot{x}_v$ and $\ddot{x}_o$, $\dot{x}_v$ and $\dot{x}_o$, x_v and x_o, are accelerations, velocities and displacements

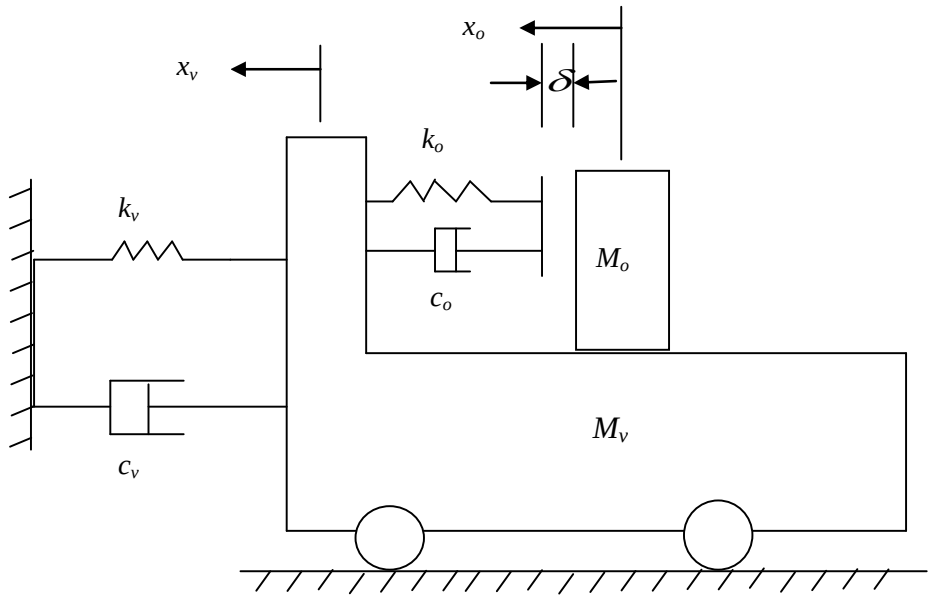

Figure 2.14: Vehicle-occupant model.

of the vehicle and occupant, respectively.

• M_v, k_1 and c_1 represent the mass of the vehicle with energy absorbers (spring k_1 and damper c_1).

• M_o, k_2 and c_2 represent the mass of the occupant with the restraint system (spring k_2 and damper c_2).

• δ is the restraint slack, a clearance distance between the occupant's torso and the restraint system.

Based on the nonlinear characteristics of velocity and displacement of the vehicle and the forward movement of the occupant, the springs and dampers in the model were modeled as piecewise linear functions. The dynamic equations for vehicle-occupant presented as a double-mass-spring-damper model, are defined in Equations 2.26 and 2.27, where k_1 and c_1- are piecewise linear spring stiffness and damper coefficient of the front vehicle structure, respectively. k_2 and c_2 are also the piecewise linear spring stiffness and damper coefficient for the restraint system, respectively.

2.3.3 Vehicle-to-vehicle model

Two sets of Kelvin models present a vehicle-to-vehicle model, a double mass-spring-damper system, as shown in Figure 2.15 where M_1 represents the mass of bullet vehicle and M_2 is the mass target vehicle.

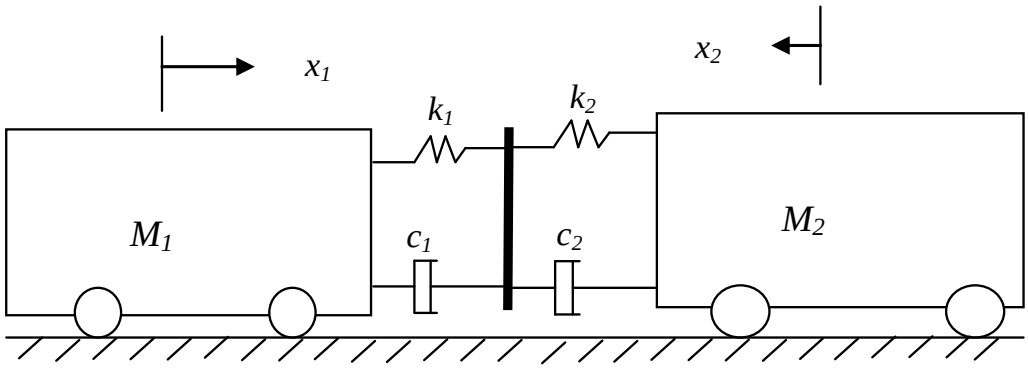

Figure 2.15: Vehicle-to-vehicle model.

To simplify the analysis, the two sets of Kelvin models were combined into one resultant Kelvin model with an effective mass, M_e, moving at a relative velocity ($\dot{x}$). Expressions for accelerations of masses M_1 and M_2 are defined in the the following and the detailed derivation can be found in Paper D.

$$\ddot{x}_1 = \gamma_1(c(\dot{x}_1 + \dot{x}_2) - k(x_1 + x_2))/M_e \tag{2.28}$$

$$\ddot{x}_2 = -\gamma_2(-c(\dot{x}_1 + \dot{x}_2) - k(x_1 + x_2))/M_e \tag{2.29}$$

where k and c are the equivalent spring stiffness and damper coefficient, respectively. M_e is the equivalent mass, γ_1 and γ_2 are mass reduction ratios, respectively.

2.3.4 Parameters optimization using genetic algorithm

The following are important steps of a genetic algorithm (GA): Initialization of populations of chromosomes, selection according to the fitness function, crossover to produce new offspring, and random mutation of new offspring.

A GA begins with a randomly chosen assortment of chromosomes, serving as the first generation (initial population). Then each chromosome in the population is evaluated by the fitness function to test how well it solves the problem [79]. The fitter a chromosome is, the more likely it is to be selected.

In this work, mathematical models for vehicle-to-barrier, vehicle-occupant, and vehicle-to-vehicle crashes were developed. To estimate and optimize the model parameters, a GA, which minimizes a fitness function in Equation (2.30), was proposed.

The fitness function was defined as follows:

$$\begin{aligned} \min_{\ddot{X},p} \quad & f(\ddot{X}_{est}, p) \\ \text{s.t} \quad & LB \leq p \leq UB \\ & E_r = \sum_{i=1}^{n} \sqrt{\left(\ddot{X}_{est} - \ddot{X}_{exp}\right)^T \times \left(\ddot{X}_{est} - \ddot{X}_{exp}\right)} \rightarrow 0, \end{aligned} \tag{2.30}$$

where p denotes a set of unknown parameters, which are the LPM (springs and dampers) in the model, LB and UB are the lower and upper bounds of parameters respectively- $\ddot{X}_{est}$ ($1 \times n$ vector) and $\ddot{X}_{exp}$ ($1 \times n$ vector) are estimated and experimental accelerations, respectively. E_r is the error between the estimated and the experimental (measured) accelerations. Basic steps of genetic algorithm are shown in Figure 2.16. When the fitness function is minimized the solver termi-

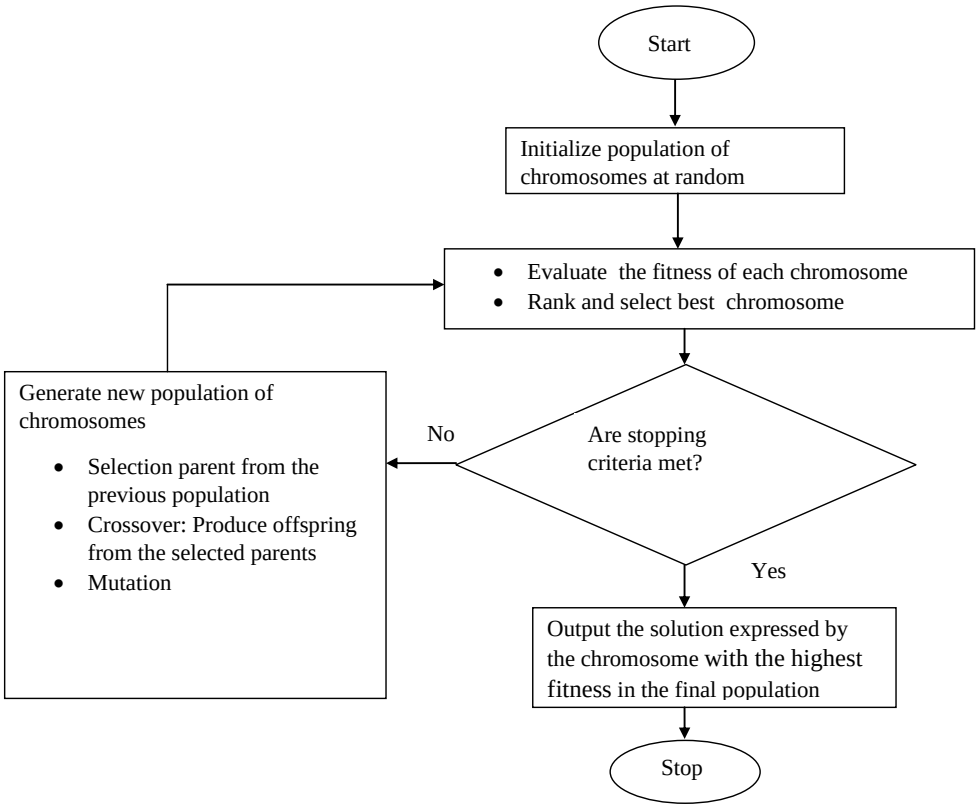

Figure 2.16: Basic steps of a Genetic Algorithm.

nates, otherwise the GA tunes the parameters so that the error between the model and experimental results is minimum. One of the following conditions may cause the GA to terminate:

- When there is no improvement in the population for a pre-defined number of generations,
- when the fitness function reaches a certain pre-defined value,
- when the maximum number of generations is reached.

In this work, the last condition was chosen as a stopping condition to optimize the parameters. Depending on the population size (the number of parameters to be estimated), the maximum number of generations equals 100 times of the parameter number.

2.4 Verification of LPM against FEM

A full-scale post-crash test for a Ford Taurus model (2004) crashing into a rigid wall and its Finite Element Model (FEM) input collected from the NHTSA, were used to verify the predictive capability of the LPM presented in subsection 2.3.1. The FEM of the vehicle consisted of 804 parts, 922007 nodes, 10 beam elements, 838926 shell elements, and 134468 solid elements. The closing velocity was set to 56 km/h, and the mass of the simulated vehicle was 1739 kg. The deceleration signal was measured from the center of gravity of the vehicle.

The rigid wall was included to the Ford-Taurus FEM, and an automatic-single-surface contact was defined between the vehicle and the rigid wall. After assembling, the model was analyzed using LS-DYNA software version R8.10, and the results were visualized using the LS-PREPOST.

A debugging was performed on the model to check the possible sources of error. A negative volume calculation was causing premature termination. To avoid the early termination, the material stress-strain curves were stiffened up at large strains. The model's credibility was tested by checking the ratio of the hourglass energy to the internal energy, which should be less or equal to the recommended value (0.1). The results of interest were obtained by activating the global statistics and the material energy key words. A D3 plot was displayed by setting a time interval between outputs to 0.005 seconds.

The model was simulated for various impact velocities (40, 48, 56, 64 and 72 km/h) with an actual computational time between one and two days for each simulation. Then a GA was applied to calibrate the LPM against full-scale crash test and FEM to test the predictive capability of the LPM. The prediction of LPM was valid

even outside the calibration point. The main contributing factors for occupant injury, such as the maximum dynamic crush and the acceleration severity index were predicted. A comparison between the piecewise linear lumped parameters model and the FEM is detailed in Paper H.

2.5 Indicator of model accuracy

To test the performance of the developed models, it is necessary to define the index that can be used to evaluate their performance. The most commonly used performance indicators in predictive model are the root mean square error (RMSE) and the mean absolute error (MAE) [80]. The RMSE is defined as

$$RMSE = \sqrt{\frac{\sum_{i=1}^{N} \left(y_i - \hat{y}_i\right)^2}{N}}, \tag{2.31}$$

and the mean absolute error (MAE) is expressed as

$$MAE = \frac{\sum_{i=1}^{N} \left|y_i - \hat{y}_i\right|}{N}, \tag{2.32}$$

where y_i and $\hat{y}_i$ are the experimental and simulated variables, respectively, and N is the number of samples in the measured data.

In this work the RMSE is chosen to measure the model's accuracy on the following kinematic variables:
$a(t)$: Acceleration time-history,
$v(t)$: Velocity time-history,
$d(t)$: Displacement time-history.
A small value of RMSE is a good indicator of the performance of the model. This index is applied in Chapter 3.

Chapter 3

Results and Discussions

This chapter presents and discusses significant key findings for vehicle crash reconstruction. The accuracy of the developed models, is tested using the Root Mean Square Error (RMSE), between the result from the simulation and experimental data. The following notations are used in Table 3.2 to 3.7: V_0: Initial velocity, V_r: Rebound velocity, C_m: Dynamic crush,C_{mo}: Maximum occupant travel, t_m: time when the vehicle reaches the dynamic crush.

3.1 Estimation of the responses of a vehicle's chassis and passenger compartment

The results from curve-fitting (CF), and state space (SS) approaches are first discussed. Here the vehicle crash configuration is a vehicle to a rigid pole. The model representing the crash is a double mass spring damper (MSD) system, where the front mass (m_1) represent the chassis and the rear mass (m_2) represents the passenger compartment.

Comparisons between the kinematic time-histories of the chassis and the passenger compartment, using the CF and SS, are presented in Figures 3.1 and 3.2, respectively. The dynamic crush from the test, is 50.6 cm and occurs after 0.075 s (see the mark on the black broken line in the plots).

After fitting the dynamic equation of the double mass-spring-damper model to real experimental displacement, it is found that displacement $d_{m_1}(t)$ curve of mass (m_1) is lagging the displacement curve $d_{m_2}(t)$ of mass (m_2).

The displacement $d_m(t)$ of the COG of a double MSD model is obtained by a cumulative average of $d_{m_1}(t)$ and $d_{m_2}(t)$.

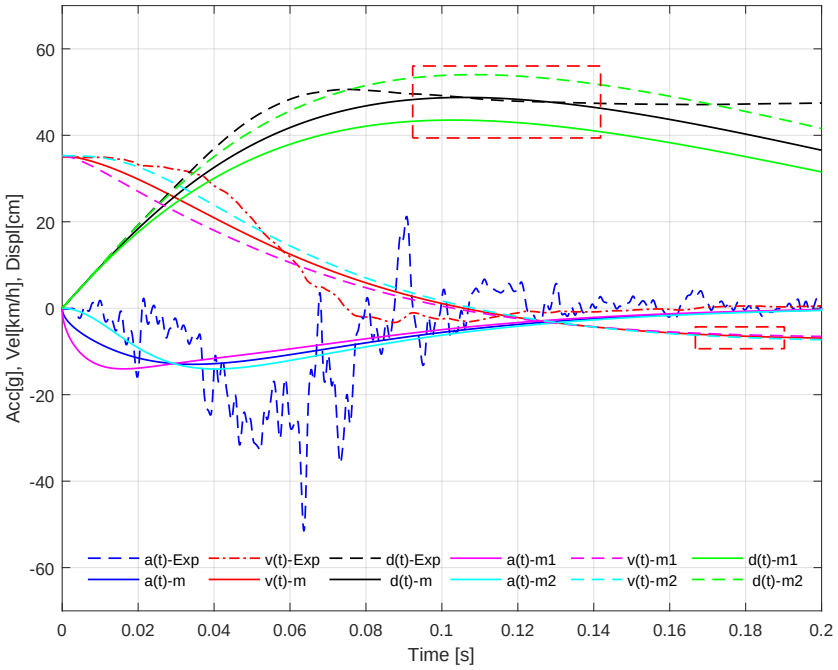

Figure 3.1: Kinematic time-histories for a VTB with a double MSD by CF.

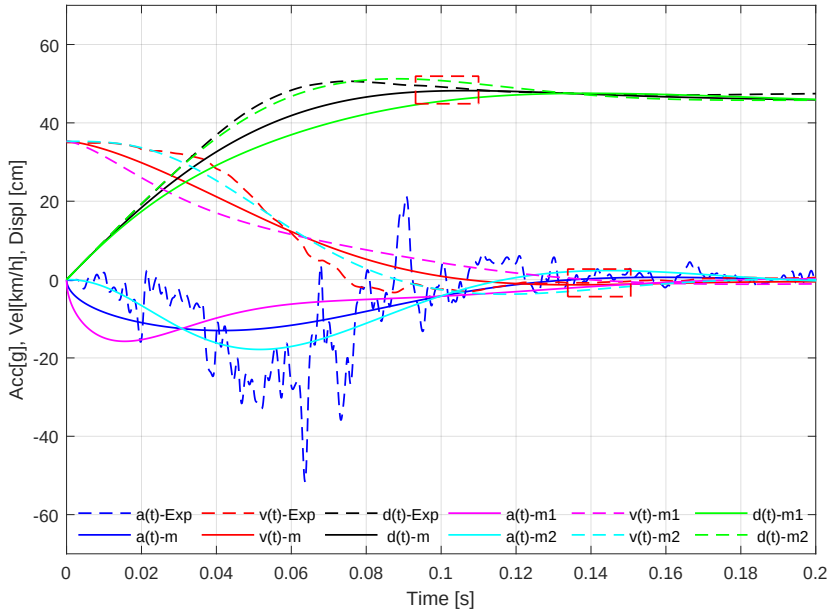

Figure 3.2: Kinematic time-histories for VTB with a double MSD by SS approach.

Results and Discussions

The dynamic crushes obtained from the CF and SS approaches are nearly equal (48.76 and 48.22 cm) and they occur around 0.10 s. However, the difference is observed on the velocity curves, where the rebound velocities are 5.66 and 1.34 km/h for CF and SS, respectively.

The maximum displacement of mass m_2 (the passenger compartment), in the SS model, is closer to that from the full-scale crash test. That indicates the dynamic crush of the state space model.

However, above approaches share the same limitation. None of the methods could reconstruct the velocity ($v(t)$) and acceleration ($a(t)$) signals. The reason for inaccuracy is attributed to the constant parameters (springs and dampers) used to model the crash. The estimated lumped parameters from both approaches are shown in Table 3.1. The crash characteristic parameters and the RMSE are shown in Table 3.2. The results are improved when the springs and dampers are modeled as piecewise functions of displacement and velocity, respectively, as can be seen in Figure 3.3.

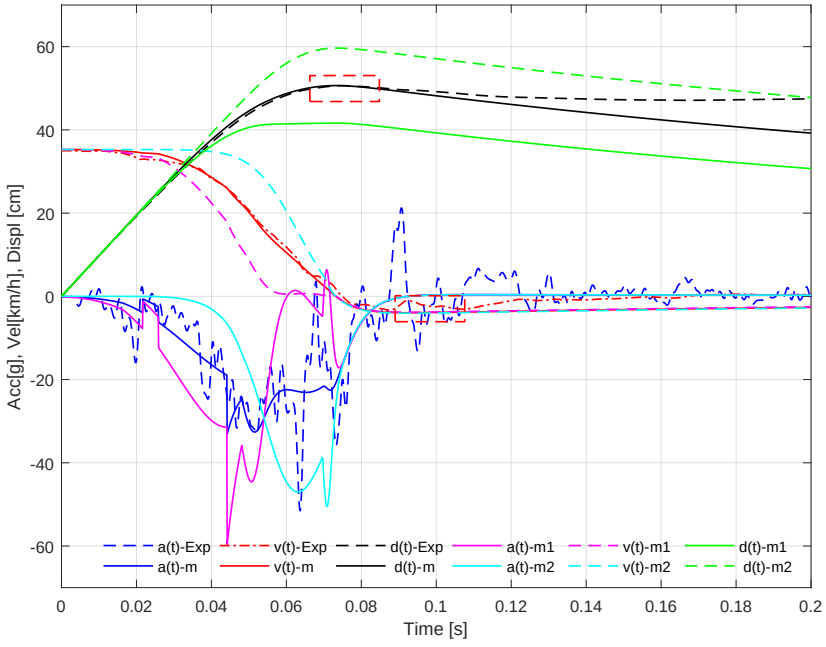

Figure 3.3: Kinematic time-histories for VTB with a double MSD optimized.

Table 3.1: Parameters estimated using curve-fitting and State-space approaches

Approach	$k_1[N/m]$	$c_1[Ns/m]$	$k_2[N/m]$	$c_2[Ns/m]$
Curve fitting	1,983,100	226,260	21,510	5,105
State-space	15,116	36,588	337,670	6,735

Table 3.2: Characteristic crash pulse parameters for VTB with double MSD

Parameter	Test	Curve-fitting	State-space	Optimized LPM
$V_0[km/h]$	35	35	35	35
$V_r[km/h]$	-3	-6	-1	-4
$C_m[cm]$	50.63	48.76	48.22	50.63
$t_m[s]$	0.075	0.107	0.104	0.074
RMSE				
$a(t)[g]$		84.7	79.45	47.77
$v(t)[km/h]$		1.41	0.99	0.67
$d(t)[cm]$		0.044	0.028	0.056

3.2 Vehicle crash reconstruction by one MSD system

The kinematic time-histories for a vehicle to barrier are presented in Figures 3.4 to 3.6. Here, the model is a single mass-spring-damper (MSD) system. Figure 3.4 represents the reproduced results from the existing approach in literature [22], where the circular natural frequency and the damping factor were extracted from the experimental data. The natural frequency ω_n extracted from the experimental data is 3.0544 rad/s, and the damping ratio ζ equals to 0.001. Then the estimated spring stiffness and damping coefficient are 321,540 N/m and 33.5082 Ns/m, respectively.

It is observed from Figure 3.4 that the maximum dynamic crush is estimated, but the displacement curve oscillates and does not follow the trend of the experimental displacement curve. The differences in the timing and magnitude of response between the test and the mass-spring-damper model are attributed to the insignificant damping in the model where the damping ratio is 0.001. By stiffening the spring with cubic nonlinearity, the results are much improved, as shown in Figure 3.5.

The results are further improved when Piecewise LPM, optimized by a genetic algorithm, is used to simulate the frontal structure of the vehicle. It can be observed that the displacement and velocity curves fit well the corresponding experimental data, as shown in Figure 3.6. However, the acceleration curve from the model does not capture the maximum peaks of the acceleration signal from the test. The characteristic crash pulse's parameters from the test and the models are shown in

Table 3.3. It is clear that the PWLPM is much more accurate than the constant and nonlinear LPm, as justified by their respective RMSE values. A smaller RMSE is a good indicator of the accuracy in reconstructing the crash scenario.

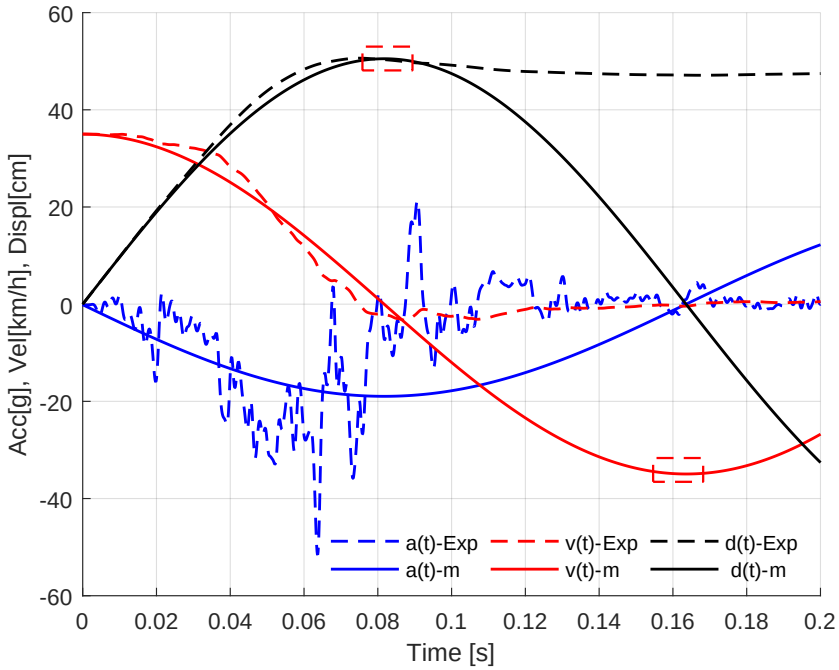

Figure 3.4: Crash responses for one MSD model using Huang's approach [22]

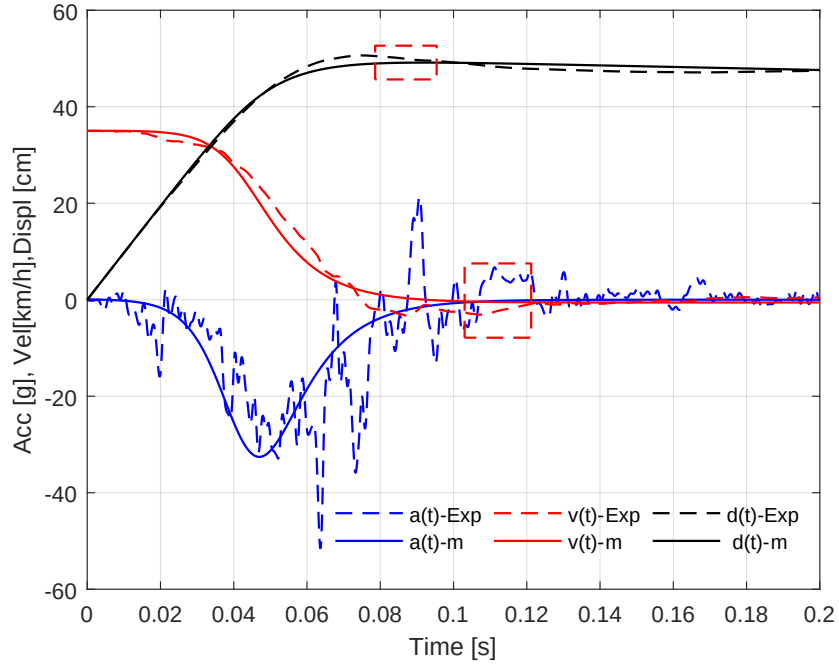

Figure 3.5: Crash responses for one MSD model with cubic nonlinear spring and damper

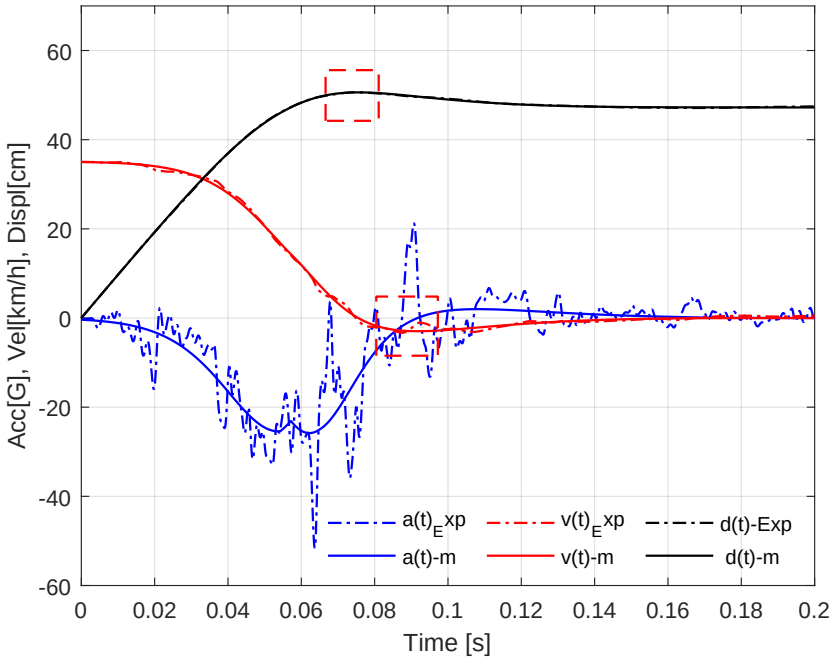

Figure 3.6: Crash responses for one MSD model with Piecewise LPM.

Table 3.3: Characteristic crash pulse parameters for VTB with single MSD

Parameter	Test	Constant LPM	Nonlinear LPM	PWLPM
$V_0[km/h]$	35	35	35	35
$V_r[km/h]$	-3	-35	-0.5	-3
$C_m[cm]$	50.63	50.51	48.99	50.61
$t_m[s]$	0.075	0.081	0.080	0.076
RMSE				
$a(t)[g]$		125.182	65.7594	53.7372
$v(t)[km/h]$		5.5278	0.4921	0.1422
$d(t)[cm]$		0.5012	0.0090	0.00089

3.3 Vehicle-occupant crash modelling

A genetic algorithm is used to optimize the spring stiffness and the damping coefficients of the proposed piecewise LPM. The test data are labeled with broken lines, while the results from the models are continuous line in Figures 3.7 and 3.8.

The test data show that the maximum occupant deceleration occurs at 0.074 s, 0.016 s before the vehicle reaches its dynamic crush at 0.090 s. The maximum occupant stopping distance (the maximum restraint deformation) is about 30 cm and occurs around 0.085 s, just before the vehicle rebounds around 0.12 s.

The first attempt to reconstruct the vehicle-occupant crash event is the introduc-

tion of linear and nonlinear component of spring and damper in the LPM. It can be shown from the kinematic time-history curves in Figure 3.7 that the model, with nonlinear spring and damper components, cannot accurately reconstruct the crash test kinematics. As it has been shown for the case of a VTB model, the piecewise LPM reconstructs the vehicle-occupant crash with sufficient accuracy, as shown in Figure 3.8. The characteristic of vehicle-occupant (V-Occ) crash pulse's parameters and the RMSE are shown in Tables 3.3 and 3.4, respectively. It is observed that the PWLPM model is accurate than the model with nonlinear spring and damper, as justified by small RMSE values.

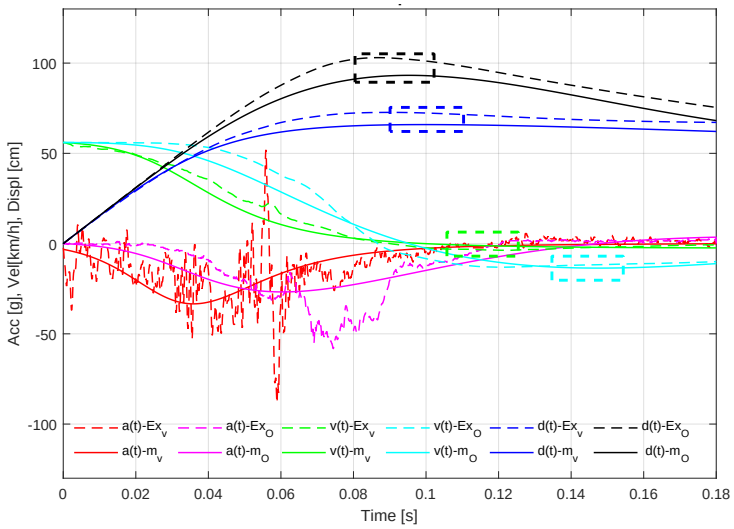

Figure 3.7: Estimation of Vehicle-occupant's kinematics by a nonlinear LPM.

Table 3.4: Characteristic crash pulse's parameters and RMSE for VO using nonlinear LPM

Parameter	Test-Vehicle	Model-Vehicle	Test-Occupant	Model-Occupant
$V_0[km/h]$	56	56	56	56
$V_r[km/h]$	-3.7	-2	-13	-13.49
$C_m[cm]$ or $C_{mo}[cm]$	73	65.87	30	27
$t_m[s]$ or $t_{mo}[s]$	0.090	0.093	0.087	0.092
RMSE				
$a(t)[g]$		109.3349		167.5613
$v(t)[km/h]$		0.8864		4.0884
$d(t)[cm]$		0.0464		0.2401

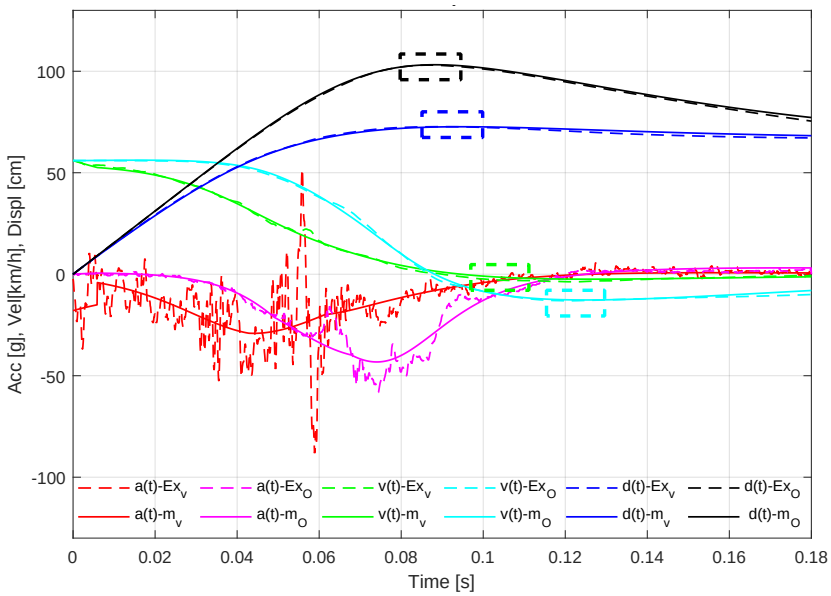

Figure 3.8: Estimation of Vehicle-occupant's kinematics by a piecewise LPM.

Table 3.5: Characteristic crash pulse's parameters and RMSE for VO using PWLPM

Parameter	Test-Vehicle	Model-Vehicle	Test-Occupant	Model-Occupant
$V_0[km/h]$	56	56	56	56
$V_r[km/h]$	-2.4	-2.4	-13	-12.6
$C_m[cm]$ or $C_{mo}[cm]$	73	72.65	37	30
$t_m[s]$ or $t_{mo}[s]$	0.090	0.093	0.087	0.086
RMSE				
$a(t)[g]$		100.18		135.79
$v(t)[km/h]$		0.25		3.4
$d(t)[km/h]$		0.0082		0.19

3.4 Vehicle-to-vehicle crash modelling

Two crash tests, a Caravan-to-Neon and a Dodge-to-Chevrolet were analysed. Here only the result for the Caravan-to-Neon are presented. Figure 3.9, shows the real after-crash test for one of the studied cases. Only a piecewise LPM is used to simulate a vehicle-to-vehicle crash scenario since its performance was sufficient for the previous cases.

The simulation results from the model are shown in Figure 3.10 and 3.10. It is observed that the model results agree with the crash test. The target vehicle (Neon) re-bounces after being impacted by the bullet vehicle (Caravan). The rebound velocities are -19.78 m/s and -19.7 m/s from the test and the model respectively. From the test, it is seen that the maximum dynamic crush of 74 cm is observed on the target vehicle, while the dynamic crash from the model is 73.9 cm, while the bullet

Figure 3.9: Vehicles deformations after crash (Caravan on right, Neon on left [1])

vehicle does not re-bounce at all. This is shown from the velocity curves of the two vehicles, with a negative velocity for the target vehicle and a positive velocity for the bullet vehicle. The frontal structure of the target vehicle's structure experiences a residual deformation (RD) of 12 cm, while the front structure of the bullet vehicle behaves elastically after the impact. The value of RD is calculated from the displacement curve in Figure 3.11 using the centroid time and the dynamic crush, according to [22]. The characteristic crash pulse's parameters from the test and the models are shown in Table 3.5. The results for Dodge-to-Chevrolet crash can be found in Paper D.

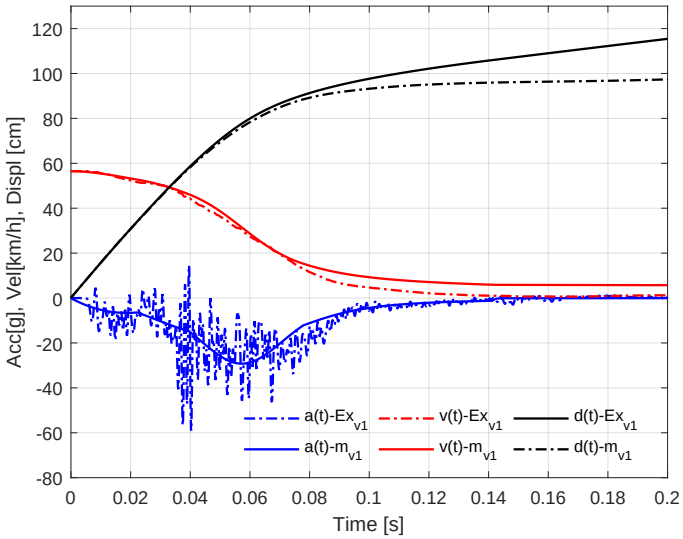

Figure 3.10: Kinematic time histories for the Bullet vehicle (Caravan) model vs test results

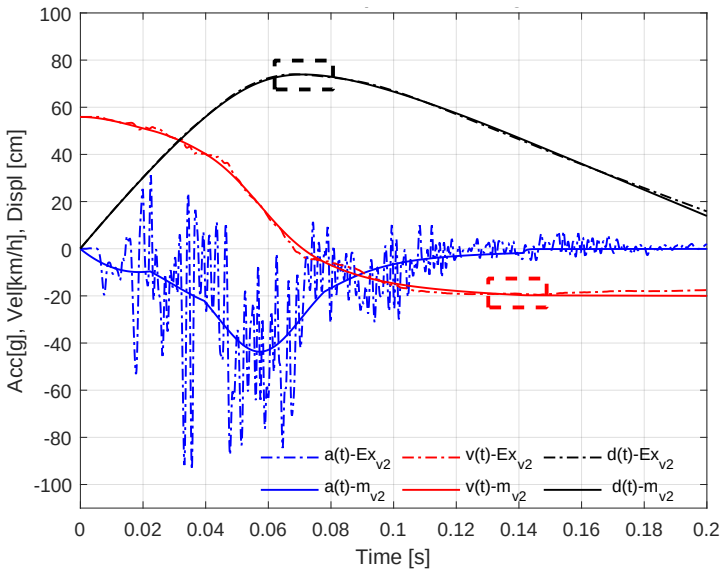

Figure 3.11: Kinematic time histories for the Target vehicle (Neon) model vs test results

Table 3.6: Characteristic crash pulse's parameters for vehicle-to-vehicle crash

Parameter	Test-Bullet	Model-Bullet	Test-Target	Model-Target
$V_0[km/h]$	58	58	58	58
$V_r[km/h]$	+1	+6	-20	-20
$C_m[cm]$	-	-	74.01	73.9
$t_m[s]$	-	-	0.068	0.0705
RMSE				
$a(t)[g]$		62.13		133.98
$v(t)[km/h]$		1.06		0.38
$d(t)[cm]$		0.085		0.0056

3.5 Verification of PWLPM against FEM

The predictive capabilities of a PWLPM are compared with those from a FEM using a Ford Taurus model obtained from the NHTSA database. The FEM is simulated for a range of velocities from 40 to 72 km/h, as illustrated in Figure 3.12. Only three plots, the lowest velocity (40 km/h), a calibration velocity (56 km/h), and the highest velocity (72km/h), are used as an illustration of the FEM simulations.

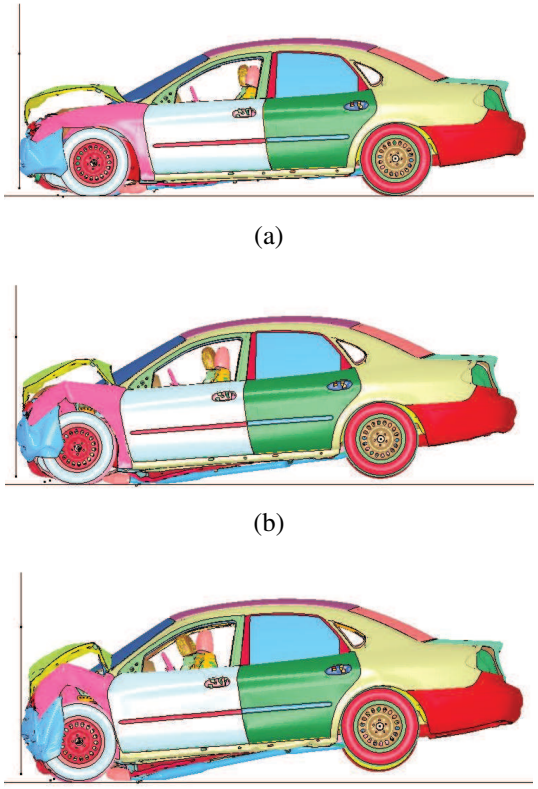

(a)

(b)

(c)

Figure 3.12: Deformed vehicle frontal structure through FEM at impact velocities of (a) 40 km/h, (b) 56 km/h and (c) 72 km/h

The PWLPM and FEM are first calibrated to the FSCT at 56 Km/h, as shown in Figure 3.13, then utilized to predict the crash at different impact velocities (below and above the calibration point) as shown in Figures 3.14 and 3.15, respectively. Additionally, PWLPM is also calibrated to the FEM. The crash pulse characteristics from the test and the models (i.e., LPM and FEM) and RME values are shown in Table 3.7. The PWLPM is well calibrated to FSCT than the FEM as it is shown in Figure 3.13a and in Table 3.7.

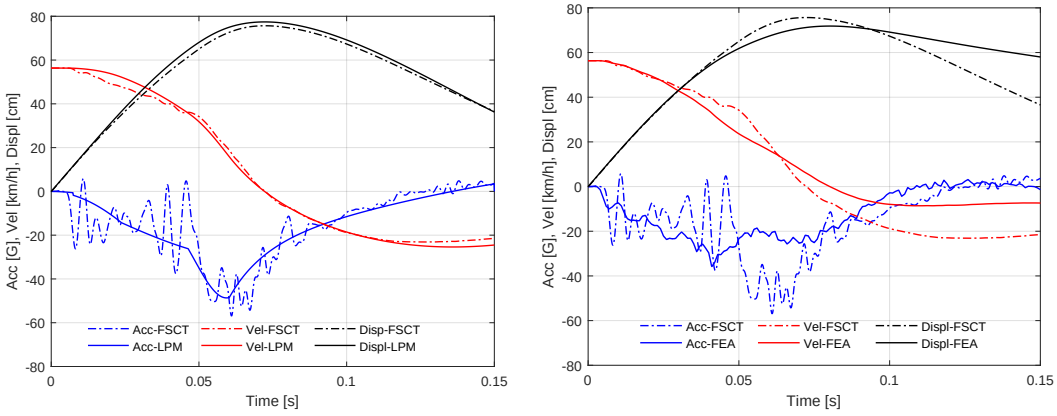

(a) (b)

Figure 3.13: Comparison of PWLPM and FEM to FSCT at 56 km/h (a) LPM vs FSCT, (b) FEM vs FSCT.

Table 3.7: Characteristic crash pulse's parameters and RMSE for FEM and PWLPM

Parameter	FSCT	FEM	PWLPM
$V_0[km/h]$	56	56	56
$V_r[km/h]$	-25	-8.5	-23
$C_m[cm]$	75.66	71.81	77.4
$t_m[s]$	0.072	0.078	0.07
RMSE			
$a(t)[g]$		114	75.33
$v(t)[km/h]$		2.64	0.59
$d(t)[cm]$		0.076	0.018

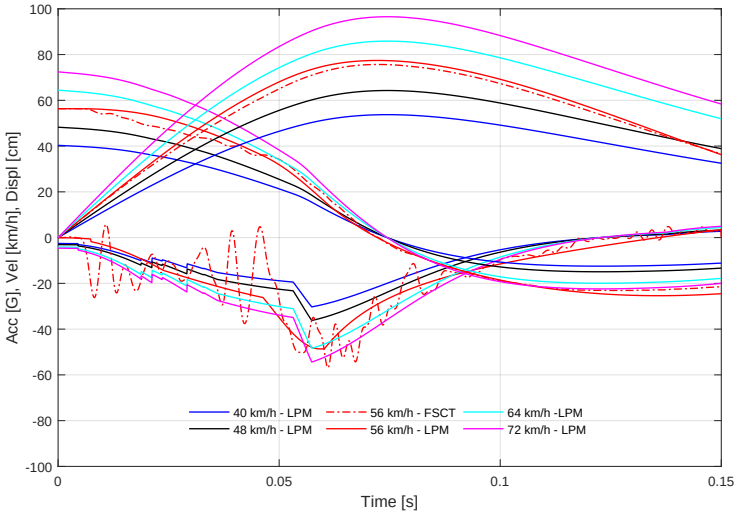

Figure 3.14: Vehicle frontal crash prediction using PWLPM

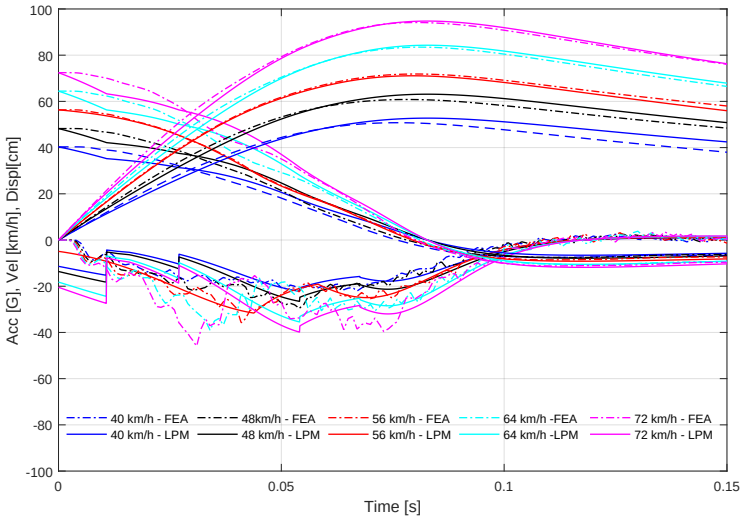

Figure 3.15: Vehicle frontal crash prediction using FEM

Small RMSE values for PWLPM for all kinematic variables are indicators of the accuracy of the proposed model. Specifically, the predictive capabilities of the PWLPM can be observed from the displacement curves in Figures 3.14 and 3.15. When the LPM is calibrated to FSCT, a constant increment of 11 cm for the maximum dynamic crush is observed for a corresponding increase of 8 km/h for the impact velocity. Similarly, a 10 cm increment is seen on the maximum dynamic crush when the LPM is calibrated to a FEM. It can be concluded, based on the observation from the prediction by FEM and PWLPM, that the PWLPM can reduce the computation time when simulating a vehicle crash event.

Further results, including the prediction of acceleration severity index at different velocities, can be found in Paper F.

Chapter 4

Concluding remarks

4.1 Conclusions

In this thesis, the performance of different vehicle crash reconstruction techniques was investigated. A nonlinear least-squares curve fitting (CF) method, an eigensystem realization algorithm (ERA), a state space (SS) approach, and a nature-inspired optimization algorithm were used for estimating model's parameters.

Initially, CF, ERA, and SS were tested on a double mass-spring-damper system, in which the front and rear masses represent the chassis and passenger compartment. It was possible to calibrate the double mass-spring-damper system parameters out of a single acceleration signal, measured from the center of gravity of the vehicle. SS produced slightly more accurate results than the CF and ERA, but the overall accuracy of the reconstruction deemed not sufficient.

Further improvement of the accuracy was achieved by introducing a genetic algorithm and upgrading the LPMs from linear to piecewise linear. GA was efficient in determining the model parameters, enabling PWLPM to reconstruct vehicle-to-barrier, vehicle-occupant, and vehicle-to-vehicle crash scenarios with sufficient accuracy. However, it takes a significant amount of time for GA to find proper initial parameters. This is attributed to the fact that the GA is a random search algorithm and it required several simulation cycles to find a good initial guess. In this work, the main focus was the accuracy of vehicle crash reconstruction, not the convergence rate of parameter calibration.

Finally, to verify the accuracy of the PWLPM, the predictive capability of the LPM was compared against that of an explicit FEM. Two parameters that characterize the collision of a vehicle with an obstacle, the maximum dynamic crush (C_m) and the acceleration severity index (ASI), were predicted and a good agreement be-

tween the two modelling approaches was observed. It can be concluded that the proposed PWLPM is a promising tool to reconstruct the crash event. It can assist vehicle designers in predicting the crash before performing physical tests or developing complex finite element models.

4.2 Further Work

Further work can be extended to include the following:

- Although LPM performed well for a vehicle to a rigid barrier, the integration of flexible barrier in the crash scenario was not considered in this work. The integration of flexible barrier could be investigated in future work.
- Finding a good guess of parameters in the optimization routine using the GA was a challenging task. The performance of other nature-inspired algorithms could be tried in future work and compared with the current results. Other algorithms could be differential evolution, simulated annealing, particle swarm optimization, etc.
- The predictive capability of LPM was verified for a vehicle to a rigid wall frontal crash. However, further studies are essential to consider the predictive capability of LPM for a vehicle-to-vehicle crash, side, oblique and offset impacts, respectively.
- Due to the stochastic behavior of the crash pulse, it was hard to reconstruct the acceleration signals from the crash test. Artificial intelligent approaches like artificial neuro network might address this challenge.

REFERENCES

[1] NHTSA, "The New Car Assessment Program Suggested Approaches for future Program Enhancements," National Highway Traffic Safety Administration, Tech. Rep., 2007, accessed, May 15, 2018. [Online]. Available: https://www.safercar.gov/staticfiles/safercar/pdf/810698.pdf

[2] T. M. Leughlin and R.A.Saul, "Crashworthiness, Aggressiveness and Crash Test Procedures," Insurance Institute for Highway Safety, Tech. Rep., 1995.

[3] W. T. Hollowell, H. C. Gabler, and S. L. S. T. S. Summers, "Review of potential test procedures for FMVSS NO. 208," 1998.

[4] Z. Wei, "Analysis, modeling and CAE validation of vehicle crashes using advanced signal processing tools," Ph.D. dissertation, University of Agder, Faculty of Engineering and Science, 2017.

[5] P. DuBois, C. C. Chou, B. B. Fileta, T. B. Khalil, A. I. King, H. F. Mahmood, H. J. Mertz, and J. Wismans, *Vehicle crashworthiness and occupant protection*. American Iron and Steel Institute, 2004.

[6] N. Saba, J. Rishmany, I. Tawk, and M. Daaboul, "Optimization of the Production Process of an A-Pillar using a Differential Thickness Profile Approach via FEA," *Athens Journal of Technology and Engineering*, vol. 4, no. 2, pp. 109–123, 2017.

[7] A. E. Ikpe, E. K. Orhorhoro, and A. Gobir, "Design and reinforcement of a B-pillar for occupants safety in conventional vehicle applications," *International Journal of Mathematical, Engineering and Management Sciences*, vol. 2, no. 1, p. 37–52, 2017.

[8] A. E. Ikpe, I. B. Owunna, and P. Satope, "Design optimization of a B-pillar for crashworthiness of vehicle side impact," *Journal of Mechanical Engineering and Sciences*, vol. 11, no. 2, p. 2693–2710, 2017.

[9] D. B. Uma, K. C. Vamsi, and S. P. Mohan, "Design simulation of crash box in car," *International Journal of Engineering Research and Technology (IJERT)*, vol. 3, no. 1, p. 978–982, 2014.

[10] K. Pelckmans, "Lecture notes for a course on system identification," accessed , February27, 2018. [Online]. Available: https://www.it.uu.se/edu/course/homepage/systemid/vt11/Sysid2011b.pdf

[11] Paul M.J. Van Den Hof and X. Bombois, "System identification for control," March 2004, accessed , February 27, 2018. [Online]. Available: ftp://ftp.unicauca.edu.co/Facultades/FIET/DEIC/Materias/Identificacion/documentos/DISC2004.pdf

[12] L. . Ljung, *System identification: theory for the user, 2nd edn*, U. S. River, Ed. PTR Prentice Hall, 1999.

[13] C. M. Pappalardo and D. Guida, "System identification algorithm for computing the modal parameters of linear mechanical systems," *Machines*, vol. 6, no. 12, pp. 1–20, 2018.

[14] T. Sands, "Nonlinear-adaptive mathematical system identification," *Computation*, vol. 5, no. 47, pp. 1–12, 2017.

[15] T. Sands and T. Kenny, "Experimental piezoelectric system identification," *Journal of Mechanical Engineering and Automation*, vol. 7, no. 6, pp. 179–195, 2017.

[16] U. N. Gandhi and S. J. Hu, "Data-based approach in modeling automobile crash," *International Journal of Impact Engineering*, vol. 16, no. 1, pp. 95–118, 1995.

[17] W. Pawlus, K. G. Robbersmyr, and H. R. Karimi, "Mathematical modeling and parameters estimation of a car crash using data-based regressive model approach," *Applied Mathematical Modelling*, vol. 35, pp. 5091–5107, 2011.

[18] W. Pawlus, H. R. Karimi, and K. G. Robbersmyr, "Investigation of vehicle crash modeling techniques: theory and application," *International Journal of Advanced Manufacturing Technology*, vol. 70, p. 965–993, 2014.

[19] L. Zhao, W. Pawlus, H. R. Karimi, and K. G. Robbersmyr, "Data-based modeling of vehicle crash using adaptive neural-fuzzy inference system," *Journal of Applied Mathematics*, vol. 19, no. 2, pp. 684–696, 2014.

[20] Q. Lu, H. R. Karimi, and K. G. Robbersmyr, "A data-based approach for modeling and analysis of vehicle collision by lpv-armax models," *Journal of Applied Mathematics*, vol. 2013, pp. 1–9, 2013.

[21] W. Pawlus, K. G. Robbersmyr, and H. R. Karimi, "Identification of a vehicle full-scale crash viscoelastic system by recursive autoregressive moving average models," *International Journal of Control Theory and Applications (IJCTA)*, vol. 4, no. 1, pp. 11–24, 2011.

[22] M. Huang, *Vehicle Crash Mechanics*. Boca Raton London New York Washington: CRC PRESS, 2002.

[23] W.Pawlus, J. E.Nielsen, H. R. Karimi, and K. G.Robbersmyr, "Mathematical modeling of a vehicle crash test based on elasto-plastic unloading scenarios of spring-mass models," *International Journal of Advanced Manufacturing Technology*, vol. 55, pp. 369–378, 2011.

[24] W. Pawlus, J. E. Nielsen, H. R. Karimi, and K. G. Robbersmyr, "Application of viscoelastic hybrid models to vehicle crash simulation," *International Journal of Crashworthiness*, vol. 55, pp. 369 – 378, 2011.

[25] W. Pawlus, H. R. Karimi, and K. G. Robbersmyr, "Development of lumped-parameter mathematical models for a vehicle localized impact," *Journal of Mechanical Science and Technology*, vol. 25, no. 7, pp. 1737–1747, 2011.

[26] J. Xin, W. Lei, L. Shixin, and Z. Yongbo, "Improved eigensystem realization algorithm and its application on ocean platforms," *Cluster Computing https://doi.org/10.1007/s10586-018-2213-0*, pp. 1–8, 2017.

[27] P. Li, S. Hu, and H. Li, "Noise issues of modal identification using eigensystem realization algorithm," in *The Twelfth East Asia-Pacific Conference on Structural Engineering and Construction*, 2011.

[28] M. D. Angelis, H. Lus, R. Betti, and R. W.Longman, "Extracting physical parameters of mechanical models from identified state space representations," *Journal of Applied Mechanics*, vol. 69, pp. 617–625, 2002.

[29] J. Juang, *Applied System Identification*, 6th ed. Printice Hall PTR, 1994.

[30] M. Majji, J.-N. Juang, and J. L. Junkins, "Time-varying eigensystem realization algorithm," *Journal of Guidance, Control, and Dynamics*, vol. 33, no. 1, pp. 13–28, 2010.

[31] J. N. Juang and R. S. Pappa, "An eigensystem realization algorithm for modal parameters identification and model reduction," *Journal of Guidance, Control, and Dynamics*, vol. 8, pp. 620–627, 1985.

[32] C. D. YANG and F. B. YEH, "Identification, reduction, and refinement of model parameters by the eigensystem realization algorithm," *Journal of Guidance, Control and Dynamics*, vol. 13, pp. 1051–1059, 1990.

[33] D. Guida, F. Nilvetti, and C. M. Pappalardo, "Parameter identification of a two degrees of freedom mechanical system," *International Journal of Mechanics*, vol. 3, no. 2, pp. 22 – 30, 2009.

[34] M. Majji, J.-N. Juang, and J. L. Junkins, "Ambient vibration studies for system identification of tall buildings," *Earthquake Engng Struct. Dyn*, vol. 32, pp. 71–95, 2003.

[35] Minh Quach and Nicolas Brunel and Florence d'Alche-Buc, "Estimating parameters and hidden variables in non-linear state-space models based on odes for biological networks inference," *Bioinformatics*, vol. 23, no. 23, p. 3209–3216, 2007.

[36] A. Emadi, "Modeling and analysis of multiconverter dc power electronic systems using the generalized state-space averaging method," *IEEE Transactions on Industrial Electronics*.

[37] J. Marzbanrad and M.Pahlavani, "A system identification algorithm for vehicle lumped parameter model in crash analysis," *International Journal of Modelind and Optimization*, vol. 1, no. 2, pp. 163–168, 2011.

[38] J. Marzbanrad and M. Pahlavani, "Parameter determination of a vehicle 5-dof model to simulate occupant deceleration in a frontal crash," *World Academy of Science, Engineering and Technology*, vol. 55, pp. 336–341, 2011.

[39] P. J. Arnoux, S. Joonekindt, L. Thollon, and K. Kayvantash, "Radioss finite element model of the thor dummy," *International journal of crashworthiness*, vol. 8, no. 6, p. 529–541, 2003.

[40] A.Yehia and A. Nasse, "Frontal crash simulation of vehicles against lighting columns using fem," *Alexandria Engineering Journa*, vol. 52, p. 295–2991, 2013.

[41] T. Teng, F. Chang, Y. Liu, and C. Peng, "Analysis of dynamic response of vehicle occupant in frontal crash using multibody dynamics method," *Mathematical and Computer Modelling*, vol. 48, pp. 1724 – 1736, 2008.

[42] L. Sousa, P. Verssimo, and J. Ambrsio, "Development of generic multibody road vehicle models for crashworthiness," *Multibody System Dynamics*, vol. 19, pp. 133 – 158, 2008.

[43] J. A. M. Carvalho and P. Eberhard, "Identification of validated multibody vehicle models for crash analysis using a hybrid optimization procedure," *Struct Multidisc Optim*, vol. 44, pp. 85–97, 2011.

[44] A. Alnaqi and A. Yigit, "Dynamic analysis and control of automotive occupant restraint systems," *Jordan Journal of Mechanical and Industrial Engineering*, vol. 5, no. 1, pp. 39–46, 2011.

[45] P. Jonsén, E. Isaksson, K. Sundin, and M. Oldenburg, "Identification of lumped parameter automotive crash models for bumper system development," *International Journal of Crashworthiness*, vol. 14, no. 6, pp. 533 – 541, 2009.

[46] H. Mooi and J. Huibers, "Simple and effective lumped mass models for determining kinetics and dynamics of car-to-car crashes," *International Journal of Crashworthiness*, vol. 5, no. 1, pp. 7–24, 2000.

[47] Z. J. Elmarakbi A M, "Crash analysis and modeling of two vehicles in frontal collisions using two types of smart front-end structures: an analytical approach using IHBM," *International Journal of Crashworthiness*, vol. 11, no. 5, pp. 67–483, 2006.

[48] W. Pawlus, H. R. Karimi, and K. G. Robbersmyr, "Development of lumped parameter mathematical models for a vehicle localized impact," *Journal of Mechanical Science and Technology*, vol. 25, no. 7, pp. 1737–1747, 2011.

[49] Hesham Kamel Ibrahim, "Design Optimization of Vehicle Structures for Crashworthiness Improvement," Ph.D. dissertation, Concordia University Montreal, Quebec, Canada, 2009.

[50] M. M. Kamal, "Analysis and simulation of vehicle to barrier impact," *SAE Technical Paper*, 1970.

[51] A. Klausen, S. S. Tørdal, H. R. Karimi, K. G. Robbersmyr, M. Jecmenica, and O. Melteig, "Firefly optimization and mathematical modeling of a vehicle crash test based on single-mass," *Journal of Applied Mathematics*, pp. 1 – 10, 2014.

[52] A. Klausen, S. S. Tørdal, H. R. Karimi, and K. G. Robbersmyr, "Mathematical modeling and numerical optimization of three vehicle crashes using a single-mass lumped parameter model," p. 44 – 49, 2015.

[53] S.M.Ofochebe, C.G.Ozoegwu;, and S.O.Enibe, "Performance evaluation of vehicle front structure in crash energy management using lumped mass-spring system," *Advanced Modeling and Simulation in Engineering*, vol. 2, p. 1–18, 2015.

[54] S. M. Ofochebe, S. O. Enibe, and C. G. Ozoegwu, "Absorbable energy monitoring scheme: new design protocol to test vehicle structural crashworthiness," *Heliyon*, vol. 2, pp. 1 – 33, 2016. [Online]. Available: https://www.journals.elsevier.com/heliyon/

[55] J. Lim, "Consideration on the offset frontal impact modeling using spring-mass model," *International Journal of Mechanical, Aerospace, Industrial, Mechatronic and Manufacturing Engineering*, vol. 9, p. 1453 – 1458, 2015.

[56] S.G.Mentzer, "The SISAME-3D Program: Structural Crash Model Extraction and Simulation," US Dept. of Transportation. National Highway Traffic Safety Administration D Report DOT HS, Tech. Rep., November 2007.

[57] S.G.Mentzer, R.Radwan, and W.Hollowel, "The SISAME methodology for extraction of optimal lumped parameter structural crash models," Society of Automotive Engineers, SAE, Tech. Rep., February 1992.

[58] J. Lim, "Lumped mass-spring model construction for crash analysis using full frontal impact test data," *International Journal of Automotive Technology*, vol. 18, p. 463 – 472, 2017.

[59] T. Belytschko, W. K. Liu, B. Moran, and K. I. Elkhodary, *Nonlinear Finite Elements for Continua and Structures*. John Wiley and Sons, 2014.

[60] *LS-DYNA Keyword User's Ma nual, VOLUME II*, Ls-dyna r9.0 ed., Livermore Software Technology Corporation, Livermore, California 94551-0712, August 2016.

[61] E. Haug, J. Clinckemaillie, X. Ni, A. K. Pickett, and T. Queckborner, "Recent trends and advances in crash simulation and design of vehicles," *Crashworthiness of Transportation Systems: Structural Impact and Occupant Protection*, vol. 332, pp. 401–417, 1997.

[62] *LS-DYNA3D theoretical manual*, Livermore Software Technology Corporation, 2876 Waverley Way, May 1998.

[63] K.-J. Bathe, *Finite Element Procedures*, 2nd ed. United States of America: Pentice Hall, 2014.

[64] J. N. Reddy, *An Introduction to the Finite Element Method*, 2nd ed. McGraw-Hill, 1993.

[65] K. Deb, A.; Srinivas, "Development of a new lumped-parameter model for vehicle side-impact safety simulation," in *Proceedings of the Institution of Me chanical Engineers, Part D: Journal of Automobile Engineering*, 2008, p. 1793–1811.

[66] M. S.Ofochebe and a. G. S. Enibe, "Absorbable energy monitoring scheme: new design protocol to test vehicle structural crashworthiness," *Heliyon, Elsevier*, vol. 2, p. 1–33, 2016.

[67] N.Tanlak, F. Sonmez, and M.Senaltun, "Shape optimization of bumper beams under high-velocity impact loads," *Engineering Structures*, vol. 95, p. 49–60, 2015.

[68] A. Eskandarian, D. Marzougui, and N. E. Bedewi, "Finite element model and validation of a surrogate crash test vehicle for impacts with roadside objects," *International Journal of Crashworthiness*, vol. 2, no. 3, pp. 239–258, 1997.

[69] J. Marzbanrad and M. Pahlavani, "Calculation of vehicle-lumped model parameters considering occupant deceleration in frontal crash," *International Journal of Crashwothiness*, vol. 16, no. 4, pp. 439 – 455, 2011.

[70] K. G. Robbersmyr, "Calibration test of a standard Ford Fiesta 1.1 l, model 1987, according to NS - EN 12767," Agder Research, Grimstad, Tech. Rep. 43, 2004.

[71] NHTSA. Vehicle crash test database on select test parameters. Accessed, May 25, 2016. [Online]. Available: http://www-nrd.nhtsa.dot.gov/database/vsr/veh/querytest.aspx

[72] International Organization for Standardization, " ISO 6487 Road vehicles - Measurement techniques in impact tests - Instrumentation," International Organization for Standardization, Switzerland, Standard, August 2015,

Accessed, May 20, 2018. [Online]. Available: https://www.sis.se/api/document/preview/919146/

[73] H. R. Karimi and K. G. Robbersmyr, "Signal analysis and performance evaluation of a vehicle crash test with a fixed safety barrier based on haar wavelets," *International Journal of Wavelets, Multiresolution and Information Processing*, vol. 21, no. 25, pp. 1– 18, 2010.

[74] "SAE J211-1 (1995): Instrumentation for Impact Test, Part 1, Electronic Instrumentation," SAE International, Standard, May 2007.

[75] N. Alem and M. Perry, "Design of digital low-pass filters for time-domain recursive filtering of impact acceleration signals," United States Army Aeromedical Research Laboratory Fort Rucker, Alabama 36362-0577, Tech. Rep., January 1995.

[76] E. L. Fasanella and K. E. Jackson, "Best practices for crash modeling and simulation," U.S. Army Research Laboratory Vehicle Technology Directorate, Langley Research Center, Hampton, Virginia, Tech. Rep., October 2002.

[77] H. Jianping and A. Pengqiang, "Modal parameter identification of structures based on combining autocorrelation function and era under ambient excitation," in *6th International Conference on Advances in Experimental Structural Engineering*, August 2015.

[78] J. N. Juang and R. S. Pappa, "An eigensystem realization algorithm for modal parameter identification and model reduction," *Journal of Guidance Control and Dynamics*, vol. 8, no. 5, p. 620–627, 1985.

[79] J. Carr. An introduction to genetic algorithms. Accessed, March 08, 2018. [Online]. Available: https://karczmarczuk.users.greyc.fr/TEACH/IAD/GenDoc/carrGenet.pdf

[80] K. M. Cort J. Willmott, "Advantages of the mean absolute error (MAE) over the root mean square error (RMSE) in assessing average model performance," *Climate Research*, vol. 30, pp. 74 – 82, 2005.

PART II

Publications

Paper A

Title:	Mathematical Modeling and Parameters estimation of Car Crash using Eigensystem Realization Algorithm and Curve Fitting Approaches
Authors:	Bernard B. Munyazikwiye[1], Hamid Reza Karimi[1] and Kjell G. Robbersmyr[1]
Affiliation:	[1] Faculty of Engineering and Science, University of Agder, P.O. Box 509, 4879 Grimstad, Norway
Article:	*Mathematical Problems in Engineering, Vol. 2013, pp. 1-13.*
Layout:	The layout of the paper has been revised to have the same format as the thesis

---

Abstract — **An Eigensystem Realization Algorithm (ERA) approach for estimating the structural system matrices is proposed in this paper using the measurements of acceleration data available from the real crash test. A mathematical model that represents the real vehicle frontal crash scenario is presented.The model's structure is a double-spring-mass-damper system, whereby the front mass represents the vehicle chassis and the rear mass represents the passenger compartment.The physical parameters of the model are estimated using curve fitting aproach and the estimated state system matrices are estimated by using the ERA approach. The model is validated by comparing the results from the model with those from the real crash test.**

Keywords— Modeling, vehicle frontal crash, curve fitting, eigensystem realization algorithm.

A.1 Introduction

Car crash test is usually performed in order to ensure safe design standards in crashworthiness (the ability of a vehicle to be plastically deformed and yet maintains a sufficient survival space for its occupants during crash scenario). Nowadays, due to advanced research in computer simulation software, simulated crash tests can be performed beforehand the full-scale crash test. Therefore, cost associated with real crash test can be reduced. Vehicle crashworthiness can be evaluated in four distinct modes: frontal, side, rear and rollover crashes. Several researches have been carried out in this field, which resulted in several novel computational models of vehicle collisions in literature. In [1], a mathematical model is proposed to estimate the maximum occupant deceleration - which is one of the main tasks in the area of crashworthiness study by a Kelvin Model which contains a mass together with spring and damper connected in parallel. An application of physical models composed of springs, dampers and masses joined together in various arrangements for simulating a real car collision with a rigid pole was presented in [2].

In [3], the authors presented an overview of the kinematic and dynamic relationships of a vehicle in a collision, where the work was to identify the parameters of the vehicle crash model using experimental data set. In [4] and [5], a lumped parameter modeling in frontal crash was investigated and analyzed in five degrees of freedom and have been used to analyze the response of occupant during the impact. In [6] and [7], an optimization procedure to assist multi-body vehicle model

development and validation was proposed. The authors first devised the topological structure of the multi-body system representing the structural vehicle components and described the most relevant mechanisms of deformation. In the work of [8], the authors proposed an approach to control the seat belt restraint system force during a frontal crash to reduce thoracic injury.
The main challenge in accident reconstruction is the system identification described as the process of constructing mathematical models of dynamical systems using measured input-output data. In case of vehicle crash, system identification algorithm consists of retrieving the unknown parameters such as the spring stiffness and damping coefficient. A possible approach is to identify these parameters directly from experimental dynamical data.
From literature, System Identification Algorithms (SIA) have been developed for different applications. Among others we can state: subspace identification, genetic algorithm, eigensystem realization algorithm and data-based regressive model approaches. Typical examples where these SIA have been used can be found in [9] and [10], [4] and [11], [12] and [13] respectively.

System identification using ERA has so far received considerable attention, as evidenced by the work of Jer-Nan Juang [14], Chiang and Chang [15], Ko and Hung [16], Juang and Papa [17] and Yang and Yeh [18]. For instance, in [17], the author developed the ERA to estimate the natural frequencies and damping ratios of a dynamical system from known Markove parameters and in [18], the authors used the ERA to identify the system matrices of a vibrating structure from the displacement-based Markov parameters, which were estimated from measured displacement responses together with the exitation forces.
The main contribution of this paper is the development of a mathematical model for a double spring-mass-damper system which reconstructs a vehicle frontal crash scenario and estimate structural parameters such as natural frequencies, spring stiffness and damping coefficients of the system. In this paper, an ERA is used to identify the system matrices of a vehicle impacting a rigid barrier, modeled by a double spring-mass-damper system. The model represents the inertia of the vehicle chassis and the passenger compartment. The state - space representation of the model is estimated from the acceleration - based Markove parameters which are extracted from the measured acceleration response. To estimate the physical parameters (stiffness and damping coefficient) of the model, a curve fitting method is used. It is noting that the effectiveness and accuracy of simulation modeling results are verified by the real physical experiments. The novelty in this paper as compared to those ref-

ered to is that the physical parameters , stiffness and damping coeficients, were first estimated and finally the model was simulated and results compared with experimental results. For instance in [2], [4] and [11] the authors validated their models from numerical examples with known parameters.

A.2 Vehicle crash experimental test

The real vehicle crash experiment was conducted on a typical mid-speed vehicle to pole collision. Its elaboration was the initiative of Robbersmyr (2004). A test vehicle was subjected to impact with a vertical, rigid cylinder. The acceleration field was 100 meter long and had two anchored parallel pipelines. The vehicle was steered using those pipelines that were bolted to the concrete runaway. Setup scheme is shown in FigureA.1.

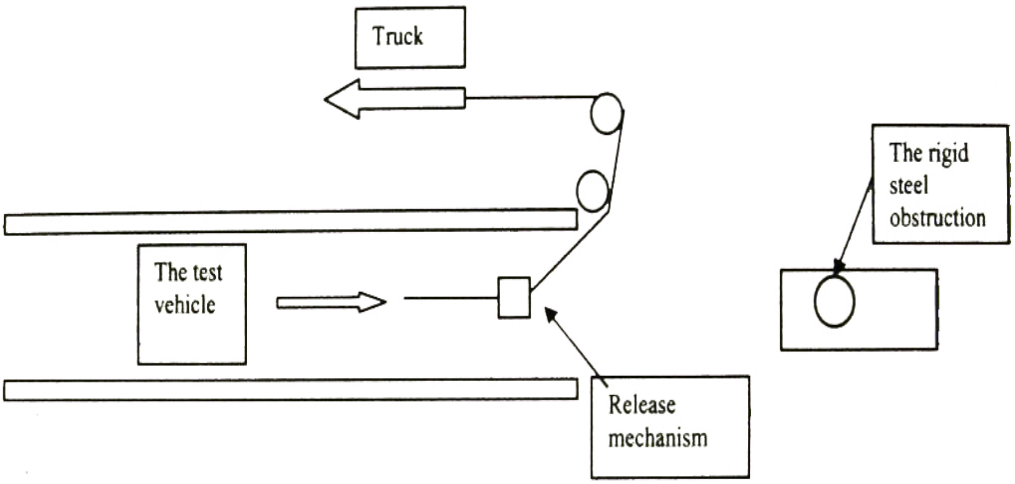

Figure A.1: Vehicle crash Experimental setup [19]

During the test, the acceleration was measured in three directions (x - longitudinal, y - lateral, and z - vertical) together with the yaw rate from the center of gravity of the car. Using normal speed and high - speed video cameras, the behavior of the safety barrier and the test vehicle during the collision was recorded. The initial velocity of the car was 35 km/h, and the mass of the vehicle (together with the measuring equipment and dummy) was 873 kg. The obstruction was constructed with two steel components - a pipe filled with concrete and a baseplate mounted with bolts on a foundation. The car undergoing the deformation is shown in Figure A.2. The accelerometer is located at the mass center of gravity of the vehicle in the pas-

senger compartment. Since we are interested in the frontal crash, only the measured acceleration in the longitudinal direction is considered in this study. The acclereration data is imported and processed in matlab for analysis. The deformation of the vehicle is obtained by integrating twice the acceleration signal.

Figure A.2: Vehicle undergoing deformation [19]

A.3 Mathematical Modeling Theoretical Background

Mathematical models describe the dynamic behavior of a system as a function of time. During frontal crash, the vehicle is subjected to an impulsive force caused by the obstacle. The model for vehicle crash simulates a rigid barrier impact of a vehicle where m_1 and m_2 represent the frame rail (chassis) and passenger compartment masses, respectively.

Parameters to be estimated are springs k_1 and k_2, dampers c_1 and c_2, as shown in Figure A.3. When the vehicle impacts on a rigid barrier, the two masses will experience an impulsive force during collision. The method for solving the impact responses of the two masses is adapted from te method used in the free vibration analysis of a two-degrees of freedom damped system [20].

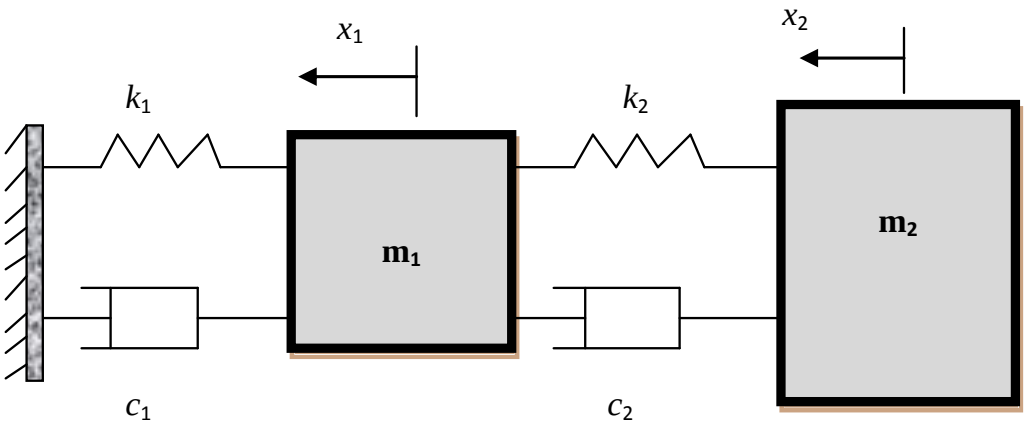

Figure A.3: A double spring-mass-damper model

The dynamic equations of the two mass-spring-damper model are shown in Equation(A.1).

$$\begin{aligned} m_1\ddot{x}_1 + (c_1 + c_2)\dot{x}_1 + (k_1 + k_2)x_1 - c_2\dot{x}_2 - k_2x_2 = 0 \\ m_2\ddot{x}_2 - c_2\dot{x}_1 + c_2\dot{x}_2 + k_2x_2 - k_2x_1 = 0 \end{aligned} \tag{A.1}$$

or

$$\begin{bmatrix} m_1 & 0 \\ 0 & m_2 \end{bmatrix} \begin{bmatrix} \ddot{x}_1 \\ \ddot{x}_2 \end{bmatrix} + \begin{bmatrix} k_1 + k_2 & -k_2 \\ -k_2 & k_2 \end{bmatrix} \begin{bmatrix} x_1 \\ x_2 \end{bmatrix} + \begin{bmatrix} c_1 + c_2 & -c_2 \\ -c_2 & c_2 \end{bmatrix} \begin{bmatrix} \dot{x}_1 \\ \dot{x}_2 \end{bmatrix} = \begin{bmatrix} 0 \\ 0 \end{bmatrix}$$

The solution for for $x_i, i = 1, 2$, can be respresented as

$$x_i = C_i e^{s_k t} \tag{A.2}$$

with *k*= 1,. . . ,4.

where C_i and s_k may be complex numbers. Substituting (A.2) into (A.1), we get

$$\begin{aligned} R_{1k}C_1 - R_{2k}C_2 = 0 \\ -S_{1k}C_1 + S_{2k}C_2 = 0 \end{aligned} \tag{A.3}$$

$$\frac{C_2}{C_1} = \frac{R_{1k}}{R_{2k}} = \frac{S_{1k}}{S_{2k}} \tag{A.4}$$

$$R_{1k} = R_{2k} * \frac{S_{1k}}{S_{2k}} \tag{A.5}$$

$$R_{1k} * S_{2k} - R_{2k} * S_{1k} = 0 \tag{A.6}$$

where

$R_{1k} = m_1 s_k^2 + (c_1 + c_2)s_k + (k_1 + k_2)$

$R_{2k} = c_2 s_k + k_2$

$S_{1k} = c_2 s_k + k_2$

$S_{2k} = m_2 s_k^2 + c_2 s_k + k_2$

After substituting R_{1k}, R_{2k}, S_{1k} and S_{2k} into (A.3), we get.

$$\begin{bmatrix} m_1 s_k^2 + (c_1 + c_2)s_k + k_1 + k_2 & -c_2 s_k - k_2 \\ -c_2 s_k - k_2 & m_2 s_k^2 + c_2 s_k + k_2 \end{bmatrix} \begin{bmatrix} C_1 \\ C_2 \end{bmatrix} = \begin{bmatrix} 0 \\ 0 \end{bmatrix} \tag{A.7}$$

Now for a nontrivial response i.e., for non-zero values of C_1 and C_2, the determinant of their coefficient matrix must vanish. That is:

$$\left[m_1 s_k^2 + (c_1 + c_2)s_k + k_1 + k_2\right]\left[m_2 s_k^2 + c_2 s_k + k_2\right] + (c_2 s_k + k_2)^2 = 0 \tag{A.8}$$

Expansion of (A.8) leads to a characteristic equation of the system, obtained as shown in (A.9).

$$s_k^4 + t s_k^3 + u s_k^2 + v s_k + w = 0 \tag{A.9}$$

where

$t = \frac{m_1 c_2 + m_2(c_1 + c_2)}{m_1 m_2}$, $u = \frac{m_1 k_2 + m_2(k_1 + k_2) + c_1 c_2}{m_1 m_2}$, $v = \frac{k_1 c_2 + k_2 c_1}{m_1 m_2}$, $w = \frac{k_1 k_2}{m_1 m_2}$

Equation (A.9) is a fourth order polynomial in s and is to be solved to get four roots. All the coefficients of this polynomial are physical parameters of the system shown in Figure A.3 and are all positive. For that reason such a polynomial cannot have positive roots. Three allowable configurations of roots are as follows [20]:

1. Two pairs of complex conjugates.

2. One pair of complex conjugates and two real and negative roots.

3. Four real and negative roots.

Case 1: ***Two pairs of complex conjugates***

The system in this case has moderate damping. The rate of decay is defined by p_1, the real part of the root, and the frequency of vibration is specified by q_1, the imaginary part. The two pairs of complex conjugates are:

$(1) s_1 = -p_1 + iq_1$, $s_2 = -p_1 - iq_1$,

$(2) s_3 = -p_2 + iq_2$, $s_4 = -p_2 - iq_2$.

where p_1, p_2, q_1, and q_2 are all positive. s_1 and s_2 are the first pair of complex conjugates, and s_3 and s_4, the second pair.

The two roots s_1 and s_2 in the first pair will yield the solutions X_{11} and X_{21}, where the first subscript refers to the mass index and the second subscript refers to the pair number of the complex conjugate. The displacement components X_{11} and X_{21} due to s_1 and s_2 respectively are given by:

$$\begin{aligned} X_{11} &= A_{11} e^{-p_1 t} \times sin(q_1 t + \phi_{11}) \\ X_{21} &= A_{21} e^{-p_1 t} \times sin(q_1 t + \phi_{21}) \end{aligned} \tag{A.10}$$

where

$$\begin{aligned} A_{11}^2 &= 4 C_{11} C_{12} \\ A_{21} &= 4 C_{21} C_{22} \\ C_{11} &= m_2 s_1^2 + c_2 s_1 + k_2 \\ C_{21} &= c_2 s_1 + k_2 \\ C_{12} &= m_2 s_2^2 + c_2 s_2 + k_2 \\ C_{22} &= c_2 s_2 + k_2 \end{aligned}$$

The general solution is:

$$\begin{aligned} X_i &= \sum_{j=1}^{2} x_{ij} \\ &= A_{i1} e^{-p_1 t} sin(q_1 t + \phi_{i1}) + A_{i2} e^{-p_2 t} sin(q_2 t + \phi_{i2}) \end{aligned} \tag{A.11}$$

Case 2: ***One pair of complex conjugate and two real and negative roots:***

The general displacement solutions are shown in (A.12).

$$X_i = A_{i1} e^{-pt} sin(qt + \phi_{i1}) + C_{i3} e^{s_3 t} + C_{i4} e^{s_4 t} \tag{A.12}$$

where *i* = 1,2.

Case 3: ***Four real and negative roots:***

The system has a large damping. When it is disturbed, the system will settle to its equilibrium configuration without oscillation. The solutions of the 4^{th} order polynomial yield four real and negative roots. In [2], the authors focused just on the first case. In this paper we will also focus on the third case. The third case is for the system which has a large damping. When it is disturbed, the system will settle to its equilibrium configuration without oscillation. The displacement signal of the real crash is simular to a case of an overdamped vibrating system. Hence the third case would represent the vehicle frontal crash reconstruction. The solution for the case 3 is:

$$X_i(t) = C_{i1}e^{s_1 t} + C_{i2}e^{s_2 t} + C_{i3}e^{s_3 t} + C_{i4}e^{s_4 t} \tag{A.13}$$

with $i = 1, 2$, where s_i are roots of the characteristic equation (A.9)

A.3.1 Estimation of model parameters by Curve Fitting

When (A.13) is curve fitted into displacement experimental data, the constants C_{ik} and s_k (i=1,2 and k=1,...,4) can be easily found and resulting in a system of equations that can be solved for k_2 and c_2.

$$C_{1k} = m_2 s_k^2 + c_2 s_k + k_2 \tag{A.14}$$

$$C_{2k} = c_2 s_k + k_2 \tag{A.15}$$

For $k = 1, \ldots, 4$, equation (A.14) can be written in a matrix form as

$$\begin{bmatrix} 1 & s_1 \\ 1 & s_2 \\ 1 & s_3 \\ 1 & s_4 \end{bmatrix} \begin{bmatrix} k_2 \\ c_2 \end{bmatrix} = \begin{bmatrix} C_{11} - m_2 s_1^2 \\ C_{12} - m_2 s_2^2 \\ C_{13} - m_2 s_3^2 \\ C_{14} - m_2 s_4^2 \end{bmatrix} \tag{A.16}$$

Let

$$\mathbf{A} = \begin{bmatrix} 1 & s_1 \\ 1 & s_2 \\ 1 & s_3 \\ 1 & s_4 \end{bmatrix}, \mathbf{B}_2 = \begin{bmatrix} C_{11} - m_2 s_1^2 \\ C_{12} - m_2 s_2^2 \\ C_{13} - m_2 s_3^2 \\ C_{14} - m_2 s_4^2 \end{bmatrix}, \mathbf{V}_2 = \begin{bmatrix} k_2 \\ c_2 \end{bmatrix}$$

Then, (A.16) can be represented as

$$\mathbf{A} * \mathbf{V}_2 = \mathbf{B}_2 \tag{A.17}$$

and, using the pseudo-inverse, we can obtain

$$\mathbf{V}_2 = (\mathbf{A}^T * \mathbf{A})^{-1} * \mathbf{B}_2 \tag{A.18}$$

The spring stiffness k_1 and damping coefficient c_1 are calculated from (A.21).

$$\begin{bmatrix} 1 & s_1 \\ 1 & s_2 \\ 1 & s_3 \\ 1 & s_4 \end{bmatrix} \begin{bmatrix} k_1 \\ c_1 \end{bmatrix} = \begin{bmatrix} R_{11} - (m_1 s_1^2 + c_2 s_1 + k_2) \\ R_{12} - (m_1 s_2^2 + c_2 s_2 + k_2) \\ R_{13} - (m_1 s_3^2 + c_2 s_3 + k_2) \\ R_{14} - (m_1 s_4^2 + c_2 s_4 + k_2) \end{bmatrix} \tag{A.19}$$

Remark 1: From (A.5), it was shown that $R_{1k} = R_{2k} * \frac{S_{1k}}{S_{2k}}$. Let

$$\mathbf{V}_1 = \begin{bmatrix} k_1 \\ c_1 \end{bmatrix}, \mathbf{B}_1 = \begin{bmatrix} R_{11} - (m_1 s_1^2 + c_2 s_1 + k_2) \\ R_{12} - (m_1 s_2^2 + c_2 s_2 + k_2) \\ R_{13} - (m_1 s_3^2 + c_2 s_3 + k_2) \\ R_{14} - (m_1 s_4^2 + c_2 s_4 + k_2) \end{bmatrix} \tag{A.20}$$

then, we have

$$\mathbf{V}_1 = (\mathbf{A}^T * \mathbf{A})^{-1} * \mathbf{B}_1 \tag{A.21}$$

A.3.2 Eigensystem Realization Algorithm

In this section, a state-space representation (SSR) of the model is derived from the dynamic equation of a vehicle subjected to a frontal crash. The same representation is also retrieved from the system Markov parameters.

A.3.2.1 Formulation of the SSR from the model dynamic equations

Considering an input force $\mathbf{u}_1$ acting on the front mass m_1, equation (A.1) can be rewritten as

$$\begin{cases} \ddot{x}_1 = -\frac{k_1+k_2}{m_1}x_1 + \frac{k_2}{m_1}x_2 - \frac{c_1+c_2}{m_1}\dot{x}_1 + \frac{c_2}{m_1}\dot{x}_2 + \frac{1}{m_1}\mathbf{u}_1 \\ \ddot{x}_2 = \frac{k_2}{m_2}x_1 - \frac{k_2}{m_2}x_2 + \frac{c_2}{m_2}\dot{x}_1 - \frac{c_2}{m_2}\dot{x}_2 \end{cases} \tag{A.22}$$

The dymamic equation (A.22) can be rewritten in matix compact form as:

$$\boldsymbol{M}\begin{bmatrix}\ddot{x}_1 \\ \ddot{x}_2\end{bmatrix} + \mathbf{L}\begin{bmatrix}\dot{x}_1 \\ \dot{x}_2\end{bmatrix} + \boldsymbol{K}\begin{bmatrix}x_1 \\ x_2\end{bmatrix} = \begin{bmatrix}\mathbf{u}_1 \\ 0\end{bmatrix} \tag{A.23}$$

with

$$\boldsymbol{M} = \begin{bmatrix} m_1 & 0 \\ 0 & m_2 \end{bmatrix}, \boldsymbol{L} = \begin{bmatrix} c_1+c_2 & -c_2 \\ -c_2 & c_2 \end{bmatrix}, \boldsymbol{K} = \begin{bmatrix} k_1+k_2 & -k_2 \\ -k_2 & k_2 \end{bmatrix}$$

In general, the equation of motion for N degrees of freedom is expressed in a matrix form as:

$$\boldsymbol{M}\ddot{\boldsymbol{x}} + \boldsymbol{L}\dot{\boldsymbol{x}} + \boldsymbol{K}\boldsymbol{x} = \mathbf{B}_c\mathbf{u} \tag{A.24}$$

or, equivalently,

$$\ddot{\boldsymbol{x}} = -\boldsymbol{M}^{-1}\boldsymbol{L}\dot{\boldsymbol{x}} - \boldsymbol{M}^{-1}\boldsymbol{K}\boldsymbol{x} + \boldsymbol{M}^{-1}\boldsymbol{B}_c\mathbf{u} \tag{A.25}$$

Where $\boldsymbol{M} \in \mathbb{R}^{N\times N}$, $\boldsymbol{L} \in \mathbb{R}^{N\times N}$ and $\boldsymbol{K} \in \mathbb{R}^{N\times N}$ are the mass, damping, and stiffness matrices respectively, while $\boldsymbol{B}_c \in \mathbb{R}^{N\times r}$, is the input matrix.
$\ddot{\boldsymbol{x}}$, $\dot{\boldsymbol{x}}$ and $\boldsymbol{x}$ are vectors of generalized acceleration, velocity and displacements respectively, and the vector $\mathbf{u}$ of dimension $r \times 1$ is the input force containing r external excitations acting on the systems.

Let define new state variables

$\mathbf{x}_1 = x_1$, $\mathbf{x}_2 = \dot{x}_1$, $\mathbf{x}_3 = x_2$ and $\mathbf{x}_4 = \dot{x}_2$.

Substituting these variables into (A.22) and combining in state equations we get

$$\begin{bmatrix} \dot{\mathbf{x}}_1 \\ \dot{\mathbf{x}}_2 \\ \dot{\mathbf{x}}_3 \\ \dot{\mathbf{x}}_4 \end{bmatrix} = \begin{bmatrix} 0 & 1 & 0 & 0 \\ -\frac{k_1+k_2}{m_1} & -\frac{c_1+c_2}{m_1} & \frac{k_2}{m_1} & \frac{c_2}{m_1} \\ 0 & 0 & 0 & 1 \\ \frac{k_2}{m_2} & \frac{c_2}{m_2} & -\frac{k_2}{m_2} & -\frac{c_2}{m_2} \end{bmatrix} \begin{bmatrix} \mathbf{x}_1 \\ \mathbf{x}_2 \\ \mathbf{x}_3 \\ \mathbf{x}_4 \end{bmatrix} + \begin{bmatrix} 0 \\ \frac{1}{m_1} \\ 0 \\ 0 \end{bmatrix} \mathbf{u} \tag{A.26}$$

Using the original state variables and interchanging rows 2 and 3, columns 2 and 3 of (A.26), we get

$$\begin{bmatrix} \dot{x}_1 \\ \dot{x}_2 \\ \ddot{x}_1 \\ \ddot{x}_2 \end{bmatrix} = \begin{bmatrix} 0 & 0 & 1 & 0 \\ 0 & 0 & 0 & 1 \\ -\frac{k_1+k_2}{m_1} & \frac{k_2}{m_1} & -\frac{c_1+c_2}{m_1} & \frac{c_2}{m_1} \\ \frac{k_2}{m_2} & -\frac{k_2}{m_2} & \frac{c_2}{m_2} & -\frac{c_2}{m_2} \end{bmatrix} \begin{bmatrix} x_1 \\ x_2 \\ \dot{x}_1 \\ \dot{x}_2 \end{bmatrix} + \begin{bmatrix} 0 \\ 0 \\ \frac{1}{m_1} \\ 0 \end{bmatrix} \mathbf{u} \tag{A.27}$$

The output equation or the measurement vector $y(t)$, which may contain any combination of modal displacements, velocities, and / or accelerations is given by:

$$\mathbf{y} = \begin{bmatrix} \mathbf{C}_p x \\ \mathbf{C}_v \dot{x} \\ \mathbf{C}_a \ddot{x} \end{bmatrix} \tag{A.28}$$

Where $\mathbf{C}_p$, $\mathbf{C}_v$ and $\mathbf{C}_a$ are the output influence matrices for position, velocity and acceleration respectively. In our experiment the acceleration is measured. Therefore, the output equation is the acceleration measurement

$$y = \mathbf{C}_a \ddot{x}_1 \tag{A.29}$$

From (A.27)

$$\mathbf{y} = \ddot{x}_1 = \begin{bmatrix} -\frac{k_1+k_2}{m_1} & \frac{k_2}{m_1} & -\frac{c_1+c_2}{m_1} & \frac{c_2}{m_1} \end{bmatrix} \begin{bmatrix} x_1 \\ x_2 \\ \dot{x}_1 \\ \dot{x}_2 \end{bmatrix} + \begin{bmatrix} \frac{1}{m_1} \end{bmatrix} u \tag{A.30}$$

Therefore, the continuous-time state-space model of the dynamic system is written as

$$\begin{aligned} \dot{\mathbf{x}} &= \mathbf{A}_c\mathbf{x} + \mathbf{B}_c\mathbf{u} \\ y &= \mathbf{C}_c\mathbf{x} + \mathbf{D}_c\mathbf{u} \end{aligned} \tag{A.31}$$

with

$$\boldsymbol{A}_c = \begin{bmatrix} 0 & 0 & 1 & 0 \\ 0 & 0 & 0 & 1 \\ -\frac{k_1+k_2}{m_1} & \frac{k_2}{m_1} & -\frac{c_1+c_2}{m_1} & \frac{c_2}{m_1} \\ \frac{k_2}{m_2} & -\frac{k_2}{m_2} & \frac{c_2}{m_2} & -\frac{c_2}{m_2} \end{bmatrix}, \boldsymbol{B}_c = \begin{bmatrix} 0 \\ 0 \\ \frac{1}{m_1} \\ 0 \end{bmatrix},$$
$$\boldsymbol{C}_c = \begin{bmatrix} -\frac{k_1+k_2}{m_1} & \frac{k_2}{m_1} & -\frac{c_1+c_2}{m_1} & \frac{c_2}{m_1} \end{bmatrix}, \boldsymbol{D}_c = \begin{bmatrix} \frac{1}{m_1} \end{bmatrix}$$

Where $\mathbf{A}_c$ is the state matrix, $\mathbf{B}_c$ is the input matrix or the state influence matrix, $\mathbf{C}_c$ is the output matrix or the measurement influence matrix and $\mathbf{D}_c$ is the feed-forward matrix or the direct transmission matrix.

Once the $\mathbf{A}_c$, $\mathbf{B}_c$, $\mathbf{C}_c$ and $\mathbf{D}_c$ matrices are known, it is easy to find the transfer function (TF) and impulse response function (IRF) of the system. By using these matrices, system's response to any input can be found in time domain or frequency domain. The state-space representation is useful for constructing the mathematical model in MATLAB environment.

The discrete-time state-space representation of a MIMO system is given by equation (A.32).

$$\begin{aligned} \mathbf{x}(k+1) &= \hat{\mathbf{A}}\mathbf{x}(k) + \hat{\mathbf{B}}\mathbf{u}(k) \\ y(k) &= \hat{\mathbf{C}}\mathbf{x}(k) + \hat{\mathbf{D}}\mathbf{u}(k) \end{aligned} \tag{A.32}$$

Where k is the integer discrete-time index at time instant $t = k\Delta t$, $x(k)$ is the state vector at the discrete-time k, $u(k)$ is the force vector, $y(k)$ is the output vector, $\hat{\mathbf{A}}$ is the discrete state system matrix, and $\hat{\mathbf{B}}$ is the discrete input influence matrix for the state vector $x(k)$. The output matrix $\hat{\mathbf{C}} = \mathbf{C}_c$ and the direct transition matrix $\hat{\mathbf{D}} = \mathbf{D}_c$ during the zero-order-hold operations. Because experimental data are discrete in nature, equation (A.32) form the basis for the system identification of linear time invariant, dynamical systems. The state matrix $\hat{\mathbf{A}}$ and the influence matrix $\hat{\mathbf{B}}$ of the discrete-time model are related to the matrices $\mathbf{A}_c, \mathbf{B}_c$ of the continuous-time model by the following expression [14]:

$$\begin{aligned} \hat{\mathbf{A}} &= e^{\mathbf{A}_c \Delta t} \\ \hat{\mathbf{B}} &= \int_0^{\Delta t} e^{\mathbf{A}_c \tau} d\tau \cdot \mathbf{B}_c \end{aligned} \tag{A.33}$$

The continuous-time model is calculated from the discrete-time model by

$$\begin{aligned} \mathbf{A}_c &= ln(\hat{\mathbf{A}})/\Delta t \\ \mathbf{B}_c &= \mathbf{A}_c(\hat{\mathbf{A}} - I)^{-1} * \hat{\mathbf{B}} \end{aligned} \tag{A.34}$$

where Δt is a constant interval.
The dimensions of the discrete-time system are equal to those of the continuous system.

A.3.2.2 ERA from the system Markov parameters

ERA is a minimum order realization technique that uses singular value decomposition technique. A Flowchart for the ERA is shown in Figure A.4.

If the excitations of the dynamic system is measured by the *m* input quantities in the vector *u*, the equations of motions and the set of output equations can both be respectively rewritten in terms of the state vector.
ERA begins with the definition of the Markov parameter of a state-space model. The method for deriving the expression for the system matrices is adapted from [14]. Consider a discrete-time state-space model (A.33).

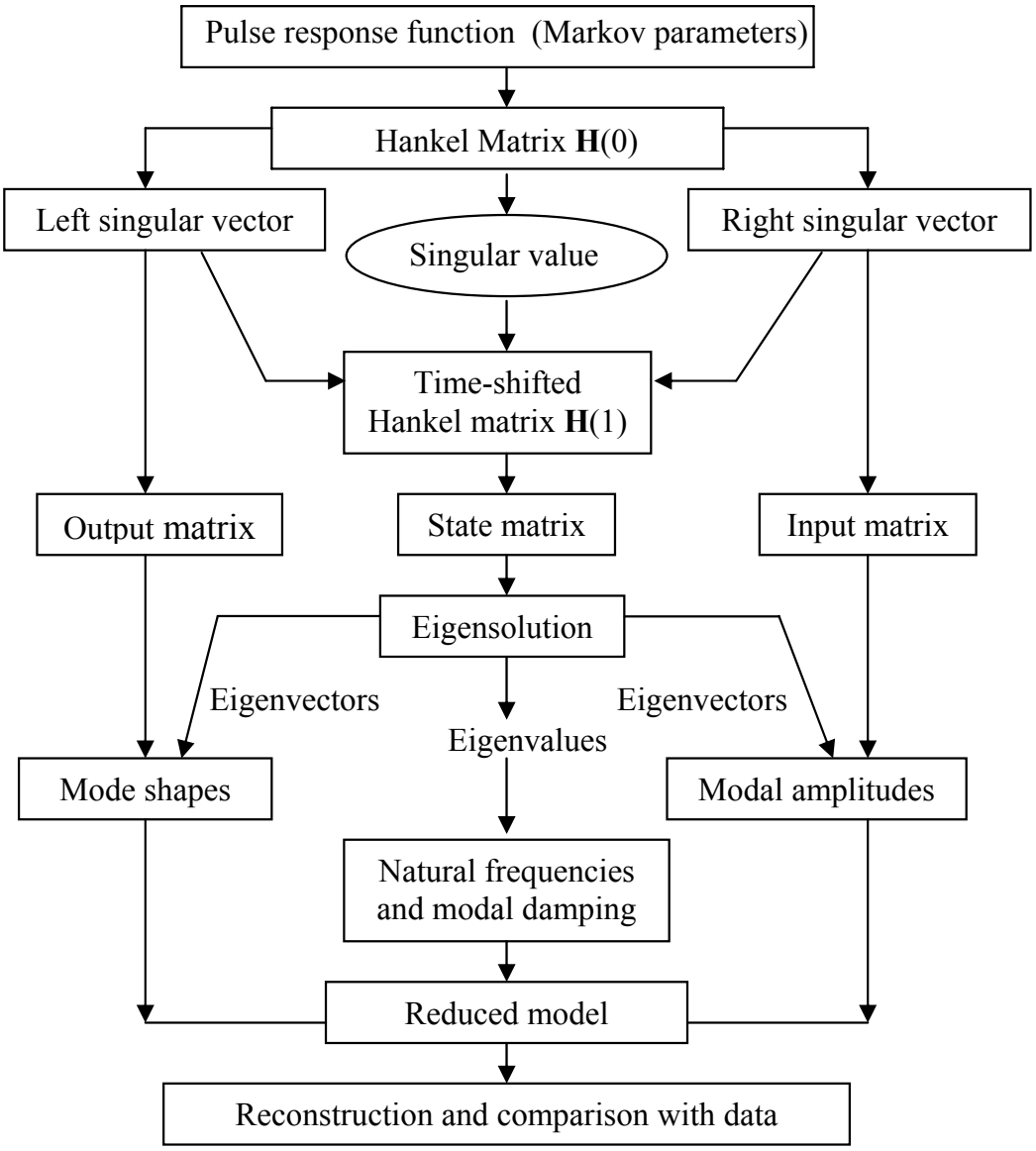

Figure A.4: Flowchart for the ERA by J.N. Juang [14]

The state-space model (A.33) has an impulse response

$$y(k) = \begin{cases} \hat{D} & k = 0, \\ \hat{C}\hat{\mathbf{A}}^{k-1}\hat{\mathbf{B}} & k \geq 1 \end{cases} \tag{A.35}$$

The discrete-time Markov parameters can be defined in the same way as (A.35). The term of $\hat{C}\hat{\mathbf{A}}^{k-1}\hat{\mathbf{B}}$ is called the Markov parameter of the system. By using these parameters one can define the impulse response of the system.

$$Y[k] = \hat{C}\hat{\mathbf{A}}^{k-1}\hat{\mathbf{B}} \tag{A.36}$$

$$Y[0] = \hat{D}, Y[1] = \hat{C}\hat{B}, Y[2] = \hat{C}\hat{A}\hat{B}, ..., Y[k] = \hat{C}\hat{\mathbf{A}}^{k-1}\hat{\mathbf{B}} \tag{A.37}$$

Consequently, the identification problem is: Given values of $Y[k]'s$, construct the constant matrices to identify the system.
The algorithm begins by constructing a $r \times s$ generalized Hankel matrix,

Given a number of input and output measurements u_k and y_k generated by a system of unknown parameters, it is requested to identify the order of the system as well as the discrete state matrices ($\hat{\mathbf{A}}$, $\hat{\mathbf{B}}$, $\hat{\mathbf{C}}$, $\hat{\mathbf{D}}$) of the system. Then the identified continuous state matrices ($\mathbf{A}_c$,$\mathbf{B}_c$, $\mathbf{C}_c$, $\mathbf{D}_c$) that has the same size as the physical model, can be estimated from (A.34) and finally extract the respective parameters.
All minimum realizations have the same set of eigenvalues and eigenvectors, which are the modal parameters of the system itself. Assume that the state matrix $\hat{\mathbf{A}}$ of order n has a complete set of linearly independent eigenvectors $\{\Psi_1, \Psi_2, ..., \Psi_n\}$ with corresponding eigenvalues $\{\lambda_1, \lambda_2, ...\lambda_n\}$:

$$\hat{\mathbf{A}}\Psi = \Psi\Lambda \tag{A.38}$$

where Λ is a diagonal matrix of the eigenvalues and Ψ is the matrix of the eigenvectors. The realization $\{\hat{A}, \hat{B}, \hat{C}\}$ can be transformed in the realization $\{\Lambda, \Psi^{-1}\hat{B}, \hat{\mathbf{C}}\Psi\}$ by using the eigenvalues and eigenvectors matrices. The diagonal matrix Λ contains the informations of modal damping rates and damped natural frequencies. The matrix $\Psi^{-1}\hat{B}$ defines the initial modal amplitudes and the matrix $\hat{\mathbf{C}}$ Ψ denotes the mode shapes at the sensor points.
All the modal parameters of a dynamic system can thus be identified by the triplet $\{\Lambda, \Psi^{-1}\hat{B}, \hat{\mathbf{C}}\Psi\}$.

The real part of Λ, into the continuous time model, gives the modal damping rates, while the imaginary part gives the damped natural frequencies.
After identifying the combined system and observer gain Markov parameters, the next step consist of forming the generalized Hankel matrix $H_{(k-1)}$:

$$H_{(k-1)} = \begin{bmatrix} Y_k & Y_{(k+1)} & \dots & Y_{(k+\beta+1)} \\ Y_{k+1} & Y_{(k+2)} & \dots & Y_{(k+\beta)} \\ \vdots & \vdots & \vdots & \vdots \\ Y_{(k+\alpha-1)} & Y_{(k+\alpha)} & \dots & Y_{(k+\alpha+\beta-2)} \end{bmatrix} \tag{A.39}$$

when *k*=1 we get:

$$H_{(0)} = \begin{bmatrix} Y_1 & Y_2 & \dots & Y_\beta \\ Y_2 & Y_3 & \dots & Y_{(\beta+1)} \\ \vdots & \vdots & \vdots & \vdots \\ Y_\alpha & Y_{\alpha+1} & \dots & Y_{\alpha+\beta-1} \end{bmatrix} \tag{A.40}$$

In order to compute a minimum order realization of the system $\{\hat{\mathbf{A}}, \hat{\mathbf{B}}, \hat{\mathbf{C}}\}$, it is necessary to construct a shifted Hankel matrix $H_{(1)}$:

$$H_{(1)} = \begin{bmatrix} Y_2 & Y_3 & \dots & Y_{\beta+1} \\ Y_3 & Y_4 & \dots & Y_{\beta+2} \\ \vdots & \vdots & \vdots & \vdots \\ Y_{(\alpha+1)} & Y_{(\alpha+2)} & \dots & Y_{(\alpha+\beta)} \end{bmatrix}$$

Substituting the Markov parameters from (A.37) into (A.39) and decomposing $H(k-1)$ into three matrices yield

$$H(k-1) = \boldsymbol{O}_b \hat{A}^{k-1} \boldsymbol{C}_t \tag{A.41}$$

where$\boldsymbol{O}_b$ and $\boldsymbol{C}_t$ are

$$\boldsymbol{O}_b = \begin{bmatrix} \hat{C} \\ \hat{C}\hat{A} \\ \hat{C}\hat{A}^2 \\ \vdots \\ \hat{C}\hat{A}^{\alpha-1} \end{bmatrix}, \boldsymbol{C}_t = \begin{bmatrix} \hat{B} & \hat{A}\hat{B} & \hat{A}^2\hat{B} & \dots & \hat{A}^{\beta-1}\hat{B} \end{bmatrix}$$

The block matrix $\boldsymbol{O}_b$ is the observability matrix, whereas the block matrix $\boldsymbol{C}_t$ is the controllability matrix.

Denote column submatrices of $\hat{B}$ by $\hat{B}_i$ and row submatrices of $\hat{C}$ by $\hat{C}_j$. The ERA data block matrix can be expressed by

$$H_{(k-1)} = [Y_{s_i+k+t_j}]; Y_{s_i+k+t_j} = C_j \hat{A}^{s_i+k-1+t_j} B_i \tag{A.42}$$

$$H(k) = \boldsymbol{O}_b \hat{A}^k \boldsymbol{C}_t \tag{A.43}$$

Assume that there exists a matrix $H^\dagger$ satisfying the relation

$$\boldsymbol{O}_b H^\dagger \boldsymbol{C}_t = I_n \tag{A.44}$$

where I_n is an identity matrix of order n. The matrix $H^\dagger$ which is the pseudo-inverse of $H(0)$ plays a major role in deriving the ERA. It is observed that

$H(0)H^\dagger H(0) = \boldsymbol{O}_b \boldsymbol{C}_t H^\dagger \boldsymbol{O}_b \boldsymbol{C}_t = \boldsymbol{O}_b \boldsymbol{C}_t = H(0)$

The ERA process starts with the factorization of the block data matrix (A.40) using singular value decomposition,

$$H_{(0)} = R \sum S^T \tag{A.45}$$

where the column of matrices R and S are orthonormal and $\sum$ is a rectangular matrix

$$\sum = \begin{bmatrix} \sum_n & 0 \\ 0 & 0 \end{bmatrix}$$

with $\sum_n = diag\{\sigma_1, \sigma_2, \dots, \sigma_i, \sigma_{i+1}, \dots \sigma_n\}$.
Let R_n and $\sum_n S_n$ be matrices formed by the first n columns of R and S respectively. Hence, the matrix $H(0)$ and $H^\dagger$ become

$$H_{(0)} = R_n \sum_n S_n^T \tag{A.46}$$

and

$$H^{\dagger} = S_n \sum_n^{-1} R_n^T \tag{A.47}$$

where $R_n^T R_n = I_n = S_n^T S_n$

Examining the singular value $\sum_n$ of the Hankel matrix $H_{(0)}$ it is possible to determine the order of the system.

Comparing (A.46) and (A.43) with k=0, we get
$\boldsymbol{O}_b = R_n \sum_n^{1/2}$ and $\boldsymbol{C}_t = \sum_n^{1/2} S_n^T$
From (A.43) , the first r columns of the observability matix $\boldsymbol{O}_b$ form the input matrix $\hat{B}$ whereas the first m rows of the controlability matix $\boldsymbol{C}_t$ form the output matrix $\hat{C}$.

With $k = 1$ in (A.43), we get

$$H_{(1)} = \boldsymbol{O}_b \hat{A} \boldsymbol{C}_t = R_n \sum_n^{1/2} \hat{A} \sum_n^{1/2} S_n^T$$

One obvious solution for the state matrix $\hat{A}$ becomes

$$\hat{A} = \sum_n^{-1/2} R_n^T H(1) S_n \sum_n^{-1/2}$$
Let O_i be a null matrix of order i, I_i an identity matrix of order i and the matrices $\mathbf{E}_m^T$ and $\mathbf{E}_r^T$ are defined as:

$$\mathbf{E}_m^T = \begin{bmatrix} \mathbf{I}_m & \mathbf{0}_m & \dots & \mathbf{0}_m \end{bmatrix}, \mathbf{E}_r^T = \begin{bmatrix} \mathbf{I}_r & \mathbf{0}_r & \dots & \mathbf{0}_r \end{bmatrix}$$

where m is the number of outputs and r is the number of inputs.
Finally, using Equations (A.42), (A.43), (A.44), (A.46) and (A.47), the basic formulation of the minimum order realization for the ERA/OKID (OKID means Observer/Kalman filter Identificationis) is:

$$Y_k = E_m^T R_n \sum_n^{-1/2} \left[\sum_n^{-1/2} R_n^T H(1) S_n \sum_n^{-1/2} \right]^{k-1} \sum_n^{-1/2} S_n^T E_r$$

Recall that in (A.36) $Y[k] = \hat{C} \hat{\mathbf{A}}^{k-1} \hat{\mathbf{B}}$.
Hence, a minimal order realisation is as follows:

$$\begin{cases} \hat{\mathbf{A}} = \sum_n^{-1/2} \mathbf{R}_n^T \mathbf{H}_{(1)} S_n \sum_n^{-1/2} \\ \hat{\mathbf{B}} = \sum_n^{-1/2} \mathbf{S}_n^T \mathbf{E}_r \\ \hat{\mathbf{C}} = \mathbf{E}_m^T \mathbf{R}_n \sum_n^{-1/2} \\ \hat{\mathbf{D}} = \mathbf{Y}_{(0)} \end{cases} \tag{A.48}$$

The continuous state matrix $\mathbf{A}_c$ and the input influence matrix $\mathbf{B}_c$ are obtained from (A.34), and the physical parameters - matrices ***M***, ***L*** and ***K*** are embedded in the state matrix $\mathbf{A}_c$.

A.4 Results and discussion

A.4.1 Parameters estimation from curve fitting approach

From the curve fitting, the values for s_i and C_{1j} (j=1,...,4) are found to be: $C_{11} = 6.65$, $C_{12} = -4.37$, $C_{13} = 1.761$, $C_{14} = -4.093$, $s_1 = -8.082$, $s_2 = -13.77$,$s_3 = 0.523$, $s_1 = -2.428$.
The result from the curve fitting is shown in Figure A.5.

A.4.2 Vehicle crash experimental data analysis

It is observed from Figure A.6, that the dynamic crash from the real vehicle crash test is 53.17 cm and occurs at time t_c= 0.078 ms, when the unfiltered data are used in the analysis. The filtered data result in a dynamic crash of 51.11 cm at time t_c= 74.5 ms as shown in Figure A.7.
The initial velociy for both filtered and unfiltered data is closer to 35 km/h (i.e. 34.99 km/h for the unfiltered data and 35.28 km/h for the filtered data).

A.4.3 Results from the model

Four different cases are considered in this section as a sample of results. Let m_1 be the mass of the chassis, m_2 the mass of passenger compartment and $m_t = 873kg$ the total mass of the vehicle.

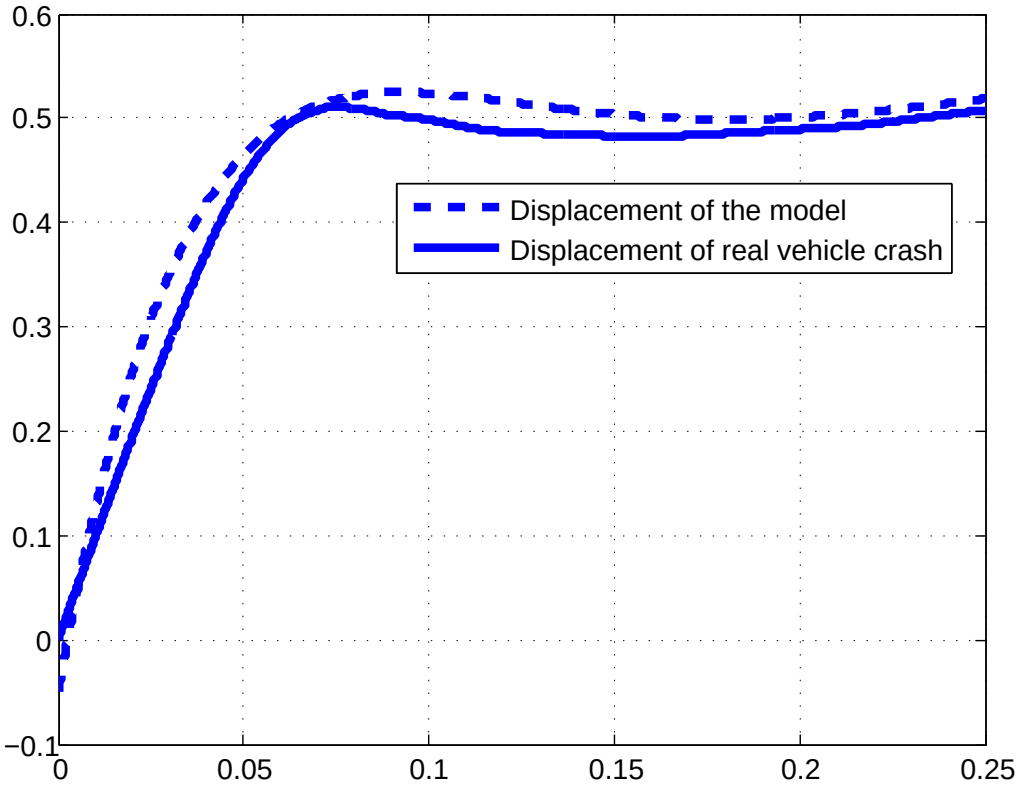

Figure A.5: Result from curve fitting

Case 1: $(m_1 < m_2)$: $m_1 = \frac{1}{3}m_t$, $m_2 = \frac{2}{3}m_t$

From Figure A.8, the dynamic crash of m_2 is 80 cm which is the displacement of the passenger compartment. Therefore this model cannot represent the vehicle crash scenarion. It is observed that, the time for dynamic crash is longer than that for the real crash (i.e. 0.17 s instead of 0.078 s).The dynamic crash of m_1 is 42.5 cm and occurs after 0.17s.

Case 2: $(m_1 > m_2)$: $m_1 = \frac{2}{3}m_t$, $m_2 = \frac{1}{3}m_t$

From Figure A.9, the dynamic crash of the passenger compartment m_2 is 66.2 cm . The time for dynamic crash increases futher up to 0.15 s. The dynamic crash of m_1 is 45.5 cm and occurs after 0.13s.Therefore for this case, the model cannot represent the vehicle crash scenario.

Case 3: $(m_1 < m_2)$: $m_1 = \frac{1}{4}m_t$, $m_2 = \frac{3}{4}m_t$

From Figure A.10, the dynamic crash of the passenger compartment m_2 is 69 cm . The time for dynamic crash is 0.15s. The dynamic crash of m_1 is 30.9 cm and occurs after 0.14s. This also cannot represent the real vehicle crash test.

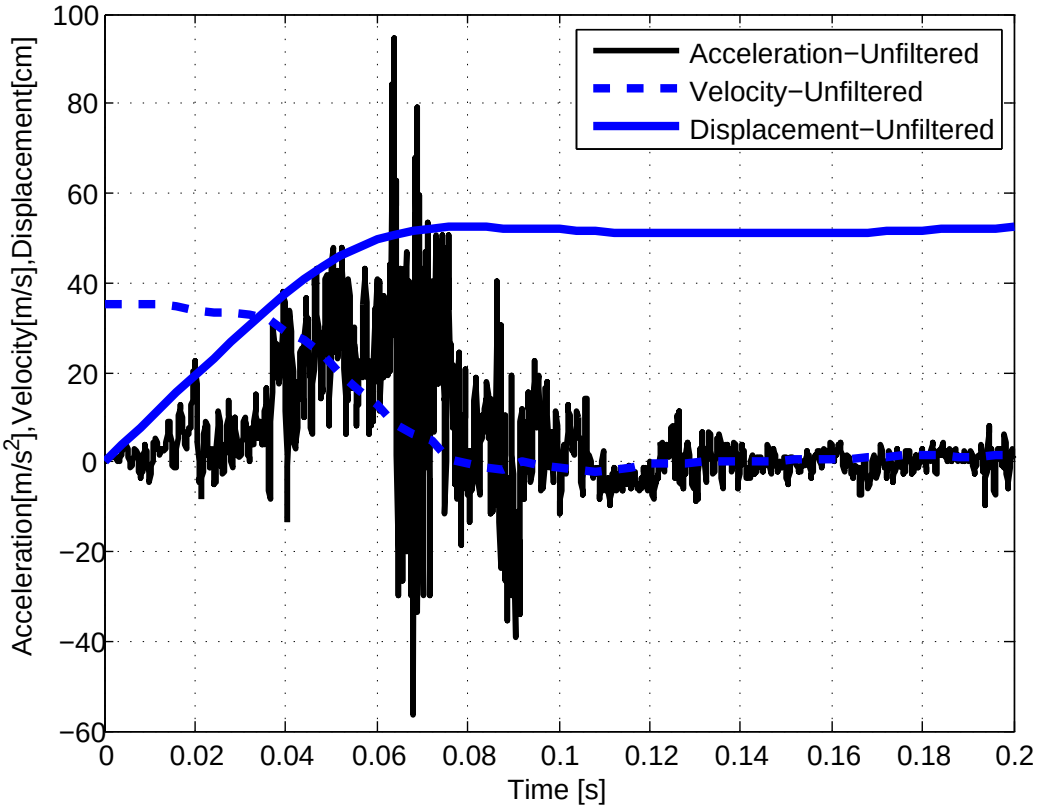

Figure A.6: Unfiltered data plot from the real vehicle crash test

Case 4: $(m_1 > m_2)$: $m_1 = \frac{3}{4}m_t$, $m_2 = \frac{1}{4}m_t$

From Figure A.11, the dynamic crash of the passenger compartment m_2 is 49.8 cm and the time for dynamic crash is 0.11s. The dynamic crash of m_1 is 35.5 cm and occurs after 0.1s. Therefore, this case can represent the vehicle crash senarion because the dynamic crash is much closer to that from the real vehicle crash and the time is relatively small as compared to other cases.

A summary of main results is shown in Table A.1. The values for k_2 and c_2 are the first and second entry of vector $\mathbf{V}_2$ in (A.18). The values for k_2 and c_2 depend on the value of mass m_2 taken into consideration. Values for k_1 and c_1 are obtained from vector $\mathbf{V}_1$ in (A.21). The stiffness coefficients which result in a closer vehicle crash reconstruction are found to be $k_1 = 74681N/m$, $k_2 = 45821N/m$ and the damping coefficients are: $c_1 = 18176Ns/m$, $c_2 = 11196Ns/m$ when the mass of the chassis is $\frac{3}{4}$ the total mass of the vehicle (m_t), where the dynamic crash of the passenger compartment is equal to 49.8 cm and occurs after 0.11s (see sub section **4.3 case 4**, Figure A.11).

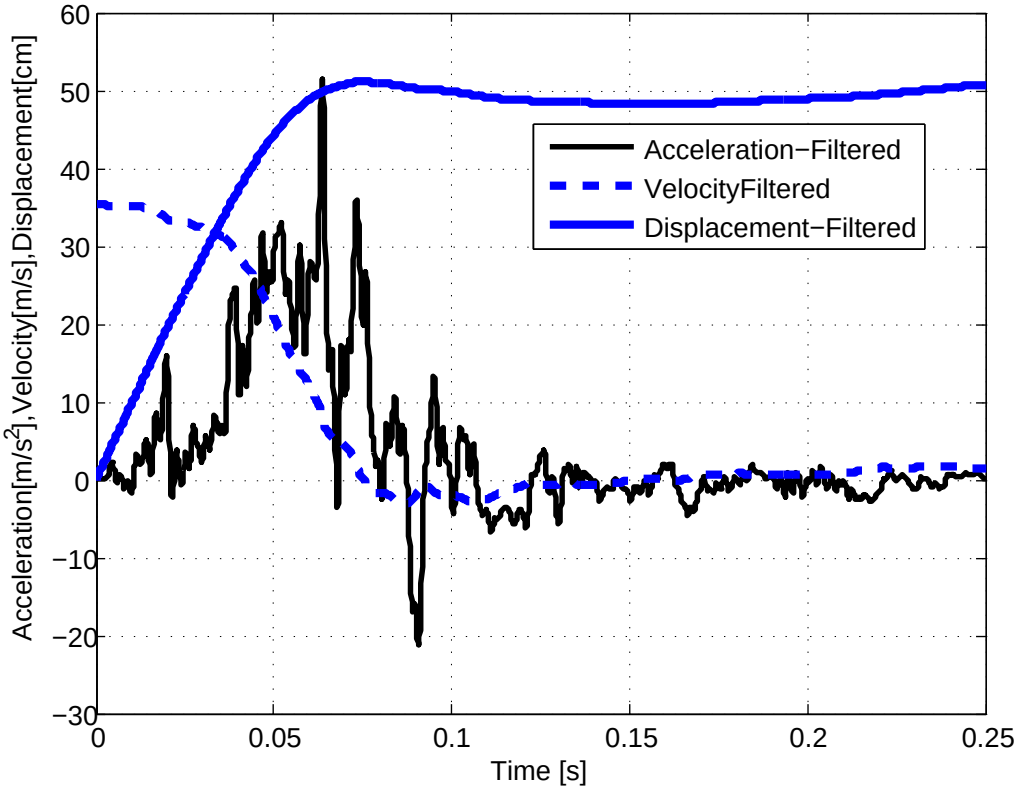

Figure A.7: Filtered data plot from the real vehicle crash test

It is observed that the passenger compartment m_2 is the one that reconstructs the vehicle crash. When the mass of the chassis is greater than that of the passenger compartment, the results from the model are closer to the expected values. For example, when m_1 =582 kg (i.e.$\frac{3}{4}$ of the total mass of the vehicle) and m_2 =291 kg (i.e. $\frac{1}{4}$ of the mass of the vehicle), the dynamic crash of the passenger compartment is 49.8 cm which is closer to 51.11 cm (the dynamic crash from the real vehicle crash).

Remark2: It is noting that optimal values for stiffness and damping coefficients are not fixed. They are dependent on the mass of passenger compartment taken into consideration.

A.4.4 State-Space Realization of the system by ERA

Consider a 2^{nd} order system (i.e n=2) for a single degree of freedom and N=100, the number of samples to assemble the Hankel matrix. It is observed that the continuous system matrices from the ERA are

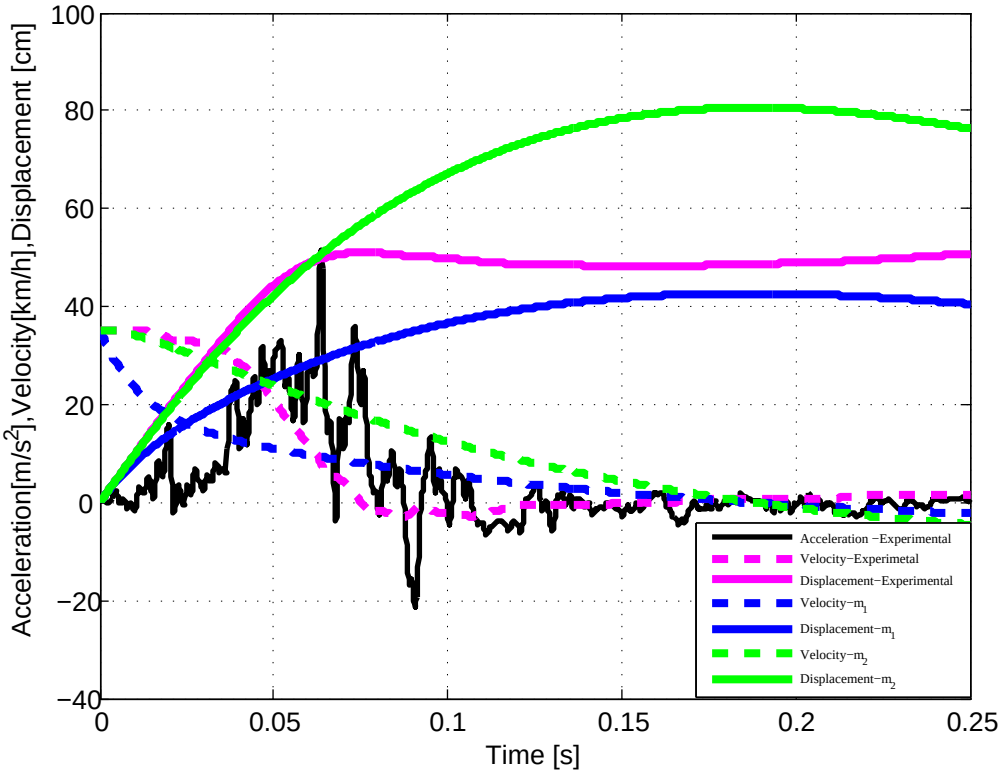

Figure A.8: Comparative analysis between Vehicle crash test and model results for $m_1 = \frac{1}{3}m_t$

Table A.1: Parameters estimation

Parameters	Case 1	Case 2	Case 3	Case4
	m_1=1/3 m_t	m_1=2/3 m_t	m_1=1/4 m_t	m_1=3/ 4 m_t
	Dynamic crash[cm]=80	Dynamic crash[cm]= 66	Dynamic crash[cm]=69	Dynamic crash[cm]=49.8
	Time of crash[s]=0.17	Time of crash[s]= 0.15	Time of crash[s]=0.14	Time of crash[s]=0.11
k_1 [N/m]	45929		74681	
k_2 [N/m]	40731		45821	
c_1 [Ns/m]	13687		18176	
c_2 [Ns/m]	9952		11196	

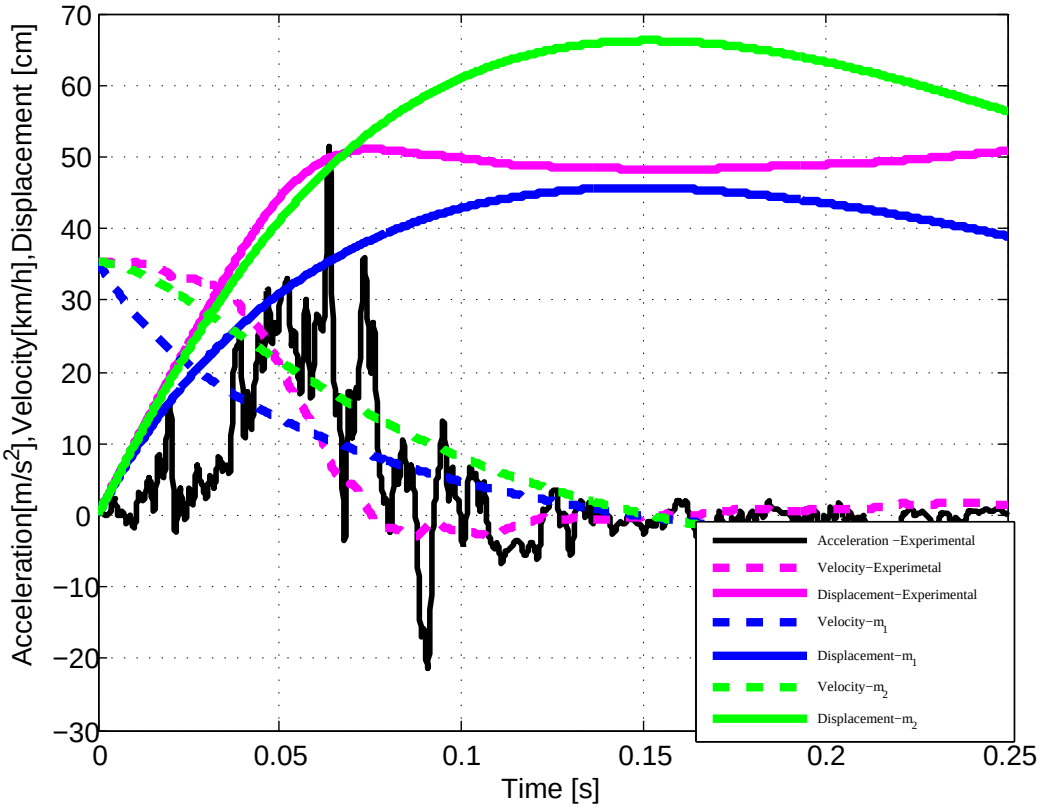

Figure A.9: Comparative analysis between Vehicle crash test and model results for $m_2 = \frac{1}{3}m_t$

$$\mathbf{A}_c = \begin{bmatrix} 95.5776 & -545.1246 \\ 545.12 & -131.6485 \end{bmatrix}; \mathbf{B}_c = \begin{bmatrix} -1474.8 \\ 5798.1 \end{bmatrix};$$
$$\mathbf{C} = \begin{bmatrix} 0.1639 & 0.5717 \end{bmatrix}; D = 0.1964$$

From the state-Matrix A_c, the eigenvectors Ψ and eigenvalues Λ were found to be

$$\Psi, \Psi^* = \begin{bmatrix} 0.1474 \pm 0.6916i \\ 0.7071 \end{bmatrix};$$

and $\Lambda = diag\{-18.04 \pm 533.15i\}$

The natural frequency and the damping ratio of a single degree of freedom are 533 rad/s and 0.0338 respectifely. The bode diagram for the system is shown in

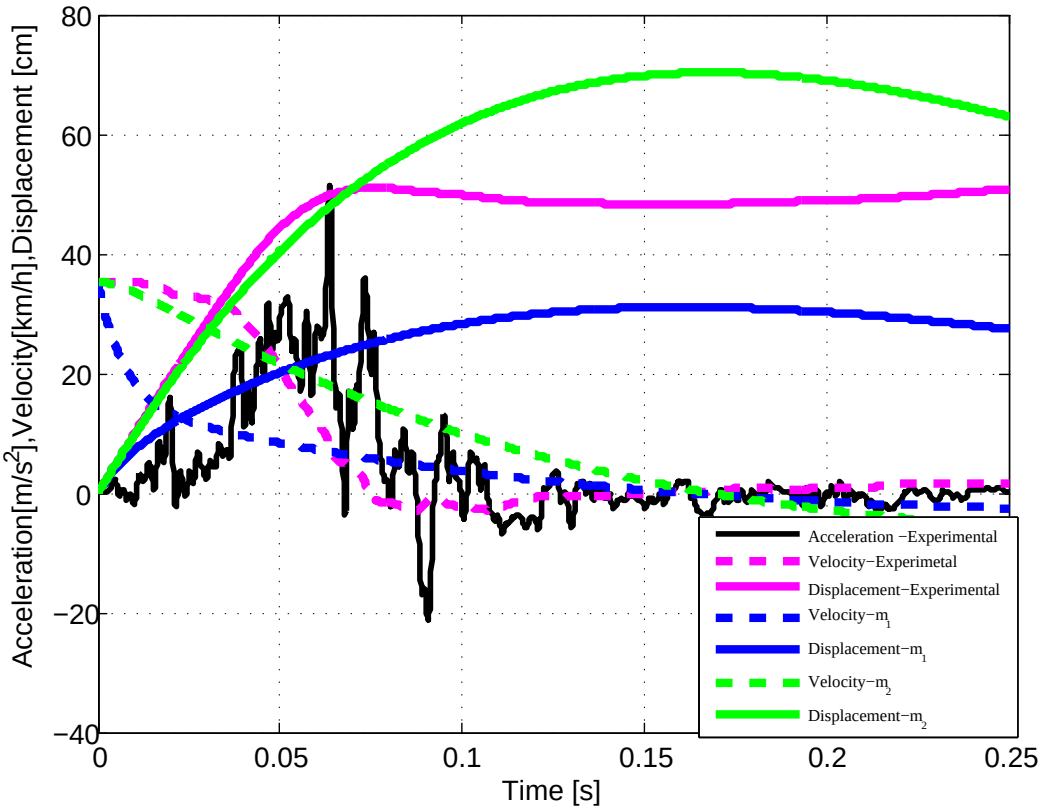

Figure A.10: Comparative analysis between Vehicle crash test and model results for $m_1 = \frac{1}{4}m_t$

Figure A.12

Considering a 4^{th} order system (i.e n=4) for a two degree of freedom and the number of samples to assemble the Hankel matrix equal to N=60, it is observed that the continuous state-space realization from the ERA are found to be:

$$\mathbf{A}_c = \begin{bmatrix} -22.5 & -526.3 & 56.2 & 141.5 \\ 526.3 & -243.8 & 631.5 & 279.9 \\ 56.2 & -631.5 & -171.2 & -1363.2 \\ -141.5 & 279.9 & 136.2 & -445.9 \end{bmatrix}; \mathbf{B}_c = \begin{bmatrix} -1990.8 \\ 5436.8 \\ 3302.4 \\ -4233.2 \end{bmatrix};$$

$$\mathbf{C} = \begin{bmatrix} 0.2149 & 0.5366 & -0.3368 & -0.3826 \end{bmatrix}; D = 0.1964$$

with

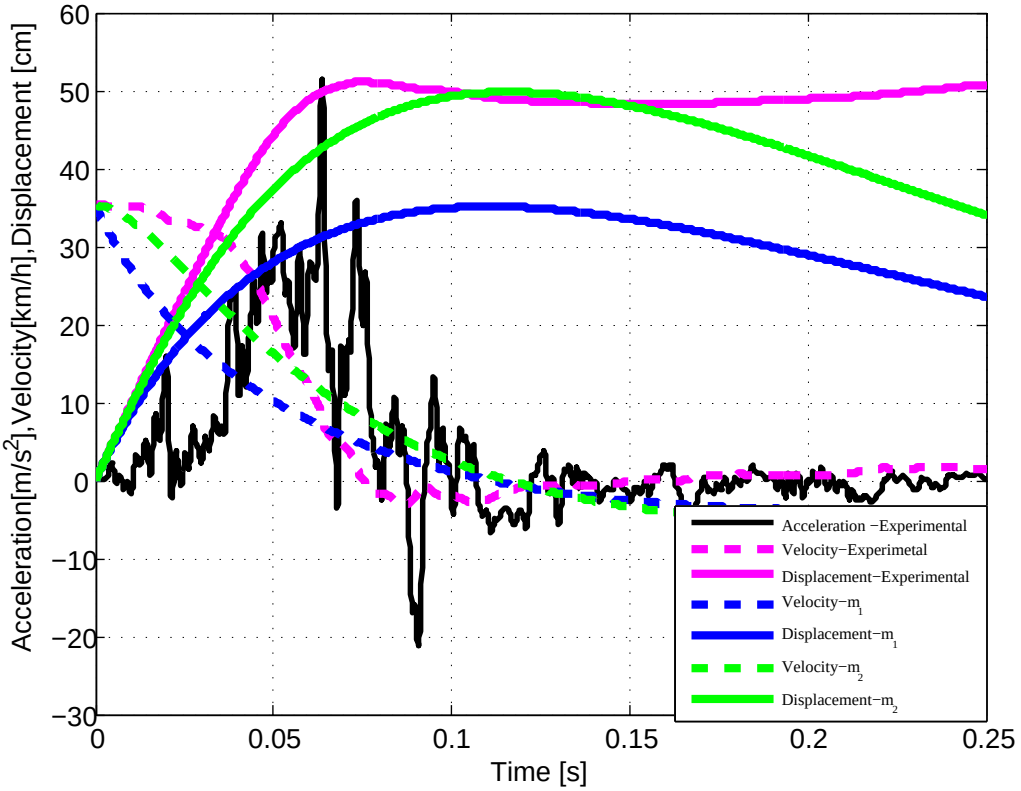

Figure A.11: Comparative analysis between Vehicle crash test and model results for $m_2 = \frac{1}{4}m_t$

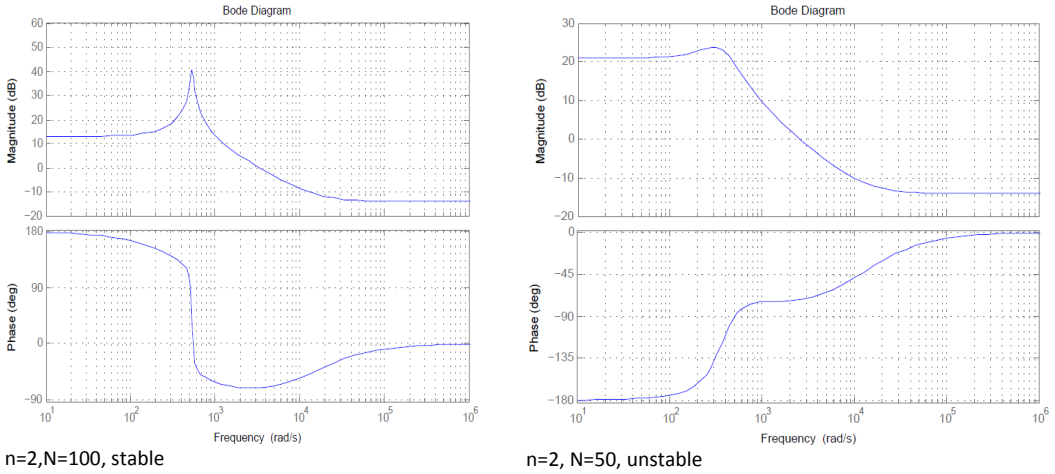

Figure A.12: Bode diagram for n=2, N=100 and N=50

$$\Psi_1, \Psi_1^* = \begin{bmatrix} 0.6864 \\ 0.2979 \mp 0.5573i \\ -0.1126 \pm 0.1269i \\ -0.0715 \pm 0.3092i \end{bmatrix}; \Psi_2, \Psi_2^* = \begin{bmatrix} 0.0537 \mp 0.0828i \\ -0.1269 \mp 0.3363i \\ 0.7002 \\ 0.0587 \mp 0.6061i \end{bmatrix};$$

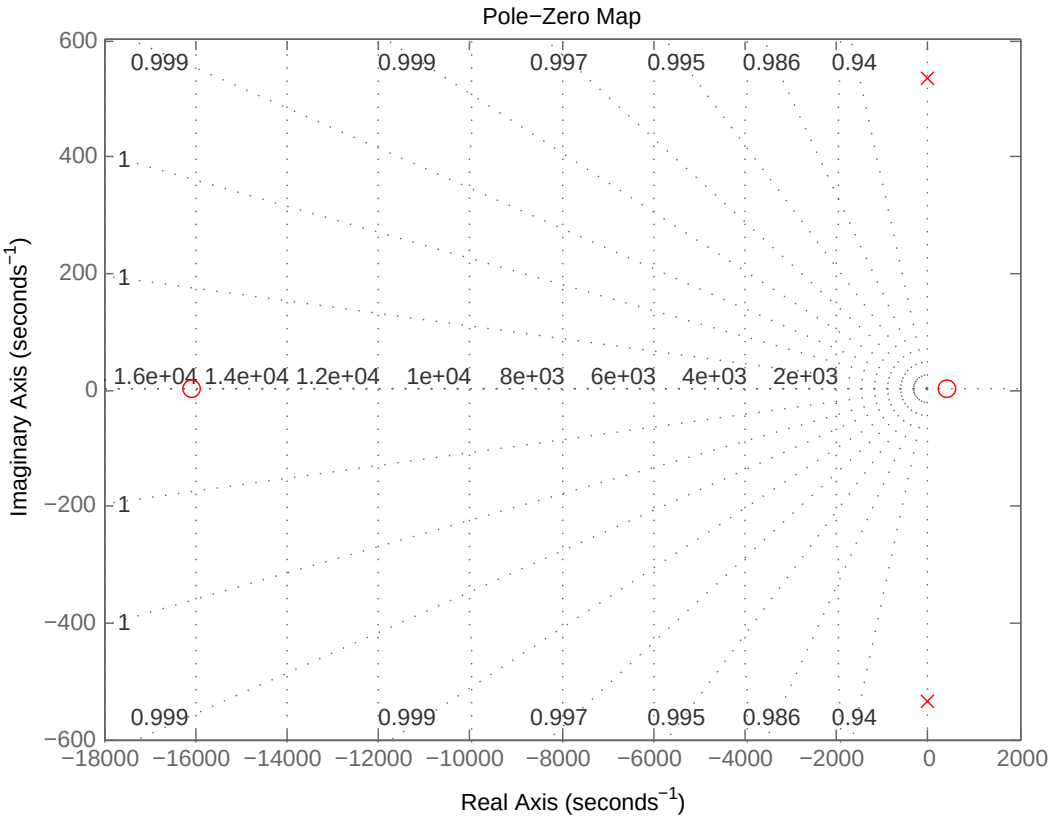

Figure A.13: Pole-zero map for n=2, N=100

and $\Lambda = diag\{-274.9 \pm 501.4i, -166.8 \pm 1476.7i\}$

The natural frequecies and damping ratios are:
ω_{n_1} = 3592.8 rad/s, ω_{n_2} = 9337.4 rad/s, ζ_1 = 0.481, ζ_2 = 0.112

For higher sample size, (i.e. N=2501 with order n=4), the system matrices are:

$$\mathbf{A}_c = \begin{bmatrix} 0.1 & -615.1 & -3.6 & -4.9 \\ 615.1 & -13.1 & -24.9 & -5.3 \\ -3.6 & 24.9 & -2.1 & -577.0 \\ -4.9 & -5.3336 & 577.0 & -0.9876 \end{bmatrix}; \mathbf{B}_c = \begin{bmatrix} 1280.1 \\ -5366.1 \\ 1636.4 \\ -946.8 \end{bmatrix};$$

$$\mathbf{C} = \begin{bmatrix} -0.144 & -0.5322 & -0.1656 & -0.0897 \end{bmatrix}; D = 0.1964$$

with

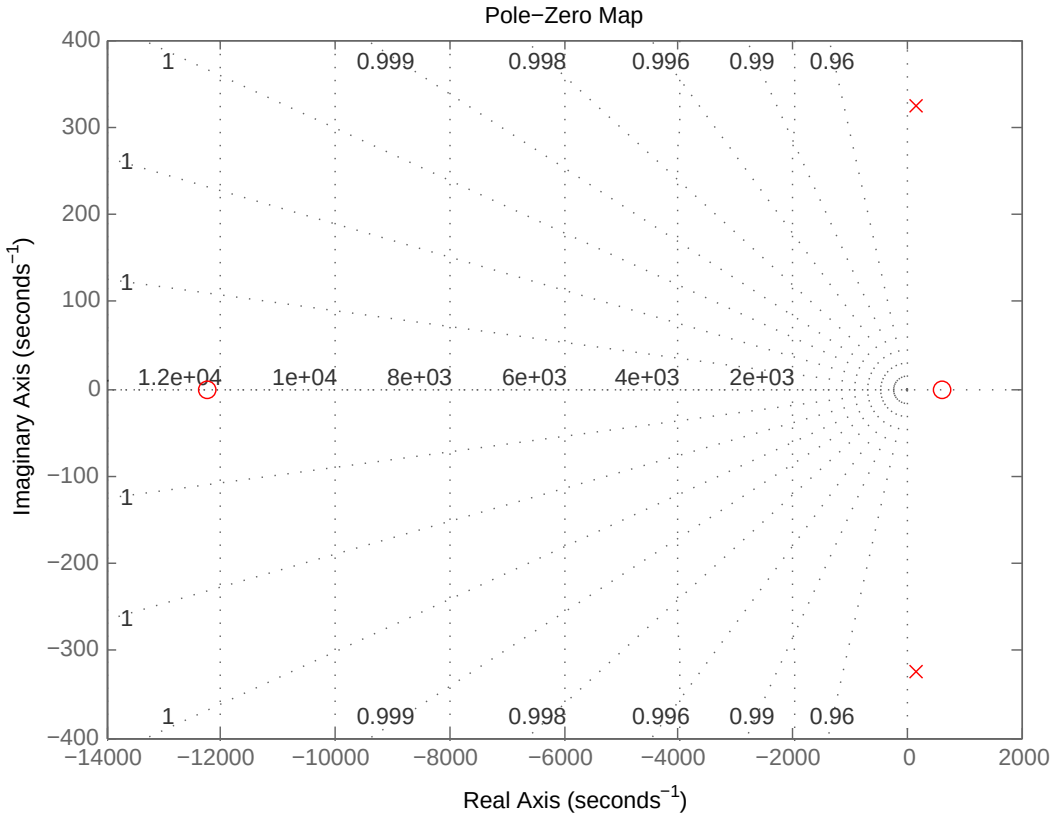

Figure A.14: Pole-zero map for n=2, N=50

$$\Psi_1, \Psi_1^* = \begin{bmatrix} 0.0053 \pm 0.6800i \\ 0.6840 \\ -0.0869 \mp 0.1733i \\ -0.1561 \pm 0.0880i \end{bmatrix}; \Psi_2, \Psi_2^* = \begin{bmatrix} 0.0878 \pm 0.1732i \\ 0.1572 \mp 0.0850i \\ -0.0027 \pm 0.6799i \\ 0.6841 \end{bmatrix};$$

and $\Lambda = diag\{-4.39 \pm 617i, -3.85 \pm 575i\}$ The natural frequecies and damping ratios are:
ω_{n_1} = 617 rad/s, ω_{n_2} = 575 rad/s, ζ_1 = 0.00712, ζ_2 = 0.006680.

Remark2: Based on the state-space realization obtained by ERA, we should be able to transfer the state matrix A_c to the original obtained from equation (A.31). Hence extract the mass, stiffness and damping matrices.

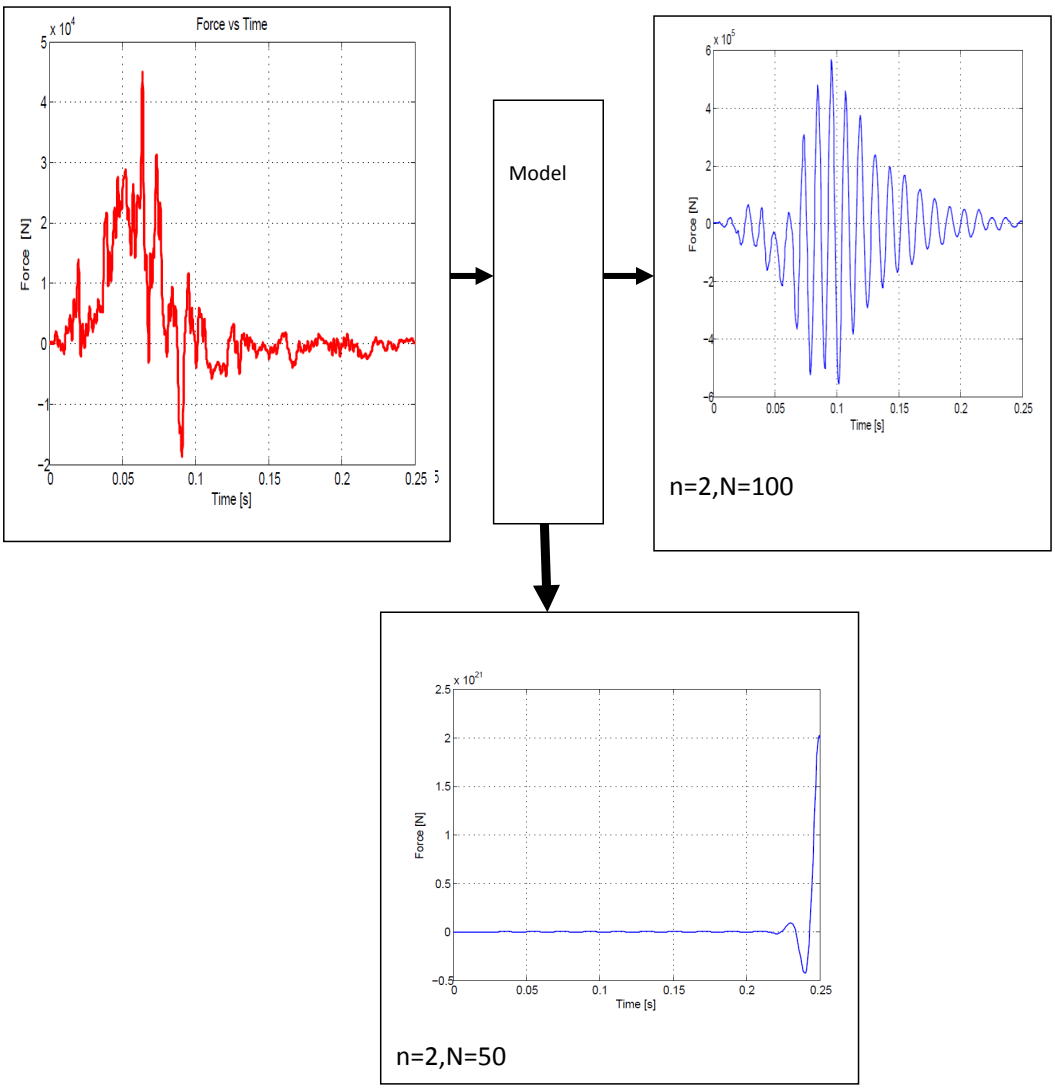

Figure A.15: Responses of a Single Degree of Freedom model to exitation force

A.5 Conclusion and future work

In this paper, it is presented a method to estimate the parameters of a double spring-mass-damper model of a vehicle frontal crash. It was observed that the model results were much closer to the experimental test results. The overall behavior of the model matches the real vehicle's crush.Two of the main parameters characterizing the collision are the maximum dynamic crush - which describes the highest car's deformation and the time at which it occurs- t_m. They are pertinent to the occupant crashworthiness since they help to assess the maximum intrusion to the passenger's compartment.

It can be concluded from this study, that a double spring-mass-damper model can

represent the real vehicle crash scenario when the mass m_1 representing the chassis of the vehicle is less than m_2, the mass representing the passenger compartment. In all cases, the front part of the vehicle undergoes smaller deformation than the passenger compartment.The time at which the maximum chassis displacement occurs is slightly shorter than the time for the passenger compartment because of its additional compression by the rest of the car. In our future work: (1) more investigation on data analysis would be interesting to consider effect of sensor delays in measurement ([21]- [22]); (2) Extraction of mass, stiffness and damping matrices from the identified state-space representation will be investigated; (3) We would like to extend our study to a three-mass-spring-damper model taking into consideration the nonlinearity of the spring and damper. The three masses will be representing the engine, the suspension and the passenger compartment mass respectively, interconnected by springs and dampers; (4) Injury mechanisms of the occupant such as Head Injury Criterion (HIC) would be considered in future work.

REFERENCES

[1] P. Witold, J. E. Nielsen, H. R Karimi, and K. G.Robbersmyr. Mathematical modeling of a vehicle crash test based on elasto-plastic unloading scenarios of spring-mass models. *Int J Adv Manuf Technol*, 55:369–378, 2011.

[2] P. Witold, J. E. Nielsen, H. R Karimi, and K. G.Robbersmyr. Application of viscoelastic hybrid models to vehicle crash simulation. *International Journal of Crashworthiness*, 16(2):195–205, 2011.

[3] P. Witold, J. E. Nielsen, H. R Karimi, and K. G.Robbersmyr. Development of lumpedparameter mathematical models for a vehicle localized impact. *Journal of Mechanical Science and Technology*, 25(7):1737–1747, 2011.

[4] J. Marzbanrad and M. Pahlavani. Parameter determination of a vehicle 5-dof model to simulate occupant deceleration in a frontal crash. *World Academy of Science, Engineering and Technology*, 55:336–341, 2011.

[5] J. Marzbanrad and M. Pahlavani. Calculation of vehicle-lumped model parameters considering occupant deceleration in frontal crash. *International Journal of Crashworthiness - International Journal of Crashwothiness*, 16(4):439–455, 2011.

[6] L. Sousa, P.Verssimo, and J. Ambrsio. Development of generic multibody road vehicle models for crashworthiness. *Multibody Syst Dyn*, 19:133–158, 2008.

[7] M. Carvalho, J. Ambrsio, and P. Eberhard. Identification of validated multibody vehicle models for crash analysis using a hybrid optimization procedure. *Struct Multidisc Optim*, 44:85–97, 2011.

[8] A.A. Alnaqi and A.S. Yigit. Dynamic analysis and control of automotive occupant restraint systems. *Jordan Journal of Mechanical and Industrial Engineering*, 5(1):39–46, 2011.

[9] P. V. Overschee and B. D. Moor. *Deterministic Identification in Subspace Identification for Linear Systems: Theory - Implementation - Applications*. Kluwer Academic Publishers, Boston / London/Dordrecht, Leuven, January 1 1996.

[10] W. Favoreel, B.D. Moor, and P.V. Overschee. Subspace state space system identificationcation for industrial processes. *Journal of Process Control*, 10:149–155, 2000.

[11] J. Marzbanrad and M. Pahlavani. A system identification algorithm for vehicle lumped parameter model in crash analysis. *International Journal of Modeling and Optimization*, 1(2):163–168, 2011.

[12] D. Guida, F. Nilvetti, and C. M. Pappalardo. Parameter identification of a two degrees of freedom mechanical system. *International Journal of Mechanics*, 3(2):23–30, 2009.

[13] P. Witold, K.G. Robbersmyr, and H. R. Karimi. Mathematical modeling and parameters estimation of a car crash using data-based regressive model approach. *Applied Mathematical Modelling*, 35:5091–5107, 2011.

[14] J.N. Juang. *Applied System Identification*. Number 6th Edtion. Printice Hall PTR, 1994.

[15] Dar-Yun and Chang-Sheng Lin. Identification of modal parameters from ambient vibration data using eigensystem realization algorithm with correlation technique. *Journal of Mechanical Science and Technology*, 24(12):2377–2382, 2010.

[16] W. J. Ko and C. F. Hung. Extraction of structural system matrices from an identified state-space system using the combined measurement of displacement, velocity and acceleration. *Journal of Sound and Vibration*, 249(5):955–970, 2002.

[17] J. N. Juang and R. S. Pappa. An eigensystem realization algorithm for modal parameters identification and model reduction. *Journal of Guidance, Control, and Dynamics*, 8:620–627, 1985.

[18] C. D. Yang and F. B. Yeh. Identification, reduction, and refinement of model parameters by the eigensystem realization algorithm. *Journal of Guidance, Control and Dynamics*, 13:1051–1059, 1990.

[19] K.G. Robbersmyr. Calibration test of a standard ford fiesta 1.1l, model year 1987, according to ns -en 12767 , technical report 43. Technical report, Agder Research, Grimstad., 2004.

[20] M. Huang. *Vehicle Crash Mechanics*. CRC PRESS, Boca Raton London New York Washington, D.C., 2002.

[21] Z. Wang, B. Shen H. Dong, and H. Gao. Finite-horizon h_∞ filtering with missing measurements and quantization effects. *IEEE Transactions on Automatic Control*, 58(7):1707–1718, 2013.

[22] Z. Wang, B. Shen, H. Shu, and G. Wei. Quantized h_∞ control for nonlinear stochastic time-delay systems with missing measurements. *IEEE Transactions on Automatic Control*, 57(6):1431–1444, Jun 2012.

Paper B.

Title:	A State-space Approach to Mathematical Modeling and Parameters Identification of Vehicle Frontal Crash
Authors:	Bernard B. Munyazikwiye [1], Kjell G. Robbersmyr [1], and Hamid Reza Karimi [1]
Affiliation:	[1] Faculty of Engineering and Science, University of Agder, P.O. Box 509, 4879 Grimstad, Norway
Article:	*Systems Science and Control Engineering, 2014, Vol. 2, 351–361*
Copyright ©:	IEEE
Layout:	The layout of the paper has been revised to have the same format as the thesis

B

Abstract — **In this paper a state-space estimation procedure that relies on the time-domain analysis of input and output signals is used for mathematical modeling of vehicle frontal crash. The model is a double-spring-mass-damper system, whereby the front mass and real mass represent the chassis and the passenger compartment respectively. It is observed that the dynamic crash of the model is closer to the dynamic crash from experimental when the mass of the chassis is greater than the mass of passenger compartment. The dynamic crash depends on pole placement and the estimated parameters. It is noted that when the poles of the model are closer to zero, the dynamic crash of the model is far from the dynamic crash from experimental data. The stiffness and damping coefficients play an important role in the dynamic crash.**
Key–Words: Modeling, vehicle frontal crash, parameters identification, state-space representation

B.1 Introduction

Car crash test is usually performed in order to ensure safe design standards in crashworthiness, the ability of a vehicle to be plastically deformed and yet maintains a sufficient survival space for its occupants during crash scenario. Nowadays, due to advanced research in computer simulation software, simulated crash tests can be performed beforehand the full-scale crash test. Therefore, cost associated with real crash test can be reduced. Vehicle crashworthiness can be evaluated in four distinct modes: frontal, side, rear and rollover crashes. System identification concerns the construction and validation of mathematical models of dynamical systems from experimental input/output data. In experiments the system reveals information about itself in terms of input and output measurements. System identification is routinely used in industry as a tool for plant modeling. There are available solutions for identification of mathematical models based on experimental test procedures. One of the most convenient and accessible solution is to use the System Identification Toolbox [1]. In addition to the general use, the System Identification Toolbox is also commonly used for creating models of vibrating mechanical systems [2, 3]. The System Identification Toolbox is largely based on the work of Ljunun (L. Ljung, 1999.) and implements common techniques used in system identification. There is substantial literature on System Identification [4]. The toolbox aids the user to fit both linear and nonlinear models to measured data sets known as black box modeling ([5]). The system identification problem is to determine the unknown sys-

tem characteristics such as mass, stiffness, and damping parameters using system responses. In the work of [6], an investigation of an adaptable crash energy management system to enhance vehicle crashworthiness was carried out. The author performed a system identification algorithm for vehicle lumped parameter model in crash analysis using a genetic algorithm procedure, an effective procedure for optimizing errors between experimental data and calculated data obtained analytically. Also a systematic investigation of vehicle frontal crash was conducted using the lumped-parameter model by [7]. Pawlus et al, [8] proposed a mathematical model to estimate the maximum occupant deceleration, which is one of the main tasks in the area of crashworthiness study by a Kelvin model which contains a mass together with spring and damper connected in parallel. An application of physical models composed of springs, dampers, and masses joined together in various arrangements for simulating a real car collision with a rigid pole was presented by [9].

Marzbanrad and Pahlavani [10], presented an overview of the kinematic and dynamic relationships of a vehicle in a collision, whereby the work was to identify the parameters of the vehicle crash model using experimental dataset. set. Munyazikwiye et al. [11] estimated the physical parameters of a frontal car crash using the eigensystem realization algorithm and curve-fitting approaches. Marzbanrad and Pahlavani [12], investigated and analyzed a lumped parameter modeling in frontal crash in five degrees of freedom, and the response of occupant during the impact was investigated.

The types of available models are low order process models, transfer functions, state-space models, linear models with static nonlinearities, nonlinear autoregressive models, etc. The identification tasks are divided into separate parts. After creating an identification and validation data set, the data is pre-processed. Identification is initialized by selecting and setting up the proper model type. Finally the models can be validated using numerous techniques such as comparing model response with measurement data, step response and a pole-zero plot.

The aim of the identification process is to identify the contents of matrices A, B, C given the input and output data set. The Matlab System Identification toolbox offers two estimation methods for state-space models:

- Subspace identification
- Iterative prediction-error minimization method.

The matrices: $\boldsymbol{A} \in \mathbb{R}^{n \times n}$, is called the (dynamical) system matrix. It describes the dynamics of the system (as completely characterized by its eigenvalues). $\boldsymbol{B} \in \mathbb{R}^{n \times m}$ is the input matrix which represents the linear transformation by

which the deterministic inputs influence the next state, $\boldsymbol{C} \in \mathbb{R}^{l \times n}$ is the output matrix which describes how the internal state is transferred to the outside world in the measurements yk. The term with the matrix $\mathbf{D} \in \mathbb{R}^{l \times m}$ is called the direct feed-through term. In continuous time systems this term is most often 0.

In this paper the state-space of the model under study was obtained and the physical parameters (stiffness and damping coefficients) were extracted from the dynamical system matix $\boldsymbol{A}$. The model was finally validated by the experimental data. The results from the model are much closer to the real crash senario. The results show that a vehicle with chassis heavier than the passanger compatment experienes less dynamic crash. Therefore care should be taken by car designer as far as the ratios (with respect to the total mass of the car) of the chassis and passenger compartment are concerned.

The novelty of the approach used in this paper is that, it is less computational time as compared to the previous approaches, like eigensysten realisation and curve fitting techniques, in the literature and the simulation results are much closer to the experimental results.

B.2 Vehicle crash experimental test

The real vehicle crash experiment was conducted on a typical mid-speed vehicle to pole collision. Its elaboration was the initiative of Robbersmyr, 2004. A test vehicle was subjected to impact with a vertical and rigid cylinder. The acceleration field was 100 meters long and had two anchored parallel pipelines. The vehicle was steered using those pipelines that were bolted to the concrete runaway. Setup scheme is shown in Figure B.1. During the test, the acceleration was measured in three directions (x - longitudinal, y - lateral, and z - vertical) together with the yaw rate from the center of gravity of the car. Using normal speed and high - speed video cameras, the behavior of the safety barrier and the test vehicle during the collision was recorded. The initial velocity of the car was 35 km/h, and the mass of the vehicle (together with the measuring equipment and dummy) was 873 kg. The obstruction was constructed with two steel components - a pipe filled with concrete and a baseplate mounted with bolts on a foundation. The car undergoing the deformation is shown in Figure B.2. The accelerometer is located at the mass center of gravity of the vehicle in the passenger compartment. Since we are interested in the frontal crash, only the measured acceleration in the longitudinal direction is consid-

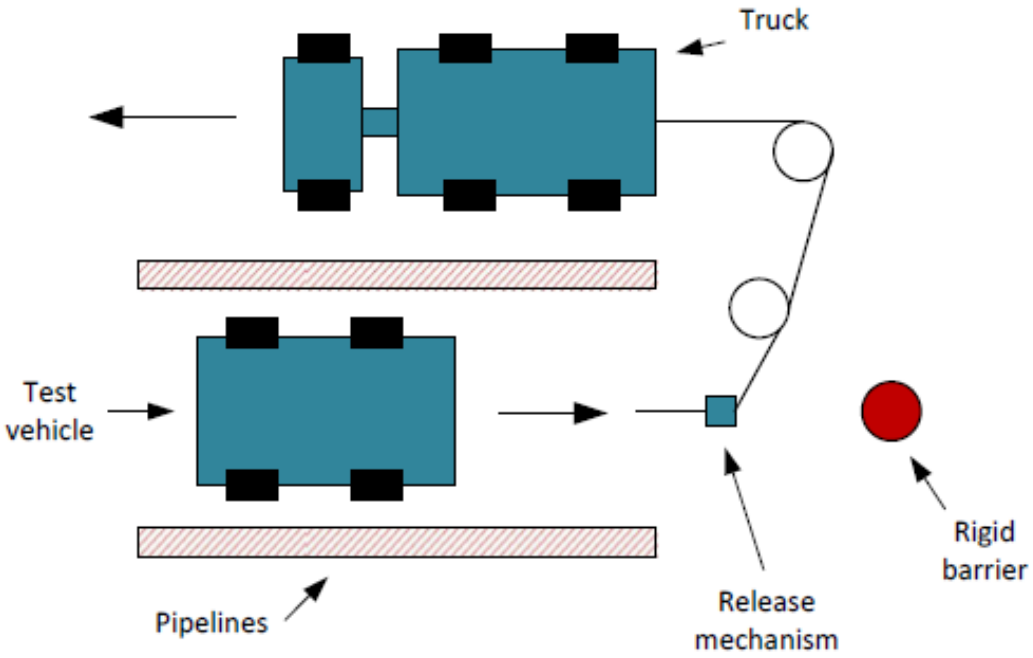

Figure B.1: **Vehicle crash Experimental setup , [13]**

ered in this study. The acclereration data is imported and processed in MATLAB for analysis. The deformation of the vehicle is obtained by integrating twice the acceleration signal.

Figure B.2: **Vehicle undergoing deformation, [13]**

B.3 Mathematical modeling

The experimental data were first imported in the Matlab Workspace and processed for being suitable for identification of the model. The measured acceleration was twice integrated to obtain the measured displacement signal. The processed data were further imported into a system identification toolbox. A transfer function model and a state-space canonical form were thereafter obtained.

Figure B.3 shows the measured input-output signals and simulated output respectively.
The transfer function from the experimental data is as follows:

$$T_e(s) = \frac{-0.0139s + 0.5942}{s^4 + 97s^3 + 3810s^2 + 87170s + 35718} \tag{B.1}$$

The estimated-state space model model of order 4 is as follows:

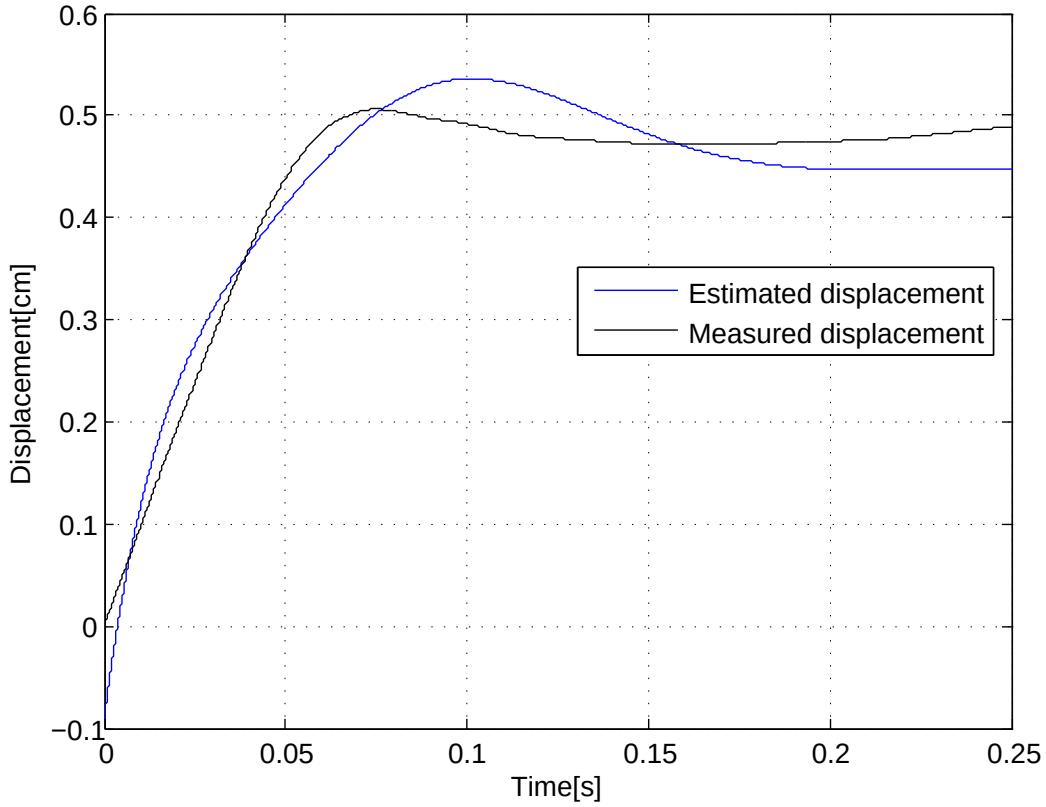

Figure B.3: **Measured and Estimated outputs**

$$\boldsymbol{A}_e = \begin{bmatrix} -97 & -3810 & -87170 & -35718 \\ 1 & 0 & 0 & 0 \\ 0 & 1 & 0 & 0 \\ 0 & 0 & 1 & 0 \end{bmatrix}, \boldsymbol{B}_e = \begin{bmatrix} 1 \\ 0 \\ 0 \\ 0 \end{bmatrix}, \tag{B.2}$$

$$\boldsymbol{C}_e = \begin{bmatrix} 0 & 0 & -0.0139 & 0.5942 \end{bmatrix}, \boldsymbol{D}_e = \begin{bmatrix} 0 \end{bmatrix} \tag{B.3}$$

Mathematical models describe the dynamic behavior of a system as a function of time. During frontal crash, the vehicle is subjected to an impulsive force caused by the obstacle. The model for vehicle crash simulates a rigid barrier impact of a vehicle where m_1 and m_2 represent the frame rail (chassis) and passenger compartment masses, respectively.

Parameters to be estimated are springs k_1 and k_2, dampers c_1 and c_2, as shown in Figure B.4. When the vehicle impacts on a rigid barrier, the two masses will experience an impulsive force during collision. The method for solving the impact responses of the two masses is adapted from te method used in the free vibration

analysis of a two-degrees of freedom damped system ([14]).

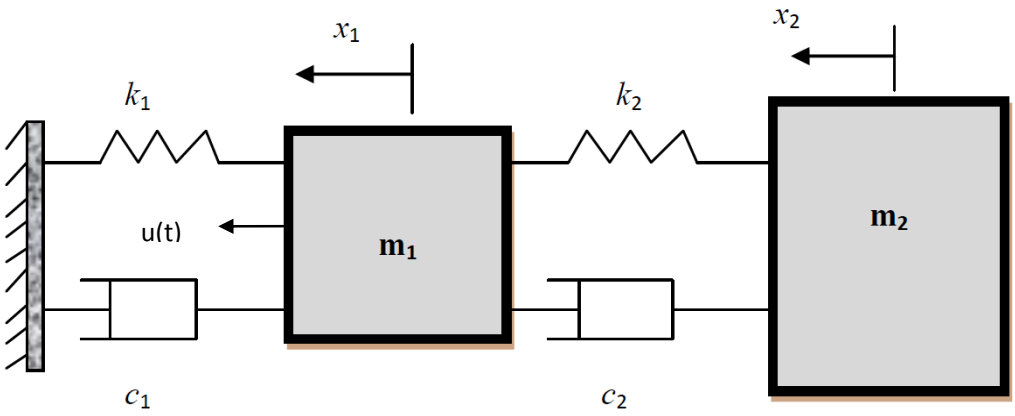

Figure B.4: **A double spring-mass-damper model**

The dynamic equations of the doble mass-spring-damper model are shown in Equation(B.4).

$$\begin{aligned} m_1\ddot{x}_1 + (c_1 + c_2)\dot{x}_1 + (k_1 + k_2)x_1 - c_2\dot{x}_2 - k_2x_2 &= u \\ m_2\ddot{x}_2 - c_2\dot{x}_1 + c_2\dot{x}_2 + k_2x_2 - k_2x_1 &= 0 \end{aligned} \tag{B.4}$$

or

$$\begin{bmatrix} m_1 & 0 \\ 0 & m_2 \end{bmatrix} \begin{bmatrix} \ddot{x}_1 \\ \ddot{x}_2 \end{bmatrix} + \begin{bmatrix} k_1 + k_2 & -k_2 \\ -k_2 & k_2 \end{bmatrix} \begin{bmatrix} x_1 \\ x_2 \end{bmatrix} + \begin{bmatrix} c_1 + c_2 & -c_2 \\ -c_2 & c_2 \end{bmatrix} \begin{bmatrix} \dot{x}_1 \\ \dot{x}_2 \end{bmatrix} = \begin{bmatrix} u \\ 0 \end{bmatrix} \tag{B.5}$$

From (B.5) a transfer function between u(t) and $x_2(t)$ is derived and given in (B.6).

$$T_{model}(s) = \frac{Num(s)}{Den(s)} \tag{B.6}$$

with

$$\begin{aligned} Num(s) &= c_2s + k_2 \\ Den(s) &= m_1m_2s^4 - (m_1c_2 + m_2(c_1 + c_2))s^3 \\ &+ (m_1k_2 + m_2(k_1 + k_2) + c_1c_2)s^2 + (c_1k_2 + c_2k_1)s + k_1k_2 \end{aligned}$$

The state-space canonical form representation from this transfer function is:

$$\boldsymbol{A}_m = \begin{bmatrix} -a_3 & -a_2 & -a_1 & -a_0 \\ 1 & 0 & 0 & 0 \\ 0 & 1 & 0 & 0 \\ 0 & 0 & 1 & 0 \end{bmatrix}, \boldsymbol{B}_m = \begin{bmatrix} 1 \\ 0 \\ 0 \\ 0 \end{bmatrix}, \boldsymbol{C}_m = \begin{bmatrix} b3 & b2 & b1 & b0 \end{bmatrix}, \quad \text{(B.7)}$$

$$\boldsymbol{D}_e = \begin{bmatrix} 0 \end{bmatrix}$$

with

$$a_0 = -\frac{(k_1 k_2)}{m_1 m_2}, a_1 = -\frac{(c_1 k_2 + c_2 k_1)}{m_1 m_2}, a_2 = -\frac{(m_1 k_2 + m_2(k_1 + k_2) + c_1 c_2)}{m_1 m_2},$$
$$a_3 = -\frac{(m_1 c_2 + m_2(c_1 + c_2))}{m_1 m_2}.$$
$$b_0 = -\frac{k_2}{m_1 m_2}, b_1 = -\frac{c_2}{m_1 m_2}, b_2 = 0, b_3 = 0.$$

The physical parameters are embedded in the state matrix. Therefore by inspection, the identified parameters are obtained by comparing the two state matrices A_e in (B.2) and A_m in (B.7), which are summarized in the following:

$$\begin{aligned} m_1 c_2 + m_2 c_1 + m_2 c_2 &= m_1 m_2 \times 97 \\ m_1 k_2 + m_2 k_1 + m_2 k_2 &= m_1 m_2 \times 3810 \\ c_1 k_2 + c_2 k_1 &= m_1 m_2 \times 87170 \\ k_1 k_2 &= m_1 m_2 \times 35718 \end{aligned} \quad \text{(B.8)}$$

A summary of estimated parameters considering different cases is shown in Table B.1. Only real values are considered.

B.4 Simulation Results

Four different cases were considered for simulation of vehicle frontal crash. The solution of (B.8) is not unique. Four solutions for each parameter were found, two real and two complex conjugate solutions. For the physical system, only real values

have meaning. Therefore the complex solutions were neglected in the development of the model. A summary of estimated real valued parameters is shown in Table B.1

Table B.1: **Parameters estimation**

Cases	Solution No	Estimated Parameters			
		k_1 [N/m]	k_2 [N/m]	c_1 [Ns/m]	c_2 [Ns/m]
Case1:m_1=1/3 m_t m_2=2/3m_t	1	3498.37	640808	22989	9440
	2	15324.66	6293.37	5247	961212.45
Case2:m_1=2/3 m_t m_2=1/3 m_t	1	7720.9	440070	33306.4	13746.15
	2	11102.14	33162.72	458205	1320210
Case3:m_1=1/4 m_t m_2=3/4 m_t	1	475.68	606207.28	20541.68	8419.68
	2	15406.26	6314.76	634.24	808276.38
Case4:m_1=3/4 m_t m_2=1/4 m_t	1	6734.92	337670.38	36588.11	15115.54
	2	9147	3778.88	26939.66	1350681.54

Case 1: $(m_1 < m_2)$. One has that $m_1 = \frac{1}{3}m_t$ and $m_2 = \frac{2}{3}m_t$

Solution of (B.8) is as follows:

$c_1 = \{22987, 524756, 2524649 \mp 2884882i, 298807 \mp 2884882i\}$

$k_1 = \{3498.37, 15324.66, 1992.02 \pm 19232.54i, 16830.99 \pm 19232.54i\}$

$c_2 = \{9440.06, 961212.45, 67992.08 \mp 747581.32i, 1094.86 \mp 1203.81i\}$

$k_2 = \{640808.30, 6293.37, 729.91 \pm 8025.41i, 45328.05 \pm 498387.54i\}$

Taking: $c_1 = 22987Ns/m$; $k_1 = 3498.37N/m$; $c_2 = 9770.06Ns/m$; $k_2 = 640808.03N/m$;

The state-space canonical form is:

$$\boldsymbol{A}_m = \begin{bmatrix} -1281 & -4597 & -669 & -13238 \\ 1 & 0 & 0 & 0 \\ 0 & 1 & 0 & 0 \\ 0 & 0 & 1 & 0 \end{bmatrix}, \boldsymbol{B}_m = \begin{bmatrix} 1 \\ 0 \\ 0 \\ 0 \end{bmatrix},$$

$$\boldsymbol{C}_m = \begin{bmatrix} 0 & 0 & 0.0557 & 3.784 \end{bmatrix}, \boldsymbol{D}_m = \begin{bmatrix} 0 \end{bmatrix} \tag{B.9}$$

and

Poles=$\{-63.7936 \pm 22.7051i, -0.0329 \pm 1.6987i\}$;

Zeros= $\{-67.8822\}$.

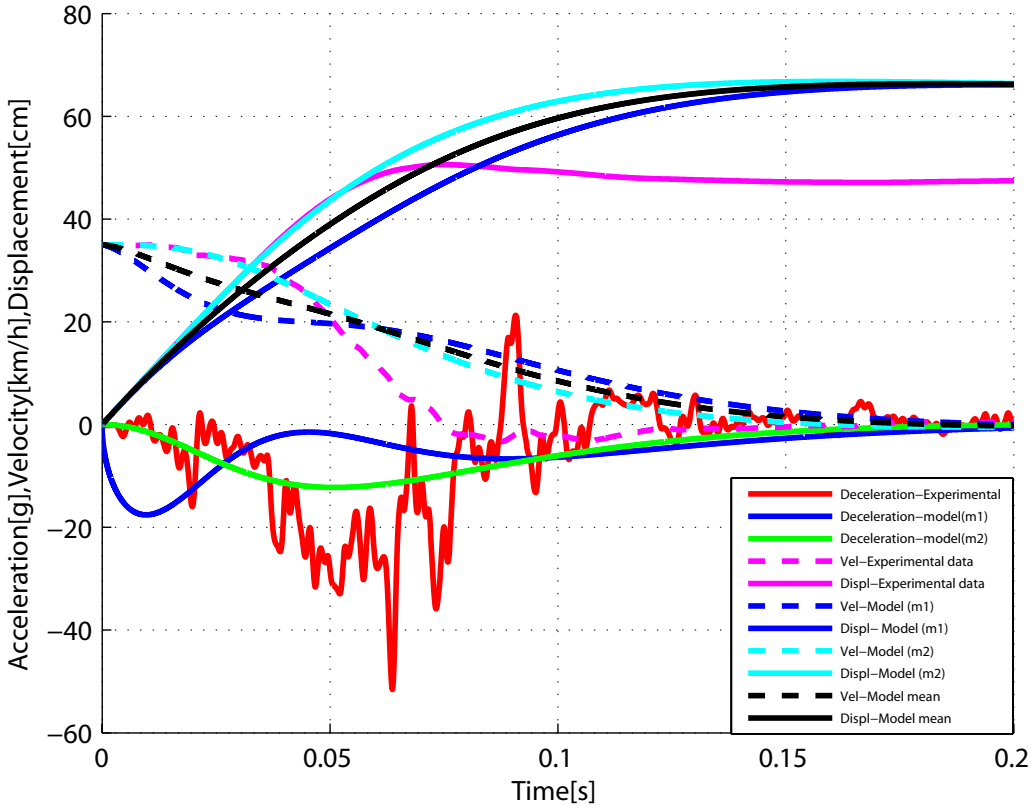

Figure B.5: **Comparative analysis between vehicle crash test and model results for** $m_1 = \frac{1}{3}m_t$

From Figure B.5, the dynamic crash of m_2 is 66.55 cm which is the displacement of the passenger compartment. Therefore this model cannot represent the vehicle crash scenarion. It is observed that, the time for dynamic crash is longer than that for the real crash (i.e. 0.14 s instead of 0.078 s).The dynamic crash of the chassis represented by m_1 is more or less equal to that of the passenger compartment -a difference of 0.43 cm is observed and but the time of crash is larger compared to that from the real crash and that from the passenger compartment (i.e. 0.17s). The model where the chassis is a third of the car cannot represent the crash scenario.

Taking:
$c_1 = 5247.56Ns/m; k_1 = 15324.66N/m; c_2 = 961212.45Ns/m; k_2 = 6293.37N/m;$

$$\boldsymbol{A}_m = \begin{bmatrix} -49652 & -2989196 & -873128 & -5686 \\ 1 & 0 & 0 & 0 \\ 0 & 1 & 0 & 0 \\ 0 & 0 & 1 & 0 \end{bmatrix},$$

$$\boldsymbol{B}_m = \begin{bmatrix} 1 \\ 0 \\ 0 \\ 0 \end{bmatrix}, \boldsymbol{C}_m = \begin{bmatrix} 0 & 0 & 55.66 & 0.371 \end{bmatrix}, \boldsymbol{D}_m = \begin{bmatrix} 0 \end{bmatrix} \tag{B.10}$$

and

Poles=$\{-4966.7, -3 \pm 2.9i, -0\}$

Zeros=$\{-0.0065\}$

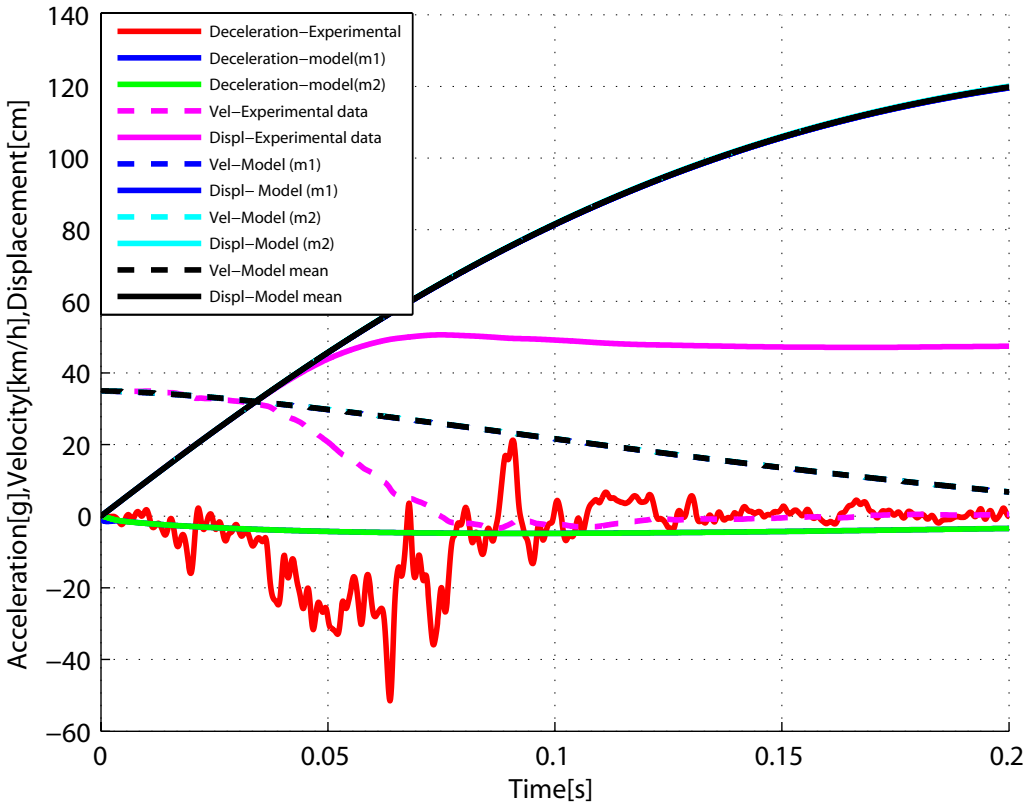

Figure B.6: **Comparative analysis between vehicle crash test and model results for** $m_2 = \frac{1}{3}m_t$

From Figure B.6 the value of dynamic crash of the passenger compartment as

represented by mass m_2 is very high and cannot be observed from the response graph, i.e. tends to ∞, resulting in a criticaly stable system because of a pole at zero. Therefore this model cannot represent the vehicle crash scenario because the deformation of the car cannot tend to ∞. The time of crash is not observed because the velocity never cross zero as an indication of maximum time of crash. Therefore the pysical parameters obtained for this model are not of much interest.

Case 2: $(m_1 > m_2)$. One has that $m_1 = \frac{2}{3}m_t$ and $m_2 = \frac{1}{3}m_t$

Solution of (B.8) is as follows:

$c_1 = \{33306.41, 23162.72, 44523.48 \pm 31912.62i, 11945.65 \mp 31991.26i\}$
$k_1 = \{7720.91, 11102.14, 3981.88 \mp 106337.54i, 14841.16 \pm 106337.54i\}$
$c_2 = \{13746.16, 1320210.06, 437015.59 \pm 1204203.36i, 483269 \mp 13316.56i\}$
$k_2 = \{440070.02, 4582.05, 1610.89 \mp 4438.85i, 145671.86 \pm 401401.12i\}$

Taking: $c_1 = 33306.4Ns/m$; $k_1 = 7720.9N/m$; $c_2 = 13746.16Ns/m$; $k_2 = 440070.02N/m$;

The state-space canonical form is:

$$\boldsymbol{A}_m = \begin{bmatrix} -1279 & -298196 & -873128 & -20063 \\ 1 & 0 & 0 & 0 \\ 0 & 1 & 0 & 0 \\ 0 & 0 & 1 & 0 \end{bmatrix}, \boldsymbol{B}_m = \begin{bmatrix} 1 \\ 0 \\ 0 \\ 0 \end{bmatrix},$$

$$\boldsymbol{C}_m = \begin{bmatrix} 0 & 0 & 0.081 & 2.598 \end{bmatrix}, \boldsymbol{D}_m = \begin{bmatrix} 0 \end{bmatrix}$$

and
Poles=$\{-63.8 \pm 29.3i, -0.16 \pm 2i\}$
Zeros= $\{-32\}$

From Figure B.7, the dynamic crash of the passenger compartment is 52.92 cm and the time for dynamic crash decreases as compared to the previous case , that is, from 0.14 s to 0.11 s. The dynamic crash of the chassis is 51.05 cm and occurs after 0.16s. Therefore for this case, the model can represent the vehicle crash scenario because the dynamic crash is much closer to that obtained from the experimental data.

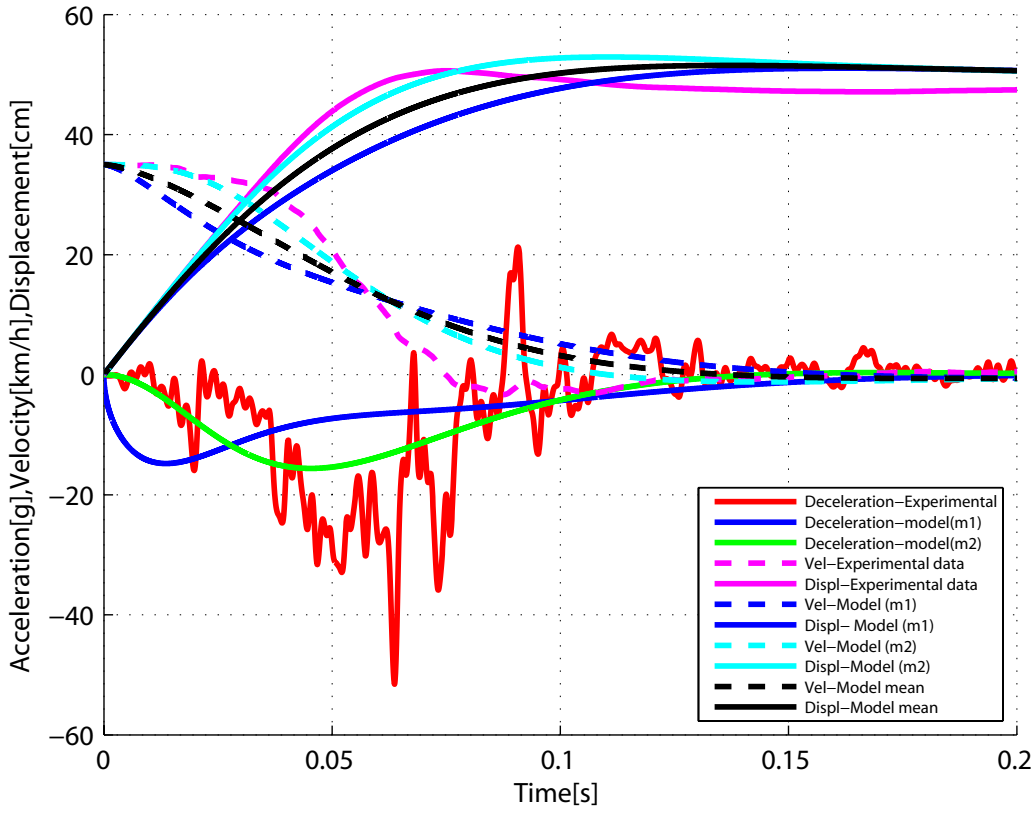

Figure B.7: **Comparative analysis between vehicle crash test and model results for** $m_1 = \frac{1}{4}m_t$

Taking:

$c_1 = 33162.72Ns/m$;$k_1 = 11102.14N/m$; $c_2 = 1320210Ns/m$; $k_2 = 458205N/m$;

$$\boldsymbol{A}_m = \begin{bmatrix} -6861 & -26081 & -8731228 & -88745 \\ 1 & 0 & 0 & 0 \\ 0 & 1 & 0 & 0 \\ 0 & 0 & 1 & 0 \end{bmatrix}, \boldsymbol{B}_m = \begin{bmatrix} 1 \\ 0 \\ 0 \\ 0 \end{bmatrix},$$

$$\boldsymbol{C}_m = \begin{bmatrix} 0 & 0 & 7.79 & 2.71 \end{bmatrix}, \boldsymbol{D}_m = \begin{bmatrix} 0 \end{bmatrix} \tag{B.11}$$

and

Poles=$\{-63.8 \pm 29.3i, -0.16 \pm 2i\}$

Zeros= $\{-32\}$

From B.8, the dynamic crash of the passenger compartment is 50.16 cm and the time for dynamic crash increases as compared to the previous case , that is, from 0.14 s to 0.16 s. The dynamic crash of the chassis is 49.82 cm and occurs after

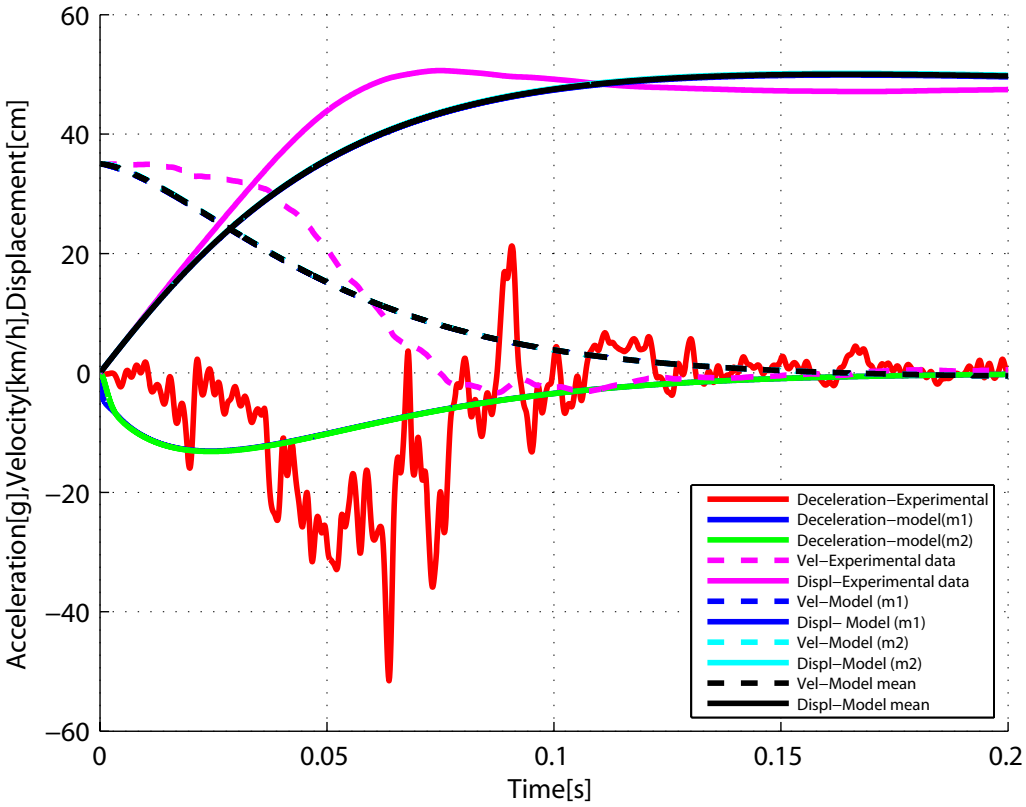

Figure B.8: **Comparative analysis between vehicle crash test and model results for** $m_2 = \frac{1}{4}m_t$

0.16s.Therefore for this case, the model can represent the vehicle crash scenario because the dynamic crash is much closer to that obtained from the experimental data.

Case 3: $(m_1 < m_2)$. One has that $m_1 = \frac{1}{4}m_t$ and $m_2 = \frac{3}{4}m_t$

Solution of (B.8) is as follows:

$$c_1 = \{20541.68, 634.24, 20494.51 \mp 6561.71i, 681.41 \mp 26561.71i\}$$
$$k_1 = \{475.68, 15406.26, 511.06 \pm 19921.28i, 15370.88 \pm 19921.28i\}$$
$$c_2 = \{8419.68, 808276.38, 7329.54 \mp 613913.15i, 132.33 \mp 11083.75i\}$$
$$k_2 = \{606207.29, 6314.76, 99.25 \pm 8312.81i, 5497.15 \pm 460434.86i\}$$

Taking:

$c_1 = 20541.68Ns/m$;$k_1 = 47.68N/m$; $c_2 = 8419.68Ns/m$; $k_2 = 606207.29N/m$;

The state-space canonical form is:

$$\boldsymbol{A}_m = \begin{bmatrix} -145.5 & -4916 & -96.4 & -2018.2 \\ 1 & 0 & 0 & 0 \\ 0 & 1 & 0 & 0 \\ 0 & 0 & 1 & 0 \end{bmatrix}, \boldsymbol{B}_m = \begin{bmatrix} 1 \\ 0 \\ 0 \\ 0 \end{bmatrix},$$

$$\boldsymbol{C}_m = \begin{bmatrix} 0 & 0 & 0.059 & 4.24 \end{bmatrix}, \boldsymbol{D}_m = \begin{bmatrix} 0 \end{bmatrix} \tag{B.12}$$

and

Poles=$\{-92.31, -53.23, -0.0037 \pm 0.6408i.\}$

Zeros= $\{-71.99\}$

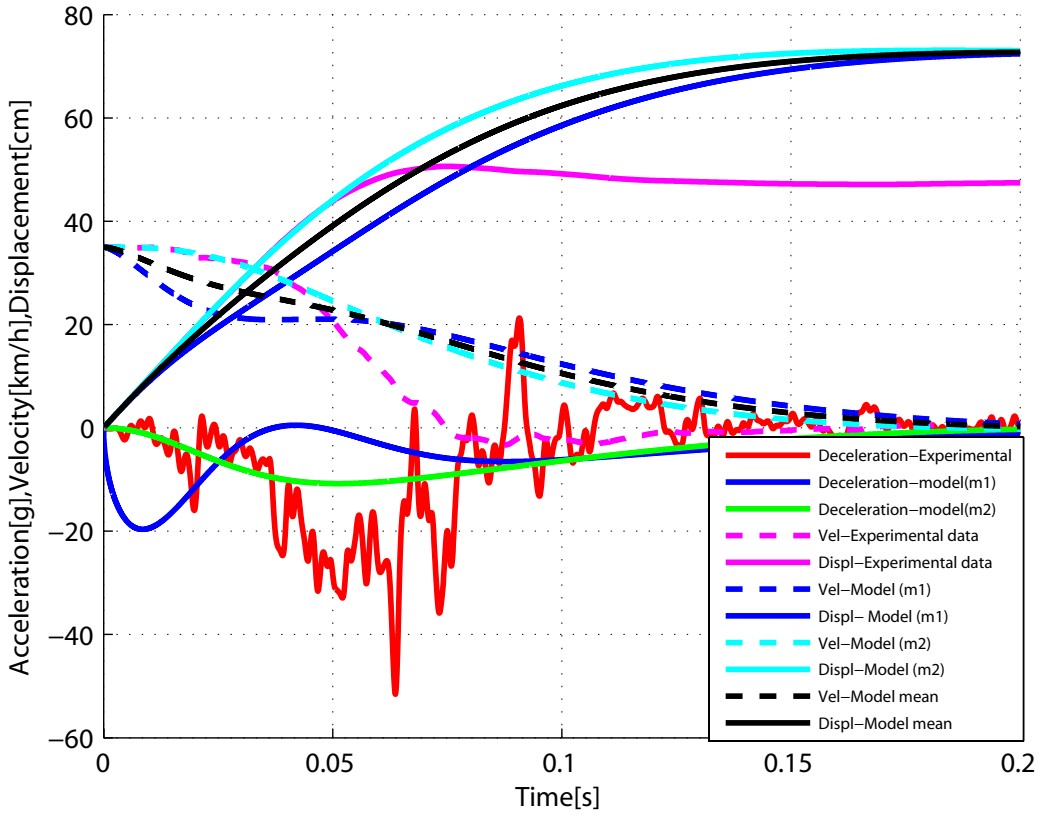

Figure B.9: **Comparative analysis between vehicle crash test and model results for** $m_2 = \frac{1}{4}m_t$

From Figure B.9, the dynamic crash of m_2 is 73.07 cm which is the displacement of the passenger compartment. Therefore this model cannot represent the vehicle crash scenario. It is observed that, the time for dynamic crash is longer than that for the real crash (i.e. 0.17 s instead of 0.078 s).The dynamic crash of the chassis represented by m_1 is more or less equal to that of the passenger compartment -a

difference of 0.62 cm is observed and the time of crash is same as that of passenger compartment and larger as compared to that from the real crash (i.e 0.17s). The model where the mass of chassis is a quarter of that of the car cannot represent the crash senario.

Taking:
$c_1 = 634.24Ns/m$;$k_1 = 15406.26N/m$; $c_2 = 808276.38Ns/m$; $k_2 = 6314.76N/m$;

The state-space canonical form is:

$$\boldsymbol{A}_m = \begin{bmatrix} -4940.5 & -7515.7 & -87193.8 & -68082.6 \\ 1 & 0 & 0 & 0 \\ 0 & 1 & 0 & 0 \\ 0 & 0 & 1 & 0 \end{bmatrix}, \boldsymbol{B}_m = \begin{bmatrix} 1 \\ 0 \\ 0 \\ 0 \end{bmatrix},$$
$$\boldsymbol{C}_m = \begin{bmatrix} 0 & 0 & 5.66 & 4.42 \end{bmatrix}, \boldsymbol{D}_m = \begin{bmatrix} 0 \end{bmatrix} \quad \text{(B.13)}$$

and
Poles=$\{-4939.3, -0.4 \pm 4.1i, -0.8.\}$
Zeros= $\{-0.7813\}$

The dynamic crah and time of crash represented in Figure B.10 are similar to those in Figure B.7. The value of dynamic crash of the passenger compartment as represented by mass m_2 is very high and cannot be observed from the response graph, i.e. tends to ∞. Therefore this model cannot represent the vehicle crash scenario.

Case 4: $(m_1 > m_2)$. One has that $m_1 = \frac{3}{4}m_t$ and $m_2 = \frac{1}{4}m_t$

Solution of (B.8) is as follows:

$c_1 = \{36588.11, 26939.66, 49693.65 \pm 311586.52i, 138334.12 \pm 31586.52i\}$
$k_1 = \{6734.92, 9147.03, 3458.53 \mp 7896.63i, 12423.41 \mp 7896.63i\}$
$c_2 = \{15115.55, 1350681.54, 558910.44 \pm 1310635.28i, 5620.72 \mp 13180.49i\}$
$k_2 = \{337670.38, 3778.88, 1405.18 \mp 3295.12i, 139727.61 \mp 327658.82i\}$

Taking:
$c_1 = 36588.11Ns/m$;$k_1 = 6734.92N/m$; $c_2 = 15115.55Ns/m$; $k_2 = 337670.38N/m$;

The state-space canonical form is:

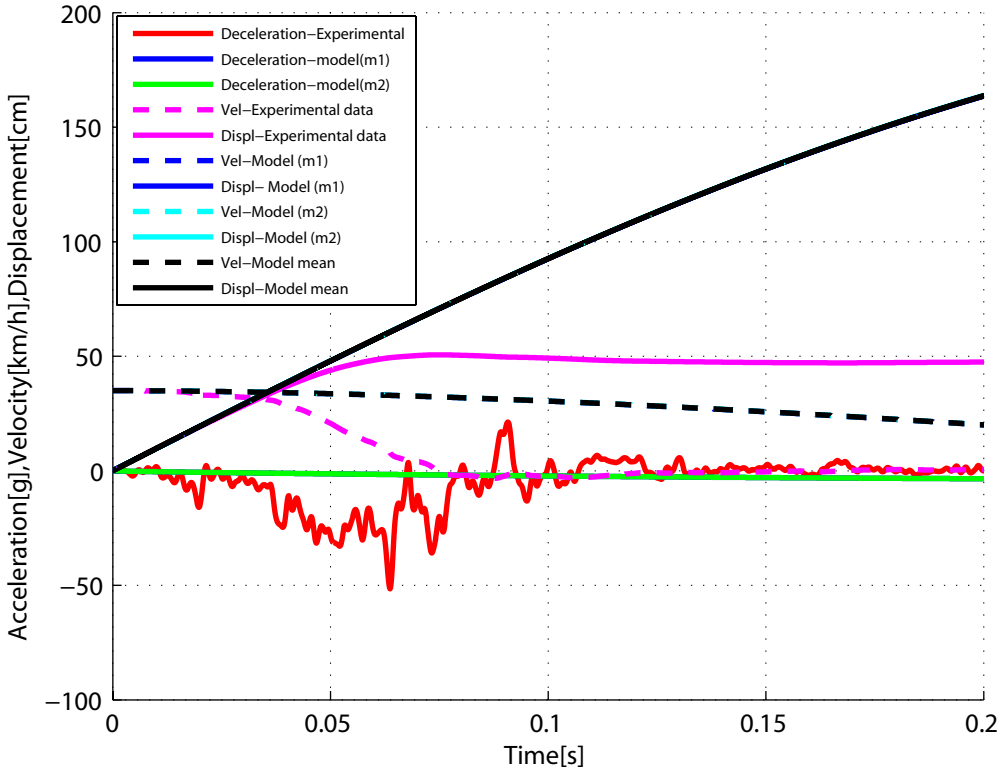

Figure B.10: **Comparative analysis between vehicle crash test and model results for** $m_2 = \frac{1}{4}m_t$

$$\boldsymbol{A}_m = \begin{bmatrix} -148.2 & -5943.3 & -2436.7 & -15913.2 \\ 1 & 0 & 0 & 0 \\ 0 & 1 & 0 & 0 \\ 0 & 0 & 1 & 0 \end{bmatrix}, \boldsymbol{B}_m = \begin{bmatrix} 1 \\ 0 \\ 0 \\ 0 \end{bmatrix},$$

$$\boldsymbol{C}_m = \begin{bmatrix} 0 & 0 & 0.11 & 2.36 \end{bmatrix}, \boldsymbol{D}_m = \begin{bmatrix} 0 \end{bmatrix} \tag{B.14}$$

and

Poles=$\{-73.94 \pm 20.55, -0.173 \pm 1.6347i.\}$

Zeros= $\{-22.34\}$

From Figure B.11, the dynamic crash of the passenger compartment is 50.48 cm and the time for dynamic crash decreases as compared to the previous case , that is, from 0.14 s to 0.11 s. The dynamic crash of the chassis is 48.14 cm and occurs after 0.16s.Therefore for this case, the model can represent the vehicle crash scenario because the dynamic crash is much closer to that obtained from the experimental data.

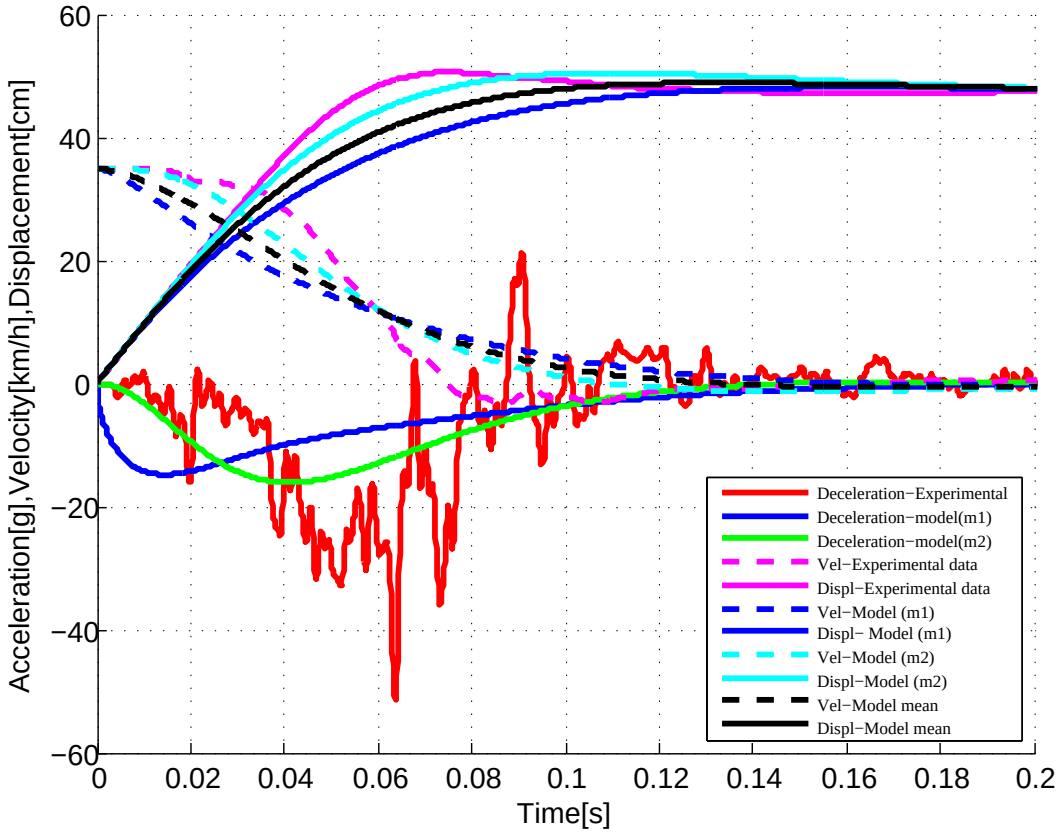

Figure B.11: Comparative analysis between vehicle crash test and model results for $m_2 = \frac{1}{4}m_t$

Taking:

$c_1 = 26939.66Ns/m$;$k_1 = 9147.03N/m$; $c_2 = 1350681.54Ns/m$; $k_2 = 3778.88N/m$;

The state-space canonical form is:

$$\boldsymbol{A}_m = \begin{bmatrix} -8292.5 & -184674.6 & -8817.3 & -24.19 \\ 1 & 0 & 0 & 0 \\ 0 & 1 & 0 & 0 \\ 0 & 0 & 1 & 0 \end{bmatrix}, \boldsymbol{B}_m = \begin{bmatrix} 1 \\ 0 \\ 0 \\ 0 \end{bmatrix},$$

$$\boldsymbol{C}_m = \begin{bmatrix} 0 & 0 & 9.45 & 0.026 \end{bmatrix}, \boldsymbol{D}_m = \begin{bmatrix} 0 \end{bmatrix} \quad \text{(B.15)}$$

and

Poles={-8261.9, -30.8, -0, -0. }

Zeros= {-0.0028}

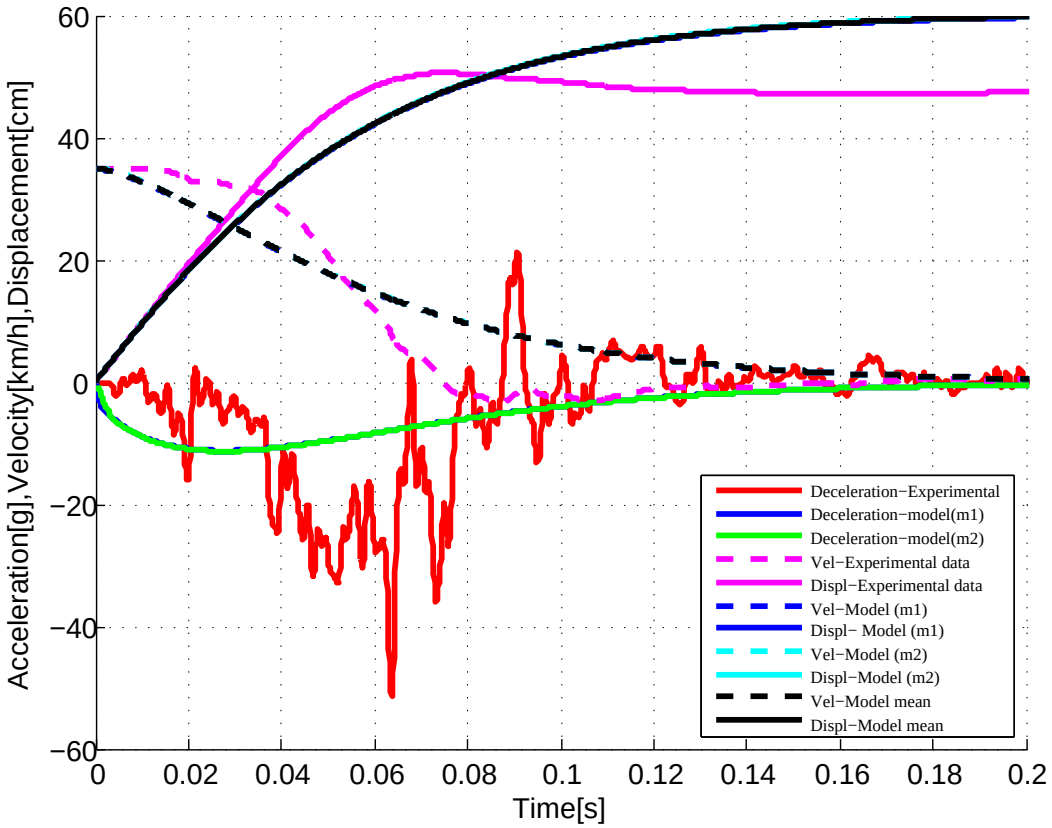

Figure B.12: **Comparative analysis between vehicle crash test and model results for** $m_2 = \frac{1}{4}m_t$

From Figure B.12 the dynamic crash of the passenger compartment m_2 is 60.24cm and the time for dynamic crash is 0.24s. The dynamic crash and time of crash of chassis are same as those of the passenger compartment.This case cannot represent the vehicle crash scenario because the dynamic crash is much diverging from the real vehicle crash.

A summary of main results is shown in Table B.2. The parameter values depend on the value of mass m_2 taken into consideration.

The stiffness coefficients which result in a closer vehicle crash reconstruction are found to be $k_1 = 74681N/m$, $k_2 = 45821N/m$ and the damping coefficients are: $c_1 = 18176Ns/m$, $c_2 = 11196Ns/m$ in the case 4, where the dynamic crash of the passenger compartment is equal to 49.8 cm and occurs after 0.11s (see Figures B.8, B.9 and B.12).

When the mass of the chassis is greater than that of the passenger compartment, the results from the model are closer to the expected values. For example:

Table B.2: **Dynamic crash and time of crash comparison**

C_{mExp} [cm]	$T_{m\text{-}Exp}$ [s]	Solution No 1	masses	C_m [cm]	T_m [s]	Solution No 2	masses	C_m [cm]	T_m [s]
50.63	0.075	Case1:m_1=1/3 m_t m_2=2/3m_t	m_2	66.55	0.14	Case1:m_1=1/3 m_t m_2=2/3m_t	m_2	∞	-
			m_1	66.13	0.19		m_1	∞	-
		Case2:m_1=2/3 m_t m_2=1/3 m_t	m_2	52.92	0.11	Case2:m_1=2/3 m_t m_2=1/3 m_t	m_2	50.16	0.16
			m_1	51.05	0.16		m_1	49.82	0.15
		Case3:m_1=1/4 m_t m_2=3/4 m_t	m_2	73.07	0.17	Case3:m_1=1/4 m_t m_2=3/4 m_t	m_2	∞	-
			m_1	72.45	0.17		m_1	∞	-
		Case4:m_1=3/4 m_t m_2=1/4 m_t	m_2	50.48	0.11	Case4:m_1=3/4 m_t m_2=1/4 m_t	m_2	60.24	0.24
			m_1	48.14	0.16		m_1	60.24	0.24

• When $m_1 = \frac{3}{4}m_t$ $m_2 = \frac{1}{4}m_t$, the identified parameters are: k_1= 6734.92 N/m , k_2= 337670.38 N/m , c_1= 36588.11 Ns/m and c_2= 15115.54 Ns/m. The dynamic crash of the chassis is 48.14 and the dynamic crash of the passenger compartment is 50.48 cm which is closer to 50.68 cm (the dynamic crash from the real vehicle crash).

• When $m_1 = \frac{2}{3}m_t$ and $m_2 = \frac{1}{3}m_t$, the identified parameters are: k_1= 11102.14 N/m , k_2= 33162.72 N/m , c_1= 4558205 Ns/m and c_2= 1320410 Ns/m. The dynamic crash of the chassis is 49.82 and the dynamic crash of the passenger compartment is 50.16 cm which is closer to 50.68 cm (the dynamic crash from the real vehicle crash).

Remark1: It is noting that optimal values for stiffness and damping coefficients are not fixed as shown in Table B.1. They are dependent on the mass of passenger compartment taken into consideration.

Remark2:

The effectiveness of obtained results showing the effect of mass of chassis and passenger compartment are clearly shown from Figure B.5 to Figure B.12 and Table B.2.

B.5 Conclusion

It is observed that the dynamic crush of the model is closer to the dynamic crush from experimental when the mass of the chassis is greater than the mass of passenger compartment. Figures B.8, B.9 and B.12 are the estimated models that reconstruct the vehicle crash with small errors in terms of dynamic crush. But the time of

crash in the three cases is still larger than the time of crash from the experimental data. It is noticed that when the poles of the model are closer to zero, the dynamic crush of the model is far from the dynamic crush from experimental data. The stiffness and damping coefficients play an important role in the dynamic crush. The smaller the stiffness and damping coefficients, the higher the dynamic crush.

REFERENCES

[1] Mathworks (r2013b).

[2] Skullestad A. and Hallingstad O. Vibration parameters identification in a spacecraft subjected to active vibration damping. *Mechatronics*, 8(6):691–705, 1998.

[3] B. Weber and G. Feltrin. Assessment of long-term behavior of tuned mass dampers by system identification. *Eng Struct*, 32(11):3670–3682, 2010.

[4] L. Ljung and T Glad. *Modeling of Dynamic Systems*. Prentice Hall, 1994.

[5] J. Marzbanrad and M.Pahlavani. A system identification algorithm for vehicle lumped parameter model in crash analysis. *International Journal of Modelind and Optimization*, 1(2):163–168, 2011.

[6] Ahmed Abd El-Rahman Khattab. *PhD Thesis, Investigation of an adaptable crash energy management system to enhance vehicle crashworthiness*. PhD thesis, Concordia University Montreal, Quebec, Canada, 2010.

[7] P. Witold, J. E. Nielsen, H. R. Karimi, and K. G. Robbersmyr. Mathematical modeling of a vehicle crash test based on elasto-plastic unloading scenarios of spring-mass models. *Int J Adv Manuf Technol*, 55:369–378, 2011.

[8] P. Witold, K. G. Robbersmyr, and H. R. Karimi. Application of viscoelastic hybrid models to vehicle crash simulation. *International Journal of Crashworthiness*, 16(2):195–205, 2011.

[9] P. Witold, H. R. Karimi, and K. G. Robbersmyr. Development of lumped-parameter mathematical models for a vehicle localized impact. *Journal of Mechanical Science and Technology*, 25(7):1737–1747, 2011.

[10] J. Marzbanrad and M Pahlavani. Parameter determination of a vehicle 5-dof model to simulate occupant deceleration in a frontal crash. *World Academy of Science, Engineering and Technology*, 55:336–341, 2011.

[11] B. Munyazikwiye, H.R. Karimi, and K.G. Robbersmyr. Mathematical modeling and parameters estimation of car crash using eigensystem realization algorithm and curve-fitting approaches. *Mathematical Problems in Engineering*, 2013:1–13, 2013. Article ID 262196, 13 pages.

[12] J. Marzbanrad and M. Pahlavani. Calculation of vehicle-lumped model parameters considering occupant deceleration in frontal crash. *International Journal of Crashwothiness*, 16(4):439–455, 2011.

[13] K. G. Robbersmyr. Calibration test of a standard ford fiesta 1.1l, model year 1987, according to ns-en 12767, tech. rep.43/2004. Technical report, Agder Research, Grimstad, Norway, 2004.

[14] M. Huang. *Vehicle Crash Mechanics*. Boca Raton London New York Washington, D.C., 2002.

Paper C

Title: A Mathematical Model for Vehicle-Occupant Frontal Crash using Genetic Algorithm

Authors: Bernard B. Munyazikwiye [1], Hamid Reza Karimi [1], and Kjell G. Robbersmyr [1]

Affiliation: [1] Faculty of Engineering and Science, University of Agder, P.O. Box 509, 4879 Grimstad, Norway, Department of Mechatronics

Conference: *2016 UKSim-AMSS 18th International Conference on Computer Modelling and Simulation 2016, pp. 141 - 146, 978-1-5090-0888-9/16 $31.00 ©2016 IEEE DOI: 10.1109/UKSim.*

Layout: The layout of the paper has been revised to have the same format as the thesis

C

Abstract — **In this paper, a mathematical model for vehicle - occupant frontal crash is developed. The developed model is represented as a double-spring-mass-damper system, whereby the front mass and the rear mass represent the vehicle chassis and the occupant, respectively. The springs and dampers in the model are nonlinear piecewise functions of displacements and velocities respectively. More specifically, a genetic algorithm (GA) approach is proposed for estimating the parameters of vehicle front structure and restraint system. Finally, it is shown that the obtained model can accurately reproduce the real crash test data taken from the National Highway Traffic Safety and Administration (NHTSA). The maximum dynamic crash of the vehicle model is 0.05% less than that in the real crash test. The displacement of the occupant is 0.09% larger than that from the crash test. Improvement of the model accuracy is also observed from the time at maximum displacement and the rebound velocities for both the vehicle and occupant.**

Keywords— Modeling; vehicle-occupant; frontal crash; parameters estimation; genetic algorithm;

C.1 Introduction

Car accidents are one of the major causes of mortality in modern society. While it is desirable to maintain the crashworthiness, car manufacturers perform crash tests on a sample of vehicles for monitoring the effect of the occupant in different crash scenarios. Car crash tests are usually performed to ensure safe design standards in crashworthiness (the ability of a vehicle to be plastically deformed and yet maintains a sufficient survival space for its occupants during the crash scenario). However, this process requires a lot of time, sophisticated infrastructure and trained personnel to conduct such a test and data analysis. Therefore, to reduce the cost associated with the real crash test, it is worthy to adopt the simulation of a vehicle crash and validate the model results with the actual crash test. Nowadays, due to advanced research in simulation tools, simulated crash tests can be performed beforehand the full-scale crash test. Therefore, the cost associated with the real crash test can be reduced. Finite element method (FEM) models and lumped parameter models (LPM) are typically used to model the vehicle crash phenomena. Vehicle crashworthiness can be evaluated in four distinct modes: frontal, side, rear and rollover crashes. Several types of research have been carried out in this field, which resulted in several novel computational models of vehicle collisions in literature, and a brief review is given

in this paper.

C.2 Literature survey and limitations of current techniques

An application of physical models composed of springs, dampers and masses joined in various arrangements for simulating a real car collision with a rigid pole was presented in [1]. In [2], a 5-DOFs lumped parameter modeling for the frontal crash was investigated to analyze the response of occupant during the impact. Ofochebe et al. in [3] studied the performance of vehicle front structure using a 4-DOFs lumped mass-spring model composed of body, engine, the cross-member and suspension and the bumper masses.

In [4] and [5], an optimization procedure to assist multi-body vehicle model development and validation was proposed. In the work of [6], the authors proposed an approach to control the seat belt restraint system force during a frontal crash to reduce thoracic injury. Klausen et al. [7] used firefly optimization method to estimate parameters of vehicle crash test based on single-mass. To reconstruct the crash event, Tørdal et al. [8] extracted the motion of a bus in an oblique crash and the kinematics of a Ford Fiesta in a pole crash from a high frame rate video. Tso-Liang et al. in [9] examined the dynamic response of the human body in a crash event and assessed the injuries sustained to the occupant's head, chest and pelvic regions.To reduce the occupant injury risks in vehicle frontal crashes, mathematical models that optimize the vehicle deceleration have been developed in [10, 11]. Apart from the commonly used approaches, recently intelligent approaches have been used in the area of vehicle crash modeling. The most commonly used are Fuzzy logic in [12], Neuro-fuzzy in [13], firefly algorithm in [7] and genetic algorithm. A genetic algorithm has been used in [14] for calculating the optimized parameters of a 12-DOFs model for two vehicle types in two different frontal crashes. In [15, 16], the author used Genetic Algorithms to optimize the performance of PID, Fuzzy and Neuro-fuzzy controllers on various systems. The main challenge in accident reconstruction is the system identification described as the process of constructing mathematical models of dynamical systems using measured input-output data. In the case of a vehicle crash, system identification algorithm consists of retrieving the unknown parameters such as the spring stiffness and damping coefficient. A possible approach is to identify these parameters directly from experimental data. From literature, System Identification Algorithms (SIA) have been developed for different applications.

Among others, we can state-space identification, eigensystem realization algorithm and data-based regressive model approaches. Typical examples where these SIA have been used can be found in [17–19].

In this paper, based on the previous research work [7], we develop a mathematical model for a double-spring-mass-damper system which reconstructs a vehicle-occupant frontal crash scenario and estimates structural parameters of the vehicle's front structure and the restraint system. The structural parameters estimated are spring and damping coefficients. To estimate the physical parameters of the model, a genetic algorithm is proposed. It is observed that the predicted results fit the experimental data very well.

C.3 The newly proposed method

The main objective of this section is to represent a dynamic model to capture the vehicle frontal crash phenomena. During the frontal crash, the vehicle is subjected to an impulsive force caused by the obstacle. The model for vehicle crash simulates a rigid barrier impact of the car, where m_1 and m_2, as shown in Figure C.1 represent the frame rail (chassis) and occupant masses, respectively. In this model, the parameters to be estimated are spring stiffness constants k_l, k_{nl} and k_2, damping constants c_l, c_{nl} and c_2. When the vehicle crashes into a rigid barrier, the two masses will experience an impulsive force during the collision. The real crash phenomenon is shown in Figure C.2 and it is observed that the value for the maximum dynamic crash of the vehicle is 72.69 cm, the time of the crash is 0.0894 s and the rebound velocity is -3.75 m/s. At the time of crash, the occupant experiences a forward movement of 30.3 cm making a total displacement of 103 cm. The rebound velocity of the occupant is -13.1 m/s.

In line of the model development to capture the values as mentioned earlier during the crash scenario, the 2-DOF dynamical model proposed in [20] for the free vibration analysis is adopted for solving the impact responses of the two masses. Then, the genetic algorithm is used to estimate the 2-DOF model parameters.

C.3.1 Model 1: Combination of linear and nonlinear springs and dampers

In model 1 the deforming spring and damping forces, developed at time of crash, are nonlinear cubic functions in x and $\dot{x}$ respectively. The spring stiffness and damper

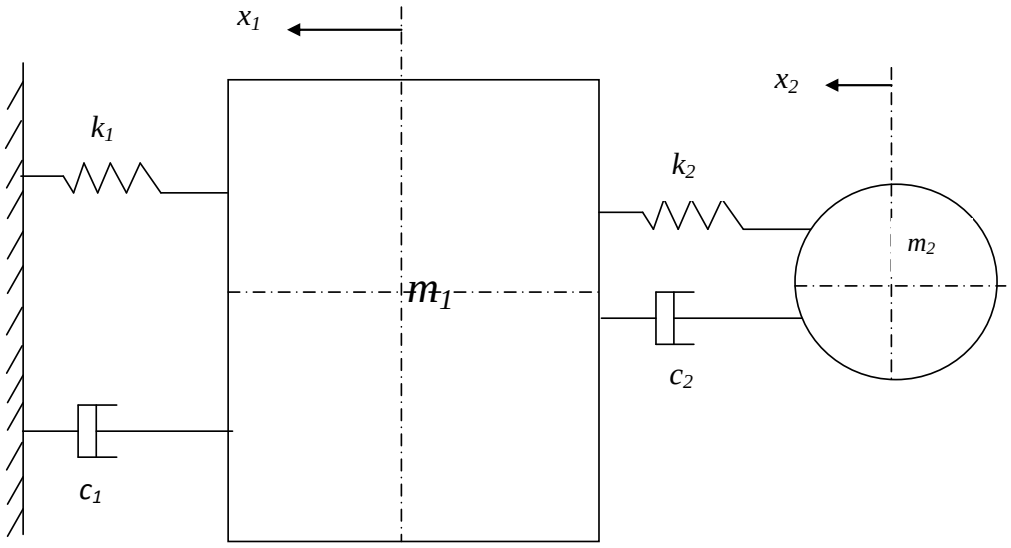

Figure C.1: A double spring-mass-damper model

constants are defined as follows:

$$k_1 = k_l + k_{nl} \tag{C.1}$$

$$c_1 = c_l + c_{nl} \tag{C.2}$$

The dynamic equations of the double-mass-spring-damper model are shown in the following:

$$F_{str} = k_l x_1 + k_{nl} x_1^3 + c_l \dot{x}_1 + c_{nl} \dot{x}_1^3 \tag{C.3}$$

$$F_{rest} = k_2(x_2 - x_1) + c_2(\dot{x}_2 - \dot{x}_1) \tag{C.4}$$

$$\ddot{x}_1 = (F_{rest} - F_{str})/m_1 \tag{C.5}$$

$$\ddot{x}_2 = (F_{rest})/m_2 \tag{C.6}$$

where F_{str} and F_{rest} are the deformation force of the vehicle frontal structure and the restraint system respectively.
k_l and k_{nl}, are linear and nonlinear springs c_l and c_{nl}, are linear and nonlinear dampers of the front vehicle structure respectively. k_2 and c_2 are spring stiffness

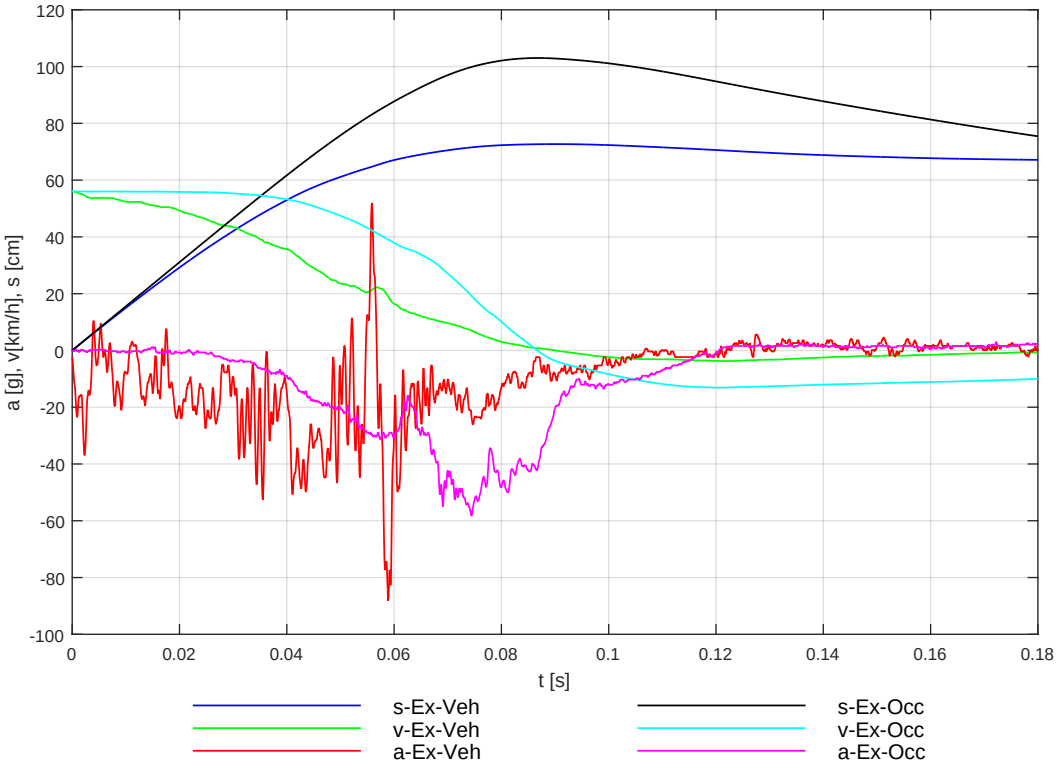

Figure C.2: Crash test data

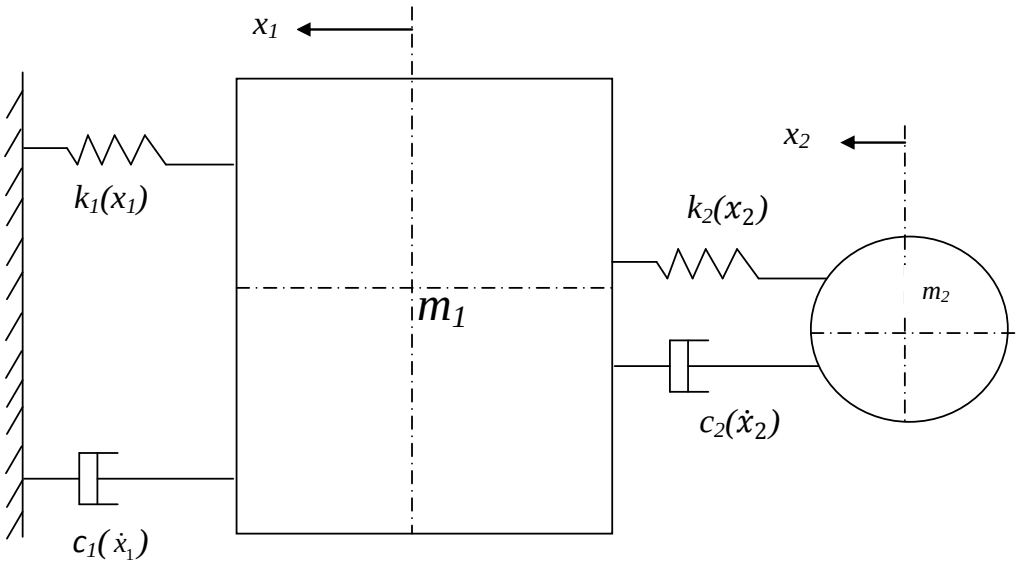

Figure C.3: The Model 2

and damper coefficients for the restraint system respectively.

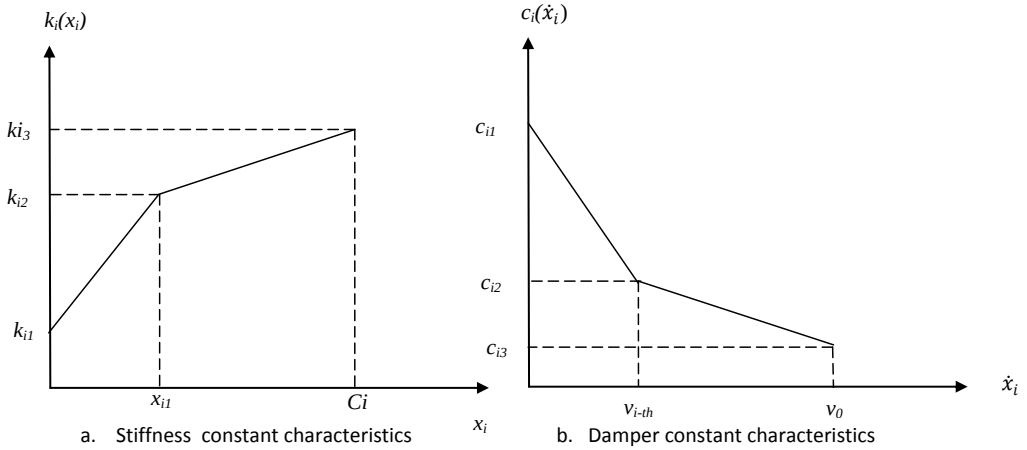

Figure C.4: Stiffness and damper characteristics of vehicle frontal structure

C

C.3.2 Model 2: Piecewise functions of springs and dampers

Figure C.3 represents the vehicle- occupant model with non-linear spring and dampers, which crashes into a fixed barrier. Based on the nonlinear characteristics of velocity and displacement of the vehicle and forward movement of the occupant shown in Figure C.2, the springs and dampers that simulate such characteristics must also be nonlinear as predefined in Figure C.4. The dynamic equation of the model is defined by:

$$F_{str} = k_1 x_1 + c_1 \dot{x}_1 \tag{C.7}$$

F_{rest}, $\ddot{x}_1$ and $\ddot{x}_2$ are identical to Eqs.(4) - (6). The piecewise functions for stiffness and dampers in the front structure of the vehicle and restrain system are defined as follows:

$$k_i(x_i) = \begin{cases} k_{i1} + \frac{k_{i2}-k_{i1}}{x_{i1}} x_i & x_i \leq x_{i1} \\ k_{i2} + \frac{k_{i3}-k_{i2}}{C_i - x_{i1}}(x_i - x_{i1}) & x_{i1} \leq x_i \leq C_i \end{cases} \tag{C.8}$$

$$c_i(\dot{x}_i) = \begin{cases} c_{i1} - \frac{c_{i1}-c_{i2}}{\dot{x}_{i1}} \dot{x}_i & \dot{x}_i \leq v_{i-th} \\ c_{i2} - \frac{c_{i2}-c_{v3}}{v_0 - \dot{x}_{i1}}(\dot{x}_i - v_{i-th}) & v_{i-th} \leq \dot{x}_i \leq v_0 \end{cases} \tag{C.9}$$

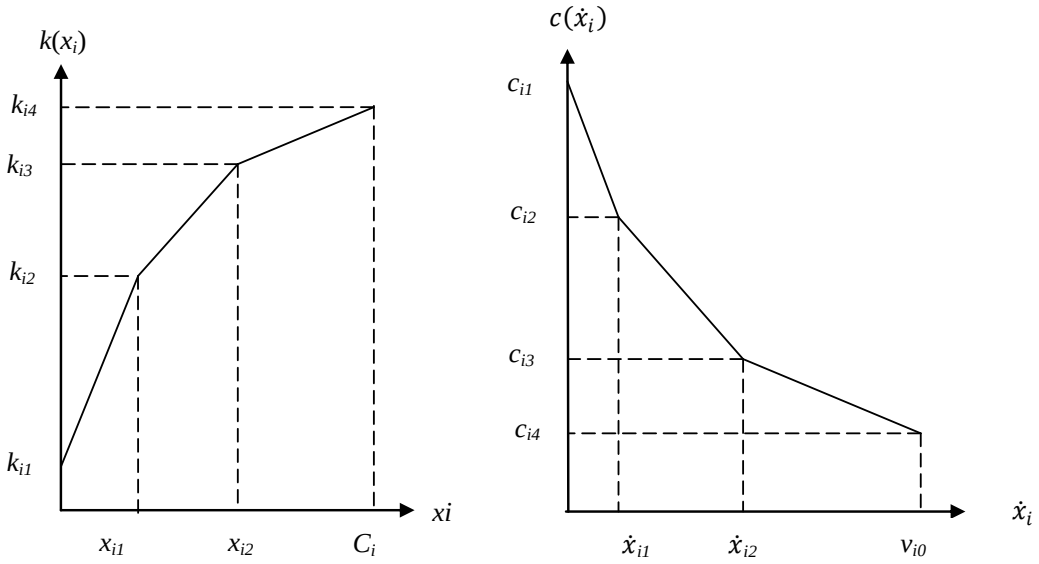

a. Stiffness constant characteristics b. Damper constant characteristics

Figure C.5: Stiffness and damper characteristics of the restraint system

where the index $i = 1, 2$ stand for 1^{st} and 2^{nd} mass respectively. C_i is the dynamic crash of the vehicle or occupant. v_0 is the initial impact velocity. v_{i-th} is the threshold velocity of i mass.

At the maximum crash, the spring stiffness is assumed to be high, but the damper coefficient is small for maintaining the shape of displacements and velocities of vehicle and occupant respectively. To get better results, the model in Figure C.4 can be modified by introducing two break point on the predefined shapes of springs and dampers as shown in Figure C.5 and defined in Eqs.(C.10) - (C.11).

$$k_i(x_i) = \begin{cases} k_{i1} + \frac{k_{i2}-k_{i1}}{x_{i1}} x_i & x_i \leq x_{i1} \\ k_{i2} + \frac{k_{i3}-k_{i2}}{x_{i2}-x_{i1}}(x_i - x_{i1}) & x_{i1} \leq x_i \leq x_{i2} \\ k_{i3} + \frac{k_{i4}-k_{i3}}{C_i-x_{i2}}(x_i - x_{i2}) & x_{i2} \leq x_i \leq C_i \end{cases} \tag{C.10}$$

$$c_i(\dot{x}_i) = \begin{cases} c_{i1} - \frac{c_{i1}-c_{i2}}{\dot{x}_{i1}}\dot{x}_i & \dot{x}_i \leq \dot{x}_{i1} \\ c_{i2} - \frac{c_{i2}-c_{i3}}{\dot{x}_{i2}-\dot{x}_{i1}}(\dot{x}_i - \dot{x}_{i1}) & \dot{x}_{i1} \leq \dot{x}_i \leq \dot{x}_{i2} \\ c_{i3} - \frac{c_{i3}-c_{i4}}{v_0-\dot{x}_{i2}}(\dot{x}_i - \dot{x}_{i2}) & \dot{x}_{i2} \leq \dot{x}_i \leq v_0 \end{cases} \tag{C.11}$$

C.3.3 Optimization algorithm

The proposed algorithm seeks to find the minimum function between several variables as can be stated in a general form $minf(p)$, where 'p' denotes the unknown variables, which are the damping and stiffness constants in the model. The cost function $f(p)$ is the objective function which should be optimized. The cost function to be minimized is the norm of the absolute error between the displacement of the simulated cash and the experimental crash data and is defined as

$$[Error] = sum(|E_{st} - E_{xp}|^T \times |E_{st} - E_{xp}) \tag{C.12}$$

where E_{st} and E_{xp} are the model and experimental variables (displacements, velocity and acceleration) respectively. All parameters defined in Eqs.(C.8) -(C.11) are embedded in E_{st} .

The GA method is used here for optimization of the cost function. The GA-type of search schemes is function-value comparison-based, with no derivative computation. It attempts to move points through a series of generations, each being composed of a population which has a set number of individuals, where individuals represent parameters to be estimated. The population size depends on the number of parameters to be estimated for a given model. For example, the Model1 has six individuals, Model 2 for a one break point piecewise function, in Figure (C.4), has eighteen individuals and twenty-four individuals for a two break points piecewise function, in Figure (C.5). Each individual is a point in the parameter space (in our case, the displacement of experimental data). The schemes that are applied to the evolution of generations have some analogy to the natural genetic evolution of species, hence the term genetic.

G.A. is an adaptive heuristic search algorithm based on the evolutionary ideas of nature selection and genetics. It represents an intelligent exploitation of a random search used to solve optimization problems and consists of five operators: Initialization, Selection, crossover, mutation and replacement. Initialization is used to

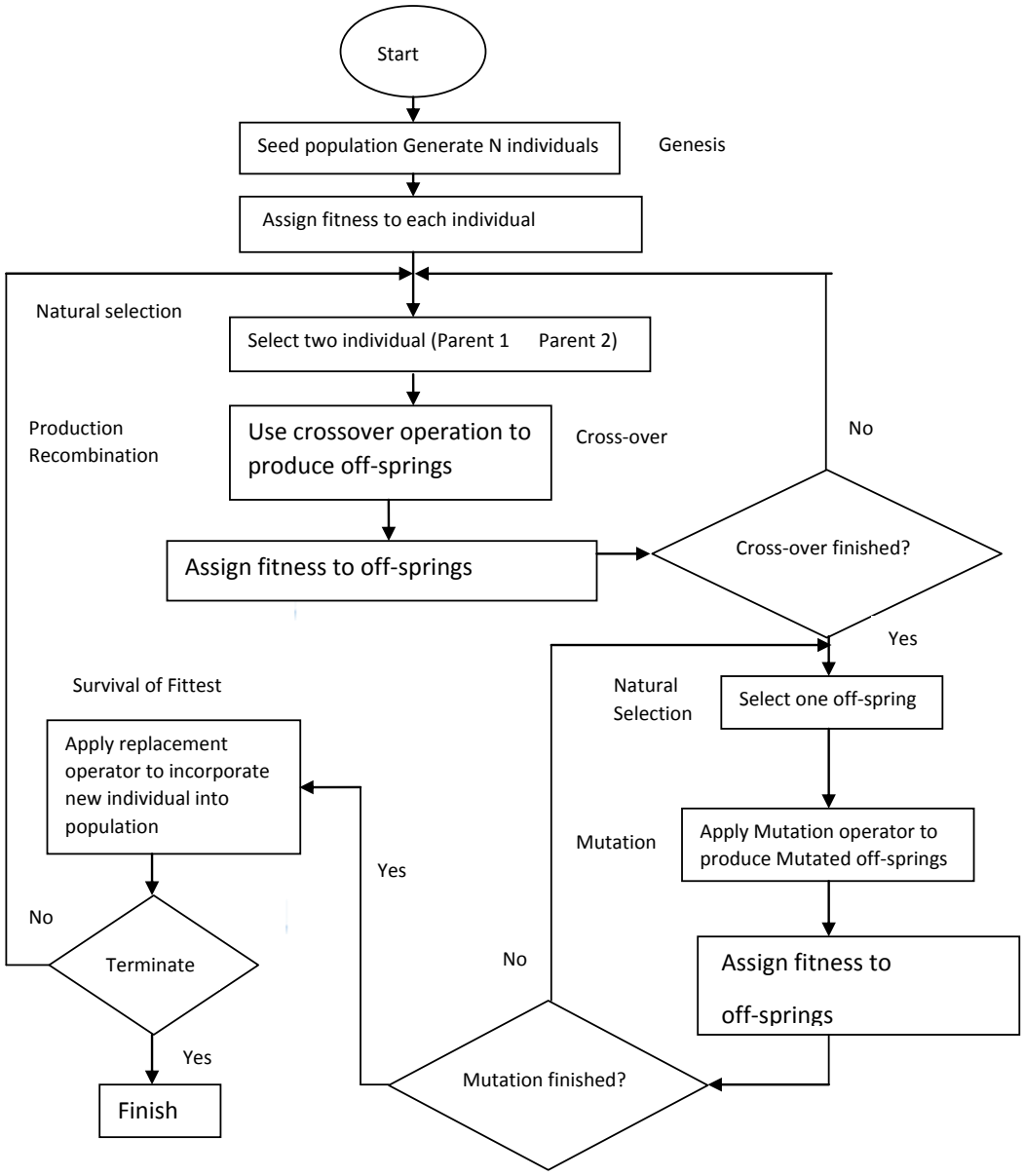

Figure C.6: GA flowchart

seed initial population randomly while selection is used to select the fittest from the population. Crossover is used to explore the search space. Mutation is used to remove the problem like genetic drift (some individuals may leave behind a few more off-springs than other individuals), and replacement is used to progress generation wise population [21]. Figure C.6 shows a general flowchart of a genetic algorithm.

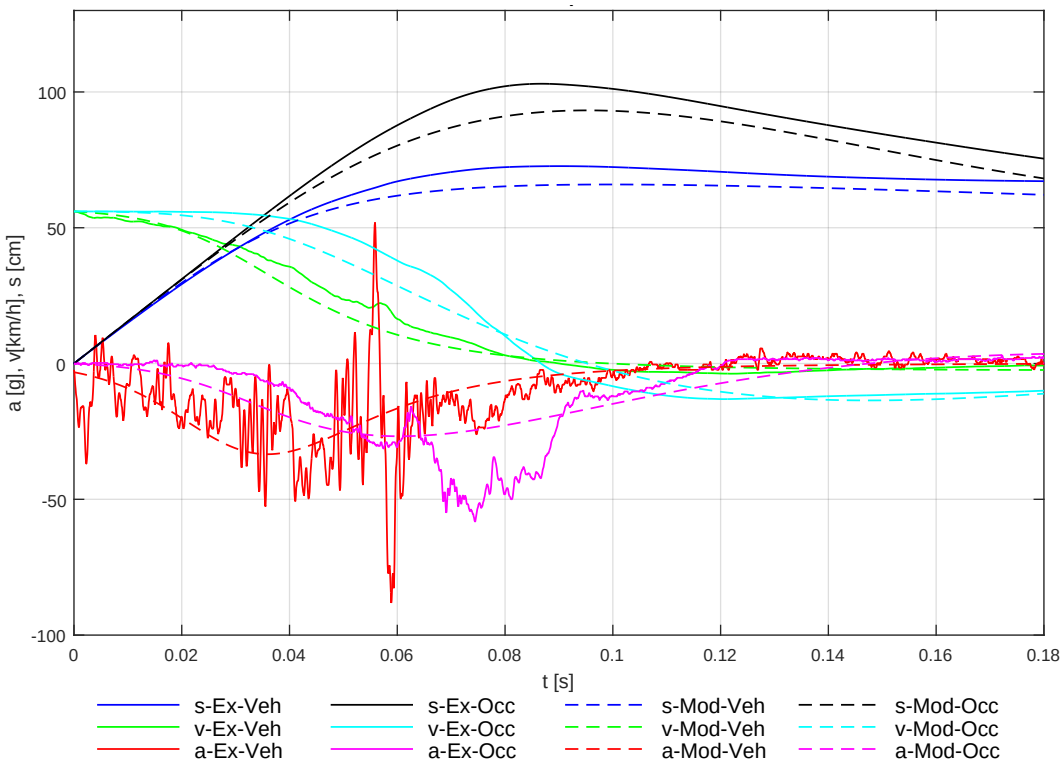

Figure C.7: Comparison between vehicle model and vehicle experimental data - Nonlinear Model1

C.4 Results and discussion

Comparisons between the model results and the experimental data are shown in Figures C.7 - C.9, where the stapled lines and continuous lines represent the simulation results and the experimental data respectively. The symbols s-Ex-Veh, v-Ex-Veh, a-Ex-Veh, s-Ex-Occ, v-Ex-Occ, a-Ex-Occ, s-Mod-Veh, v-Mod-Veh, a-Mod-Veh, s-Mod-Occ, v-Mod-Occ, a-Mod-Occ, on the legends stand for displacement (s), velocity(v) and acceleration(a) of the vehicle(Veh) and occupant(Occ) respectively. Ex and Mod stand for Experimental and Model, respectively.

It is noted from Figure C.7 that the maximum displacements of the vehicle and occupant models are 9.2% and 9.5% less those from the experimental data respectively. The time of the dynamic crush is far from the experimental data. The maximum crash of the vehicle is 0.089 s while that from the model is 0.098 s. This is also observed on the occupant time at maximum displacement; that is 0.146 s instead of 0.12 s from data. The rebound velocity of $-2.3m/s$ for the vehicle model is slightly less than that in the real crash (i.e. $-3.75m/s$), but the occupant rebound velocity of $-13.5m/s$ is almost closer to the real crash data (i.e.$-13.1m/s$). This

Table C.1: Parameters estimation Model1

Parameter	*Value*	*Unit*
k_l	6.4270e+04	N/m
k_{nl}	30.3830	N/m^3
c_l	6.2029e+04	Ns/m
c_{nl}	246.2119	Ns^3/m^3
k_2	4.3159e+04	N/m
c_2	2.0797e+03	Ns/m

Table C.2: Parameters estimation Model2- one break point piecewise function

Parameter	*Value*	*Unit*	*Parameter*	*Value*	*Unit*
k_{11}	6.3993e+04	N/m	k_{21}	6.2502e+03	N/m
k_{12}	3.5743e+04	N/m	k_{22}	3.8618e+04	N/m
k_{13}	6.3669e+04	N/m	k_{23}	7.5718e+04	N/m
x_{11}	0.3034	m	x_{21}	0.0529	m
c_{11}	8.3497e+04	Ns/m	c_{21}	3.1340e+03	Ns/m
c_{12}	3.2983e+03	Ns/m	c_{22}	3.0876e+03	Ns/m
c_{13}	1.9725e+05	Ns/m	c_{23}	3.1159	Ns/m
$v_{1\text{-}th}$	15.5035	m/s	$v_{2\text{-}th}$	0.1013	m/s

shows that the model presented in Figure C.1, with combined linear and nonlinear force elements cannot accurately reconstruct the vehicle occupant crash scenario. The estimated parameters, linear and nonlinear springs and dampers: k_l, k_{nl}, c_l, c_{nl}, k_2 and c_2 , are shown in Table C.1.

An improvement is noted in Figure C.8 where the stiffness and dampers in the model are piecewise functions with one break point shown in Figure C.4. The maximum dynamic crush of the vehicle model is 0.3% less than that in the real crash test. The displacement of the occupant is 0.4% larger than that from the crash test. Improvement of the model accuracy is also observed from the time at maximum displacement and the rebound velocities for both the vehicle and occupant. The estimated parameters are shown in Table C.2.

From Figure C.9, the model accuracy is obtained by using force elements with

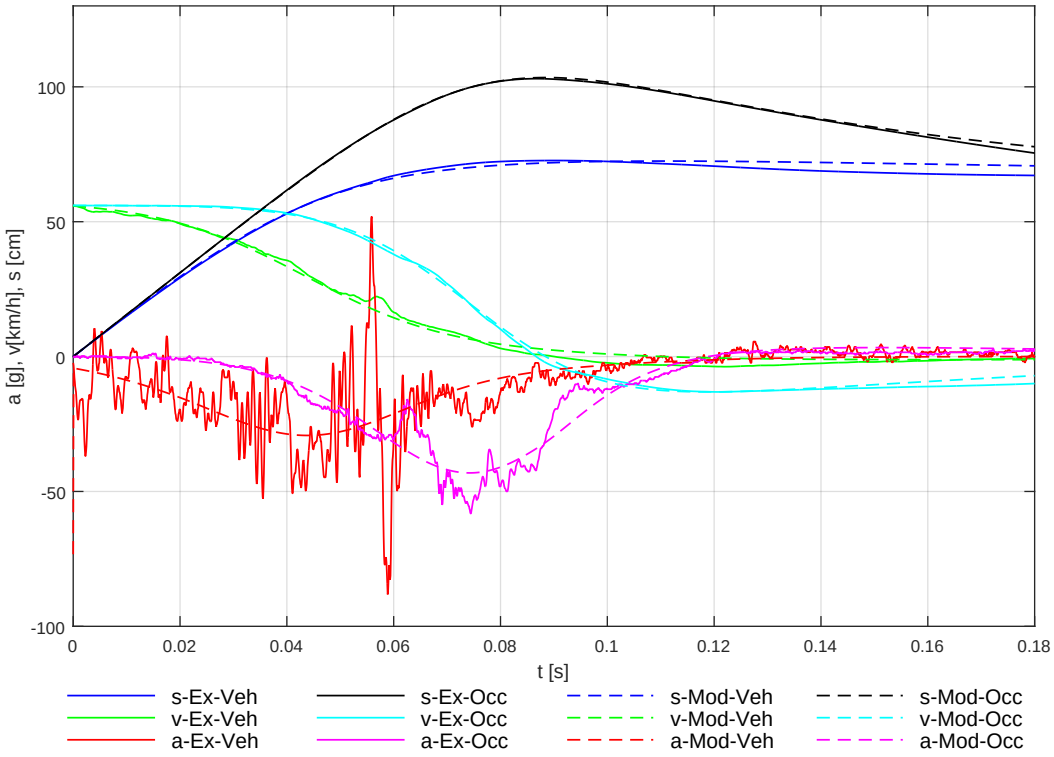

Figure C.8: Comparison between vehicle model and vehicle experimental data - piecewise function with 1 break point

Table C.3: A summary of kinematics results from the models

Model type		C_m [cm]	T_m [s]	v_{reb} [m/s]
Model1: Mixed of linear and nonlinear springs / dampers	Vehicle	65.93	0.0978	-2.26
	Occupant	93.22	0.09473	-13.58
Model2:1 break point piecewise function	Vehicle	72.48	0.1085	-1.15
	Occupant	103.4	0.08617	-13.1
Model2: 2 break points piecewise functions	Vehicle	72.65	0.093	-2.43
	Occupant	103.2	0.0863	-12.68

two break point piecewise functions as shown in Figure C.5. The maximum dynamic crash of the vehicle model is 0.05% less than that in the real crash test. The displacement of the occupant is 0.09% larger than that from the crash test. Improvement of the model accuracy is also observed from the time at maximum displacement and the rebound velocities for both the vehicle and occupant. A summary of kinematics results from the models is tabulated in Table C.3 and the optimized estimated parameters are shown in Table C.4. The deformation force and loading characteristics of the vehicle front structure and restraint system are shown in Figure C.10. A maximum force of $1,352,000N$ is observed at the time of collision and

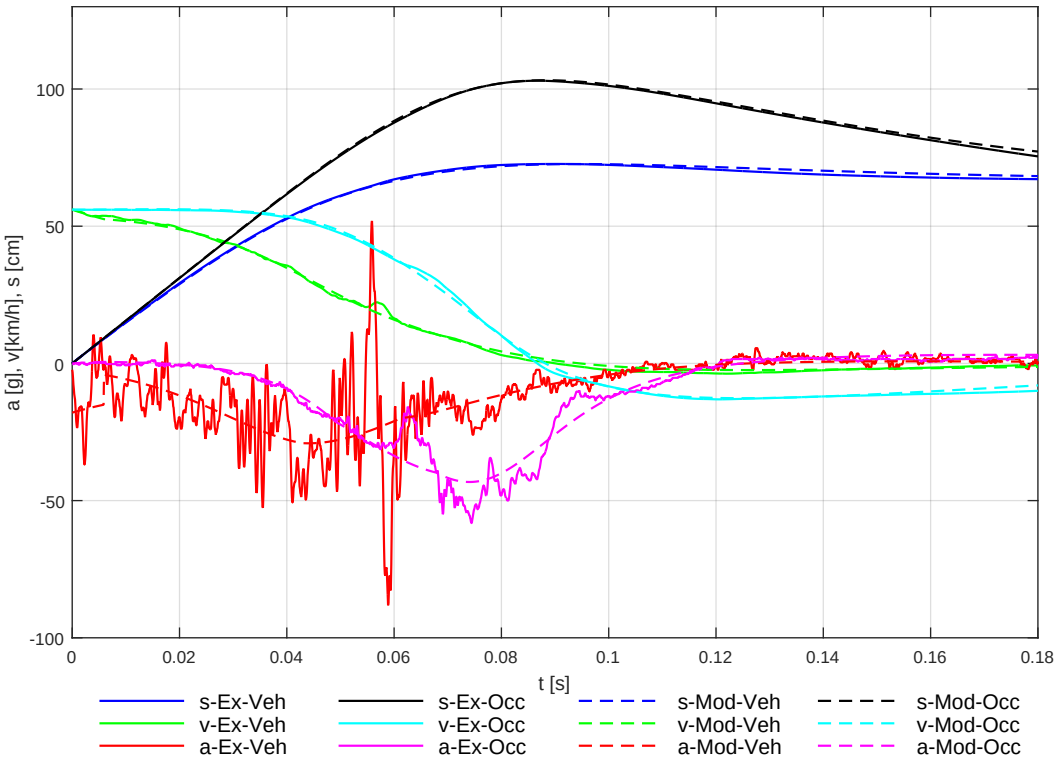

Figure C.9: Comparison between vehicle model and vehicle experimental data - piecewise function with 2 break points

Table C.4: Parameters estimation Model2- two break points piecewise function

Parameter	*Value*	*Unit*	*Parameter*	*Value*	*Unit*
k_{11}	7.6665e+04	N/m	k_{21}	6.8536e+03	N/m
k_{12}	7.9498e+04	N/m	k_{22}	2.5529e+04	N/m
k_{13}	9.6887e+03	N/m	k_{23}	9.9998e+04	N/m
k_{14}	9.9998e+04	N/m	k_{24}	7.2212e+04	N/m
x_{11}	0.5533	m	x_{21}	3.3735e-05	m
x_{12}	0.6711	m	x_{22}	0.7498	m
c_{11}	8.4895e+04	Ns/m	c_{21}	4.8212e+03	Ns/m
c_{12}	2.8460e+03	Ns/m	c_{22}	1.3677e+03	Ns/m
c_{13}	3.3299e+03	Ns/m	c_{23}	3.2491e+03	Ns/m
c_{14}	1.4046e+04	Ns/m	c_{24}	2.2323e+03	Ns/m
$\dot{x}_{11}$	10.4951	m/s	$\dot{x}_{21}$	7.8176	m/s
$\dot{x}_{12}$	14.6044	m/s	$\dot{x}_{22}$	15.6884	m/s

decreases up to $-36,680N$. The restraint system reaches the maximum force of $57,590N$ at $0.054s$. Spring and damper characteristics are shown in Figure C.11 and Figure C.12 respectively.

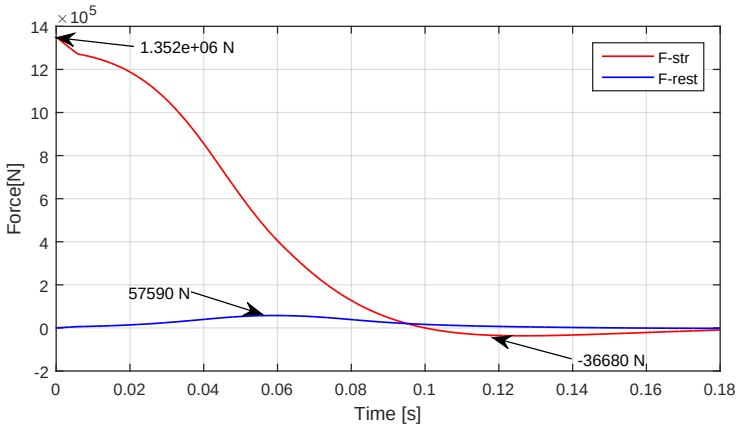

Figure C.10: Deformation of the vehicle frontal structure

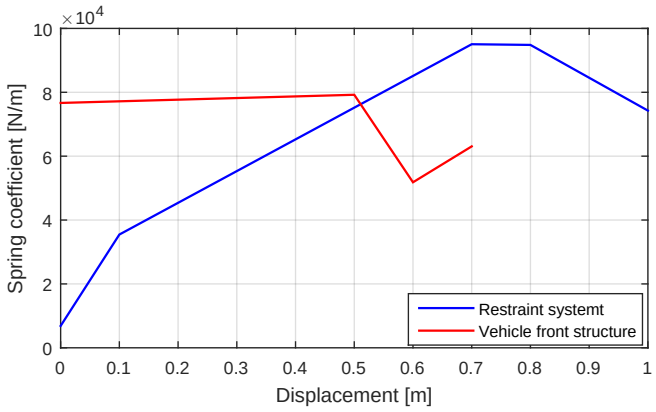

Figure C.11: Spring coefficient characteristics

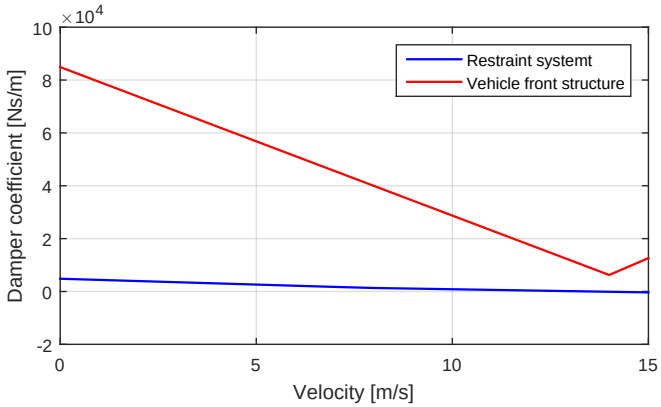

Figure C.12: Damper coefficient characteristics

C.5 Conclusion and future work

In this paper, a mathematical-based method is presented to estimate the parameters of a double-spring-mass-damper model of a vehicle-occupant frontal crash. It is

observed that the model results in responses are closer to the experimental crash test. Therefore, the overall behavior of the model matches the real vehicle's crush well. Two of the main parameters characterizing the collision are the maximum dynamic crush - which describes the highest car's deformation and the time at which it occurs- t_m. They are pertinent to the occupant crashworthiness since they help to assess the maximum intrusion into the passenger's compartment.

The model with combined linear and nonlinear force elements showed results with a significant error. It is noted that the stepwise nonlinear springs and dampers model 2, gives better results than the model 1. Introducing more break points on the piecewise functions increases the accuracy of the model. The force due to structure deformation decreases, and the loading due to the restraint system increases and become maximum at the time of crash. These forces are almost zero after rebound phase.

The authors will extend the work by including other parts of the vehicle such as an engine in the model. Further investigations of the proposed approach to vehicle-to-vehicle crash scenario is also under study.

Acknowledgment

Thanks to The Dynamic Research Group members, at the University of Agder, for their constructive comments and criticisms. The inspiration for this paper is a result of regular meetings of the group.

REFERENCES

[1] W. Pawlus, J. E. Nielsen, H. R. Karimi, and K. G. Robbersmyr. Application of viscoelastic hybrid models to vehicle crash simulation. *International Journal of Crashworthiness*, 55:369 – 378, 2011.

[2] J. Marzbanrad and M. Pahlavani. Calculation of vehicle-lumped model parameters considering occupant deceleration in frontal crash. *International Journal of Crashwothiness*, 16(4):439 – 455., 2011.

[3] S. M. Ofochebe, C. G. Ozoegwu, and S. O. Enibe. Performance evaluation of vehicle front structure in crash energy management using lumped mass spring system. *Advanced Modeling and Simulation in Engineering*, 2(2):1–18, April 01 2015.

[4] L. Sousa, P.Verssimo, and J. Ambrsio. Development of generic multibody road vehicle models for crashworthiness. *Multibody Syst Dyn*, 19:133 – 158, 2008.

[5] M. Carvalho, J. Ambrsio, and P. Eberhard. Identification of validated multibody vehicle models for crash analysis using a hybrid optimization procedure. *Struct Multidisc Optim*, 44:85 – 97, 2011.

[6] A.A. Alnaqi and A.S. Yigit. Dynamic analysis and control of automotive occupant restraint systems. *Jordan Journal of Mechanical and Industrial Engineering*, 5(1):39 – 46, 2011.

[7] A. Klausen, S. S. Tørdal, H. R. Karimi, K. G. Robbersmyr, M. Jecmenica, and O. Melteig. Firefly optimization and mathematical modeling of a vehicle crash test based on single-mass. *Journal of Applied Mathematics*, pages 1 – 10, 2014.

[8] S. S. Tørdall, A. Klausen, H. R. Karimi, K. G. Robbersmyr, M. Jecmenica, and O. Melteig. An application of image processing in vehicle crash motion detection from high frame rate video. *international Journal of Innovative Computing, Informationand Control*, 11(5):1667 – 1680, 2015.

[9] T.L. Teng, F.A. Chang, Y.S. Liu, and C.P. Peng. Analysis of dynamic response of vehicle occupant in frontal crash using multibody dynamics method. *Mathematical and Computer Modelling*, 48:1724 – 1736, 2008.

[10] K. Mizuno, T. Itakura, S. Hirabayashi, E. Tanaka, and D. Ito. Optimization of vehicle deceleration to reduce occupant injury risks in frontal impact. *Traffic Injury Prevention*, 15:48 – 55, 2014.

[11] D. Ito, Y. Yokoi, and K. Mizuno. Crash pulse optimization for occupant protection at various impact velocities. *Traffic Injury Prevention*, 16:260 – 267, 2015.

[12] L. Zhao, H. R. Karimi W. Pawlus, and K. G. Robbersmyr. Data-based modeling of vehicle crash using adaptive neural-fuzzy inference system. *IEEE / ASME Transactions on mechatronics*, 19(2):684 – 696, April 2014.

[13] W. Pawlus, H. R. Karimi, and K. G. Robbersmyr. A fuzzy logic approach to modeling a vehicle crash test. *Central European Journal of Engineering*, pages 1 – 13, 2012.

[14] M. Pahlavani and J. Marzbanrad. Crashworthiness study of a full vehicle-lumped model using parameters optimization. *International Journal of Crashworthiness*, 20(6):573 – 591, 2015.

[15] D. Pelusi. Genetic-neuro-fuzzy controllers for second order control systems. In *2011 UKSim 5th European Symposium on Computer Modeling and Simulation*, pages 12 – 17, 2011.

[16] D. Pelusi. Optimization of a fuzzy logic controller using genetic algorithms. In *2011 Third International Conference on Intelligent Human-Machine Systems and Cybernetics*, pages 143 – 146, 2011.

[17] B. B. Munyazikwiye, K. G. Robbersmyr, and H. R. Karimi. A state-space approach to mathematical modeling and parameters identification of vehicle frontal crash. *Systems Science and Control Engineering*, 2:351 – 361, 2014.

[18] B. B. Munyazikwiye, H. R. Karimi, and K. G. Robbersmyr. Mathematical modeling and parameters estimation of car crash using eigensystem realization algorithm and curve-fitting approaches. *Mathematical Problems in Engineering*, pages 1 – 13, 2013.

[19] W. Pawlus, K.G. Robbersmyr, and H. R. Karimi. Mathematical modeling and parameters estimation of a car crash using data-based regressive model approach. *Applied Mathematical Modelling*, 35:5091 – 5107, 2011.

[20] M. Huang. *Vehicle Crash Mechanics*. CRC PRESS, Boca Raton London New York Washington, 2002.

[21] R. Kumar, G. Gopal, and R. Kumar. Novel crossover operator for genetic algorithm for permutation problems. *International Journal of Soft Computing and Engineering (IJSCE)*, 3(2):252–258, May 2013.

Paper D

Title:	Optimization of Vehicle-to-Vehicle Frontal Crash Model based on Measured Data using Genetic Algorithm
Authors:	Bernard B. Munyazikwiye [1], Hamid Reza Karimi [2], and Kjell G. Robbersmyr [1]
Affiliation:	[1] Faculty of Engineering and Science, University of Agder, P.O. Box 509, 4879 Grimstad, Norway [2] Department of Mechanical Engineering, Politecnico di Milano 20156 Milan, Italy
Article:	*IEEE Access* , Special Section on Recent Advances on Modelling, Optimization , and Signal.Processing Methods in Vehicle Dynamics and Crash-Worthiness, March 2017,Vol.5, pp. 3131-–3138, DOI: 10.1109/ACCESS.2017.2671357
Copyright ©:	IEEE
Layout:	The layout of the paper has been revised to have the same format as the thesis

Abstract — **In this paper, a mathematical model for vehicle-to-vehicle frontal crash is developed. The experimental data are taken from the National Highway Traffic Safety Administration (NHTSA). To model the crash scenario, the two vehicles are represented by two masses moving in opposite directions. The front structures of the vehicles are modeled by Kelvin elements, consisting of springs and dampers in parallel, and estimated as piecewise linear functions of displacements and velocities respectively. To estimate and optimize the model parameters, a genetic algorithm (GA) approach is proposed. Finally, it is observed that the developed model can accurately reproduce the real kinematic results from the crash test.**

Keywords— Modeling, vehicle-to-vehicle crash, parameters estimation, genetic algorithm.

D.1 Introduction

Car accidents are one of the major causes of mortality in modern society. While it is desirable to maintain the crash-worthiness, car manufacturers perform crash tests on a sample of vehicles for monitoring the effect of the occupant in different crash scenarios. Car crash tests are usually performed to ensure safe design standards in crash-worthiness (the ability of a vehicle to be plastically deformed and yet maintains a sufficient survival space for its occupants during the crash scenario). However, this process is very time consuming and requires sophisticated infrastructure and trained personnel to conduct such a test and data analysis. Therefore, to reduce the cost associated with the real crash test, it is worthy to adopt the simulation of a vehicle crash and validate the model results with the actual crash test. Nowadays, due to advanced research in simulation tools, simulated crash tests can be performed beforehand the full-scale crash test. Therefore, the cost associated with the real crash test can be reduced. Finite element method (FEM) models and lumped parameter models (LPM) are typically used to model the vehicle crash phenomena and hence can help the designer to better design the vehicle with less number of crash tests. Vehicle crash-worthiness can be evaluated in four distinct modes: frontal, side, rear and rollover crashes.

In the past few decades, much research has been carried out in the field of vehicle crash-worthiness, which resulted in several novel computational models of vehicle collisions in the literature, and a brief review is given in this paper. An ap-

plication of physical models composed of springs, dampers and masses joined in various arrangements for simulating a real car collision with a rigid pole, was presented in [1]. The same authors in [2], proposed a method of modeling for vehicle crash systems based on viscous and elastic properties of the materials and explained the differences in simulating vehicle-to-rigid barrier collision and vehicle–to-pole collision. A method to reproduce car kinematics during a collision using a non-linear autoregressive (NAR) model, where parameters are estimated by the use of feed-forward neural network model, was proposed in [3]. In [4], a Five-Degrees of Freedom (5-DOFs) lumped parameter model for the frontal crash was investigated to analyze the response of occupant during the impact. Ofochebe et al. in [5], studied the performance of vehicle front structure using a 4-DOFs lumped mass-spring model composed of body, engine, the cross-member, the suspension and the bumper masses.

In [6] and [7], an optimization procedure to assist multi-body vehicle model development and validation was proposed. In the work of [8], the authors proposed an approach to control the seat belt restraint system force during a frontal crash to reduce thoracic injury. Klausen et al. [9] used firefly optimization method to estimate parameters of vehicle crash test based on a single-mass. Munyazikwiye et al. in [10] and [11], used different approaches to model the vehicle frontal crash using a double-spring-mass-damper model. In [12], a mathematical model for vehicle-occupant frontal crash was studied using genetic algorithm. Tso-Liang et al. in [13], examined the dynamic response of the human body in a crash event and assessed the injuries sustained to the occupant's head, chest and pelvic regions.

Apart from the commonly used approaches, recently intelligent approaches have been used in the area of vehicle crash modeling. The most commonly used, are Fuzzy logic in [14], Neuro-fuzzy in [15], genetic algorithm and firefly algorithm in [9]. Vangi in [16] developed an approach to determine the impact severity indexes of oblique impact with a non-zero restitution. While in [17], the authors developed a fuzzy logic model for vehicle frontal crash to predict vehicle crash severity from acceleration data. The kinetic energy and jerk inputs data were used to find the crash severity index. Vangi and Begani [18], demonstrated the usefulness of the triangle method for evaluating the kinetic energy loss of a vehicle during road traffic accident, while in [19], the authors used a fuzzy approach to reconstruct the accident history at time of crash and calculated the velocity of an impacting vehicle. A genetic algorithm has been used in [20] for calculating the optimized parameters of a 12-DOFs model for two vehicle types in two different frontal crashes.

The main challenge in accident reconstruction is the system identification, described as the process of constructing mathematical models of dynamical systems using measured input-output data, where the input data is the acceleration measurement and output data is the deformation of the vehicle. In [21], a novel wavelet-based approach was introduced to reproduce acceleration pulse of a vehicle involved in a crash event. In the case of a vehicle crash, system identification algorithm is used to retrieve the unknown parameters such as the spring stiffness and damping coefficient. A possible approach is to identify these parameters directly from experimental data. From the literature, System Identification Algorithms (SIA) have been developed based on various methodologies, for instance, subspace identification, genetic algorithm, eigensystem realization algorithm and data-based regressive model approaches. After scanning through the literature, it is noted that the authors could reconstruct the kinematics of the car crash, but less attention was taken on the nonlinearity behavior of the deformed vehicles involved in crash scenarios. To the best of our knowledge, the problem of reconstruction of a piecewise linear model for a vehicle-to-vehicle frontal crash scenario based on the genetic algorithm has not yet been completely considered in the literature and this forms our motivation for the present study.

The main contribution of this paper is threefold: 1) A mathematical model is developed to reconstruct a vehicle-to-vehicle frontal crash scenario and to estimate the nonlinear behaviors of the front parts of the vehicle undergoing crash deformation; 2) A genetic algorithm is proposed to estimate the parameters of the vehicle's front structures in terms of piecewise linear functions, which can assist car designers or manufacturers to reduce the cost associated with the real physical crashes which are generally costly and time consuming; 3) The accuracy of the predicted results are verified using the available experimental data. It should be mentioned that according to the methodology proposed in this paper, the dynamic crash can be predicted and allows the designer to redesign the vehicle for vehicle crashworthiness.

D.2 Experimental set up

Two physical crash tests data sets for the Caravan crashing into the Neon and the Chevrolet crashing into the Dodge are obtained from the NHTSA Database [22]. These tests were carried out on typical mid-speed vehicles colliding each other in the frontal direction. The test set up consisting of vehicle-to-vehicle crash (Caravan into Neon) is shown in Figure D.1. The data were obtained relative to the Federal

Motor Vehicle Safety Standards (FMVSS) No. 208 - Occupant Crash Protection. In the first test, the target vehicle (a 1996 Plymouth Neon) and the bullet vehicle (a 1997 Dodge Caravan) were instrumented with seven longitudinal axis accelerometers, three lateral axis accelerometers, four vertical axis accelerometers, and their specified impact velocity range was 55.5 km/h to 57.1 km/h.

The bullet vehicle's centerline was aligned with the target vehicle's centerline. This test was a full frontal car-to-car moving test. The test weights and impact speeds of the target and bullet vehicles were: 1378.0 kg and 55.9 km/h, and 2059.5 kg and 56.5 km/h respectively.

The same test set up was used on a Chevrolet car crashing into a Dodge car. The test weights and impact speeds of the Chevrolet and Dodge cars were: 2109 kg and 50.3km/h, and 1997 kg and 50 km/h respectively.

In general during vehicle frontal crash, the vehicles are subjected to impulsive forces. When a vehicle crashes into another vehicle, the heavier one is less deformed than the lighter one and at time of crash, both vehicles loose their kinetic energy in a fraction of a second through front-end structural deformations. The amount of deformation is equal to the stopping distance of the vehicle. Since the stopping distance of a vehicle in the crash is normally short, a much higher force is generated at the front interface. The vehicle stopping distance (or dynamic crash) in vehicle-to-vehicle crash tests largely depends on crash pulses. The dynamic crash can be determined by double integration of the vehicle crash pulse with known initial impact velocity. The decelerations for both, bullet and target vehicles are shown in Figure D.2.

Figure D.1: Vehicles deformations after crash (Caravan left front-view, Neon right front-view)

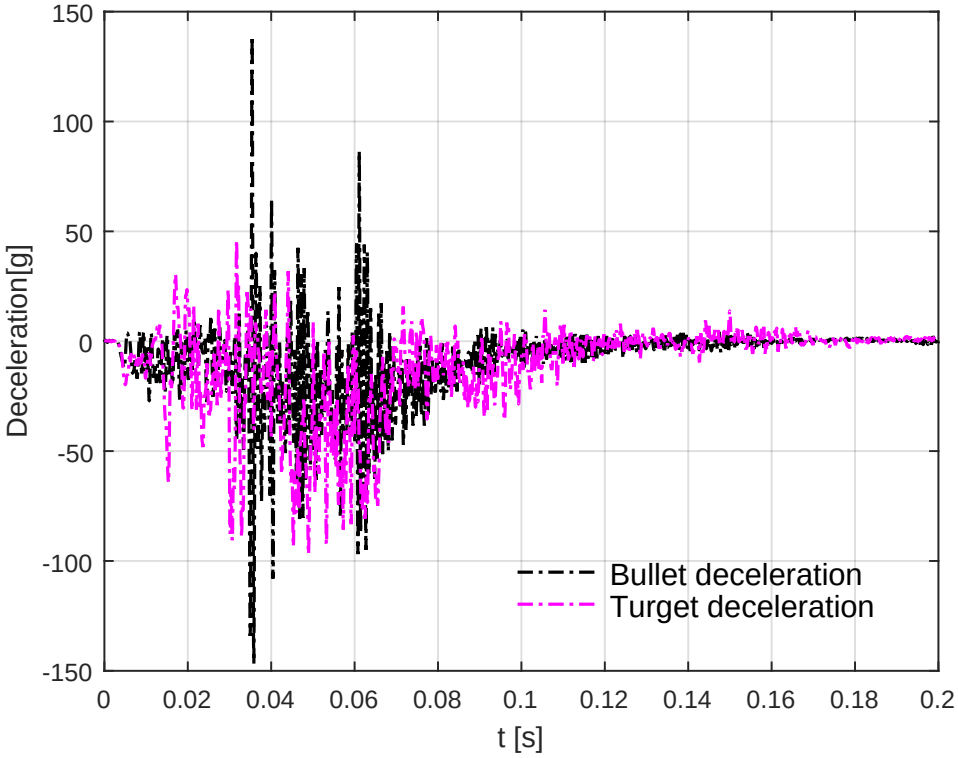

Figure D.2: Test decelerations for bullet and target vehicles

D.3 Model development

The main objective of this section is to develop a dynamic model which can represent a vehicle-to-vehicle frontal crash scenario. The real crash test results are shown in Figure D.2, and the model which can reproduce these results consists of two masses moving in opposite directions, as shown in Figure D.3. In line of the model development to capture the values as mentioned earlier during the crash scenario, the dynamical model proposed in [23] for the free vibration analysis are adopted for solving the impact responses. Then, the genetic algorithm is used to estimate the model parameters.

D.3.1 Vehicle-to-Vehicle crash model

An impact between two masses can be represented schematically as in Figure D.3, where each of the two masses has a contact with the Kelvin element, a set of spring and damper in parallel. If the connection between the mass and the element is a rigid contact, the element may undergo tension and compression. If not, due to separation between the mass and element, the element can only be subjected

to compression. To simplify the analysis, the two sets of Kelvin elements can be combined into one resultant Kelvin element as shown in Figure D.4. The parametric relationship between the two individual Kelvin elements and the resultant Kelvin element can be obtained in the sequel. From the spring deformation relationship, the total deformation of the combined spring k is equal to the sum of the deformations of the two individual springs (an additive deflection relationship). The spring force relationship can then be established as follows:

$$\alpha = x_1 + x_2 \tag{D.1}$$

$$\frac{F_k}{k} = \frac{F_k}{k_1} + \frac{F_k}{k_2} \tag{D.2}$$

where α and F_k are total deflection and force due to mass m_1 and m_2 respectively. Similarly, by taking the time derivative of the deformation relationship, the deformation rates are also found to be additive for the dampers. The damping relationship is shown as follows.

$$\dot{\alpha} = \dot{x_1} + \dot{x_2} \tag{D.3}$$

$$\frac{F_c}{c} = \frac{F_c}{c_1} + \frac{F_c}{c_2} \tag{D.4}$$

The equivalent relationships for spring stiffness and damping coefficients are then established as follows:

$$k = \frac{k_1 k_2}{k_1 + k_2}$$

$$c = \frac{c_1 c_2}{c_1 + c_2}$$

In a two-mass system, shown in Figure D.4, the mass M_2 is impacted by M_1 at an initial relative speed (or closing speed) of v_{12} where $v_{12} = v_1 + v_2 = v_0$. If one of the masses in the two-mass system is infinite, the system becomes a vehicle-to-barrier (VTB) model.

The only mass moving in this system is referred to as the effective mass, M_e. The relative motion of the mass with respect to the fixed barrier is the same as the ab-

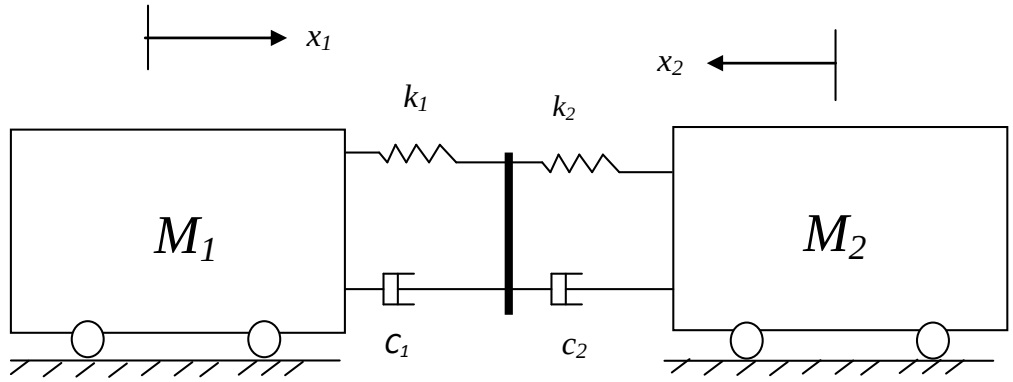

Figure D.3: A vehicle-to-vehicle impact model - Two Kelvin elements in series [23]

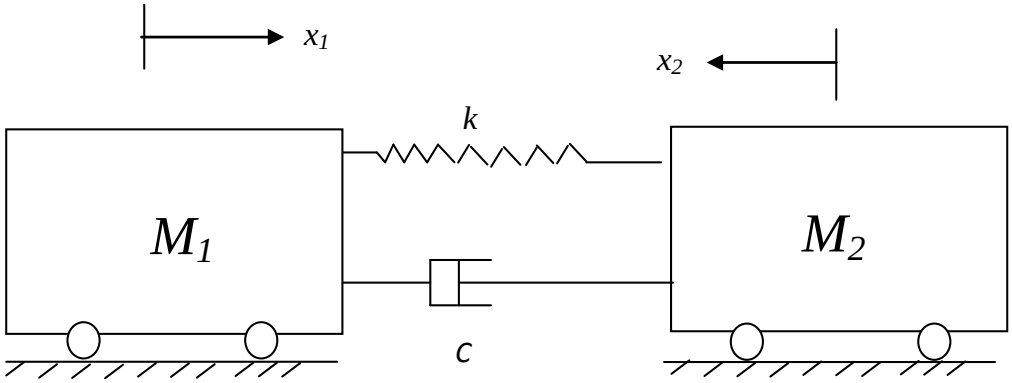

Figure D.4: A vehicle-to-vehicle impact model - A Kelvin model

solute motion of the mass with respect to a fixed reference frame. In a system where there are multiple masses involved in an impact, the analysis can be simplified by using the relative motion and effective mass approaches. The relative displacement of the effective mass, M_e, is α. The dynamic responses of the two-mass system and one effective mass system are summarized as [23]:

$$\ddot{x}_1 = \gamma_1 \ddot{\alpha} \qquad \ddot{x}_2 = \gamma_2 \ddot{\alpha} \tag{D.5}$$

where

$$\ddot{\alpha} = -v_{12}\omega_e sin(\omega_e t) \tag{D.6}$$

$$\omega_e = \sqrt{\frac{k}{M_e}} \tag{D.7}$$

$$\gamma_1 = \frac{M_2}{M_1 + M_2} \tag{D.8}$$

$$\gamma_2 = \frac{M_1}{M_1 + M_2} \tag{D.9}$$

$$M_e = \frac{M_1 M_2}{M_1 + M_2} \tag{D.10}$$

where ω_e is the natural frequency, γ_1 and γ_2 denote mass reduction factors and M_e is the effective mass. The dynamic equation of the effective mass system is represented as follows:

$$M_e\ddot{\alpha} = -c\dot{\alpha} - k\alpha \tag{D.11}$$

or

$$\ddot{\alpha} = (-c\dot{\alpha} - k\alpha)/M_e \tag{D.12}$$

Substituting (D.1) and (D.3) into (D.12), we get:

$$\ddot{\alpha} = (-c(\dot{x}_1 + \dot{x}_2) - k(x_1 + x_2))/M_e \tag{D.13}$$

From the response obtained from the test, the displacement and velocity are nonlinear. Therefore the Kelvin element of the model should be estimated as nonlinear parameters. In the first estimation the spring and the damping forces in the model are nonlinear cubic function of x and $\dot{x}$, respectively. Therefore, the dynamic responses of the two-mass system in Equation (D.5) are:

$$\begin{aligned}\ddot{x}_1 = \gamma_1(&-c(\dot{x}_1 + \dot{x}_2) - c_{nl}(\dot{x}_1 + \dot{x}_2)^3 \\ &- k(x_1 + x_2) - k_{nl}(x_1 + x_2)^3)/M_e\end{aligned} \tag{D.14}$$

$$\begin{aligned}\ddot{x}_2 = -\gamma_2(&-c(\dot{x}_1 + \dot{x}_2) - c_{nl}(\dot{x}_1 + \dot{x}_2)^3 \\ &- k(x_1 + x_2) - k_{nl}(x_1 + x_2)^3)/M_e\end{aligned} \tag{D.15}$$

where c_{nl} and k_{nl} are nonlinear components of the damping coefficient and the spring stiffness in the model respectively.

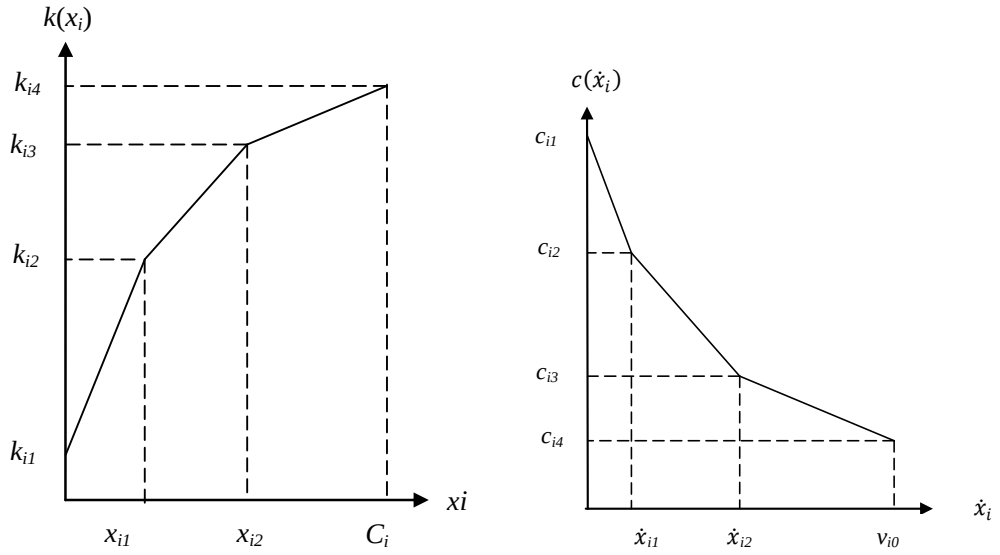

(a) Stiffness coeficients (b) Damping coefficients

Figure D.5: Predefined stiffness and damping coefficient characteristics of the vehicle's front structure

D.3.2 Piecewise linear approximations for springs and dampers

The springs and damping coefficients in the model described in the previous sections, are defined by the piecewise functions in (D.16) - (D.17) and shown graphically in Figure D.5.

The predefined shape of the spring and damper characteristics in Figure D.5, are chosen based on the shapes of the displacement and velocity responses from the crash test. The maximum displacement occurs when the velocity of the target vehicle reduces to zero, during the breaking phase, where the vehicle is overdamped and undamped during low and high velocities respectively. This justifies a high damping coefficient at the time of crash and a low value of damping coefficient at the initial velocity. The stiffness is low during elastic deformation, but after crash, the vehicle is plastically deformed, therefore the stiffness increases drastically to maintain the deformation.

$$k(x_i) = \begin{cases} k_{i1} + \frac{k_{i2}-k_{i1}}{x_{i1}} x_i & x_i \leq x_{i1} \\ k_{i2} + \frac{k_{i3}-k_{i2}}{x_{i2}-x_{i1}}(x_i - x_{i1}) & x_{i1} \leq x_i \leq x_{i2} \\ k_{i3} + \frac{k_{i4}-k_{i3}}{C_i-x_{i2}}(x_i - x_{i2}) & x_{i2} \leq x_i \leq C_i \end{cases} \tag{D.16}$$

$$c(\dot{x}_i) = \begin{cases} c_{i1} - \frac{c_{i1}-c_{i2}}{\dot{x}_{i1}} \dot{x}_i & \dot{x}_i \leq \dot{x}_{i1} \\ c_{i2} - \frac{c_{i2}-c_{i3}}{\dot{x}_{i2}-\dot{x}_{i1}}(\dot{x}_i - \dot{x}_{i1}) & \dot{x}_{i1} \leq \dot{x}_i \leq \dot{x}_{i2} \\ c_{i3} - \frac{c_{i3}-c_{i4}}{v_0-\dot{x}_{i2}}(\dot{x}_i - \dot{x}_{i2}) & \dot{x}_{i2} \leq \dot{x}_i \leq v_0 \end{cases} \tag{D.17}$$

Therefore, using the piecewise linear functions defined in Equations (D.16) and (D.17), the dynamic responses in Equation (D.5) can be represented as follows:

$$\ddot{x}_1 = \gamma_1(c(\dot{x}_1 + \dot{x}_2) - k(x_1 + x_2))/M_e \tag{D.18}$$

$$\ddot{x}_2 = -\gamma_2(-c(\dot{x}_1 + \dot{x}_2) - k(x_1 + x_2))/M_e \tag{D.19}$$

D.3.3 Optimization Scheme of the Genetic Algorithm

Genetic Algorithm (GA) is an adaptive heuristic search based on the evolutionary ideas of nature selection and genetics. It represents an intelligent exploitation of a random search used to solve optimization problems. This Evolutionary Algorithm holds a population of individuals (chromosomes), which evolve by means of selection and other operators like crossover and mutation. Every individual in the population gets an evaluation of its adaptation (fitness) to the environment. In the terms of optimization this means that the function which is maximized or minimized is evaluated for every individual. The selection chooses the best gene combinations (individuals), which through crossover and mutation should drive to better solutions in the next population. The Genetic Algorithm consists of seven steps [24], itemized below.

1. Generate initial population: in most of the algorithms the first generation is randomly generated, by selecting the genes of the chromosomes among the

allowed alphabet for the gene. Because of the easier computational procedure, it is accepted that all populations have the same number (N) of individuals. In our problem N is 24, the number of parameters to be estimated.

2. Calculation of the values of the function that we want to minimize or maximize. In our work the cost function minimizes the error between the experimental results and the model results.

3. Check for termination of the algorithm: as in the most optimization algorithms, it is possible to stop the genetic optimization by:
   - Value of the function: the value of the function of the best individual is within defined range around a set value. It is not recommended to use this criterion alone, because of the stochastic element in the search the procedure, the optimization might not finish within sensible time;
   - Maximal number of iterations: this is the most widely used stopping criteria. We have set 10^9 iterations to get the optimum solution. It guarantees that the algorithm will give some results within some time, whenever it has reached the extremum or not;
   - Stall generation: if within the initially set number of iterations (generations) there is no improvement of the value of the fitness function of the best individual, the algorithms stops.

4. Selection: this is used to select the fittest from the population among all individuals. This step is followed by crossover and mutation, which produce the population offspring. At this stage the best n individuals are directly transferred to the next generation.

5. Crossover: this is used to explore the search space.

   Here, the aim is to get offspring individuals that inherit the best possible combination of the characteristics (genes) of their parents.

6. Mutation: is used to remove the problem like genetic drift (some individuals may leave behind a few more off-springs than other individuals), and replacement is used to progress to the next new generation.

7. New generation: the elite individuals chosen from the selection are combined with those who passed the crossover and mutation, and form the next generation.

The proposed algorithm seeks to find the minimum function between several variables as can be stated in a general form $minf(p)$,

The cost function $f(p)$ is the objective function which should be optimized. The cost function to be minimized is the norm of the absolute error between the displacement, velocity and acceleration of the simulated cash and the experimental crash data and is defined as:

$$[Error] = sum(|Est - Exp|^T \times |Est - Exp|) \tag{D.20}$$

where Est and Exp are the model and experimental variables (displacement, velocity and acceleration) respectively.

The algorithm for solving the problem defined by Equations (D.14) and (D.15) is shown in Figure D.6. An initial guess of parameters is chosen and substituted in equations (16) and (17). Then the obtained stiffness and damping coefficients are substituted into equations (14) and (15) which in turn are numerically solved using time integration to get the simulated kinematic results i.e., accelerations, velocities and displacements. These kinematic results are finally compared with the time history from the crash test. Then the cost function is evaluated. When the cost function is minimum the solver terminates. Otherwise the GA is used to tune the parameters to match the experimental results.

The GA method is used here for optimization of the cost function. The GA-type of search schemes is function-value comparison-based, with no derivative computation. It attempts to move points through a series of generations, each being composed of a population which has a set number (population size, 24 in this work) of individuals or parameters. Each individual is a point in the parameter space (in our case, the displacement and velocity of experimental data). The schemes that are applied to the evolution of generations have some analogy to the natural genetic evolution of species, hence the term genetic.

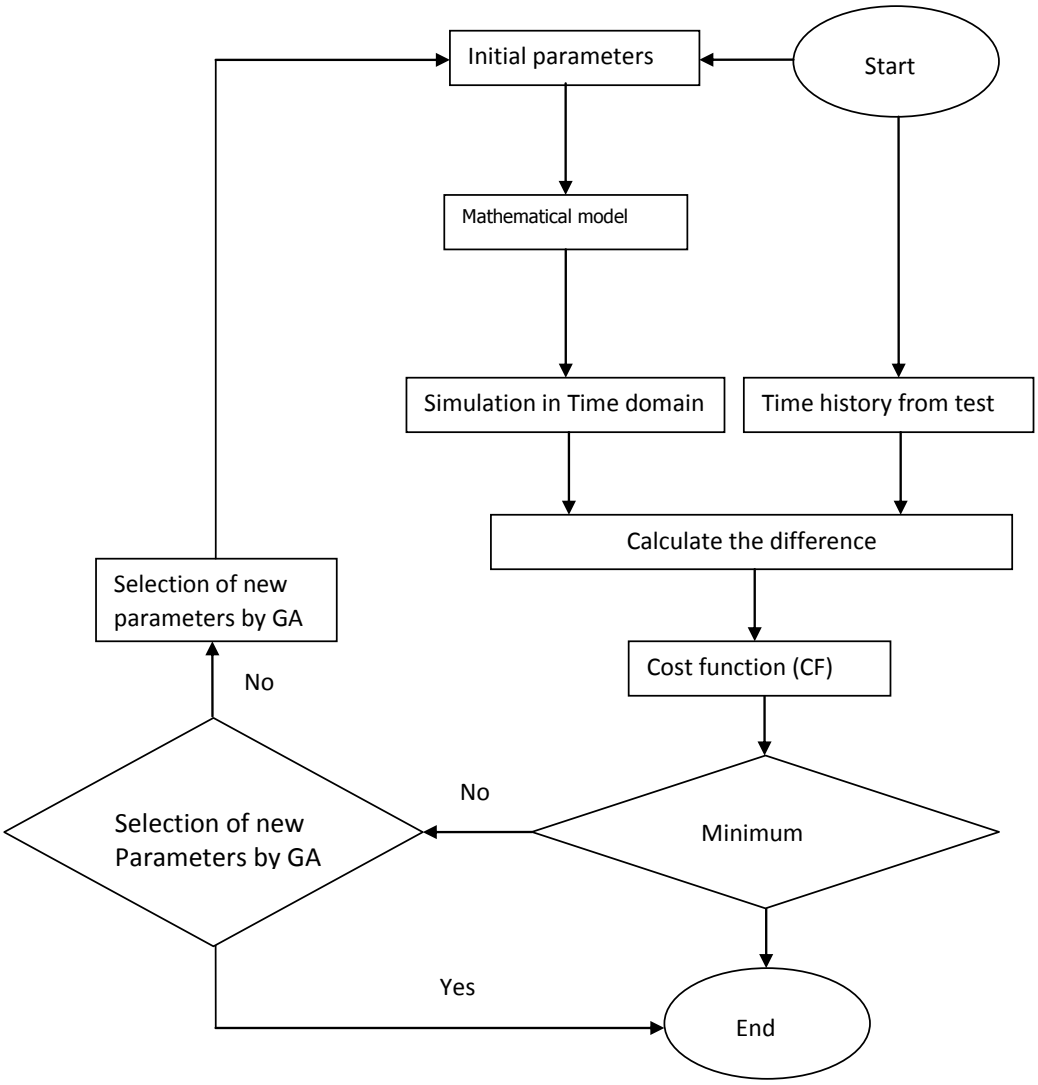

Figure D.6: A flowchart for problem solving

D.4 Results and discussion

This section presents the simulation results for two crash tests. The fist crash scenario is a Caravan car crashing into a Neon car, and the second is the Dodge car crashing into a Chevrolet car. Finally, some concluding remarks in regards to implementation of GA to the vehicle-to-vehicle model development are drawn.

The results of the model presented in (D.14) and (D.15) are shown in Figure D.7 which reconstructs the dynamic crush of a Caravan crashing into a Neon. The results show a trend similar to that obtained from the test. But the maximum dynamic crash is less than that from the test. The result presented in Figure D.7 were obtained using $fmincon$, an optimization function available in MATLAB, with interior point

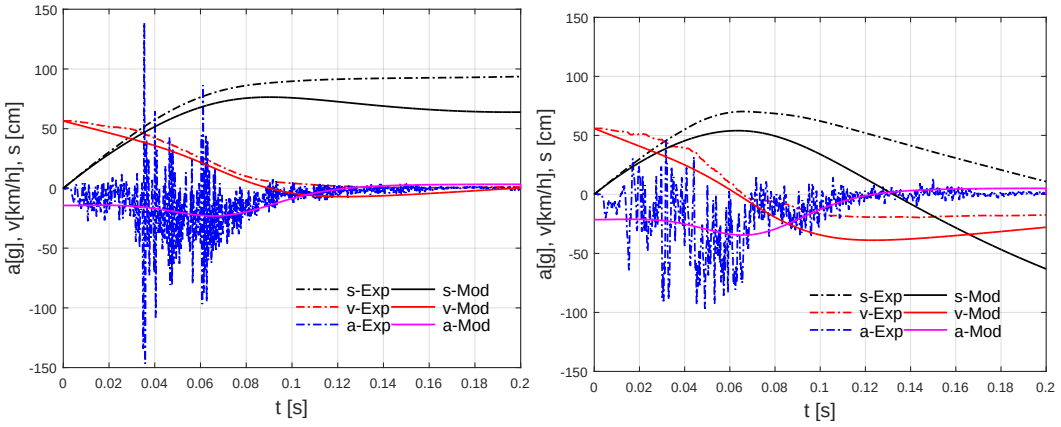

(a) Caravan (b) Neon

Figure D.7: Model vs Experimental results for vehicle-to-vehicle (Caravan-Neon) crash using IPA

algorithm (IPA). A big difference between the bullet (Caravan) model response and the test results is noted. The bullet model presents a re-bounces velocity which is not observed on the test results.

To solve this problem, the genetic algorithm was used to optimize the parameters defined by the piecewise functions presented in Figure D.5 and Equations (D.16) and (D.17), where the stiffness and damping coefficients are a function of x and $\dot{x}$ respectively. The improved results are presented in Figure D.8. It is noted that the model results are much closer to the experimental results from the crash test. The maximum dynamic crash of 70.24 cm is observed on the target (Neon) from the test, while the dynamic crash from the model is 69.92 cm. At the maximum dynamic crash, the bullet vehicle keeps on moving in the same direction as before crash, but the target vehicle re-bounces. The rebound velocities are -19.6 m/s and -18.3 m/s from the test and the model respectively. This is observed by the velocity curves of the two vehicles, where a negative velocity is noted for the target vehicle and a positive velocity is noted for the bullet vehicle after the maximum dynamic crash. The front structure of the target vehicle is plastically deformed, while the front structure of the bullet vehicle experiences an elastic deformation. The accuracy of the model is also observed on the time at the maximum dynamic crash, t_m. The time at the maximum dynamic crash, t_m is 0.06568 s from the test and 0.06824 s from the model respectively, as observed on the Neon's kinematic results.

The labels s-Exp, v-Exp, a-Exp, s-Mod, v-Mod, a-Mod, in Figures D.7 and D.8 stand for: experimental and model displacements, velocities and accelerations, respectively.

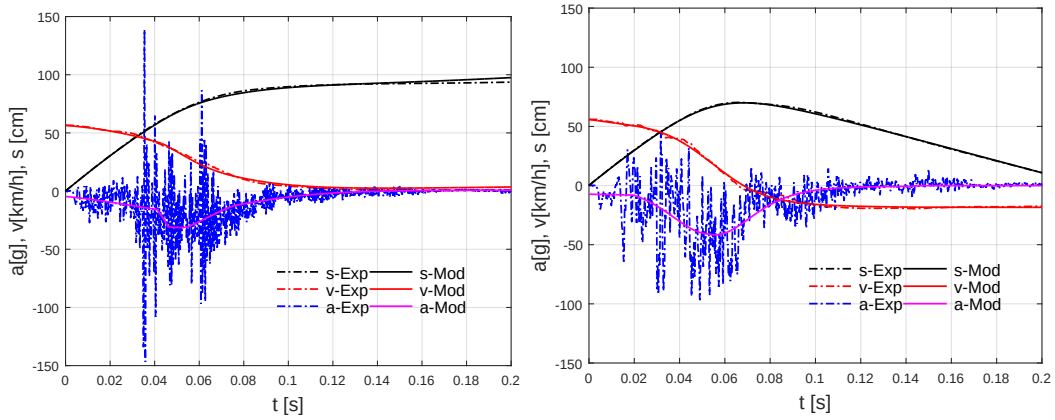

(a) Caravane (b) Neon

Figure D.8: Model vs Experimental results for vehicle-to-vehicle (Caravan-Neon) crash using GA

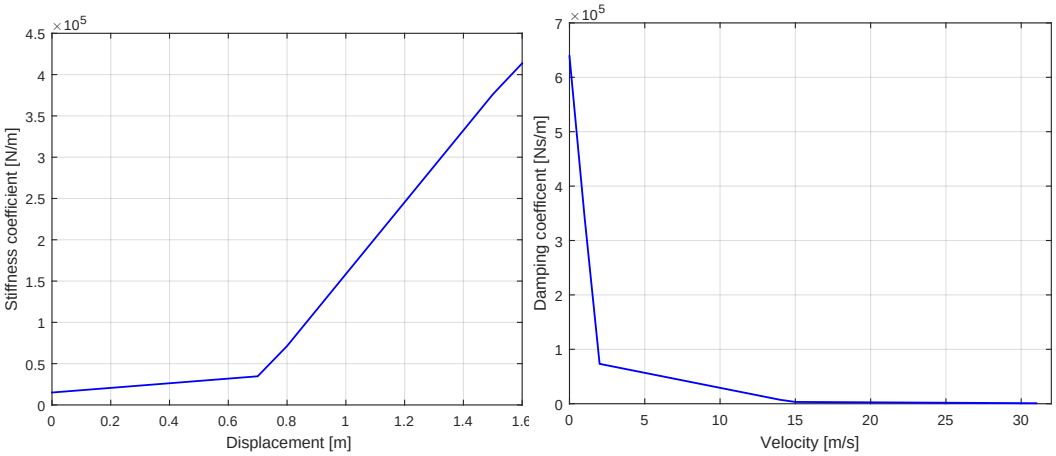

(a) Stiffness coeficients (b) Damping coefficients

Figure D.9: Piecewise spring and damper coefficients of the Neon's front structure

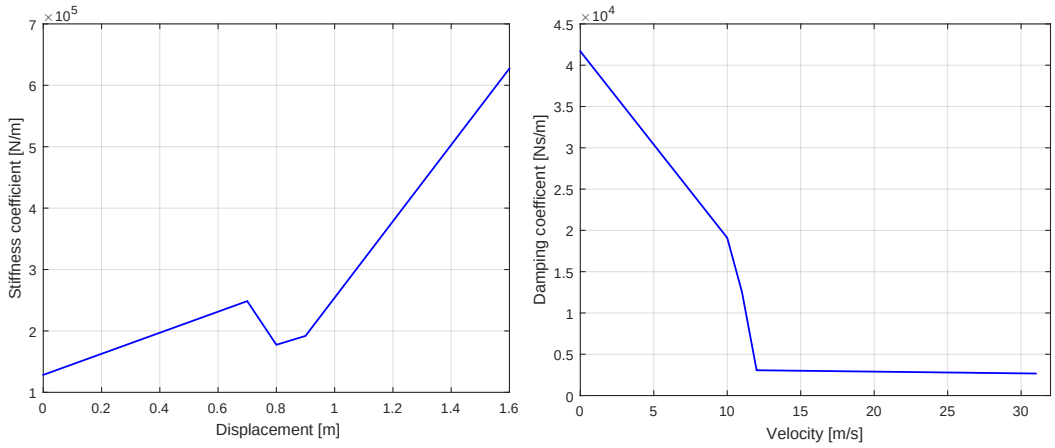

(a) Stiffness coefficients (b) Damping coefficients

Figure D.10: Piecewise spring and damper coefficients of the Caravan's front structure

Table D.1: Estimated Parameters for the Caravan-to-Neon model

Parameter for Bulet vehicle	*Value*	*Unit*	*Parameter for Target vehicle*	*Value*	*Unit*
k_{11}	1.2843e+05	N/m	k_{21}	1.5030e+04	N/m
k_{12}	2.5142e+05	N/m	k_{22}	3.5161e+04	N/m
k_{13}	1.4932e+05	N/m	k_{23}	4.1930e+05	N/m
k_{14}	6.5159e+05	N/m	k_{24}	5.1878e+04	N/m
x_{11}	0.7168	m	x_{21}	0.7168	m
x_{12}	0.8316	m	x_{22}	1.5994	m
c_{11}	4.1688e+04	Ns/m	c_{21}	6.3884e+05	Ns/m
c_{12}	1.7727e+04	Ns/m	c_{22}	7.3768e+04	Ns/m
c_{13}	3.0696e+03	Ns/m	c_{23}	3.3250e+03	Ns/m
c_{14}	2.6614e+03	Ns/m	c_{24}	860.3030	Ns/m
$\dot{x}_{11}$	10.6044	m/s	$\dot{x}_{21}$	1.9138	m/s
$\dot{x}_{12}$	11.7252	m/s	$\dot{x}_{22}$	14.6957	m/s

The stiffness coefficient (k) and damping coefficient (c) characteristics of the target and bullet vehicle's front structure are shown in Figure D.9 and Figure D.10, respectively. From these Figures it is noted that the stiffness and damping coefficients are piecewise functions with high magnitude at the maximum dynamic crash,

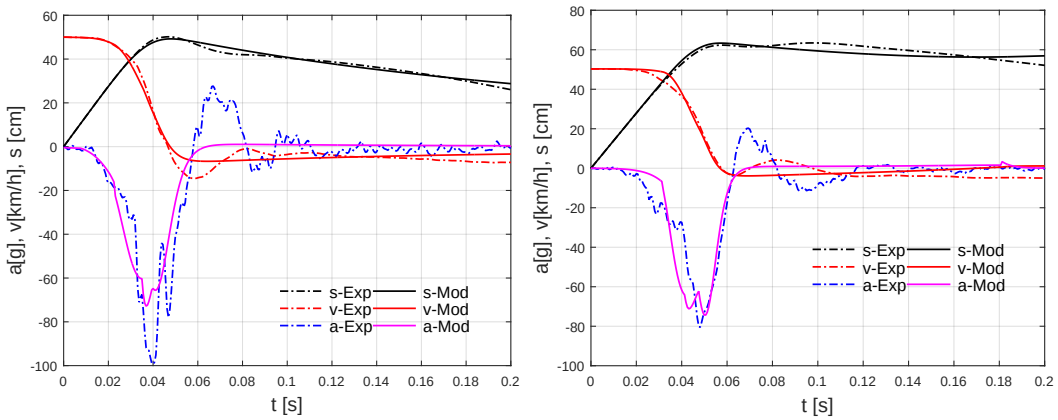

(a) Dodge (b) Chevrolet

Figure D.11: Model vs Experimental results for the Dodge-to-Chevrolet crash using GA

when the velocity of the target vehicle is reduced to zero. This justifies the forced breaking of the target vehicle at the time of collision. A high damping coefficient at the time of crash and a low value of damping coefficient at the initial velocity are observed. It is also noted that the stiffness is low during elastic deformation, but after crash, the vehicle is plastically deformed, therefore stiffness increases drastically to maintain deformation. A summary of estimated parameters for the Caravan - Neon crash is shown in Table D.1.

To verify the model, the Chevrolet-Dodge crash test was used to demonstrate the accuracy of the GA. The comparison between the model and the crash test results are shown in Figure D.11. It is observed from Figure D.11 that the maximum dynamic crushes and their occurrence time , for both vehicles, are almost equal to those observed from the physical crash tests. The maximum dynamic crashes and the times of crash, for the Chevrolet and Dodge cars are: 62.20 cm and 0.055 s, and 49.63 cm and 0.048 s respectively.

A summary of estimated parameters for Dodge- Chevrolet crash is shown in Table D.2. The stiffness and damping coefficients characteristics of the Dodge's and Chevrolet's front structures are shown in Figures D.12 and D.13 respectively.

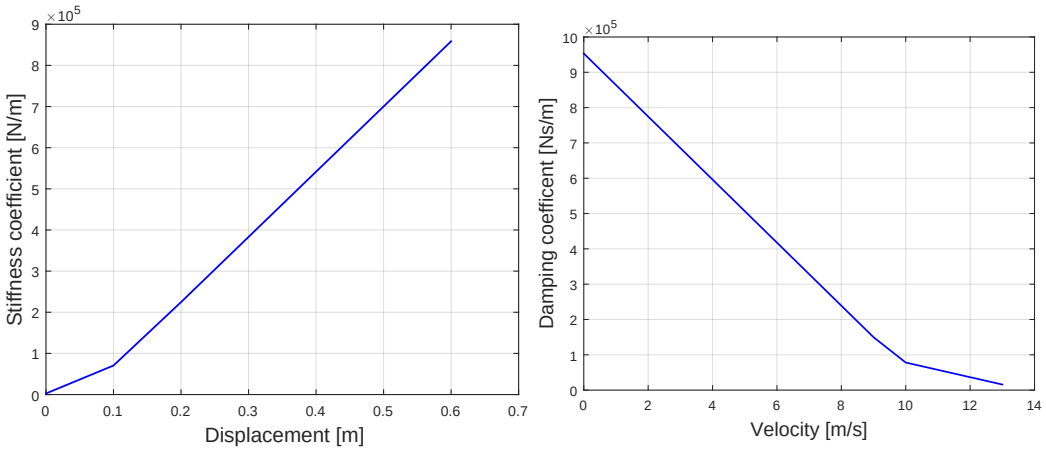

(a) Stiffness coeficients (b) Damping coefficients

Figure D.12: Piecewise spring and damper coefficients of the Dodge's front structure

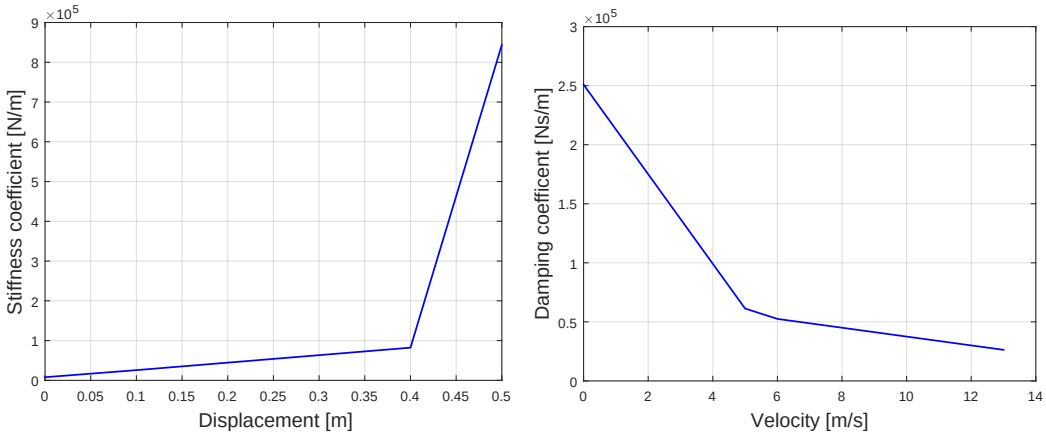

(a) Stiffness coeficients (b) Damping coefficients

Figure D.13: Piecewise spring and damper coefficients of the Chevrolet's front structure

Table D.2: Estimated Parameters for the Dodge-to-Chevrolet model

Parameters for Dodge	***Value***	***Unit***	***Parameters for Chevrolet***	***Value***	***Unit***
k_{11}	2.5726e+03	N/m	k_{21}	7.9266e+03	N/m
k_{12}	4.9029e+03	N/m	k_{22}	6.8819e+03	N/m
k_{13}	7.3699e+04	N/m	k_{23}	8.9521e+04	N/m
k_{14}	9.1342e+05	N/m	k_{24}	8.6448e+05	N/m
x_{11}	2.8633e-06	m	x_{21}	1.5314e-06	m
x_{12}	0.1048	m	x_{22}	0.4387	m
c_{11}	9.5321e+05	Ns/m	c_{21}	2.5087e+05	Ns/m
c_{12}	8.3382e+04	Ns/m	c_{22}	5.5703e+04	Ns/m
c_{13}	7.4707e+03	Ns/m	c_{23}	5.2663e+03	Ns/m
c_{14}	5.0879e-07	Ns/m	c_{24}	363.1498	Ns/m
$\dot{x}_{11}$	9.7443	m/s	$\dot{x}_{21}$	5.1470	m/s
$\dot{x}_{12}$	13.4024	m/s	$\dot{x}_{22}$	13.6221	m/s

D.5 Conclusion and future work

In this paper, a mathematical-based method is presented to estimate the parameters of a vehicle-to-vehicle frontal crash. It is observed that the model results in responses in vehicle crash model match with the experimental crash tests. Therefore, the overall behavior of the models matches the real vehicle's crash well. Hence the implication of the proposed model is that it can help vehicle designer to better design the vehicle with fewer physical crash tests. Two of the main parameters characterizing the collision are the maximum dynamic crash (C_m), which describes the highest car's deformation, and the time (t_m) at which it occurs. They are pertinent to the occupant crashworthiness since they help to assess the maximum intrusion into the passenger's compartment. The results show that we can obtain an optimum solution with GA Toolbox Matlab than the $fmincon$ optimization algorithm. It has been demonstrated that the model and the GA parameter optimization procedure used in this work can be successfully extended for different range of crash speeds.

The authors will extend the work by including other parts of the vehicle such as an engine in the model. The authors also intend to investigate the application of genetic algorithm for different crash scenarios such as oblique crash and side impact. Further investigations will be carried out using Finite Element Model (FEM) approach for validation of the results form Lumped Parameter model of vehicle-to-

vehicle crash scenario.

Acknowledgment

The authors would like to thank the Dynamic Research Group members, at the University of Agder, for their constructive comments to improve this research work. The authors would also like to thank the editor and anonymous reviewers for their valuable and constructive comments and suggestions to improve the quality of this work.

REFERENCES

[1] W. Pawlus, J. E. Nielsen, H. R. Karimi, and K. G. Robbersmyr. Application of viscoelastic hybrid models to vehicle crash simulation. *International Journal of Crashworthiness*, 55:369 – 378, 2011.

[2] W. Pawlus, H. R. Karimi, and K. G. Robbersmyr. Development of lumped-parameter mathematical models for a vehicle localized impact. *Journal of Mechanical Science and Technology*, 25(7):1737–1747, 2011.

[3] W. Pawlus, H. R. Karimi, and K. G. Robbersmyr. Data-based modeling of vehicle collisions by nonlinear autoregressive model and feedforward neural network. *Information Sciences*, 235:65–79, 2013.

[4] J. Marzbanrad and M. Pahlavani. Calculation of vehicle-lumped model parameters considering occupant deceleration in frontal crash. *International Journal of Crashwothiness*, 16(4):439 – 455., 2011.

[5] S. M. Ofochebe, C. G. Ozoegwu, and S. O. Enibe. Performance evaluation of vehicle front structure in crash energy management using lumped mass spring system. *Advanced Modeling and Simulation in Engineering*, 2(2):1–18, April 01 2015.

[6] L. Sousa, P.Verssimo, and J. Ambrsio. Development of generic multibody road vehicle models for crashworthiness. *Multibody Syst Dyn*, 19:133 – 158, 2008.

[7] M. Carvalho, J. Ambrsio, and P. Eberhard. Identification of validated multibody vehicle models for crash analysis using a hybrid optimization procedure. *Struct Multidisc Optim*, 44:85 – 97, 2011.

[8] A.A. Alnaqi and A.S. Yigit. Dynamic analysis and control of automotive occupant restraint systems. *Jordan Journal of Mechanical and Industrial Engineering*, 5(1):39 – 46, 2011.

[9] A. Klausen, S. S. Tørdal, H. R. Karimi, K. G. Robbersmyr, M. Jecmenica, and O. Melteig. Firefly optimization and mathematical modeling of a vehicle crash test based on single-mass. *Journal of Applied Mathematics*, pages 1 – 10, 2014. Article ID 150319.

[10] B. B. Munyazikwiye, K. G. Robbersmyr, and H. R. Karimi. A state-space approach to mathematical modeling and parameters identification of vehicle frontal crash. *Systems Science and Control Engineering*, 2:351 – 361, 2014.

[11] B. B. Munyazikwiye, H. R. Karimi, and K. G. Robbersmyr. Mathematical modeling and parameters estimation of car crash using eigensystem realization algorithm and curve-fitting approaches. *Mathematical Problems in Engineering*, pages 1 – 13, 2013. Article ID 262196.

[12] B. B. Munyazikwiy, H. R. Karimi, and K. G. Robbersmyr. A mathematical model for vehicle-occupant frontal crash using genetic algorithm. In *2016 UKSim-AMSS 18th International Conference on Computer Modelling and Simulation*, 2016.

[13] T.L. Teng, F.A. Chang, Y.S. Liu, and C.P. Peng. Analysis of dynamic response of vehicle occupant in frontal crash using multibody dynamics method. *Mathematical and Computer Modelling*, 48:1724 – 1736, 2008.

[14] C. S. Lin, K. D. Chou, and C. C.YU. Numerical simulation of vehicle crashes. *Applied Mechanics and Materials*, 590:135–143, May 2014.

[15] W. Pawlus, H. R. Karimi, and K. G. Robbersmyr. A fuzzy logic approach to modeling a vehicle crash test. *Central European Journal of Engineering*, pages 1 – 13, 2012.

[16] D. Vangi. Impact severity assessment in vehicle accidents. *International Journal of Crashworthiness*, 19(6):576 – 587, 2014.

[17] B. B. Munyazikwiye, H. R. Karimi, and K. G. Robbersmyr. Fuzzy logic approach to predict vehicle crash severity from acceleration data. In *Proceedings of 2015 International Conference on Fuzzy Theory and Its Applications (iFUZZY)*, pages 44 – 49, The Evergreen Resort Hotel (Jiaosi), Yilan, Taiwan, Nov. 18-20 2015.

[18] D. Vangi and F . Begani. Performance of triangle method for evaluating energy loss in vehicle collisions. *Journal of Automobile Engineering*, 226:338 – 347, 14 July 2012.

[19] D. Vangi. A fuzzy approach for vehicle-pedestrian collision reconstruction. *Vehicle system dynamics*, 47(9):1115 – 1135, 2009.

[20] M. Pahlavani and J. Marzbanrad. Crashworthiness study of a full vehicle-lumped model using parameters optimization. *International Journal of Crashworthiness*, 20(6):573 – 591, 2015.

[21] H. R. Karimi, W. Pawlus, and K. G. Robbersmyr. Signal reconstruction, modeling and simulation of a vehicle full-scalecrash test based on morlet wavelets. *Neurocomputing*, 93:88 – 99, 2012.

[22] NHSA. http://www-nrd.nhtsa.dot.gov/database/vsr/veh/querytest.aspx.

[23] M. Huang. *Vehicle Crash Mechanics*. CRC PRESS, Boca Raton London New York Washington, 2002.

[24] *Genetic Algorithms for Optimization-User Manual. Andrey Popov, TU-Sofia, 2003*.

Paper E

Title:	Application of Genetic Algorithm on Parameter Optimization of Three Vehicle Crash Scenarios
Authors:	Bernard B. Munyazikwiye [1], Hamid R. Karimi [2], and Kjell G. Robbersmyr[1] [2] Department of Mechanical Engineering, Politecnico di Milano 20156 Milan, Italy
Affiliation:	[1] Faculty of Engineering and Science, University of Agder, P.O. Box 509, 4879 Grimstad, Norway
Conference:	*International Federation of Automatic Control (IFAC)*, Toulouse, France, July 2017. DOI:10.1016/j.ifacol.2017.08.564
Copyright ©:	Elsevier
Layout:	The layout of the paper has been revised to have the same format as the thesis

Abstract — **This paper focuses on the development of mathematical models for vehicle frontal crashes. The models under consideration are threefold: a vehicle into barrier, vehicle-occupant and vehicle to vehicle frontal crashes. The first model is represented as a simple spring-mass-damper and the second case consists of a double-spring-mass-damper system, whereby the front mass and the rear mass represent the vehicle chassis and the occupant, respectively. The third model consists of a collision of two vehicles represented by two masses moving in opposite directions. The springs and dampers in the models are nonlinear piecewise functions of displacements and velocities respectively. More specifically, a genetic algorithm (GA) approach is proposed for estimating the parameters of vehicles front structure and restraint system for vehicle-occupant model. Finally, using the existing test-data, it is shown that the obtained models can accurately reproduce the real crash test data.**

Keywords— Modeling, vehicle-occupant, frontal crash, parameters estimation, genetic algorithm.

E.1 Introduction

Vehicle crashes are one of the major causes of mortality in modern society. To maintain the crash-worthiness, car manufacturers carry out crash tests on a sample of vehicles for checking the effect of the occupant during crash scenarios. Crash-worthiness is the ability of a vehicle to be plastically deformed and still maintains a sufficient survival space for its occupants. However, this process very expensive and time consuming. To minimize the cost associated with the physical crash test, it is better to adopt the simulation of a vehicle crash and validate the model results with the actual crash test. Due to advanced research in simulation tools during the last decades, simulated crash tests can be performed prior to the full-scale crash test. The common approaches are based on Finite element method (FEM) or lumped parameter modeling (LPM). In the literature, much work has been conducted in the field of vehicle crash-worthiness and resulted in several computational models. A brief review is given in this paper. A car crashing into a rigid pole was modeled by a suitable spring-mass-damper arrangement as presented in [1]. The response of an occupant during a vehicle crash was investigated in [2] where the author used a 5-DOF lumped parameter model (LPM), while in [3], using a 4-DOF LPM the authors studied the performance of vehicle front structure. An optimiza-

tion procedure to assist a multi-body vehicle model was proposed in [4] and [5] and in [6] the author reduced the thoracic injury during a frontal crash by controlling the force on the seat belt restraint system. [7], through a firefly optimization approach, estimated the model parameters of vehicle crash into barrier based on a mass- spring-damper model . Diffent methods for modeling vehicle frontal crash scenarios were developed by [8, 9]. In [10], the authors developed a mathematical model for vehicle-Occupant and a vehicle-to-vehicle frontal crash using Genetic Algorithm in [11]. [12], examined the dynamic response of the human body (the head, chest and pelvic injuries of an occupant, respectively) in a crash event. The problem of reconstruction of a piecewise linear model for vehicle crash scenario based on the genetic algorithm has received less attention in the literature and this forms our motivation for the present study.

In this paper, a genetic algorithm is used to estimate and optimize the parameters of different models, namely: a vehicle-to-barrier, a vehicle-occupant and a vehicle-to-vehicle frontal crash models respectively. The structural parameters estimated are spring and damping coefficients. It is observed that the predicted results fit the experimental data very well.

E.2 Experimental set-up

Three experimental crash texts were conducted. Data for vehicle into barrier were taken from a calibration test done by Agder Research, Norway. The second and third test data were taken from the National Highway Traffic Safety Administration (NHTSA), open-source database [13]. The first test was carried out on a typical mid-speed vehicle to pole collision. A test vehicle was subjected to an impact with a vertical, rigid cylinder. During the test, the acceleration was measured in three directions (x - longitudinal, y - lateral, and z - vertical) together with the yaw rate from the center of gravity of the car. The initial velocity of the car was 35 km/h, and the mass of the vehicle (together with the measuring equipment and driver) was 873 kg. Only the measured acceleration in the longitudinal direction was considered in this study because we were interested in the frontal crash. In the second test, a load cell barrier consisting of 36 load cells was impacted by a Volkswagen Scirocco at a velocity of 56.5 km/h. A 50^{th} percentile male Anthropomorphic Test Dummy was placed in the car in the driver's seating position. The target vehicle (a 1996 Plymouth Neon) and the bullet vehicle (a 1997 Dodge Caravan) were instrumented with seven longitudinal axis accelerometers, three lateral axis accelerometers, four

vertical axis accelerometers. The test weights and velocities of the target(Plymouth Neon) and bullet(a Dodge Caravan) vehicles were 1378.0 kg, 55.9 km/h and 2059.5 kg, 56.5 km/h respectively.

E.3 Model development

The main objective of this section is to represent dynamic models to capture the vehicle frontal crash phenomena. When the vehicle crashes into a rigid barrier, the two masses will experience an impulsive force during the collision. The second model consists of two masses as shown in Figure E.1, where m_v and m_o represent the vehicle and the occupant masses, respectively. The third model consists of two masses moving in opposite directions, as shown in Figure E.2. In line of the model development to capture the values as mentioned earlier during the crash scenario, the dynamical models proposed in [14] for the free vibration analysis are adopted for solving the impact responses. Then, the genetic algorithm is used to estimate the model parameters.

E.3.1 Model 1: Vehicle-to-rigid barrier crash model

Initially a real vehicle crash experiment was conducted on a typical mid-speed vehicle to pole collision. In vehicle into barrier model, the deforming spring and damping forces, developed at time of crash, are piecewise functions in x and $\dot{x}$ respectively. But for vehicle to barrier cash, the prefix i is dropped. The forces F_k and F_c due to spring stiffness and damper constants are defined as follows ([14]):

$$F_k = kx \tag{E.1}$$

$$F_c = c\dot{x} \tag{E.2}$$

$$\ddot{x} = (-F_k - F_c)/m \tag{E.3}$$

where m, x and $\dot{x}$ are mass, displacement and velocity of the vehicle, respectively. k and c are spring stiffness and damping coefficients of the vehicle's front structure, respectively.

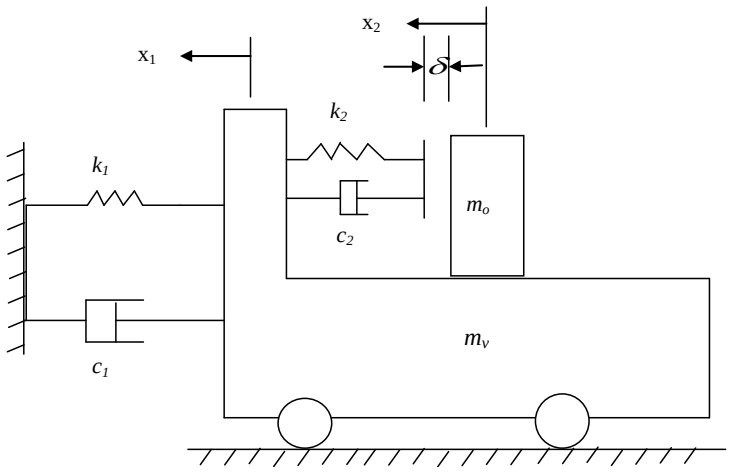

Figure E.1: Vehicle - occupant model

E.3.2 Model 2: Vehicle-Occupant frontal crash model

Figure E.1 represents the vehicle-occupant model with non-linear spring and dampers that crashes into a fixed barrier. Based on the nonlinear characteristics of velocity and displacement of the vehicle and forward movement of the occupant the springs and dampers that simulate such characteristics are modeled as piecewise linear functions. The dynamic equations of the double-mass-spring-damper model are shown in the following:

$$F_{str} = k_1 x_1 + c_1 \dot{x}_1 \tag{E.4}$$

$$F_{rest} = \begin{cases} k_2(x_2 - x_1) + c_2(\dot{x_2} - \dot{x_1}); & x_1 - x_2 \geq \delta \\ 0; & elsewhere \end{cases} \tag{E.5}$$

where k_1, k_2, c_1 and c_2 are piecewise linear functions defined in Equations (E.25) - (E.26).

$$\ddot{x}_1 = (F_{rest} - F_{str})/m_v \tag{E.6}$$

$$\ddot{x}_2 = (F_{rest})/m_o \tag{E.7}$$

where F_{str} and F_{rest} are the deformation force of the vehicle frontal structure and the restraint system respectively.

k_1 and c_1, are nonlinear spring damper of the front vehicle structure respectively. k_2 and c_2 are spring stiffness and damper coefficients for the restraint system respectively.

E.3.3 Model 3: Vehicle-to-Vehicle crash model

An impact between two masses can be represented schematically, as in Figure E.2. Each of the two masses having a contact with the Kelvin element, a set of spring and damper in parallel. If the connection between the mass and the element is a rigid contact, the element may undergo tension and compression. If not, due to separation between the mass and element, the element can only be subjected to compression. To simplify the analysis, the two sets of Kelvin elements can be combined into one resultant Kelvin element. The parametric relationship between the two individual Kelvin elements and the resultant Kelvin element can be obtained as in the following. The spring force (F_k) and damping force (F_c) relationships can then be established as follows:

$$\alpha = x_1 + x_2 \tag{E.8}$$

$$\frac{F_k}{k} = \frac{F_k}{k_1} + \frac{F_k}{k_2} \tag{E.9}$$

$$\dot{\alpha} = \dot{x_1} + \dot{x_2} \tag{E.10}$$

$$\frac{F_c}{c} = \frac{F_c}{c_1} + \frac{F_c}{c_2} \tag{E.11}$$

$$k = \frac{k_1 k_2}{k_1 + k_2} \tag{E.12}$$

$$c = \frac{c_1 c_2}{c_1 + c_2} \tag{E.13}$$

In a two-mass system shown in Figure E.2, the mass M_2 is impacted by M_1 at an initial relative speed (or closing speed) of v_{12} where $v_{12} = v_1 + v_2 = v_0$. If one of the masses in the two-mass system is infinite, the system becomes a vehicle-to-barrier (VTB) model. The only mass moving in this system is referred to as the effective

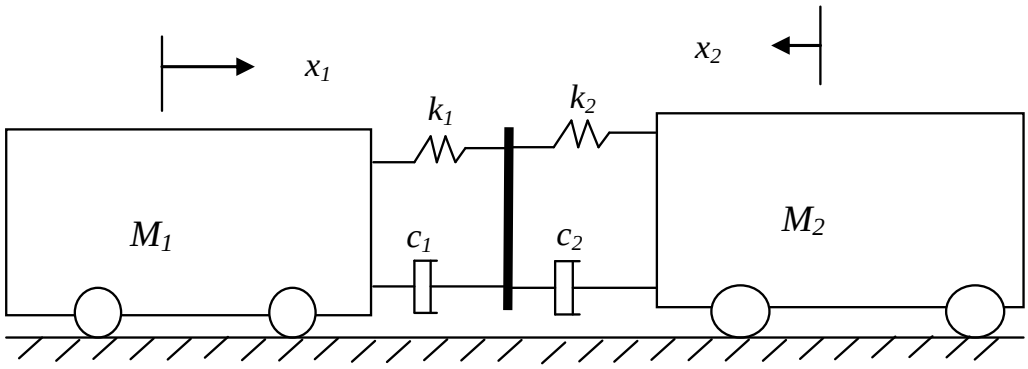

Figure E.2: Vehicle to vehicle impact model - two Kelvin elements in series

mass, M_e. The relative motion of the mass with respect to the fixed barrier is the same as the absolute motion of the mass with respect to a fixed reference frame. In a system where there are multiple masses involved in an impact, the analysis can be simplified by using the relative motion and effective mass approaches. The relative displacement of the effective mass, M_e, is α. The dynamic responses of the two-mass system and one effective mass system are summarized as follows:

$$\ddot{x}_1 = \gamma_1 \ddot{\alpha} \qquad\qquad \ddot{x}_2 = \gamma_2 \ddot{\alpha} \tag{E.14}$$

where

$$\ddot{\alpha} = -v_{12}\omega_e sin(\omega_e t) \tag{E.15}$$

$$\omega_e = \sqrt{\frac{k}{M_e}} \tag{E.16}$$

$$\gamma_1 = \frac{M_2}{M_1 + M_2} \tag{E.17}$$

$$\gamma_2 = \frac{M_1}{M_1 + M_2} \tag{E.18}$$

$$M_e = \frac{M_1 M_2}{M_1 + M_2} \tag{E.19}$$

where ω_e is the natural frequency, γ_1 and γ_2 denote mass reduction factors and M_e is the effective mass. The dynamic motion of the effective mass system can be expressed as:

$$M_e\ddot{\alpha} = -c\dot{\alpha} - k\alpha \tag{E.20}$$

$$\ddot{\alpha} = (-c\dot{\alpha} - k\alpha)/M_e \tag{E.21}$$

substituting (E.8) and (E.10) into (E.21), we get:

$$\ddot{\alpha} = (-c(\dot{x_1} + \dot{x_2}) - k(x_1 + x_2))/M_e \tag{E.22}$$

Therefore, the dynamic responses of the two-mass system in Equation (E.14) can be presented as follows:

$$\ddot{x}_1 = \gamma_1(-c(\dot{x}_1 + \dot{x}_2) - k(x_1 + x_2))/M_e \tag{E.23}$$

$$\ddot{x}_2 = -\gamma_2(-c(\dot{x}_1 + \dot{x}_2) - k(x_1 + x_2))/M_e \tag{E.24}$$

E.3.4 Piecewise linear approximations for springs and dampers

The springs and damping coefficients in the types of models in the previous sections, are defined by the piecewise functions. The predefined spring and damper characteristics are chosen based on the shapes of the displacement and velocity responses from the crash test. The predefined spring and damper are defined by Equations (E.25) and (E.26).

$$k(x_i) = \begin{cases} k_{i1} + \frac{k_{i2}-k_{i1}}{x_{i1}}x_i & x_i \le x_{i1} \\ k_{i2} + \frac{k_{i3}-k_{i2}}{x_{i2}-x_{i1}}(x_i - x_{i1}) & x_{i1} \le x_i \le x_{i2} \\ k_{i3} + \frac{k_{i4}-k_{i3}}{C_i-x_{i2}}(x_i - x_{i2}) & x_{i2} \le x_i \le C_i \end{cases} \tag{E.25}$$

$$c(\dot{x}_i) = \begin{cases} c_{i1} - \frac{c_{i1}-c_{i2}}{\dot{x}_{i1}}\dot{x}_i & \dot{x}_i \leq \dot{x}_{i1} \\ c_{i2} - \frac{c_{i2}-c_{i3}}{\dot{x}_{i2}-\dot{x}_{i1}}(\dot{x}_i - \dot{x}_{i1}) & \dot{x}_{i1} \leq \dot{x}_i \leq \dot{x}_{i2} \\ c_{i3} - \frac{c_{i3}-c_{i4}}{v_0-\dot{x}_{i2}}(\dot{x}_i - \dot{x}_{i2}) & \dot{x}_{i2} \leq \dot{x}_i \leq v_0 \end{cases} \tag{E.26}$$

where the index $i = 1, 2$ stand for 1^{st} and 2^{nd} mass respectively. C_i is the dynamic crash of the vehicle or occupant. v_0 is the initial impact velocity. The index i designates the models with two masses such as vehicle-to-vehicle and vehicle-occupant models respectively. The same piecewise functions, without the index i, are used to model the vehicle into barrier crash. At the maximum crash, the spring stiffness is assumed to be high, but the damper coefficient is small for maintaining the shape of displacements and velocities respectively.

E.4 Optimization Scheme of the Genetic Algorithm

Genetic Algorithm (GA) is an adaptive heuristic search based on the evolutionary ideas of nature selection and genetics. It represents an intelligent exploitation of a random search used to solve optimization problems.This Evolutionary Algorithm holds a population of individuals (chromosomes), which evolve by means of selection and other operators like crossover and mutation. Given a clearly defined problem to be solved and a bit string representation for candidate solutions, a simple GA works as follows in [15]:

1. Start with a randomly generated population of n l-bit chromosomes (candidate solutions to a problem).
2. Calculate the cost function $f(x)$ of each chromosome x in the population.
3. Repeat the following steps until n offspring have been created:
4. Replace the current population with the new population.
5. Go to Step 2

Each iteration of this process is called a generation. A GA is typically iterated for anywhere from 50 to 500 or more generations. The proposed algorithm seeks to find the minimum function between several variables as can be stated in a general form $minf(x)$, where 'x' denotes the unknown variables, which are the damping and

stiffness constants in the model. The cost function $f(x)$ is the objective function which should be optimized. The cost function to be minimized is the norm of the absolute error between the displacement of the simulated cash and the experimental crash data and is defined as:

$$[Error] = sum(|Est - Exp|^T \times |Est - Exp|) \tag{E.27}$$

where Est and Exp are the model and experimental variables (displacements, velocity and acceleration) respectively. A Genetic Algorithm shown is developed to solve the problems defined by Equations (E.3), (E.6), (E.7), (E.23) and (E.24).

E.5 Results and discussion

This sections is a summary of major findings observed on the three vehicle crash models. Namely: vehicle into barrier, vehicle-occupant into barrier and vehicle-to-vehicle models respectively. The label symbols s,v and s in Figure E.3 to Figure E.5 stand for displacement, velocity and acceleration respectively. Exp and Mod stand for Experimental and Model. Figure E.3 shows the comparison between the model response and the experimental test results for a vehicle into a barrier crash. It is noted that the dynamic crush from the model is exactly equal to that obtained from the test. The maximum dynamic crash, the time of crash and the rebound velocity for both, the model and test results are summarized in Table E.1. Using the

Table E.1: Estimated Parameters for vehicle into barrier model

Spring	Value	Damper	Value
k_1	3.9880e+03 N/m	c_1	8.7727e+04 Ns/m
k_2	2.8403e+04 N/m	c_2	6.6938e+04 Ns/m
k_3	0.44386e+01 N/m	c_3	3.0115e+04 Ns/m
k_4	2.2337e+05 N/m	c_4	5.9893e+04 Ns/m

same algorithm as in vehicle into barrier, a comparison between the crash test from vehicle-occupant crash and the model shown in Figure E.1 is shown in Figure E.4. The results show that the model is very accurate.

From Figure E.4, the model accuracy is obtained by using force elements with two break point piecewise functions. The maximum dynamic crash of the vehicle model is 0.05% less than that in the real crash test. The displacement of the occupant

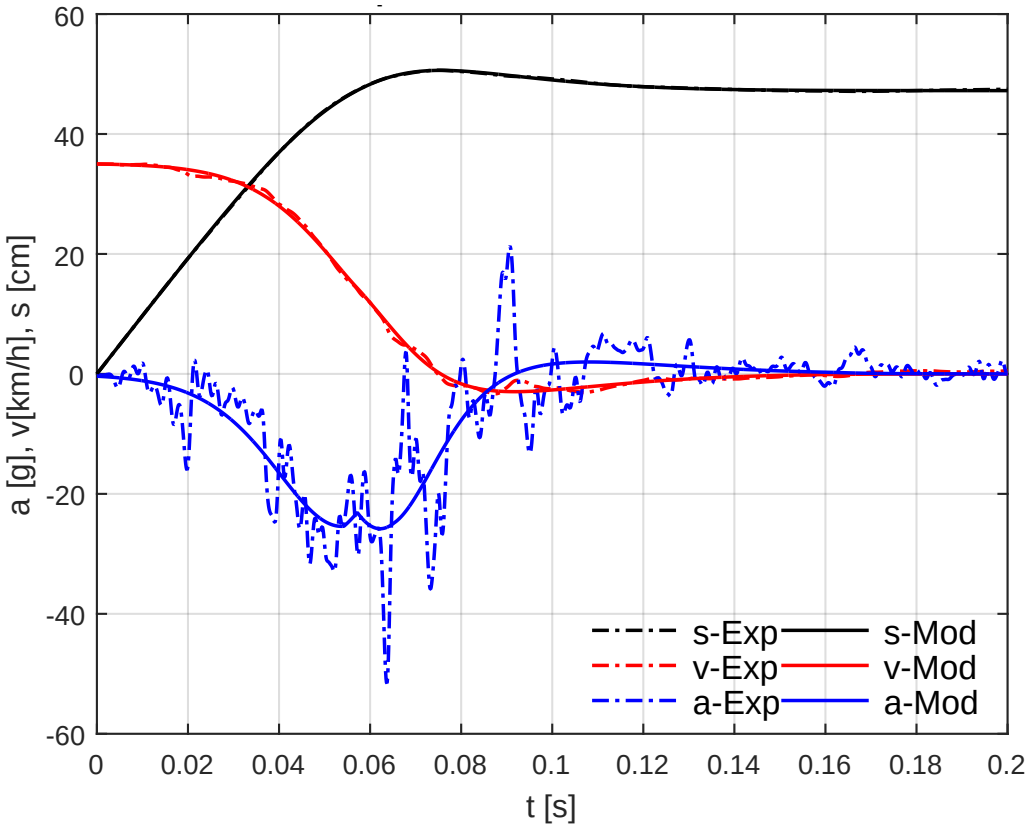

Figure E.3: Model vs Experimental results for Vehicle into fixed pole frontal crash

is 0.09% larger than that from crash test. Improvement of the model accuracy is also observed from the time at maximum displacement and the rebound velocities for both the vehicle and occupant. The optimized estimated parameters are shown in Table E.2. The main results for vehicle-to-vehicle crash modeling are presented in Figs. E.5. It is noted that the model results are much closer to the experimental results for crash test. The maximum dynamic crash of 70.24cm is observed on the target from the test, while the dynamic crash from the model is 69.92 cm. At maximum dynamic crash, the bullet vehicle keeps on moving in the same direction as before crash but the target vehicle re-bounces. The rebounce velocities are -19.6 m/s and -18.3 m/s from the test and the model respectively. This is observed by the velocity curves of the two vehicles, where a negative velocity is noted for the target vehicle and a positive velocity is noted for the bullet vehicle after maximum crash. The accuracy of the model is also observed on the time of maximum crash, t_m. The time of maximum crash, t_m is 0.06568 s from the test and 0.06824 s from the model respectively.

The deformation of the target vehicle is due to the compressive force at dynamic crash. A summary of kinematics results from all models studied is tabulated in Table

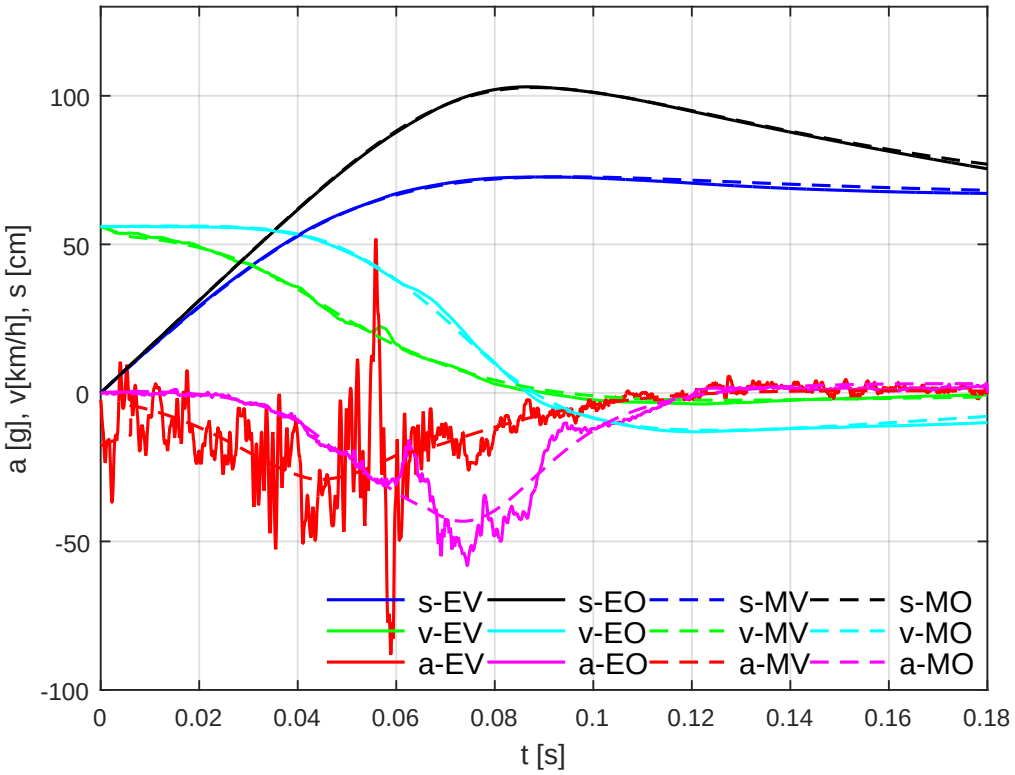

Figure E.4: Model vs Experimental results for vehicle-occupant frontal crash

Table E.2: Estimated Parameters for vehicle-Occupant model

Vehicle	Value	Occupant	Value
k_{11}	7.6665e+04 N/m	k_{21}	6.8536e+03 N/m
k_{12}	7.9498e+04 N/m	k_{21}	2.5529e+04 N/m
k_{13}	9.6887e+03 N/m	k_{23}	9.9998e+04 N/m
k_{14}	9.9998e+04 N/m	k_{24}	7.2212e+04 N/m
c_{11}	8.4895e+04 Ns/m	c_{21}	4.8212e+03 Ns/m
c_{12}	2.8460e+03 Ns/m	c_{22}	1.3677e+03 Ns/m
c_{13}	3.3299e+03 Ns/m	c_{23}	3.2491e+03 Ns/m
c_{14}	1.4046e+04 Ns/m	c_{24}	2.2323e+03 Ns/m

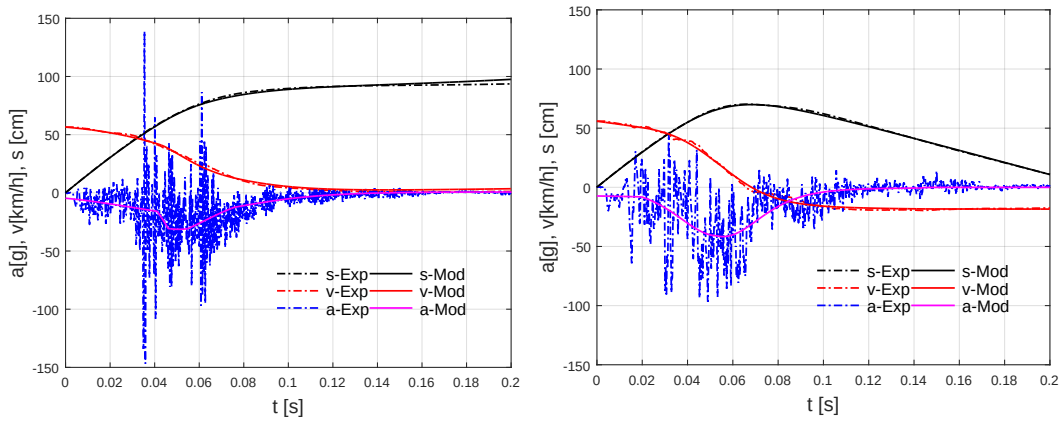

(a) Bullet (b) Target

Figure E.5: Model vs Experimental results for vehicle-to-vehicle frontal crash (a) Bullet (b) Target

Table E.3: Estimated Parameters for vehicle-to-vehicle model

Bullet	Value	Target	Value
k_{11}	1.2843e+05 N/m	k_{21}	1.5030e+04 N/m
k_{12}	2.5142e+05 N/m	k_{21}	1.5030e+04 N/m
k_{13}	1.4932e+05 N/m	k_{23}	4.1930e+05 N/m
k_{14}	6.5159e+05 N/m	k_{24}	5.1878e+04 N/m
c_{11}	4.1688e+04 Ns/m	c_{21}	6.3884e+05 Ns/m
c_{12}	1.7727e+04 Ns/m	c_{22}	7.3768e+04 Ns/m
c_{13}	3.0696e+03 Ns/m	c_{23}	3.3250e+03 Ns/m
c_{14}	2.6614e+03 Ns/m	c_{24}	0.8603e+03 Ns/m

E.4, where VTB, V-Occ and VTV stand for vehicle to Barrier, vehicle-Occupant and Vehicle-to-Vehicle models respectively. T and M stand for Test and Model results, respectively.

Table E.4: A summary of kinematics results from tests (T) and the models (M)

	VTB	V-Occ		VTV	
Results		Veh	Occ	Bulet	Target
$C_m[m] - T$	0.5063	0.7269	1.03	0.9359	0.7024
$C_m[m] - M$	0.5061	0.7274	1.028	0.9613	0.6992
$t_m[s] - T$	0.0749	0.0894	0.086	0.1984	0.065
$t_m[s] - M$	0.0748	0.093	0.087	0.1981	0.068
$V_{reb}[m/s] - T$	-3.3	-3.7	-13	0.9	-19.6
$V_{reb}[m/s] - M$	-2.96	-2.4	-12.6	2.7	-18.3

E.6 Conclusion

In this paper, a mathematical-based method is presented to estimate the parameters of three different vehicle crashes. It is observed that the developed mathematical model results in responses in all vehicle crash models are closer to the experimental crash tests. Therefore, the overall behavior of the models matches the real vehicle's crush well. Two of the main parameters characterizing the collision are the maximum dynamic crush - which describes the highest car's deformation and the time at which it occurs- t_m. They are pertinent to the occupant crash-worthiness since they help to assess the maximum intrusion into the passenger's compartment.

Acknowledgment

The authors would like to thank the Dynamic Research Group members at the University of Agder for their constructive comments to improve this research work.

REFERENCES

[1] W. Pawlus, J. E. Nielsen, H. R. Karimi, and K. G. Robbersmyr. Application of viscoelastic hybrid models to vehicle crash simulation. *International Journal of Crashworthiness*, 55:369 – 378, 2011.

[2] J. Marzbanrad and M. Pahlavani. Calculation of vehicle-lumped model parameters considering occupant deceleration in frontal crash. *International Journal of Crashwothiness*, 16(4), 439 – 455, 2011.

[3] S. M. Ofochebe, C. G. Ozoegwu, and S. O. Enibe. Performance evaluation of vehicle front structure in crash energy management using lumped mass spring system. *Advanced Modeling and Simulation in Engineering*, 2(2):1–18, April 01 2015.

[4] L. Sousa, P.Verssimo, and J. Ambrsio. Development of generic multibody road vehicle models for crashworthiness. *Multibody Syst Dyn*, 19:133 – 158, 2008.

[5] M. Carvalho, J. Ambrsio, and P. Eberhard. Identification of validated multibody vehicle models for crash analysis using a hybrid optimization procedure. *Struct Multidisc Optim*, 44, 85 – 97, 2011.

[6] A. Alnaqi and A. Yigit. Dynamic analysis and control of automotive occupant restraint systems. *Jordan Journal of Mechanical and Industrial Engineering*, 5(1), 39 – 46, 2011.

[7] A. Klausen, S. S. Tørdal, H. R. Karimi, K. G. Robbersmyr, M.Jecmenica, and O. Melteig. Firefly optimization and mathematical modeling of a vehicle crash test based on single-mass. *Journal of Applied Mathematics*, 1 – 10, 2014.

[8] B. B. Munyazikwiye, H. R. Karimi and K. G. Robbersmyr. Mathematical modeling and parameters estimation of car crash using eigensystem realization algorithm and curve-fitting approaches. *Mathematical Problems in Engineering*, 1 – 13, 2013.

[9] B. B.Munyazikwiye, K. G.Robbersmyr, and H. R. Karimi. A state-space approach to mathematical modeling and parameters identification of vehicle frontal crash. *Systems Science and Control Engineering*, 2, 351 – 361, 2014.

[10] B. B.Munyazikwiye, H. R.Karimi, and K. G.Robbersmyr. A mathematical model for vehicle-occupant frontal crash using genetic algorithm. *2016 UKSim-AMSS 18th International Conference on Computer Modelling and Simulation, 6-8 April 2016*.

[11] B. B.Munyazikwiye, H. R.Karimi, and K. G.Robbersmyr. Optimization of vehicle-to-vehicle frontal crash model based on measured data using genetic algorithm. *IEE Access*, 5(1), 3131–3138, 2017.

[12] T. L. Teng, F. A. Chang, Y. S. Liu, and C. P. Peng. Analysis of dynamic response of vehicle occupant in frontal crash using multibody dynamics method. *Mathematical and Computer Modelling*, 48:1724 – 1736, 2008.

[13] N.H.T.S.A. Vehicle crash test database on select test parameters. *http://www-nrd.nhtsa.dot.gov/database/vsr/veh/ querytest.aspx*. Accessed , May 25, 2016.

[14] M. Huang. *Vehicle Crash Mechanics*. CRC PRESS, Boca Raton London New York Washington, 2002.

[15] M. Melanie. *An Introduction to Genetic Algorithms*. Massachusetts Institute of Technology, 1999.

Paper F

Title: Prediction of Vehicle Crashworthiness Parameters using Piecewise Lumped Parameters and Finite Element Models

Authors: Bernard B. Munyazikwiye[1,2], Dmitry Vysochinskiy[1], Mikhail Khadyko[3] and Kjell G. Robbersmyr[1]

Affiliation: [1] Department of Engineering Sciences, University of Agder, Jon Lilletuns Vei 9, 4879, Grimstad, Norway
[2] Department of Mechanical and Energy Engineering, College of Science and Technology, University of Rwanda, Avenue de l'Armée, Po.Box 3900, Kigali, Rwanda
[3] Department of Structural Engineering, Norwegian University of Science and Technology, Richard Birkelands Vei 1A, 7491, Trondheim, Norway

Article: *Designs, Special Issue Road Vehicle Safety: Design and Assessment, 2018 Vol.2(4) pp. 1-16*

Layout: The layout of the paper has been revised to have the same format as the thesis

---

Abstract — **Estimating the vehicle crashworthiness experimentally is expensive and time-consuming. For these reasons, different modelling approaches are utilised to predict the vehicle behaviour and reduce the need for full-scale crash testing. The earlier numerical methods used for vehicle crashworthiness analysis were based on the use of lumped parameters models (LPM), a combination of masses and nonlinear springs interconnected in various configurations. Nowadays, the explicit nonlinear finite element analysis (FEA) is probably the most widely recognised modelling technique. Although informative, finite element models (FEM) of vehicle crash are expensive both in terms of man-hours put into assembling the model and related computational costs. A simpler analytical tool for preliminary analysis of vehicle crashworthiness could greatly assist the modelling and save time. In this paper, the authors investigate whether a simple piecewise LPM can serve as such a tool. The model is first calibrated at an impact velocity of 56 km/h. After the calibration, the LPM is applied to a range of velocities (40, 48, 64 and 72 km/h) and the crashworthiness parameters such as the acceleration severity index (ASI) and the maximum dynamic crush are calculated. The predictions for crashworthiness parameters from the LPM are then compared with the same predictions from the FEA.**

Keywords— piecewise lumped parameters; finite element analysis; dynamic crush; acceleration severity index

F.1 Introduction

Car accidents are among the major causes of mortality in modern society. In the automotive industry, safety is one of the main design considerations. When there is a progressive collapse of the vehicle structure during a frontal crash, two basic requirements should be fulfilled for preventing death or serious injury to the occupants. The first requirement ensures that occupants do not sustain injuries caused by high inertia forces. It dictates that the parameters that characterise the inertia forces felt by the occupant are kept below the threshold values specified in the corresponding standards.

According to the European Standard EN1317-1 [1], a measure of potential injury due to inertia forces during a crash event is the acceleration severity index (ASI), which is calculated from the acceleration measurement at the centre of grav-

ity of the car. The second requirement ensures that occupants are not clamped by the car structure during the crash event. To fulfil this requirement the deformation of the passenger compartment needs to be limited. The severity of car deformation can be estimated by maximum dynamic crush, which is the maximum displacement of the car front with respect to its centre of gravity [2].

Usually, full-scale crash tests (FSCT) are performed to ensure the safe range of risk. Prior to the development of powerful computers, up until the early 1970s, crash studies relied almost exclusively on experimental full-scale testing. However, FSCT is expensive, time-consuming and requires sophisticated infrastructure and highly qualified personnel. Therefore, numerical modelling and simulation are actively used to study and analyse car crashes. Simulation of vehicle crashworthiness has been evolving over the past 45 years. The earlier numerical methods used for vehicle crashworthiness were based on the use of the lumped masses and nonlinear springs. The models built with these methods, known as lumped parameters models (LPM), used lumped masses to represent parts of the vehicle, such as engine block and the passenger compartment, considered rigid during the analysis, and the springs to represent the structural elements responsible for absorbing the kinetic energy.

Various examples of the use of LPM to vehicle crash reconstruction and evaluation of vehicle crashworthiness can be found in the literature. One of the earliest and successful examples of the use of LPM is the model developed by Kamal in 1970s for simulation of vehicle frontal crash at velocities between 0 and 30 mph (48 km/h) [3]. The model was a 3 degrees of freedom (DOF) system composed of three masses and eight springs. In the past few decades, much research has been carried out in the field of vehicle crashworthiness using LPM which resulted in several novel computational models of vehicle collisions. In [4], Marzbanrand expanded the Kamal model to a 5-DOF LPM for the frontal crash and analysed the response of occupant during the impact. Meler et al. [5], performed a system identification for a vehicle frontal crash using a multi-objective optimisation approach. The front end of the vehicle was modelled as a 3 DOF system composed by the passenger compartment; the front wheels, cross-member, and suspension system; and engine interconnected by springs. Kim et al. [6], developed simple approaches for optimising vehicle structure crashworthiness using a single mass-spring-damper system. Huang [7], developed several mathematical models for vehicle crashworthiness using the LPM approach. Inspired by Huang 's work, Pawlus et al. [2, 8] presented results for vehicle crashworthiness assessment using a single

mass-spring-damper system. In [9], the authors proposed an approach to control the seat belt restraint system force during a frontal crash to reduce thoracic injury. Klausen et al. [10, 11] introduced a firefly optimisation method to estimate parameters of vehicle crash test based on a single mass-spring-damper model. Ofochebe et al. [12], studied the performance of a vehicle front structure using a 5-DOF lumped mass-spring model composed of body, engine, the cross-member, the suspension, and the bumper masses. Munyazikwiye et al. [13, 14], applied piecewise linear lumped parameters models and a genetic algorithm (GA) to simulate a vehicle impact (accommodating an occupant) into the barrier and a vehicle-to-vehicle frontal crash, respectively. This GA was also used in [15] for calculating the optimised parameters of a 12-DOF model for two vehicle types in two different frontal crashes.

Lim [16, 17], using SISAME software, presented various research results based on the extraction of lumped parameters from the experimental data to reconstruct the vehicle crash kinematics. Also Mentzer et al. [18, 19], presented the essential formulation of SISAME for extracting the LPM from crash test. Gabler et al. [20], developed LPMs for vehicle into barrier and vehicle-to-vehicle crashes using the SISAME code to extract the model parameters. Recently, Mazurkiewicz et al. [21] used the LPM to improve the safety of children transported in motor vehicles subjected to a side impact during a vehicle crash. Vangi et al. [22] proposed a step-by-step procedure to collect data for a two vehicles accident reconstruction. In [23–26] the authors proposed an optimisation procedure to assist multi-body vehicle model development for vehicle crashworthiness. Tso-Liang et al. [24], examined the dynamic response of a human body in a crash event and assessed the injuries sustained to the occupant's head, chest and pelvic regions.

Even though LPMs have shown useful results in terms of crash reconstruction, some of their limitations have been pointed out in literature. The major challenge of the LPM for vehicle crash analysis is the dependency of LPM on the availability of calibration data. That is, the spring characteristics of the system are determined from existing data, either from a full-scale crash test or from a FE model [27, 28]. A previous work, on a similar study, concluded that LPMs are valid only for data which are used for their creation and could not be simulated for different velocities [2]. This left an open question which needed to be addressed.

The other commonly used approach for vehicle crash analysis is the Finite Element Analysis (FEA). Among the various vehicle crash simulation techniques, explicit FEA is probably the most frequently used and it has been used to calibrate the LPM effectively. Deb and Srinivas in [29] calibrated an LPM for vehicle side

impact based on data from a FEM. In [30], the authors developed an LPM of crash energy absorbing structure for frontal crash. The stiffness characteristics of the structure was obtained from the result of a FEM. Ofochebe et al. [31], developed an absorbable energy monitoring scheme for testing the vehicle structural crashworthiness by calibrating an LPM to an equivalent front-half FEM of a vehicle. Tanlak et al. [32], calibrated an LPM from a FEA of a bumper beam subjected to high impact velocity. However, finite element models have some limitations: They are relatively complex and require a large amount of computational time.

Although out-shined by the more sophisticated finite element modelling techniques, simple lumped parameters models are still used today, especially when it comes to reconstruction of the crash event. The availability of a simpler numerical tool for estimation of basic vehicle crashworthiness parameters can assist the designer and speed up the design process. LPM might serve as such a tool.

Although LPMs have been extensively used for reconstruction of crash scenario at specific impact velocity, it is still worthy to explore more the use of LPM, for predicting the crash event at various impact velocities as complement to the existing results e.g. in [11, 33, 34]. In this paper, the authors investigate whether it is possible to accurately estimate the basic crashworthiness parameters such as maximum dynamic crush and ASI, using the earlier proposed LPM [13, 14]. The piecewise linear LPM is calibrated to the acceleration signal from FSCT and from FEM. Then, the model prediction capability is validated by comparing its predictions with those from a FEA at different impact velocities.

F.2 Materials and Methods

A full-scale crash test of a Ford Taurus (2004 model) in Figure F.1 is chosen as a baseline for the LPM and FEA used in this paper. The test weight and impact speed of the vehicle were 1739 kg and 56 km/h, respectively. The acceleration signal and the finite element analysis model inputs used in this study were obtained from NHTSA open database [35, 36].

The processing of the acceleration signal, calculation of ASI and maximum dynamic crush; and the FEA were done by the authors.

F.2.1 Experimental data and signal filtering

In this paper, the acceleration signal is first filtered using a Finite Impulse Response (FIR) filter before performing a numerical integration to obtain the velocity and

Figure F.1: Full-scale crash test of a Ford Taurus (2004 model) at 56 km/h [35].

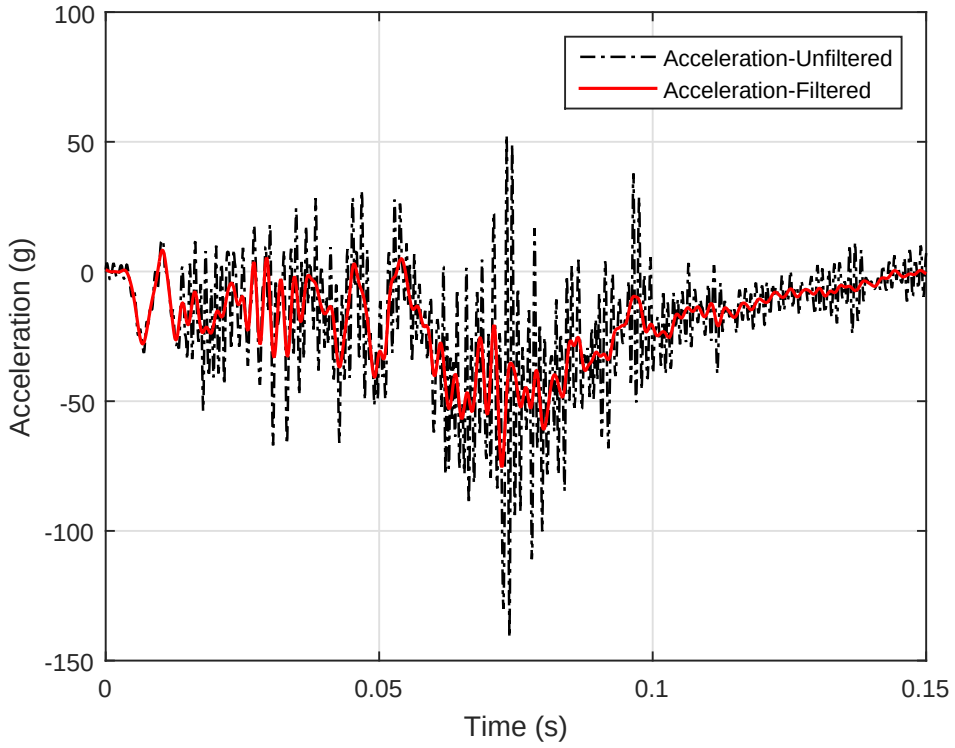

Figure F.2: Noisy and Filtered acceleration signals for full-scale frontal crash

displacement responses, respectively. Figure F.2 shows the noisy and filtered acceleration signals for a vehicle crashing into a barrier. A cut-off frequency of 0.5 kHz with a sampling rate of 10 kHz is chosen while designing a suitable low pass filter. A filter order of 30 and a Kaiser window are used for filtering the acceleration signal.

F.2.2 Piecewise linear lumped parameters model

The model consists of a Kelvin model shown in Figure F.3. The mathematical expression of the model is a normal second order differential equation as shown in the following

$$\ddot{x} = (-F_k - F_c)/m \tag{F.1}$$

where $\dot{x}$ and x are the velocity and displacement of the centre of gravity of mass m (the mass of the vehicle); and F_k , F_c are the built-up spring and damping forces defined in the following equations

$$F_k = k(x) \cdot x, \tag{F.2a}$$

$$F_c = c(\dot{x}) \cdot \dot{x}, \tag{F.2b}$$

Equation (F.1) is solved using a numerical integration to get the model velocity and displacement time-histories, respectively and are then expressed as

$$\dot{x}(i+1) = \dot{x}(i) + \ddot{x}(i)\Delta t \tag{F.3}$$

$$x(i+1) = x(i) + \dot{x}(i)\Delta t; \tag{F.4}$$

with i = 1:(length(t)-1), t is the time vector and Δt is a time step.

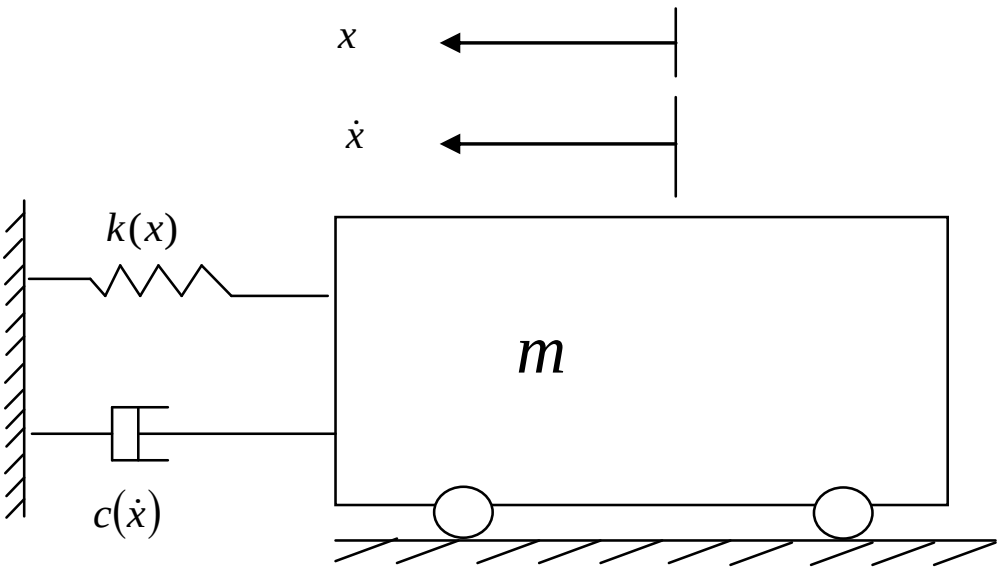

Figure F.3: Lumped parameter model

The spring stiffness and damping coefficients in the model, are defined as the piecewise linear functions of x and $\dot{x}$, respectively. These functions are

$$k(x) = \begin{cases} k_1 + \frac{k_2 - k_1}{x_1} x & 0 \leq x \leq x_1 \\ k_2 + \frac{k_3 - k_2}{x_2 - x_1}(x - x_1) & x_1 \leq x \leq x_2 \\ k_3 + \frac{k_4 - k_3}{C_m - x_2}(x - x_2) & x_2 \leq x \leq C_m \end{cases}, \tag{F.5a}$$

$$c(\dot{x}) = \begin{cases} c_1 - \frac{c_1 - c_2}{\dot{x}_1} \dot{x} & 0 \leq \dot{x} \leq \dot{x}_1 \\ c_2 - \frac{c_2 - c_3}{\dot{x}_2 - \dot{x}_1}(\dot{x} - \dot{x}_1) & \dot{x}_1 \leq \dot{x} \leq \dot{x}_2 \\ c_3 - \frac{c_3 - c_4}{v_0 - \dot{x}_2}(\dot{x} - \dot{x}_2) & \dot{x}_2 \leq \dot{x} \leq v_0 \end{cases}, \tag{F.5b}$$

where the upper limits C_m and v_0 are the maximum dynamic crush and initial velocity from the FSCT or FEM used for calibration of the LPM at v_0 = 56 km/h. Equations (F.5a) - (F.5b) were used to calibrate the LPM. The intention was to reconstruct the crash event by simplest LPM possible and the model with three intervals was shown to be accurate enough during the earlier studies [13, 14]. The prediction is performed by excluding the lower and upper limits in equation (F.5) and subjecting the calibrated LPM to different impact velocities. Then, the piecewise linear functions are

$$k(x) = \begin{cases} k_1 + \frac{k_2 - k_1}{x_1} x & x \leq x_1 \\ k_2 + \frac{k_3 - k_2}{x_2 - x_1}(x - x_1) & x_1 \leq x \leq x_2 \\ k_3 + \frac{k_4 - k_3}{C_m - x_2}(x - x_2) & x \geq x_2 \end{cases}, \tag{F.6a}$$

$$c(\dot{x}) = \begin{cases} c_1 - \frac{c_1 - c_2}{\dot{x}_1} \dot{x} & \dot{x} \leq \dot{x}_1 \\ c_2 - \frac{c_2 - c_3}{\dot{x}_2 - \dot{x}_1}(\dot{x} - \dot{x}_1) & \dot{x}_1 \leq \dot{x} \leq \dot{x}_2 \\ c_3 - \frac{c_3 - c_4}{v_0 - \dot{x}_2}(\dot{x} - \dot{x}_2) & \dot{x} \geq \dot{x}_2. \end{cases} \tag{F.6b}$$

F.2.3 LPM estimation and Calibration scheme using the GA

The procedure for solving the problem defined in equation (F.1) is shown in Figure F.4. The genetic algorithm (GA) attempts to move points through a series of generations, each being composed of a population which has a set number (population size, 200 in this work) and 12 parameters (four stiffness values, four damping coefficient values, two position values, x_1 and x_2, two intermediate velocities $\dot{x}_1$ and $\dot{x}_2$).

The proposed algorithm seeks to find the minimum of an objective function as can be stated in a general form $minf(p)$, where p denotes the unknown variables in the model. In this paper, the two objective functions to be minimised are the error functions $E_1(p,t)$ and $E_2(p,t)$ between the acceleration time-history obtained from the LPM and the calibration data. From the estimated acceleration, the displacement and velocity time-histories are thereafter derived by numerical integration. The objective functions are defined in equations (F.7a) and (F.7b).

$$E_1(p,t) = \sum_{i=1}^{N} \sqrt{\left[a_{FSCT}(t_i) - a_{LPM}(p,t_i)\right]^T \times a_{FSCT}(t_i) - a_{LPM}(p,t_i)}, \quad \text{(F.7a)}$$

$$E_2(p,t) = \sum_{i=1}^{N} \sqrt{\left[a_{FEA}(t_i) - a_{LPM}(p,t_i)\right]^T \times a_{FEA}(t_i) - a_{LPM}(p,t_i)}, \quad \text{(F.7b)}$$

where a_{FSCT}, a_{LPM} and a_{FEA} are accelerations from the FSCT, LPM and FEA, respectively and N is the number of data points. An initial guess of parameters is chosen and substituted in the piecewise linear functions defined in equations (F.5a) and (F.5b). The obtained spring stiffness and damping coefficients are substituted into equations (F.2a) and (F.2b), which are respectively substituted in the dynamic equation (F.1). Then, equation (F.1) is solved numerically to get the simulated kinematic results. Finally, these kinematic results are compared with the calibration data. The objective functions in equations (F.7a) and (F.7b) are evaluated, and when the stop criterion is met the solver terminates, otherwise the GA keeps on tuning the model parameters until the LPM results match the calibration data (experimental or FEA results).

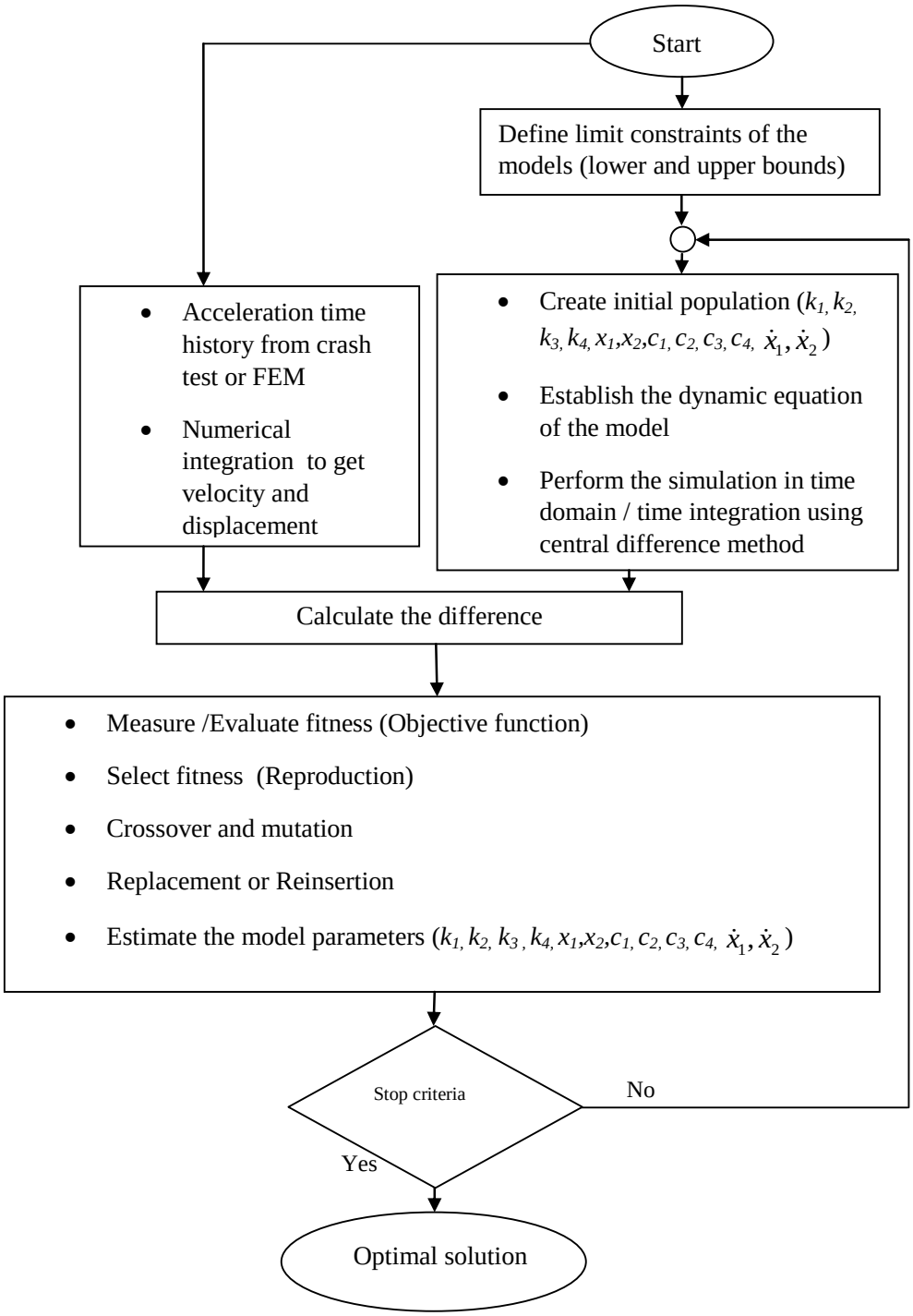

Figure F.4: Calibation procedure using genetic algorithm

F.2.4 Finite element analysis

As mentioned earlier, the input to finite element analysis was obtained from the National Highway Traffic Safety and Administration (NHTSA) open database [36].

The following is a summary describing the studied FEM:

- Number of parts: 804
- Number of nodes: 922,007
- Number of beam elements: 10
- Number of shell elements: 838,926
- Number of solid elements: 134,468

The simulations were performed using the LS-DYNA software Version R8.10 (Revision R8.105896). The impact velocities of 40, 48, 56, 64, and 72 km/h were simulated. Acceleration signal was recorded at the centre of gravity (CG) of the finite element model.

In the case when the finite element analysis uses the under-integrated shell and solid elements, non-physical, zero-energy deformation modes such as hourglass modes might occur. Some small amount of hourglass energy can be tolerated, but this non-physical deformation mode needs to be kept under control. The ratio of the hourglass energy to the internal energy should not exceed the recommended value. In the presented analysis, this ratio was carefully controlled and kept below 10 % of the peak internal energy, which is the recommended value according to [37, 38]. The ratio of hourglass energy to the highest internal energy was 0.078. The actual computation time for a single crash simulation supported by the LS-DYNA was between 1 and 2 days.

F.2.5 Acceleration Severity Index (ASI)

The ASI is intended to give a measure of the severity of inertia force experienced by a person seated in the proximity of the CG of the vehicle during impact. The ASI is derived from the acceleration time-histories measured at the CG of the impacting vehicle and is computed as follows [39]:

$$ASI(t_i) = \sqrt{\left(\frac{\overline{a}_x}{\hat{a}_x}\right)^2 + \left(\frac{\overline{a}_y}{\hat{a}_y}\right)^2 + \left(\frac{\overline{a}_z}{\hat{a}_z}\right)^2} \tag{F.8}$$

where $\hat{a}_x = 12g, \hat{a}_y = 9g, \hat{a}_z = 10g$ are limit values for the components of the acceleration along the body axes x (longitudinal direction), y (lateral direction) and z (vertical direction), respectively. These values are obtained from the human body tolerance limits, interpreted as the values below which passenger risk is very small

(light injury if any) and $g = 9.81m/s^2$ is the acceleration due to gravity, while $\overline{a}_x, \overline{a}_y, \overline{a}_z$ are the components of acceleration of a selected point at the CG of the vehicle, averaged over a moving time interval δ = 0.050 seconds and the ASI is the maximum value of ASI(t). The average acceleration components are defined in equation (F.9).

$$\begin{aligned} \overline{a}_x &= \frac{1}{\delta}\int_t^{t+\delta} a_x dt \\ \overline{a}_y &= \frac{1}{\delta}\int_t^{t+\delta} a_y dt \\ \overline{a}_z &= \frac{1}{\delta}\int_t^{t+\delta} a_z dt \end{aligned} \tag{F.9}$$

In case of a full frontal crash, the acceleration components in the lateral and vertical directions are less significant as compared to the longitudinal acceleration. Hence, in this work, the computation of ASI involves only the longitudinal component and its associated $12g$ threshold acceleration. That is:

$$ASI = \frac{|\overline{a}_x|}{12g} \tag{F.10}$$

In case of collision with a rigid barrier, all the impact energy is absorbed by the vehicle structure. Thus, the European standard EN 1317-2:2010 [39] does not specify any standard values of ASI on impact with the rigid barriers. For reference, the prescribed values of ASI for flexible barriers are:

- Class A: ASI ≤ 1
- Class B: 1.0 $\leq$ ASI ≤ 1.4
- Class C: 1.4 $\leq$ ASI ≤ 1.9

The impact Severity Class A indicates a greater level of safety for vehicle occupants than Class B and the same for class B compared to class C. The more the ASI exceeds unity, the more the impact consequences for the passengers are dangerous [40].

F.3 Results

The spring stiffness and damping coefficient characteristics of the vehicle's front structure, optimised through the GA, are shown in Table F.1. The crashworthiness

parameters in terms of maximum dynamic crush (C_m), time of crush (t_m) and ASI for the range of velocities are summarized in Table F.2.

Table F.1: Estimated structural parameters of the vehicle frontal crash model calibrated at 56 km/h.

Parameters	**LPM Calibrated to FSCT**	**LPM Calibrated to FEM**
k_1	7195 N/m	25,718 N/m
k_2	7210 N/m	31,444 N/m
k_3	25,386 N/m	45,476 N/m
k_4	711,060 N/m	467,830 N/m
x_1	0.0526 m	0.2448 m
x_2	0.1023 m	0.2923 m
c_1	59,444 Ns/m	80,827 Ns/m
c_2	51,590 Ns/m	7775 Ns/m
c_3	4997 Ns/m	38,812 Ns/m
c_4	1382 Ns/m	5703 Ns/m
$\dot{x}_1$	7.0585 m/s	4.7855 m/s
$\dot{x}_2$	8.9272 m/s	8.2880 m/s

LPM: Lumped Parameters Model , FSCT: Full-Scale Crash Test, FEM: Finite Element Model

Figure F.5 illustrates three out of five FEA simulations of a Ford-Taurus (2004 model) crashing into a fixed rigid wall at initial velocities of 40, 56, and 72 km/h, respectively. The convergences of the objective functions are satisfied since their fitness values are constant across a large number of generations as shown in Figure F.6. The kinematic time-history (displacements, velocities, and accelerations) are compared as shown in Figures F.7 and F.8. These Figures show the predictions of the LPM for a range of velocities (40, 48, 56, 64, and 72 km/h, respectively). Figure F.9, presents a summary of kinematics results of the LPM calibrated at 56 km/h against the FSCT and FEA, respectively.

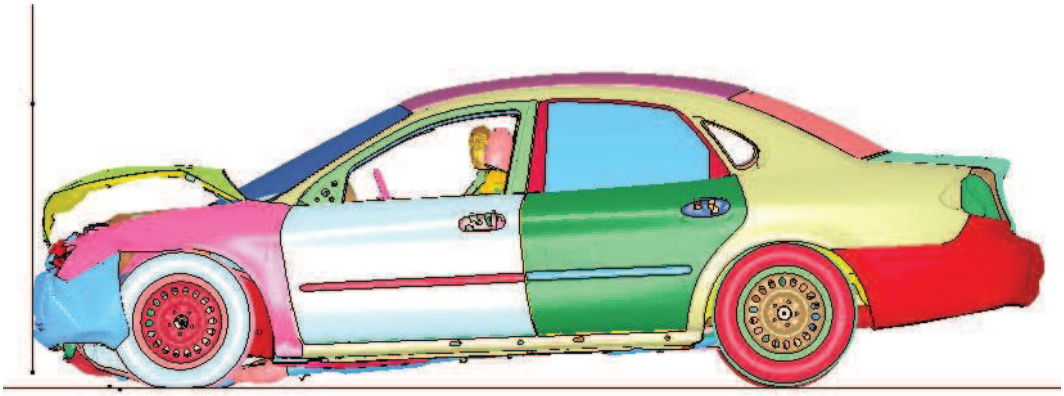

(a)

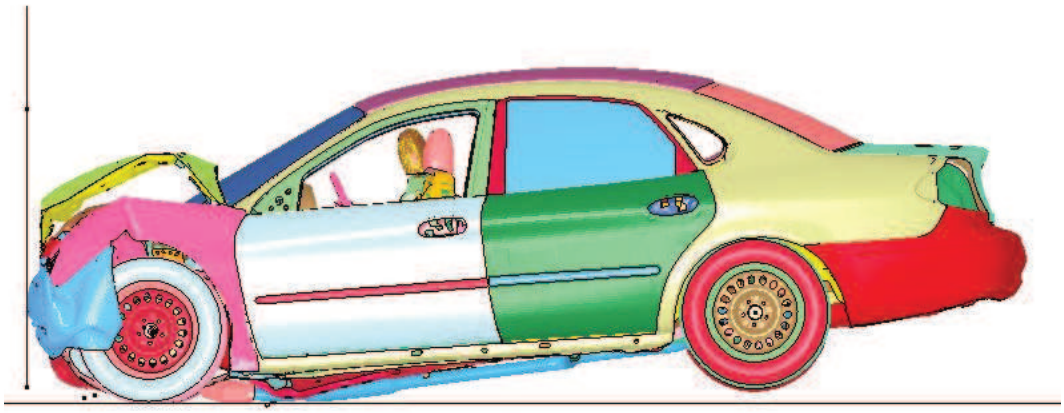

(b)

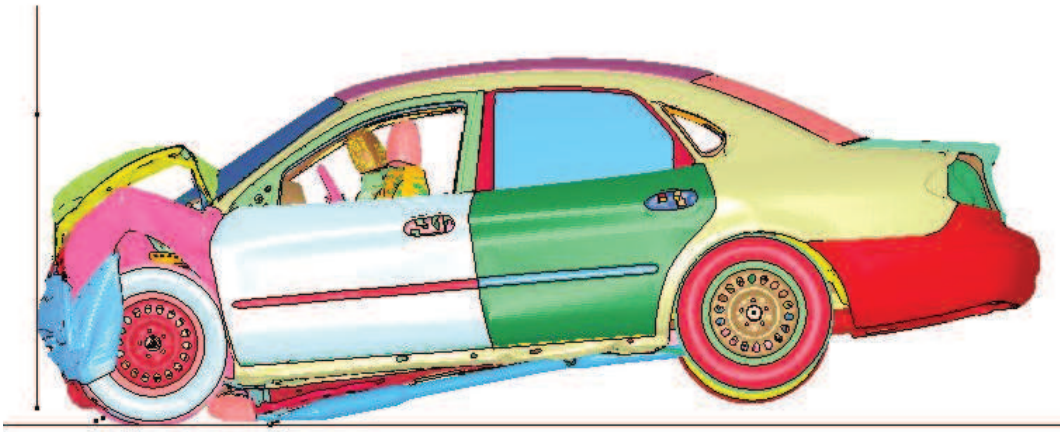

(c)

Figure F.5: Deformed vehicle frontal structure through FEA at impact velocities of (a) 40 km/h, (b) 56 km/h and (c) 72 km/h

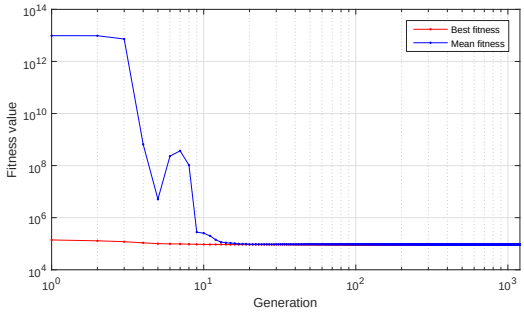

(a)

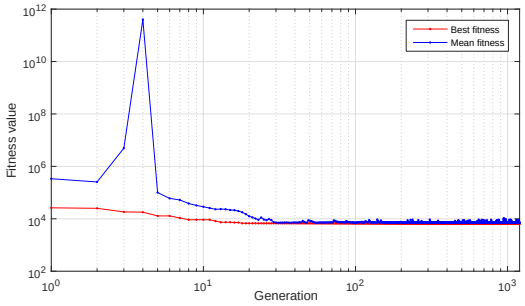

(b)

Figure F.6: Convergence of the objective function using GA (a) LPM calibrated to FSCT (b) LPM calibrated to FEM.

Table F.2: Estimated crashworthiness parameters for FSCT, LPM and FEA .

		Impact velocities				
Approaches	Parameters	**40 km/h**	**48 km/h**	**56 km/h**[c]	**64 km/h**	**72 km/h**
FSCT	t_m [s]	-	-	0.0723	-	-
	C_m [m]	-	-	0.7551	-	-
	ASI [-]	-	-	2.5	-	-
LPM calibrated to FSCT	t_m [s]	0.0736	0.0740	0.0738	0.0741	0.0741
	C_m [m]	0.5373	0.6429	0.7508	0.8588	0.9653
	ASI [-]	1.7	2.1	2.6	2.7	3.1
FEA	t_m [s]	0.0755	0.0781	0.0801	0.0804	0.0800
	C_m [m]	0.5077	0.6077	0.7180	0.8331	0.9408
	ASI [-]	1.5	1.8	2.0	2.3	2.5
LPM calibrated to FEA	t_m [s]	0.0824	0.0825	0.0793	0.0822	0.0805
	C_m [m]	0.5231	0.6258	0.7108	0.8360	0.9396
	ASI [-]	1.4	1.6	2.0	2.3	2.5

[c]Calibration point, t_m is the time at maximum dynamic crush, C_m is the maximum dynamic crush and ASI is the acceleration severity index.

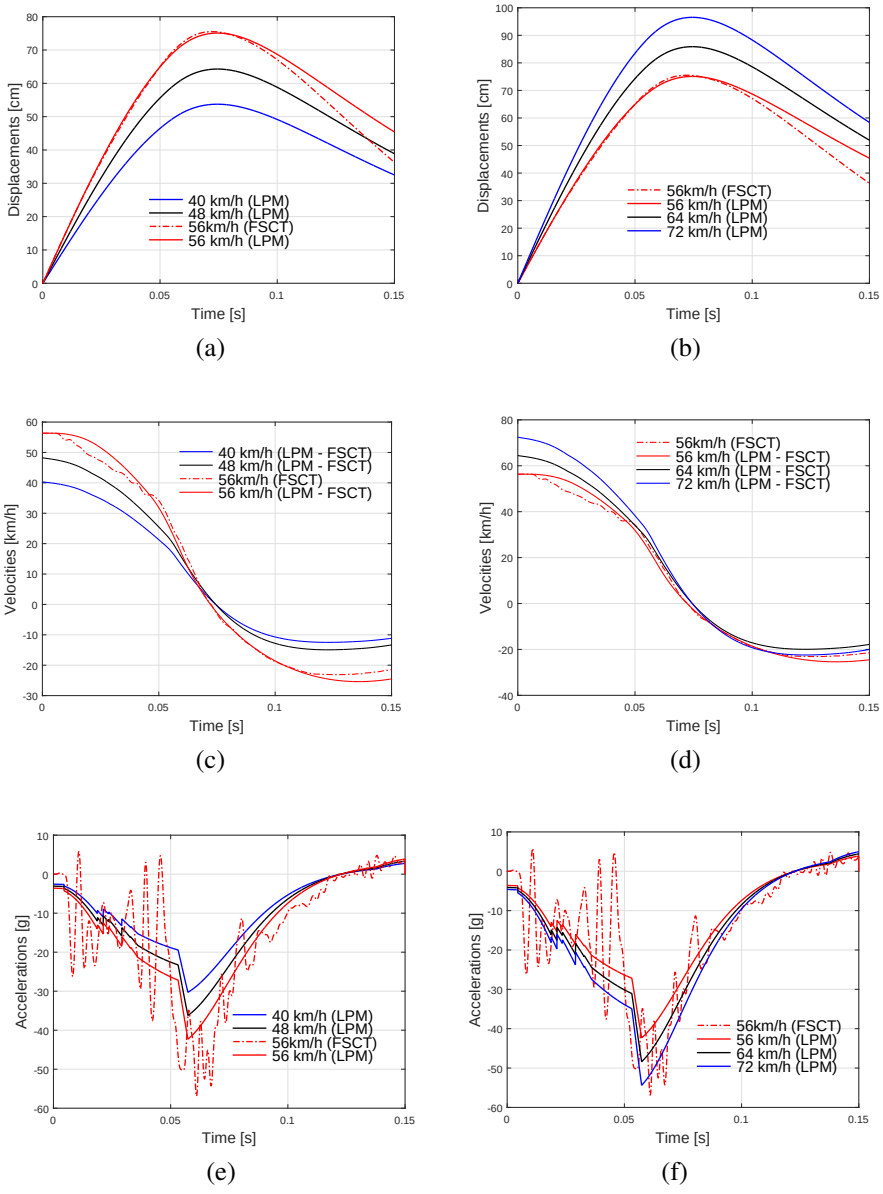

Figure F.7: Displacement, velocity, and acceleration plot comparison in case of LPM calibrated to FSCT, (a), (c) and (e) impact velocities lower than the calibration point (56 km/h); (b), (d) and (f) impact velocities higher than the calibration point.

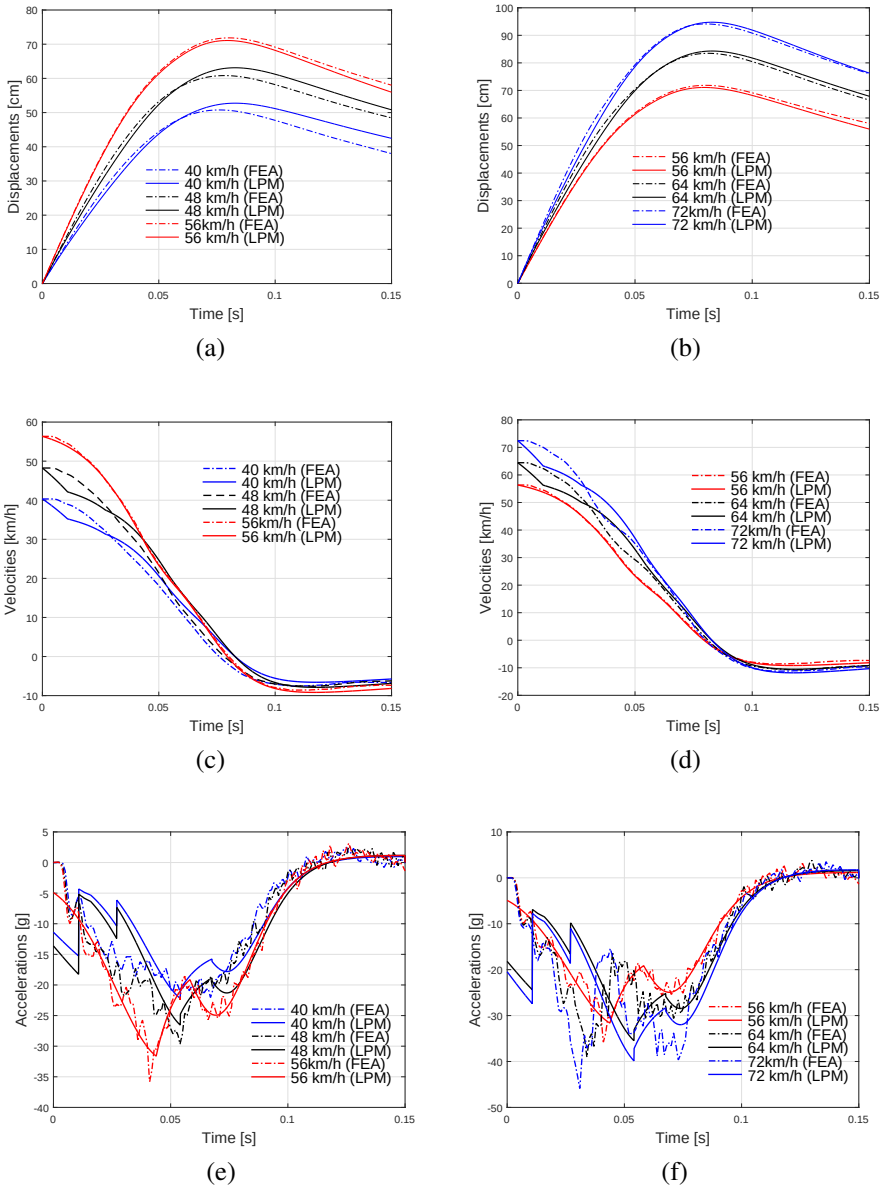

Figure F.8: Displacement, velocity, and acceleration plots comparison in case of LPM calibrated to FEA, (a), (c) and (e) impact velocities lower than the calibration point (56 km/h); (b), (d) and (f) impact velocities higher than the calibration point.

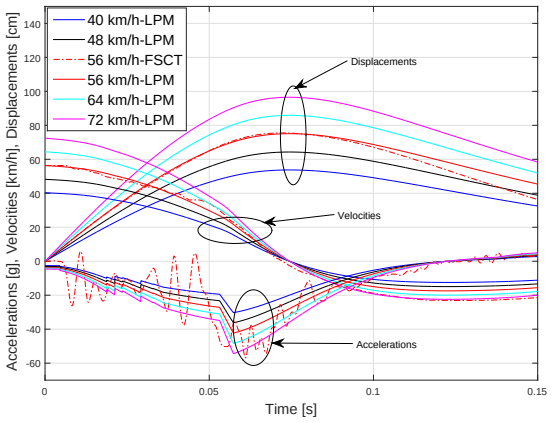

(a)

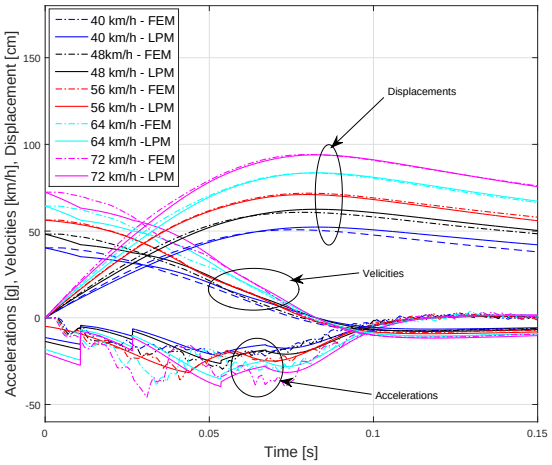

(b)

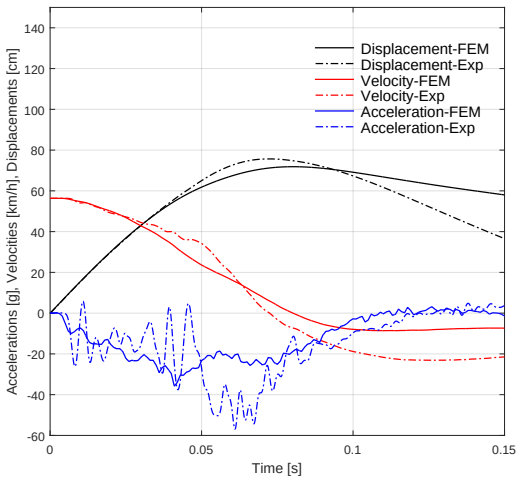

(c)

Figure F.9: A summary of kinematic time histories for (a) LPM calibrated to FSCT, (b) LPM calibrated to FEM, (c) comparison between FEA and FSCT at 56 km/h.

F.4 Discussion

During the real vehicle crash event, the front structure of the car is deformed plastically and the amount of deformation is measured by the maximum dynamic crush. At maximum dynamic crush, the car stops when the velocity decreases up to zero and then increases negatively when the car gets separated from the barrier. In this study, the LPM simulates the crash event. This was achieved by first calibrating the model with acceleration signal from FSCT and FEM for a portion of deformation from the time of contact with the barrier up to time of maximum dynamic crush. From Table F.1, it is observed that the estimated stiffness value increases at the maximum dynamic crush while, at the same time, the damping coefficient decreases. The kinematics results from the LPM match those from FSCT up to the maximum dynamic crush. From Table F.1, it is shown that the maximum dynamic crashes from the FSCT and LPM are 0.7551 m and 0.7508 m, respectively and occur after 0.0723 s for FSCT and 0.0738 s for LPM. From Figure F.7, a deviation is observed just after the time of maximum dynamic crush.

In case of FEM, the frontal structure of the model absorbs enough kinetic energy. From Figure F.5, the hood and fender are bent and the bumper is deformed plastically at the highest velocity (72 km/h). This is due to many elements that buckle together when the front structure is completely compressed at the maximum dynamic crush. When the LPM is calibrated to the FEM, a reasonable agreement between the results from LPM and those from FEA is observed as shown in Figure F.8. It is shown that the maximum error between the maximum dynamic crush C_m, from the FEA and LPM is less than 3 cm for all impact velocities. This is evidenced by the dynamic crushes with their respective time of occurrence. It is noted from Table F.2 that the maximum dynamic crush and the ASI for LPM and FEM are similar at a specific impact velocity. The results show that the ASI is high (greater than 1.9) when the impacting velocity of the vehicle is greater than 48 km/h.

The predictions show that a constant increment of 11 cm of the maximum dynamic crush is observed for a corresponding increment of 8 km/h for the impact velocity when the LPM is calibrated to a FSCT. Likewise, an increment of 10 cm is observed on the maximum dynamic crush when the LPM is calibrated to a FEM. The high values of ASI reported in this work are due to the rigidity of the barrier. The results show that the LPM agrees with the experimental data obtained from the NHTSA, collected on a FORD TAURUS model crashing into a flat load cell barrier at 56 km/h with Test No.5143, Curve No.122 [35] and the conventional FEA. The

calibration time for the LPM is between 15 and 30 minutes and the simulation takes less than 20 seconds, while the actual computational time for the FEA is between 1 and 2 days excluding the undefined time spent in developing the complex FEM of a complete vehicle.

F.5 Conclusions and future work

It is obvious that simple LPM cannot replace the complex FE model with regard to crash simulations, but it can assist to speed up the analysis. Due to the complexity of the FEM, the analyst typically needs several iterations with adjustment of simulation parameters before a successful simulation is produced. In this work three to five iterations were necessary, each taking about half of the full simulation time before the analysis termination. Hence to produce a single successful FE analysis of the crash event required about a week of working time. To produce an N number of successful FE simulations for a range of velocities would typically take less time than N weeks since once a successful combination of parameters is found, it can be used for most of the simulations and only minor adjustments are needed for different velocities. In the current study, the FE analysis for the five different velocities was produced within a month. Using a LPM allows to perform one FEA instead of five, calibrate the LPM to FEM and obtain the estimate of the crash parameters for a range of velocities. Hence combining LPM and FEM extracts preliminary results of a month work within a week.

In future work, the integration of flexible barrier in LPM could be investigated. Other evolutionary-based algorithms such as the Differential Evolution (DE), Covariance Matrix Adaptation Evolution Strategy (CMA-ES), and Particle Swarm Optimization (PSO) could be tried for further improvement on the current results obtained using the GA. The extension of this work could be the consideration of the predictive capabilities of the LPM for other crash scenarios such as an oblique crash, side impact, and vehicle-to-vehicle crash, respectively. The expected challenges could be the representation of bending, of multi-dimensional/multi-axial deformations in other vehicle crash configurations. Other challenges expected when analysing the oblique and side crash with LPM could be the complexity in extracting of parameters in case of a multi-dimension model.

Author contributions

Bernard B. Munyazikwiye, the main author, proposed the approach, processed the data, analysed the results and wrote the article; Dmitry Vysochinskiy and Kjell G. Robbersmyr, scientific advisers, supervised the work and revised the article; Mikhail Khadyko, performed the FEA and the final revision of the article.

Conflicts of interest

The authors declare no conflict of interest. The research is part of the main author's PhD-project and is funded by the University of Agder,Kristiansand and Grimstad, Norway.

REFERENCES

[1] European Standard EN 1317-1. Road restraint systems Part 1, Terminology and general criteria for test methods. Technical report, European Committee of Standardization, 2010.

[2] Pawlus, W.; Karimi, H.R.; Robbersmyr, K.G. Development of lumped-parameter mathematical models for a vehicle localized impact. *Journal of Mechanical Science and Technology* **2011**, *25*, 1737–1747.

[3] M.Kamal, M. Analysis and Simulation of Vehicle to Barrier Impact. *SAE International , Technical Paper* **1970**, pp. 1 – 6.

[4] Marzbanrad, J.; Pahlavani, M. Calculation of vehicle-lumped model parameters considering occupant deceleration in frontal crash. *International Journal of Crashworthiness* **2011**, *16*, 439 – 455.

[5] Marler, R.T.; Kim, C.H.; Arora, J.S. System identification of simplified crash models using multi-objective optimization. *Computer Methods in Applied Mechanics and Engineering* **2006**, *195*, 4383–4395.

[6] Kim, C.H.; Mijar, A.R.; J.S.Arora. Development of simplified models for design and optimization of automotive structures for crashworthiness. *Struct Multidisc Optim* **2001**, *22*, 307–321.

[7] Huang, M. *Vehicle Crash Mechanics*, 1st ed.; CRC PRESS: Boca Raton, FL, USA, 2002.

[8] Pawlus, W.; Nielsen, J.E.; Karimi, H.R.; Robbersmyr, K.G. Application of viscoelastic hybrid models to vehicle crash simulation. *International Journal of Crashworthiness* **2011**, *55*, 369 – 378.

[9] Alnaqi, A.; Yigit, A. Dynamic Analysis and Control of Automotive Occupant Restraint Systems. *Jordan Journal of Mechanical and Industrial Engineering* **2011**, *5*, 39 – 46.

[10] Klausen, A.; Tørdal, S.S.; Karimi, H.R.; Robbersmyr, K.G.; Jecmenica, M.; Melteig, O. Firefly Optimization and Mathematical Modeling of a Vehicle Crash Test Based on Single-Mass. *Journal of Applied Mathematics* **2014**, pp. 1 – 10. Article ID 150319.

[11] Klausen, A.; Tørdal, S.S.; Karimi, H.R.; Robbersmy, K.G. Mathematical Modeling and Numerical Optimization of Three Vehicle Crashes using a Single-Mass Lumped Parameter Model. 24th International Technical Conference on the Enhanced Safety of Vehicles (ESV); , 2015; pp. 44 – 49.

[12] Ofochebe, S.M.; Ozoegwu, C.G.; Enibe, S.O. Performance evaluation of vehicle front structure in crash energy management using lumped mass spring system. *Advanced Modeling and Simulation in Engineering* **2015**, *2*, 1–18.

[13] Munyazikwiy, B.B.; Karimi, H.R.; Robbersmyr, K.G. A Mathematical Model for Vehicle-Occupant Frontal Crash using Genetic Algorithm. 2016 UKSim-AMSS 18th International Conference on Computer Modelling and Simulation, Cambridge, United Kingdom, 6-8 April, 2016.

[14] Munyazikwiye, B.B.; Karimi, H.R.; Robbersmyr, K.G. Optimization of Vehicle-to-Vehicle Frontal Crash Model Based on Measured Data Using Genetic Algorithm. *IEEE Access, Special Section on Recent Advances on Modelling, Optimization, and Signal Processing Methods in Vehicle Dynamics and Crashworthiness* **2017**, *5*, 3131–3138.

[15] Pahlavani, M.; Marzbanrad, J. Crashworthiness study of a full vehicle-lumped model using parameters optimization. *International Journal of Crashworthiness* **2015**, *20*, 573 – 591.

[16] Lim, J.M. A Consideration on the Offset Frontal Impact Modeling Using Spring-Mass Model. *International Journal of Mechanical, Aerospace, Industrial, Mechatronic and Manufacturing Engineering* **2015**, *9*, 1453 – 1458.

[17] Lim, J.M. Lumped Mass-Spring Model Construction for Crash Analysis using Full Frontal Impact Test Data. *International Journal of Automotive Technology* **2017**, *18*, 463 – 472.

[18] Mentzer, S.G. The SISAME-3D Program: Structural Crash Model Extraction and Simulation. Technical report, US Dept. of Transportation. D Report DOT HS, 2007.

[19] Mentzer, S.; Radwan, R.; Hollowel, W. The SISAME methodology for extraction of optimal lumped parameter structural crash models. *SAE Technical Paper 920358,* **1992**.

[20] Gabler, H.C.; Hollowell, W.; Summers, S. Systems modeling of frontal crash compatibility. *Proceedings of the 2000 SAE International Congress and Exposition, Detroit, USA Paper No. 2000-01-0878* **2000**, pp. 1–8.

[21] Mazurkiewicz, L.; Baranowski, P.; Karimi, H.R.; Damaziak, K.; Malachowski, J.; Muszynski, A.; Muszynski, A.; Robbersmyr, K.G.; Vangi, D. Improved child-resistant system for better side impact protection. *Int J Adv Manuf Technol* **2018**, pp. 1–11.

[22] Vangi, D.; Cialdai, C.; Gulino, M.S.; Robbersmyr, K.G. Vehicle Accident Databases: Correctness Checks for Accident Kinematic Data. *Designs* **2018**, *2*, 1–11.

[23] Sousa, L.; P.Verssimo.; Ambrosio, J. Development of generic multibody road vehicle models for crashworthiness. *Multibody Syst Dyn* **2008**, *19*, 133 – 158.

[24] Teng, T.; Chang, F.; Liu, Y.; Peng, C. Analysis of dynamic response of vehicle occupant in frontal crash using multibody dynamics method. *Mathematical and Computer Modelling* **2008**, *48*, 1724 – 1736.

[25] Carvalho, M.; Ambrosio, J.; Eberhard, P. Identification of validated multibody vehicle models for crash analysis using a hybrid optimization procedure. *Struct Multidisc Optim* **2011**, *44*, 85 – 97.

[26] Carvalho, M.; Ambrósio, J. Identification of multibody vehicle models for crash analysis using an optimization methodology. *Multibody Syst Dyn* **2010**, *24*, 325–345.

[27] Ibrahim, H.K. Design Optimization of Vehicle Structures for Crashworthiness Improvement. PhD thesis, Concordia University, Montreal, Quebec, Canada, 2009.

[28] Mahmood, H.F.; Fileta, B.B., Vehicle Crashworthiness and Occupant Protection; American Iron and Steel Institute, 2004; chapter 2. Design of vehicle structures for crash energy management, pp. 20–21.

[29] Deb, A.; Srinivas, K.C. Development of a new lumped-parameter model for vehicle side-impact safety simulation. *Proceedings of the Institution of Mechanical Engineers, Part D: Journal of Automobile Engineering* **2008**, pp. 1793–1811.

[30] Piyush Dube, M. L. J. Suman, V.B. Lumped Parameter Model for Design of Crash Energy Absorption Tubes. *MSRUAS-SAS Tech Journal* **2014**, *13*, 5–7.

[31] M.Ofochebe, S.; Enibe, S.; G.Ozoegwu, C. Absorbable energy monitoring scheme: new design protocol to test vehicle structural crashworthiness. *Heliyon, Elsevier* **2016**, *2*, 1–33.

[32] Tanlak, N.; Sonmez, F.; Senaltun, M. Shape optimization of bumper beams under high-velocity impact loads. *Engineering Structures* **2015**, *95*, 49–60.

[33] Lu, Q.; Karimi, H.R.; Robbersmyr, K.G. A Data-Based Approach for Modeling and Analysis of Vehicle Collision by LPV-ARMAX Models. *Hindawi Publishing Corporation, Journal of Applied Mathematics* **2013**, *2013*, 1– 10.

[34] Prasad, P.; Padgaonkar, A.J. Static-to-Dynamic Amplification Factors for Use in Lumped-Mass Vehicle Crash Models. *Society of Automotive Engineers (SAE) 810475* **1981**, p. 1–43.

[35] *NHTSA. Vehicle Crash Test Database, http://www-nrd.nhtsa.dot.gov/database/vsr/veh/ querytest.aspx*, 2016. Accessed, May 25, 2016.

[36] NHTSA. *LS-DYNA FE Crash Simulation Vehicle Models, https://www.nhtsa.gov/crash-simulation-vehicle-models*, 2016. Accessed, June 15, 2016.

[37] Livermore Software Technology Corporation, Livermore, California 94551-0712. *LS-DYNA Keyword User's Manual, VOLUME II*, ls-dyna r9.0 ed., 2016.

[38] *LSDYNA Supports, https://www.dynasupport.com/howtos/element/hourglass*. Accessed, May 29, 2018.

[39] European Standard EN 1317-2. Road restraint systems Part 2, Performance Classes, impact test acceptance criteria and test method for safety barriers including vehicle parapets. Technical report, European Committee of Standardization, 2010.

[40] Shojaat, M. Correlation between injury risk and impact severity index ASI. Swiss Transport Research Conference, Monte Verità / Ascona, Sweden, 20 - 22 March, 2003.